

NASA CONTRACTOR
REPORT



NASA CR-925

NASA CR-925

FACILITY FORM 602

N68-16351

(ACCESSION NUMBER)

(THRU)

193
(PAGES)

(CODE)

(NASA CR OR TMX OR AD NUMBER)

03
(CATEGORY)

TWO-STAGE POTASSIUM TEST TURBINE

Volume IV

Materials Support of Performance
and Endurance Tests

by W. F. Zimmerman, R. B. Hand, D. S. Engleby,
and J. W. Semmel, Jr.

Prepared by
GENERAL ELECTRIC
Cincinnati, Ohio
for Lewis Research Center

TWO-STAGE POTASSIUM TEST TURBINE

Volume IV

Materials Support of Performance and Endurance Tests

By W. F. Zimmerman, R. B. Hand,
D. S. Engleby, and J. W. Semmel, Jr.

Distribution of this report is provided in the interest of information exchange. Responsibility for the contents resides in the author or organization that prepared it.

Prepared under Contract No. NAS 5-1143 by
GENERAL ELECTRIC
Cincinnati, Ohio

for Lewis Research Center

NATIONAL AERONAUTICS AND SPACE ADMINISTRATION

For sale by the Clearinghouse for Federal Scientific and Technical Information
Springfield, Virginia 22151 - CFSTI price \$3.00

PRECEDING PAGE BLANK NOT FILMED.

FOREWORD

This materials support program covers work associated with construction, test, and operation of the two-stage potassium test turbine under NASA contract NAS 5-1143. It supplements work reported in volume I of this series, which describes the materials support work associated with turbine design and material selection. The work was performed under the Technical Management of J. P. Joyce with the assistance of T. A. Moss, R. L. Davies, and R. N. Weltmann, all of the Space Power Systems Division, NASA-Lewis Research Center.

PRECEDING PAGE BLANK NOT FILMED.

ABSTRACT

The use of superalloys and refractory alloys in the fabrication and operation of a two stage potassium vapor turbine is described. Operating conditions consisted of turbine inlet vapor temperatures between 1450°F and 1550°F and rotational speeds from 15,400 rpm to 21,000 rpm during a 35-hour turbine checkout period and a 68-hour performance test period. A final steady state endurance test run of 2000 hours, of which 1750 hours were continuous, was completed at 1500°F inlet vapor temperature and at a rotational speed of 18,250 rpm. Impurity levels in the potassium were maintained at about 5-12 ppm by continuous hot trapping with zirconium foil in the boiler by-pass and condenser hot traps. Turbine components consisted of an A-286 shaft, U-700 turbine wheels, U-700, TZC and TZM blades, and L-605 nozzle partitions. The amount of contamination of various refractory alloys such as F-48, AS-30, TZM and TZC with carbon, oxygen, nitrogen and hydrogen under turbine operating conditions was evaluated and limited tensile tests were performed on refractory alloy specimens subjected to potassium vapor conditions.

Overall, the turbine operation and material behavior were highly satisfactory; no failures, of a nature which would limit future turbine operation, were noted. During early performance testing, various examples of metal loss by solution corrosion were observed; for example, gross corrosion of turbine blade airfoils occurred when large quantities of liquid potassium were deliberately sprayed into the turbine inlet. Limited metal transport from the boiler to various portions of the facility and turbine components was also noted during this period. Metal foil was deposited on the surface of the vapor line from the boiler and on turbine wheel and blade components. These deposits contained predominantly iron, chromium and nickel and were believed to have resulted from the drying out of liquid droplets from the boiler and containing dissolved metal as solute. These adverse corrosion and metal transport conditions were virtually eliminated during the 2000-hour endurance test by means of improvements in both the boiler system and its method of operation. The endurance test indicated that long time operation of alkali metal vapor turbines is practical.

CONTENTS

	Page
I. SUMMARY	1
II. INTRODUCTION	6
III. SIGNIFICANT TURBINE EVENTS RELATED TO MATERIALS SUPPORT	7
A. Turbine Description	7
B. Summary of Events	9
IV. NON-REFRACTORY MATERIALS EVALUATION	11
A. Rotating Parts	11
B. Non-Rotating Parts	15
V. REFRACTORY ALLOY MATERIALS EVALUATION	18
A. Blade Material Properties	18
B. Refractory Alloy Contamination	22
VI. CORROSION, EROSION, AND MATERIAL TRANSFER	32
A. Corrosion and Erosion	32
1. Corrosion During Initial Turbine Testing	32
2. Lack of Corrosion During Performance Testing	37
3. Corrosion/Erosion During Endurance Testing	38
B. Material Transfer	49
1. C. D. Nozzle Testing	50
2. Performance Testing	50
3. Endurance Testing	52
VII. PROCUREMENT, HANDLING, AND ANALYSIS OF POTASSIUM	54
A. General Considerations	54
B. Procurement and Initial Purification of Potassium	57
C. Initial Facility Testing	58
D. Initial Turbine Testing	59
E. Turbine Performance Testing	60
F. Turbine Endurance Testing	63
VIII. CONCLUSIONS AND RECOMMENDATIONS	68
REFERENCES	70

I. SUMMARY

The successful operation of the two stage potassium vapor turbine during preliminary performance tests and throughout the 2000-hour endurance test was accomplished with a proper consideration for the utilization of materials. This was done first, in the original selection of materials, secondly, in the identification and resolution of minor materials and process problems during the fabrication and test of the turbine and, finally, in the observation and documentation of the characteristics and properties of materials as the result of their use in the turbine.

Fabrication Improvements (pp 11 to 17) For the most part, the original materials and processes selected for the fabrication of the turbine, as presented in GE63FPD238¹, were successfully employed in the final turbine testing. However, the fabrication and testing of the turbine did provide experience which permitted the introduction of various improvements in the details of the design and of the use of materials and fabrication processes. These included:

1. The use of all welded construction instead of bolted metal "O"-ring flanges in both the outer weld assembly of turbine components and the inner weld assembly of the hydrodynamic seal liquid metal supply system. Techniques were also developed for assembling the turbine with a minimum of weld distortion.
2. The Type 316 stainless steel tubes supplying argon, oil and potassium to the bearing housing experienced thermal cracking and were replaced by heavier walled tubing; welding was used as the method of joining these tubes to the housing instead of the original cobalt base, H-33 braze (see Table XV, Composition Analysis), since individual repairs could be made, when required, without submitting the entire housing to a high temperature brazing cycle.
3. Turbine bucket locking strips were increased in thickness for the performance test. These strips failed by strain age cracking in the sharply bent forward radius. This problem was eliminated by using a more generous bend radius and by re-solution treating the fabricated locking strips before installing them in the turbine wheel assembly; the locking strips were aged in place during turbine operation.

Refractory Alloy Evaluation (pp 18 to 31) Refractory alloy blades of columbium base alloys, F-48 and AS-30, and of the molybdenum base alloy, TZM,

were originally considered for use in the turbine. Prior to installation of these second stage blades for endurance test, extensive evaluation was made of these refractory alloys as ring specimens in the Type 316 stainless steel turbine facility to determine their possible contamination with carbon, oxygen, nitrogen and hydrogen. Because of the enormous ratio of Type 316 stainless steel to columbium alloy specimens, both in mass and in surface area, the possibility of contamination of the columbium was great. Evidences of significant contamination in the columbium base alloys resulted in a decision to install only molybdenum base alloy blades in the turbine during endurance testing. This type of refractory alloy ring testing was continued during the 2000-hour endurance test. The molybdenum alloys were least affected; their total specimen weight changes were only a few tenths of a milligram (0.0001 g/cm^2 of outer surface area) as contrasted to total weight losses per specimen in columbium base alloys of approximately 100 milligrams (0.0035 g/cm^2 of outer surface area). The weight losses were generally greater aft of the turbine where more liquid droplet condensate was available. Similarly, the contamination pickup in the refractory alloys was greater in the columbium alloys than in the molybdenum alloys. Carbon, oxygen and nitrogen contents in a 30-mil thick surface layer of the F-48 alloy specimens increased significantly; the carbon content more than doubled and the oxygen and nitrogen contents increased by about 200 ppm in 254 hours of testing. The contamination appeared to be greater forward of the turbine where the temperature was higher, but the greater surface weight losses in the specimens located aft of the turbine may have resulted in lower apparent contamination values in those specimens. In the higher carbon alloys, such as AS-30 and TZC, carbon variations were less significant. It was also observed that the major portion of contamination occurred during the test periods immediately following installation of turbine components; specimens installed after turbine operation and without cutting into the turbine were much less affected by the potassium vapor environment. It was because of the high levels of contamination observed in the columbium base alloys that these alloys were not tested in the turbine facility as turbine blades.

TZC molybdenum alloy turbine blades were prepared and installed in the turbine along with previously prepared TZM blades. Because of a complete lack of ductility at room temperature in the heat of TZC available for this purpose, extensive testing was accomplished to certify the TZC for use in the turbine facility. Tensile testing above room temperature indicated the alloy had acceptable ductility of 8-10 percent elongation above 250°F; preheating the turbine to 600°F assured that this material would have ample ductility during turbine start-up and operation. TZC tensile bars, which were suspended in the potassium vapor stream during 1746 hours of the turbine endurance test, indicated some additional loss of low temperature ductility; but adequate ductility was available above 250°F.

Corrosion (pp 32 to 44) Metal loss from turbine blades and other components took various forms during different periods of turbine operation. A gross loss of metal occurred during the 35-hour initial turbine checkout period when potassium condensate was deliberately sprayed into the turbine; these losses occurred on the convex leading edges of the first stage U-700 blades, the leading side of the bucket dovetail and bucket locking strips, the rear surfaces of the first stage nozzle partitions and the first stage turbine tip shroud. A lesser degree of metal loss occurred on the second stage components. When the liquid potassium spray and suspected droplet carry-over from the boiler were eliminated, or were greatly reduced, as occurred during the 68-hour period of performance testing, no serious metal loss was observed. In the final 2000-hour endurance test, highly localized metal losses were observed at aerodynamically controlled locations principally along the concave leading edge and convex trailing edge surfaces of the blades. The corrosion appeared to be only slightly more severe in the first stage U-700 blades. The molybdenum alloy blades in the second stage were slightly more affected than the U-700 blades, but the depth of localized corrosion was only 3-4 mils deep compared to 2-3 mils in U-700. Metal loss in all instances was believed to be the result of solution corrosion; no evidence of mechanical impact erosion damage was noted in the turbine components.

Erosion (pp 45 to 49) A major purpose of the 2000-hour endurance test was the evaluation of the effect of impacting liquid droplets on the erosion of turbine components. No evidences of such hardware erosion were observed. In order to

increase the probability of observing erosion in the 2000-hour test, erosion specimens of U-700, stress-relieved TZM, recrystallized TZM and as-received TZC were installed aft of the second stage where they would be impacted by liquid droplets leaving the second stage blades. While some liquid metal corrosion was observed in the refractory metal specimens, only in the U-700 insert did metal loss occur which gave indications of impact erosion damage. A cluster of deep holes about 2-3 mils in diameter and 7-10 mils deep were located on this insert at the expected point of droplet impact. Micro-cracks, indicative of mechanical damage, were observed in these holes.

Metal Transfer (pp 49 to 53) Limited amounts of metal transfer were observed in the turbine facility and on turbine components on various occasions. Metal deposits up to 30 mils thick were found downstream of the converging-diverging nozzle after the nozzle test and were believed to be due to the expansion and drying out of liquid droplets containing dissolved metal. During the modification of the boiler, dust-like metal particles were found in the upper boiler header; these deposits were believed to have formed when liquid potassium droplets, saturated with metal solute from the boiler, were evaporated to dryness in the upper header. Metal foil deposits from 5-10 mils in thickness and of a porous nature formed in a highly localized area on the 8-inch vapor line downstream of the partly closed throttling valve during the performance tests; this foil became disengaged from the wall and went through the turbine. These disengaged metallic foil deposits were found on one of the contamination ring specimen probes, on the leading edge of the first stage nozzle partitions, and impacted on the leading edge convex airfoil surfaces of the first stage blades, and, to a lesser extent, on the second stage blades. A uniform 0.5-mil film of metal deposit on the first stage blades and a 0.2-mil film on the second stage blades also occurred during performance testing as the probable result of some liquid metal carry-over from the boiler. Changes in boiler operating conditions apparently minimized the formation of such films during endurance testing; however, a metal film was found on the forward surface of the first stage wheel and on the first stage blades. On the wheel, the film was 2 mils thick at the hub and less than 1-mil thick at the rim. The metal film on the blade airfoils was 0.1-mil to 0.5-mil in thickness. Except for

those deposits noted during the endurance test, which contained cobalt (probably from the first stage L-605 nozzle partitions or H-33 braze alloy), all the deposits contained constituents indicating they had come from the boiler as solute in liquid metal droplets.

Analysis of Potassium (pp 54 to 67) During the development and testing of the turbine, the potassium was analyzed periodically for oxygen, carbon and metallic impurities. The impurity concentrations remained low except when malfunctions or repair procedures resulted in contamination of the interior of the loop. The combined purification processes of hot trapping in both the boiler and condenser and of vaporization in the boiler resulted in the rapid removal of impurities during startup and the maintenance of extremely high purity during testing with respect to oxygen and metallic impurities. Oxygen was usually present as only 5-12 ppm. The carbon content was probably maintained at very low levels also, but the analytical results for carbon showed a considerable amount of unexpected scatter - a problem which was not resolved.

In summary, the turbine performed most satisfactorily during performance and endurance tests. While some metal loss and mass transfer occurred, solution corrosion rather than impact erosion was responsible; the effects were not of sufficient magnitude to jeopardize the performance or functional operation of the turbine either during these tests or as a consideration for continued testing.

II. INTRODUCTION

Much of the materials work in support of the two stage potassium test turbine was previously reported in GE63FPD238¹; that report covered selection and technical justification of materials, the preparation of materials and process specifications, drawing review, initial fabrication development and manufacturing, and the evaluation of specific materials and process problems which could be foreseen.

This report covers the materials and process work associated with the final fabrication of the turbine as it evolved during the course of the turbine test program. It covers the period from May 8, 1963 to February 8, 1966 and includes both turbine performance testing and a 2000-hour turbine endurance test; it concerns itself principally with the evaluation of selected components of refractory and conventional alloys for resistance to turbine erosion, corrosion and mass transfer effects.

While the basic design approach and initial materials selections proved highly reliable in most respects, the evolutionary nature of the turbine development resulted in the identification of various operational problems; it was necessary to conduct various items of experimental, fabrication or evaluation work to resolve these problems and to identify improvements in design, materials, processes or analytical methods. As a result of this optimization of materials and design, the final performance test and the 2000-hour endurance test were conducted in a routine and reliable manner with a minimum of interruptions and no catastrophic hardware failure or damage.

III. SIGNIFICANT TURBINE EVENTS RELATED TO MATERIALS SUPPORT

An understanding of the contributions of the materials support effort to the successful development and operation of the two stage potassium vapor turbine requires a brief description of the turbine itself and a chronological outline of some of the more significant events which occurred during the project.

A. Turbine Description

The turbine, shown in Figure 1 in its original configuration, was designed to operate at 1600°F potassium vapor inlet temperature on 92% quality vapor and to deliver 260 horsepower at 19,200 rpm. The turbine diameter was about 9 inches. The two stage Astroloy turbine wheel and U-700 bucket assembly were overhung from an A-286 shaft which was supported by oil lubricated bearings within a Type 316 stainless steel bearing housing. The forward, pivoted-pad bearing took the larger part of the radial load and the rear, ball bearing took the thrust loads. The oil lubricated bearings were separated from the potassium vapor in the turbine by means of a rotating cup, liquid potassium hydrodynamic seal; argon gas was introduced between two rotating, multiple-toothed labyrinth seals and the flow of argon through these seals toward the oil, in one case, and toward the potassium, in the other case, prevented mixing of oil and potassium. An additional seal at the forward end of the pad-bearing sleeve prevented leakage and mixing of oil and potassium along the shaft. An "X" type seal was compressed between the U-700 tie bolt (which fastened the wheels to the shaft through a series of curvic couplings) and the forward I.D. of the shaft; this prevented leakage of potassium along the I.D. of the shaft.

Oil, argon and liquid potassium, for the operation of bearings and seals within the bearing housing, were supplied by means of Type 316 stainless steel tubes; these entered behind the mid-flange of the housing, passed along the outside of the housing and entered the forward portion of the housing at the appropriate places. A Type 316 stainless steel sheet metal can was welded to the forward and mid-flanges of the bearing housing to protect these tubes from contact with potassium vapor which might enter between the bearing housing and the turbine exhaust scroll.

The bearing housing was cantilever supported by means of a joint at its mid-

flange with the aft-flange of the turbine exhaust scroll; this joint also was responsible for prevention of potassium leakage to the atmosphere.

The Type 316 stainless steel stator casing was installed as split halves and required both axial joints between the two halves and circumferential joints both to the bullet-nose inlet duct in front and to the exhaust scroll in back.

To illustrate the changes in the design of the turbine and its use of materials and fabrication processes, the turbine configuration is shown in its final form in Figure 2. The more significant changes were as follows:

1. Welded turbine flanges replaced the "O"-ring flange seals.
2. A copper plated chevron seal and a Viton "A" "O"-ring were used to replace a metal "O"-ring shaft seal and prevent leakage of oil along the shaft.
3. The pad bearing was moved aft to provide room for a stainless steel oil screw seal with weld-inlaid silver alloy surfaces to restrict the forward flow of oil from the bearing.
4. The lead-indium alloy on the silver plated pad bearing surfaces was eliminated.
5. The pad bearing was provided with direct oil lubrication to each pad which permitted the elimination of an "O"-ring seal between the bearing housing and the bearing support ring. Oil leakage toward the labyrinth seals was minimized.
6. A spider type support was provided to maintain concentricity between the bearing housing and the bearing support ring during differential expansion of these components. This minimized the possibility of seal rubbing and permitted closer seal clearances.
7. The nickel plated labyrinth seals were replaced with copper with better rub characteristics and adequate potassium corrosion resistance.
8. The Type 316 stainless steel service tubes supplying argon, oil and potassium to the bearing housing were replaced with heavier walled tubing and the joining method was changed from the H-33 braze to TIG welding because of, (1) the development of numerous cracks and leaks and, (2) the difficulty of their repair.
9. Various changes were made in the location and number of bearing housing tubing supply lines for argon, oil and potassium to improve pressure relationships around the buffer seal.

10. The method of joining the hydrodynamic seal assembly to the bearing housing was changed from a bolted assembly to a welded assembly method to eliminate the possibility of slinger seal potassium escaping to the loop.

11. A more flexible sheet metal cover for the bearing housing tube cavity was utilized to reduce the possibility of weld cracking and of leakage of potassium vapor into the tube cavity.

B. Summary of Events

During mechanical tests on the turbine, while the turbine facility was being used for potassium vapor nozzle testing, it was determined that modifications in the bearing housing tube assembly were required to utilize heavier wall tubing and weld joining. The necessity of complete weld assembly of the turbine into the facility was apparent when a failure occurred in the "O"-ring/welded can method of installing the C.D. nozzle in the test facility. Weld flanges were added to the turbine components and the turbine was installed in the facility for its preliminary checkout on April 13, 1964.

Minor, but significant leakage of oil from the lubrication system into the hydrodynamic seal potassium system occurred during checkout of the hydrodynamic seal using potassium liquid; this required minor modifications in shaft seal materials and design features. The turbine was operated on potassium vapor for four hours for the first time on July 13, 1964; this period of operation identified speed control problems and the need for all-welded construction in the hydrodynamic seal assembly operations to prevent liquid metal loss to the main loop.

Additional improvements were made in the bearing housing and hydrodynamic seal assembly and the turbine was again operated on potassium vapor for 35 hours in October 1964 with major emphasis devoted to operational techniques necessary to control turbine speed during preliminary performance tests. A failure in the boiler system on October 13, 1964 provided the opportunity for significant revisions in the turbine facility designed to provide a higher quality, a more stable supply of potassium vapor and more stable turbine speed control. Examination of the turbine at this point indicated significant liquid metal corrosion in the blades, which was caused by spray nozzle injection of liquid metal upstream of the turbine.

When boiler repairs were completed and the turbine was rebuilt in March 1965, the turbine operated successfully with good speed control during two periods of turbine performance testing of 12 hours and 56 hours each in March and April. During these tests, refractory alloy specimens were installed in the facility to evaluate environmental effects on alloy contamination. Some mass transfer of metal foil deposits was noted at this time and a thin uniform metallic film of metal was found to have been deposited on the turbine blades.

During the early summer of 1965 a decision was made to incorporate TZC and possibly Cb-132M refractory alloy blades along with TZM blades in the 2000-hour endurance test. These blades were fabricated and the TZC material was qualified for use under limited test conditions to avoid its adverse low temperature ductility characteristics.

The 2000-hour endurance test was successfully completed on December 20, 1965; for purposes of metallurgical evaluation, it provided, in addition to conventional turbine components, 12 erosion inserts of various materials located aft of the second stage, 4 each molybdenum blades of the TZM and TZC alloy compositions, three sets of refractory metal probe insert specimens each comprised of duplicate rings of TZM, TZC and F-48, and 4 TZM tensile test bars.

During turbine testing, various turbine temperatures and turbine speeds were experienced as a part of the test program. While the complete schedule of test conditions is covered in the other turbine topical reports, the following was representative of the level of operating conditions of interest from a materials viewpoint:

<u>Type of Test</u>	<u>First Stage Inlet °F</u>	<u>Second Stage Inlet °F</u>	<u>Speed RPM</u>
Checkout	1450	1350	15,400-20,000
Performance	1450-1550	1350-1450	15,400-20,000
Endurance	1500	1400	18,250

IV. NON-REFRACTORY MATERIALS EVALUATION

The non-refractory materials in the turbine components performed, during the 2000-hour endurance test, in a highly satisfactory manner indicating the basic conservatism in the original design and the adequacy of the properties of the materials selected. During initial operation and performance testing of the turbine, minor design and materials changes were made to improve operational reliability or to resolve problems encountered in controlling the supply of lubricating oil, argon and hydrodynamic seal potassium. The details of these improvements are covered more completely in a topical report on mechanical design and have been listed only briefly in this report under Turbine Description(III-A).

Much of the materials technology used in this work is based upon past experience in the field of aircraft gas turbines. Materials technology differs in the potassium turbine from that of gas turbines in the following ways: Longer test periods and design life are expected; turbine wheels are uncooled at their hubs (except for some conduction cooling to the bearing lubricant); liquid metal corrosion resistance rather than oxidation resistance is required; turbine wheel assembly is dependent upon the tie bolt's resistance to stress relaxation; and an extensive, leak-tight system of running seals and of liquid and gas supply lines is required.

The following summarizes some of the more significant aspects of the successful use of the non-refractory alloys, but excludes, for later discussion, matters pertaining to liquid metal corrosion, impact erosion and metal transfer.

A. Rotating Parts

The rotating components, for the purpose of materials evaluation, included (1) the hydrodynamic seal, (2) the turbine wheels, blades and locking strips, and (3) the shaft and tie bolt.

Hydrodynamic Seal - The hydrodynamic seal, composed of a Type 316 stainless steel stationary seal and an A-286 alloy rotating cup, operated successfully at the 800°F operating temperature with no apparent deterioration from the constant flow of liquid potassium passing through the seal at approximately 2 gpm. On opening the rotating cup after 2000 hours of endurance testing, the interior surfaces had been darkened in color, but a close examination disclosed no indication of erosion

or corrosion. A granular, magnetic deposit was removed from the bottom of the cup; when analyzed by qualitative spectrographic analysis this deposit was found to contain chromium, iron, and nickel as major elements (greater than 10% by weight) and titanium as a minor element (less than 10% by weight). This deposit appeared to have been centrifuged from the potassium rather than having been uniformly deposited from solution. The quantity of the deposit was inconsequential and its presence is reported here as a matter of record.

Turbine Wheels - The Astroloy (U-700)* turbine wheels and U-700 blades did not experience creep during either the performance testing or during the 2000-hour endurance test as determined by post-test dimensional analysis. Inspection of wheels after each test did not disclose any corrosion of the wheels, and only during the 2000-hour endurance test did any significant amount of metal transfer occur to deposit metallic elements onto the wheel surfaces. The operating temperature of the first stage wheel rim and buckets was calculated to be approximately 50°F above the 1400°F aging temperature of the alloy, whereas the second stage wheel, rim and blade operating temperature was always below the aging temperature of the alloy. Accordingly, the first stage wheel would be expected to show the effects of over-aging produced by 2000 hours operation above the appropriate aging temperature, both in mechanical property variations and in microstructure; the second stage U-700 wheel properties and structures accordingly would not be expected to deviate measurably from those of the fully heat treated U-700 material. No destructive tests were performed on these wheels since they were intended to be used for an additional 3000 hour turbine endurance test.

Turbine Blades - In order to determine the effects of the 2000-hour endurance test on the blade material, miniature tensile test bars were machined from both first stage and second stage U-700 blades, and from a fully heat treated

* Note: Although the wheels were designated as Astroloy wheels, the very close similarity of this alloy with U-700 permits its subsequent designation as U-700 for purposes of simplification.

U-700 turbine blade blank; three tensile tests of each were performed at room temperature. One of these tensile bars is shown with a second stage blade for comparison in Figure 3. The results, which are shown in Table I, indicate only minor changes in strength but a decided reduction in ductility (from 19% elongation to 12% elongation).

The changes in mechanical properties indicated that the microstructure of U-700 underwent some change over extended periods of time at turbine operating temperatures. A study of the electron photomicrographs, presented in Figures 4 and 5 for a first stage blade before and after the 2000-hour endurance test, disclosed coalescence of the gamma prime precipitate within the grains and the coalescence of the $M_{23}C_6$ intergranular carbides. Accicular structures, indicative of sigma phase (as noted by the characteristic 60° orientation angle between needles), were observed in the dovetail structure of a first stage blade after the 2000-hour endurance test. These structures can be seen in the photomicrographs presented in Figures 6 and 7. The presence of sigma phase in the structure could also have contributed toward the decrease in the turbine blade ductility.

Locking Strips - During the original selection of Rene' 41 as the turbine blade locking strip material¹, 0.020-inch and 0.032-inch thick strips were bent in the aged condition (1400°F-16 hours) over a 0.060-inch radius. Sufficient ductility was available in this heat treated condition to develop crack-free bends in the 0.020-inch thick sheet, but the ductility was marginal in the thicker section and some cracking tendency was observed. The 0.020-inch sheet was used to fabricate locking strips for the first turbine operation; these strips were aged before installation in the turbine and operated successfully without cracking. However, the gross corrosion experienced on these locking strips in preliminary turbine testing required that, (1) the thicker lock strips be used in the solution treated condition where bend ductility was good and, (2) the locking strips be permitted to age during turbine operation.

Following performance testing the forward ends of some of these locking strips had failed by strain age cracking in the machine-bent radius. These cracks are shown in photomicrographs in Figures 8 and 9. High magnification examination

disclosed aging precipitation along strain lines associated with the observed cracks; it was concluded that the bend radius had been too small in those cases where strain age cracking occurred. In subsequent turbine wheel assemblies, a more generous radius was provided in the forward machine-made bend and the formed strips were solution annealed prior to their installation.

Because the Rene' 41 alloy ductility was marginal when bent in the aged condition, the practice of allowing aging to occur during operation was not changed. The locking strips performed thereafter without a single failure. Figure 10 shows the tensile properties of aged and solution treated Rene' 41 alloy; it indicates that the Rene' 41 alloy has sufficient strength to be used in the solution treated condition, and that aging in place during turbine operation is a satisfactory procedure.

Diffusion Bonding - The possibility of diffusion bonding was anticipated between the wheels and the shaft at the curvic couplings because of the high temperature of operation and the local contact pressure produced by the tie bolt tensile stresses. Apparently, either the surface oxides of the U-700 alloy wheels and the A-286 shaft were retained at the close fitting interfaces of the curvic coupling, or the temperature-load-time conditions were not sufficient for diffusion to occur; disassembly of these components was never difficult. Furthermore, diffusion bonding did not occur between the blades and the wheels, probably because of blade vibration, in addition to the previous suggestions. Some of the 2000-hour endurance test blades were more difficult to remove than those of other tests; but, the difficulty of their removal could be attributed to the presence of mass transport material deposited along the dovetail surfaces.

Tie Bolt - Stress relaxation did not occur in the U-700 alloy tie bolt during any of the turbine tests. During assembly, the tie bolt was pre-stressed, within the elastic limit, with a pre-determined load which resulted in an extension of 0.016-inch. After each test, the tie bolt was again stressed with the same load and the locking-nut torque was measured. Since this torque and the free length of the tie bolt were identical before and after test, it was concluded that stress relaxation did not occur.

Turbine Shaft - No evidence of deterioration of the shaft could be found following any of the tests.

B. Non-Rotating Parts

"O"-Ring Seals - The need for reliable, leak-tight flange joints in the turbine components and in the test facility was demonstrated during the convergent-divergent nozzle tests when a leak developed in the bolted, metal "O"-ring sealed joints. Investigations into the cause of leakage proved that the nickel electroplate on the metal "O"-rings was hard, as deposited, and that this electroplate cracked when the "O"-ring was compressed between the flanges, allowing potassium to leak across the seal. Tests were performed with experimental "O"-rings and flanges to determine a suitable metal sealing ring combination for these large flanges, but no acceptable solution could be found.

Welded Flange Sealing - Because of these leaks in mechanically sealed joints, the bolted "O"-ring flanges, intended for potassium retention and for ease of turbine assembly, were replaced with re-weldable flanges which have since proved completely satisfactory. It was necessary to alter the existing turbine hardware to replace the "O"-ring flanges with re-weldable flanges; the possibility was considered that weld-induced distortion of finished parts, occasioned by the addition of the weld flanges or by weld assembly of components, might alter turbine blade tip clearances and other critical internal dimensions. To determine the possible extent of weld distortion and to develop weld assembly procedures which would minimize distortion, dummy turbine components were prepared, a welding procedure was devised, and the welding was performed; various diameter measurements were taken periodically to record the distortion of the turbine casing and other components. As a result of the data from this dummy assembly, the turbine components were weld assembled with insignificant distortion and the required internal component clearances were assured. This same procedure was applied to subsequent turbine weld assemblies with the same success.

Bearing Housing Welds - The installation of stainless steel tubing in the bearing housing was originally performed using a high temperature cobalt-

base braze (H-33). See Table XV for analysis. After the operation of the turbine on steam for flow testing and efficiency measurements, these tubes were removed and replaced by new, heavier wall tubing installed by weld assembly methods. Welding was used since operation of the C.D. nozzle with braze assembled instrumentation tubing had indicated the difficulties of repairing leaks, or the possibility of fatigue failures in such thin-walled brazed assemblies. The corrosion resistance of the H-33 braze proved satisfactory, as indicated by the successful operation of the brazed nozzle partitions.

Following the first brief period of turbine operation on potassium vapor on July 13, 1964, the bolted-on hydrodynamic seal was found to leak at its outer metal "O"-ring seal. Potassium, supplied to the seal, leaked along the interface between the bearing housing and the hydrodynamic seal. In order to provide a positive, weld-tight potassium supply system to the seal, electron beam welding techniques were developed to attach a small diameter potassium supply tube to the aft face of the hydrodynamic seal. When the seal was installed at the front of the bearing housing, this supply tube extended aft, through the front bearing housing flange, where it could later be weld assembled to its potassium supply line. A circumferential TIG weld was used to join the seal to the bearing housing and to prevent loss of overflow potassium and argon from the seal to the main loop. This innovation is described more fully in the topical report on mechanical design.

Buffer Seals - After preliminary operation on potassium vapor, a labyrinth seal rub was noted in which the labyrinth teeth were damaged equally as severely as the nickel electroplate of the seal face. A series of rub test experiments were performed on several alternate materials to identify a better seal face material. Copper was ultimately selected as a replacement for nickel when it was found that copper, in addition to resisting attack from potassium at the hydrodynamic seal temperature of 800°F, would plastically deform to accommodate the labyrinth teeth during a rub. Copper was subsequently applied to the bearing housing seal surfaces by electroplating. The superiority of the copper was demonstrated when, during one rub, the sealing ability of the labyrinth was improved; in other instances when rubs occurred, the copper deformed ductily and the sealing ability of the labyrinth was not impaired.

Plating turned out to be highly unpredictable for these thick deposits and very dependent upon (1) surface preparation, (2) the plating operation setup and (3) the experience of personnel. Three attempts were required before acceptable copper buffer seals were obtained for the 2000-hour endurance test; however, after 600 hours of operation the copper electroplate separated from the base metal, a fact which was deduced by minor changes in the seal characteristics. Despite this separation at the electroplated interface the seal still worked satisfactorily.

Screw Seals - After the first period of turbine operation, which was necessary to check out the turbine seal systems, minor oil leakage into the potassium hydrodynamic seal system required the addition of a shaft screw seal immediately forward of the main pad bearing. An aluminum bronze material (85 Cu - 11 Al - 3.7 Fe - 0.3 Mn) was used for this seal; later operation of the turbine on potassium vapor resulted in bearing run-out which caused damage to this screw seal and demonstrated its chip-forming tendencies. At this point, the bronze screw seal was replaced by a stainless steel component with a ductile, copper-silver alloy puddle-welded in place to later form the screw seal surfaces. This alloy Handy and Harmon No. 655 (65% Ag - 28% Cu - 2% Ni - 5% Mn), has demonstrated very good ductility under rubbing conditions.

Exhaust Scroll - Stresses from thermal shock and differential thermal expansion did not present complications in any of the components, except in the exhaust scroll. During manufacturing assembly of the scroll, the struts were first welded in place and then a braze fillet was formed between sheet and scroll by back brazing. After the first high temperature turbine operation, cracks were apparent in the braze fillets around the leading edges of the struts. These cracks increased in length during each subsequent high temperature operation; however, there was no evidence of weld cracking, and no evidence of loss of structural integrity since the welds bore the load in these joints. Though a few of these cracks eventually penetrated completely through the brazed and welded joint, potassium leakage was of no concern since the struts connected only internal members which directed the flow of the exhaust vapors and did not form a leakage path to the atmosphere.

V. REFRACTORY ALLOY MATERIALS EVALUATION

The use of refractory alloy turbine blades in the 3000 K.W. Type 316 stainless steel facility was intended to demonstrate the utility of such molybdenum base alloys as TZM and TZC and of such columbium alloys as AS-30, F-48 and Cb-132M. It was also intended to evaluate the nature of potential problems which might occur as the result of erosion, corrosion and/or metal transport during turbine operation. At the operating temperatures within the 3000 K.W. loop, the turbine bucket temperatures in the 2nd stage were about 1240-1300°F; this temperature is well below that for typical refractory alloy material applications and well within the temperature range where elastic, rather than plastic properties are the controlling factor. Material strength is not usually the limiting consideration for high strength refractory alloys at these temperatures. On the other hand, the possibility of low ductility at room temperature and the contamination of these alloys with interstitial elements in a non-refractory alloy system must both be considered. Furthermore, corrosion and erosion of refractory alloys may very well be influenced by the presence of contaminants in the system. When the refractory alloys make up only a negligible portion of the total system weight, these adverse contamination effects may assume more significance than would be the case in an all refractory alloy system even at the same apparent levels of liquid metal impurity.

The following describes the mechanical property testing done to assure mechanical reliability in refractory alloy blades and to measure the contamination of refractory alloys in the 3000 K.W. system under actual operating conditions.

A. Blade Material Properties

Blade Material Selections - For the turbine endurance run, refractory alloy turbine blades of AS-30, F-48 and TZM were originally prepared and their mechanical properties and microstructure were thoroughly documented in GE63FPD238¹. These evaluations included; (1) room temperature and elevated temperature tensile strengths and ductility properties, (2) room temperature and 1400°F tensile property effects of 1000-hour aging in vacuum at 1400°F and of 1000-

hour exposure to liquid potassium and, (3) elevated temperature stress-rupture characteristics. Their room temperature and 1400°F tensile properties are summarized again in Table II for comparison with TZC and Cb-132M. NASA's desire to operate the turbine with TZC molybdenum alloy blades and Cb-132M columbium alloy blades required that some limited confirmation testing of these materials be accomplished in order to assure the safety and mechanical integrity of the turbine. Sufficient material was originally available for only duplicate tensile tests at room temperature and 1400°F to examine the low temperature ductility and high temperature, short-time strength properties.

Materials Processing History - Initially, NASA delivered to G. E. one piece of Cb-132M sufficient to make 5 blades and 3 tensile bars and one piece of TZC sufficient to make 2 blades and 4 tensile specimens. Some time later a second piece of Cb-132M, from the same heat and processing history as the first, was provided by NASA; additional TZC material identical with the first was also procured. A portion of these additional materials was immediately supplied to the bucket manufacturer to insure the delivery of at least 4 turbine blades of each material.

The layout diagrams of these pieces following ultrasonic inspection and showing the rolling and extrusion directions are indicated in Figures 11 and 12; their composition, interstitial element analysis and processing history, where available, are given in Tables III and IV. Both materials were extruded and cross rolled. Since the TZC was rolled at 1700°C (3092°F), no further heat treatment was given to it; a complete recrystallization of the TZC alloy at 3250°F, according to Chang's² data, would have reduced the 1400°F yield strength to 24,000 psi, well below the bucket dovetail stresses which were estimated in the range of 50,000 psi. The Cb-132M alloy, which was reputed to have been rolled at 2400°F, was given a one-hour stress relief at 2200°F in a vacuum of 1×10^{-5} torr. Photomicrographs taken of the TZC showed it to be fibrous in both the rolling and extrusion directions as shown in Figures 13 and 14. The Cb-132M had large equiaxed grains and showed evidence of a grain boundary precipitate as seen in Figures 15 and 16.

Specimen Preparation - The turbine blade and tensile specimen blanks were cut from the plate stock using a water-cooled silicon carbide cut-off wheel. Surface cracks, which penetrated to depths of 0.0005 to 0.020-inch, were noted along the cut edges of the Cb-132M blanks. All edges were checked by Zyglo inspection for cracks and stress-free grinding was used to remove these defects. All blade blanks were freed of surface cracks by this method, as indicated by final Zyglo inspection. Cracks in the gauge length portion of the Cb-132M tensile blanks were removed during stress-free grinding of these finished specimens; however, all the cracks were not removed from the larger, outer diameter of the button-head ends of the tensile specimens.

Tensile Testing - Both the TZC and the Cb-132M specimens, prepared as indicated above, failed in a brittle fashion when tested at room temperatures in an Instron Tensile Test Machine at a cross-head speed of 0.05 inch/inch/minute. In addition, a Cb-132M tensile specimen was stress relieved and heat treated at 2600°F for 1 hour in a 10^{-5} torr vacuum, pickled in 20 HF - 20 HNO₃ - 60 H₂O to remove 0.001-inch of the surface, and then tested at a slower strain rate of 0.005 inch/inch/minute cross-head speed; this specimen also failed in a brittle manner. The large grain size and the poor room temperature ductility of the Cb-132M indicates that the reported processing history may have been incorrect and that the material may have received a recrystallization treatment which developed the large equiaxed grains from hot cold-worked material. Because of its apparent poor properties and of the contamination being experienced with columbium base alloys operated within the potassium vapor turbine facility, as discussed under VI B, Refractory Alloy Contamination, Cb-132M was no longer considered as a turbine blade material for evaluation in the present facility.

The poor room temperature ductility of the TZC alloy was thought to be the result of carbon remaining in solution; the high temperatures at which the alloy was worked may not have resulted in strain energy necessary to precipitate dissolved carbon as TiC. In contrast, a TZC alloy prepared by Prater³ and worked at lower temperatures exhibited good ductility and strength at room temperature; see Table V.

* The effects of heat treatment on the strengths of molybdenum base alloys have been covered quite extensively by Chang² and by Chang and Perlmuter⁴; the sluggishness of TiC aging reactions in the absence of a highly strained structure suggested that a limited possibility for improving ductility might exist by long time aging at temperatures near 2750°F. As shown in Table V, TZC tensile specimens #3 and #4 were aged for 35 hours at 2750°F in vacuum, pickled to remove up to one mil of surface layer and tested at room temperature and at 1400°F; a crosshead speed of 0.005 inch/inch/minute was used up to 0.6% elongation and was then increased to 0.05 inch/inch/minute to failure. Test results indicate some improved room temperature ductility and very adequate hot ductility; significantly lower room temperature ductility and yield strength were obtained than have been previously demonstrated for TZC alloy. The lower yield and ultimate strength at 1400°F suggested that the alloy would be very marginal in this condition for meeting the bucket dovetail stress requirements of 56,200 psi at 23,000 rpm (the top turbine design speed) even if the 7 percent elongation and 10 percent reduction in area at room temperature were considered acceptable. The fact that the room temperature specimen failed in a brittle manner, away from the minimum area where the reduction in area was only 3.5 percent, attests to its still brittle nature. It was concluded that attainment of room temperature ductility in this particular heat of TZC was unlikely without serious losses in 1400°F strength and no further heat treatment studies were made. Instead, the transition temperature from ductile-to-brittle tensile failure was determined in the pickled, and unpickled condition. Since the minimum tensile ductility of 8% was achieved at 150°F, the TZC alloy was used in the as-received condition for this turbine blade application, relying on the preheat of the turbine to attain ductility in the blade dovetails.

TZC Creep Testing - A creep test of TZC at 1400°F and 50,000 psi stress reached 73 hours without deformation. A second creep test specimen was loaded to 55,000 psi at 1400°F for 150 hours then step loaded to 60,000 psi, again without deformation. Since the high temperature yield strength of approximately 58,000 psi for TZC is substantially greater than the TZC blade dovetail stresses of 35,400 psi at 18,250 rpm, the turbine rotational speed during the 2000-hour endurance test, and the material is obviously not creep limited at this temperature;

this heat of TZC had adequate hot strength even though it developed only about 70-90% of its true strength capabilities at room temperature. A turbine speed of about 23,000 rpm would be required to initiate yielding of the blade dovetails assuming the yield strength at the bucket operating temperature of 1260°F is not significantly increased over its 1400°F tested value. Nevertheless, the TZC strengths were significantly less than those of TZM; at 1400°F the TZM had a yield strength of 81,000 psi compared to only 58,000 for this particular lot of TZC alloy.

TZC Transverse and Aged Tensile Properties - The transverse tensile properties of TZC and its tensile properties after aging 1000 hours in vacuum at 1400°F were also determined. For the 1000 hour ageing treatment, the TZC tensile specimens were wrapped in several layers of tantalum foil and sealed under a vacuum of 10^{-5} torr in a Type 316 stainless steel capsule; the capsule was heated to 1400°F in an electric furnace in an air atmosphere and held for 1000 hours. The results of tensile tests, which were run at room temperature and at 1400°F, are shown in Table VI for transverse, and for aged specimens.

The transverse properties at low temperature gave some limited evidence of slightly reduced strengths and lowered ductility. The 1400°F properties were roughly equivalent to those in the longitudinal direction. No serious deterioration of properties was noted in the aged TZC specimens. Although the ductility of the aged specimen at 150°F appears to have been reduced, the ductility is very good at 250°F; a possible slight increase in transition temperature might be implied but was not considered significant in relation to turbine operating conditions.

The above testing and evaluation of the TZC alloy offered sufficiently satisfactory results to assure the successful operation of this particular heat of TZC alloy as turbine blade materials in the two-stage potassium turbine.

B. Refractory Alloy Contamination

Refractory Alloy Probes - In preparation for the operation of refractory alloy turbine blades in the endurance test of the turbine, selected refractory

alloy specimens were inserted in the potassium vapor upstream of the turbine for the purpose of determining any possible contamination effects. A Type 316 stainless steel probe, shown in Figure 17, was designed to support 6 refractory alloy specimens each 1/2" O.D. x 1/4" I.D. x 3/8" high. A perforated stainless steel sleeve was installed over the refractory alloy rings to prevent any gross particles from entering the turbine should significant deterioration of the specimens occur in the turbine facility environment. A thermocouple was installed within the stainless steel probe at a point adjacent to the first refractory alloy ring; during operation in the test facility, the temperature indicated by this thermocouple was within 10°F of the potassium vapor temperature.

During the 12- and 56-hour turbine performance tests of March and May, 1965, refractory alloy duplicate specimens of F-48, AS-30, and TZM were installed on a probe located upstream of the turbine at Station One. During the turbine endurance testing which began in September 1965, two additional probes were installed without protective screens in the condenser; in these tests the three probes each contained duplicate specimens of TZC, TZM and F-48 alloys.

After 12 hours of performance testing above 1400°F the single probe at Station One, containing specimens of F-48, AS-30 and TZM was removed, the specimens were weighed and one specimen of each composition was replaced with a new specimen of similar composition. The test was continued for an additional 56 hours at temperatures above 1400°F; following this, all of the F-48, AS-30 and TZM specimens were removed for evaluation.

After 254 hours of the endurance testing, one complete probe with all of its F-48, TZM and TZC specimens was removed from the condenser and replaced with a caged probe containing four TZC tensile bars; on the probe upstream of the turbine (Station One), one ring specimen of each of these alloy compositions was removed and replaced with a fresh specimen; one additional probe in the condenser was not disturbed. After the 2000-hour endurance test these specimens were evaluated.

After removal from their probes, the specimens were cleaned in hexane and alcohol; they were evaluated by means of weight change, metallography, and C, N, O and H analyses at the surface and core of each specimen. Specimen weights were determined to 0.0001 gram with an accuracy better than ± 0.0005 gram using an Ainsworth Type SC balance. Surface specimens were prepared by machining away all but 0.030-inch of the surface; core specimens were prepared by removing 0.030-inch from the I.D., O.D. and ends. The results of these evaluations are discussed below.

Performance Test Refractory Alloy Contamination Results - The weight change and chemical analyses data from the refractory alloy rings exposed in the potassium test facility at Station One during the performance tests are shown in Table VII. The weight changes in the TZM alloy specimens were generally insignificant in comparison to those for the columbium base alloys.

With the exception of one unexpectedly high carbon analysis, the data on refractory alloy specimens from the performance run test indicated that the TZM alloy was quite stable in the turbine environment, whereas the columbium alloys gettered appreciable amounts of carbon, oxygen and nitrogen. Surprisingly, the F-48 specimen, which experienced only the turbine loop operating conditions in May, appeared to be generally more contaminated than the specimen which experienced both the March and May, 1965 turbine loop operating conditions. These unexpected results may have been due to a protective metallic foil deposit which was draped over the perforated sleeve covering the first 3 specimens in the probe tested in May.

Metallographic examination of the surface of the refractory alloy probe specimens revealed subtle indications of contamination of the F-48 alloy in the form of a new phase which is apparently non-metallic in nature. It could be seen in the as-polished conditions and became more apparent when etched with 60% Glycerine - 20% Hf - 20% HNO_3 etchant. The phase is best defined by an electrolytic anodizing treatment, as is shown in Figures 18 and 19. The pale yellow color of the phase is similar to that observed by Harrison and Delgrosso⁵ in the low pressure oxidation of Cb-1Zr and which they identified as CbO. A

complete confirmation of the nature of this phase would require extensive work in the calibration of etching techniques against known standards, which was beyond the scope of present efforts. Attempts were made to separate the phase using bromine extraction techniques, but sufficient quantities of the phase could not be accumulated for x-ray diffraction identification purposes.

Liquid droplet carry-over from the boiler, the argon gas, and outgassing of the loop components are possible sources of the contamination of the refractory alloy specimens. The unexpected high carbon content (980 ppm) of TZM Specimen No. 5 of the May test was rechecked and found to be 1210 ppm; metallographic examination and hardness traverses did not reveal a carbide layer or carburization of the subsurface.

The contamination of the columbium base alloys, particularly by oxygen and nitrogen, was sufficient to cause concern for the successful operation of F-48 or AS-30 blades in the facility during endurance testing. For example, if the weight loss of F-48 Specimen No. 1 from the March test was considered to have been lost as CbO , then the true pickup of oxygen within 0.030-inch of the original surface can be calculated to be 1086 ppm. Similarly, the large weight losses in AS-30 Specimen No. 6 may be associated with its apparent contamination during weld assembly of the stainless steel probe components in air. The AS-30 Specimen No. 1-5, which was not contaminated in welding, did not experience this large weight loss in either the first or the second run. Nevertheless, the pickup of carbon, oxygen and nitrogen in the AS-30 specimens appeared equally severe in both AS-30 specimens. Because of these high contamination rates for columbium alloys, and their possible resultant embrittlement, it was decided to utilize only molybdenum base alloys, such as TZC and TZM, in the turbine endurance tests.

Possible Sources of Contamination - The gaseous pickup and carbon contamination could conceivably come from, (1) argon gas from one or more of 3 sources, (a) the argon from the liquid argon source used to originally fill the loop, (b) the argon from the recirculating system which might occasionally escape through the hydrodynamic seal during a dip in speed (speed dips occurred during the early performance tests), and (c) the recirculating argon from the

efflux pressure instrumentation system, (2) the liquid metal drops which are carried over from the boiler and which contain dissolved gases and carbon and/or (3) outgassing from the Type 316 stainless steel in the facility itself. Calculations were made involving impurity levels in the contaminating medium, the rate of the medium's recirculation and estimated sticking factors for impurities. These calculations indicated that contamination of the columbium alloys could occur under conservative conditions from the impurities in either the argon or the liquid potassium carry-over, as well as from the outgassing of stainless steel.

Carburization Experiments - Even after the decision was made to delete the use of columbium alloy blades from the turbine and to use molybdenum alloys instead, the single instance of high carbon pickup in a TZM probe specimen caused concern; if a condition carburizing to molybdenum alloys existed in the turbine, the ductile-to-brittle transition temperature might be increased to a temperature beyond that to which the turbine could be conveniently preheated. Such a condition would have prevented the operation of the turbine for reasons of TZC blade brittleness and possible catastrophic failure. Prior to operation of the turbine, additional evaluation work on the ductility of surface carburized TZC was undertaken and is discussed below. It is also expected that more extensive evaluation of TZM probe specimens for evidences of carbon pickup in the turbine facility during the first part of the endurance test would provide additional information to confirm or deny the presence of a carburizing or embrittlement environment.

It was appropriate to determine if carburization of the TZC material could occur by contact with liquid potassium containing carbon and to determine the effect of such deliberate carburization on the low temperature ductility of TZC. For this purpose, four TZC tensile specimens were heated in liquid potassium, containing excessive amounts of carbon, for 100 hours at 1400°F; tensile tests at elevated temperature were then performed to evaluate the ductility of the carburized specimens.

A 1 1/4-inch, Schedule 80, Type 321 stainless steel capsule 7 3/4-inches

long was prepared. The four tensile specimens were assembled in a parallel array by means of stainless steel wire fastened at the heads of the tensile specimens. An amount of carbon sufficient to carburize all the molybdenum to MoC and all of the chromium in the stainless steel capsule to Cr_3C_2 was calculated as 33.5 grams. The amount of carbon was added as four, 5-inch lengths of 1/4-inch diameter spectrographic grade carbon electrodes; they were located in positions parallel to the test bars, around the inner surface of the capsule. The capsule was filled with approximately 80 cc of potassium which was sufficient to occupy 80% of the capsule volume at the test temperature. Transfer of the potassium to the capsule was done in an electron beam welding chamber modified for the filling and weld sealing of capsules in a vacuum of 10^{-5} and 10^{-6} torr⁶. Analyses taken from potassium in the transfer line to the weld chamber indicated 8, 12 and 15 ppm oxygen.

After exposure of the capsule in an air furnace at 1400°F for 100 hours, the capsule was opened in an argon atmosphere, the potassium was melted and removed, the test specimens were collected under mineral oil, and these specimens were subsequently cleaned using hexane and alcohol.

Table VIII shows the tensile test results of these TZC test specimens; they exhibited no ductility at temperatures as high as 650°F, which is the maximum reasonable temperature for turbine preheat. Ductile failure occurred at 1200°F. Figure 20 shows the presence of 0.0002-inch thick carbide film which was identified by x-ray diffraction as Mo_2C and MoC. Carbon analysis of a 0.030-inch thick section from the end of a tensile specimens indicated a carbon content of 2200-2500 ppm compared to an original vendor analysis of 1470 ppm.

This experiment suggested that, if a condition which is highly carburizing to the molybdenum alloys occurred in the turbine facility, the molybdenum alloy blades would probably remain ductile at the operating temperature, but would have very low ductility under turbine restart conditions. It also emphasized the need for a rapid evaluation of the refractory alloy probe specimens after the first shut down of the turbine during endurance testing with TZC buckets in place. Fortunately, evaluation of these probes indicated that a carburizing condition toward the molybdenum alloys did not exist in the turbine facility, as will be discussed below.

Endurance Test Refractory Alloy Contamination Results - When the turbine was shut down after 254 hours of endurance run, evaluation of the TZC, TZM and F-48 probe specimens was made. The probe at Station One, which operated at 1520°F, and one of the probes from the condenser, which operated at 1260°F, were removed and cleaned in hexane and alcohol. These two probes are shown in Figure 21. One ring specimen of each of the alloy compositions on the probe at Station One was removed and replaced with a fresh specimen. The condenser probe which was removed for specimen evaluation, was modified to contain four TZC tensile bars for subsequent exposure during potassium turbine testing.

The evaluation data for the probe materials is shown in Table IX and X and summarized in graph form in Figure 22. The F-48 alloy specimens, each weighing about 10 grams, lost about 0.0400- to 0.0700-gram at Station One and lost 0.0900- to 0.1100-gram in the condenser. In comparison, the molybdenum weight changes were very much less; they gained only 0.0002- to 0.0004-gram at Station One and lost only 0.0005- to 0.0012-gram in the condenser. The specimen weight losses in the condenser were probably greater because of the lower quality of the vapor entering the condenser (94% as compared to 99.5% at Stage 1) and the greater purity of the freshly condensed liquid potassium droplets striking the specimens; also, the specimens in the condenser were not protected by a perforated sleeve as were those at Station One.

Within the range of experimental error there were no significant indications of carbon contamination in the molybdenum alloys. The TZC specimen at Station One appeared to have decarburized somewhat. While TZC specimen II-4, located in the condenser, gave two unexpectedly high carbon analyses of 2850 and 4730 ppm, three other analyses, at 1170, 1260 and 1180 ppm, were well within the expected range, and the other TZC specimen in the condenser experienced no significant change. It is suggested that the above two high carbon analyses resulted from the retention of Zyglo inspection fluid in cracks which were formed during the mechanical testing discussed below. The TZM specimen at Station One appeared to have decarburized at the surface, but those in the condenser were not appreciably affected. The range of carbon variation in unexposed TZC specimens is indicated by values of 1760 and 1490 ppm obtained from consecutive analyses

of the same specimen. This compares well with an original vendor carbon analysis of 1470 ppm. The original vendor analyses for TZM and F-48 are also given. Because of the observed variation in carbon analyses, the comparison of any two values is not sufficient for conclusions; however, a general carburizing condition toward the molybdenum alloys did not appear to exist. In all cases the F-48 columbium base alloy increased in carbon content. A comparison between the gas analyses for columbium and molybdenum alloys confirmed past experience; the F-48 alloy was contaminated significantly in oxygen and nitrogen but there was generally little change in the molybdenum alloys. Gas analyses were not performed on the surface specimens of the TZC rings since these were diverted to flattening tests for measurement of bend ductility as described below.

The TZC ring specimens were machined along their inside diameter to produce thin walled cylinders with a wall thickness of about 0.044-inch, a nominal diameter of 1/2-inch and a length of about 3/8-inch. A section of each ring was removed to form a "C"-shaped specimen. After each ring specimen was Zygl inspected to detect the location of any cracks, the "C"-section of each ring was bent under compression loading at temperatures of 500°F or 650°F; all TZC rings taken from the turbine facility were very ductile under this type of test as indicated in Table XI. These ductility results and the absence of carbon pickup supported the decision to continue turbine endurance testing beyond 254 hours with little expectancy of carbon pickup or loss of ductility.

Carbon and gas analyses of TZC, TZM and F-48 conducted on specimens taken from the various probes at the end of the 2000-hour endurance test generally confirmed earlier observations. These data were shown in Table X. Insignificant changes in weight occurred in the molybdenum specimens. The F-48 specimens again lost a significant amount of weight and these weight losses were greater in F-48 specimens at the location downstream of the turbine than in those at the upstream location. The loss in weight in the F-48 alloy was less for the longer duration, latter portion of the 2000-hour endurance test than it was for the first 254 hours. A possible explanation could lie in the higher initial oxygen concentration within the loop at the early part of the test; once the loop and all newly installed parts in the loop were operated with potassium for the

254-hour period, the hardware surface contamination was undoubtedly reduced. Except for replacement of probe specimens, no entries were made into the loop at the 254-hour shut down.

There appeared to be some minor reduction in carbon content in the high carbon level TZC alloy, some increases in carbon level in the TZM and substantial increases in carbon in the F-48 alloy.

The oxygen and nitrogen levels increased for all refractory alloy specimens, but were greater, by far, for the F-48 alloy. The contamination levels increased significantly with time; again the increase was more noticeable for the F-48 alloy.

The non-linear rate of contamination pickup is shown by an examination of data on new specimens installed at Station One after 254 hours of the 2000-hour endurance test; oxygen and nitrogen pickup in the new F-48 sample was less than half that in a similar originally installed sample which remained on test for the full 2000 hours. This same newly installed F-48 specimen was contaminated after 1746 hours much less than was the original F-48 specimen, which was exposed for only the first 254 hours of the test. This clearly demonstrated that the contamination potential of the turbine facility toward refractory alloys decreased significantly after the first period of endurance test operation; a logical explanation appears to be that flushing with potassium during turbine startup has decontaminated exposed parts of the previously opened portions of the turbine facility and of newly installed turbine components.

Metallographic evaluation of the refractory alloy specimens after 254 hours and after 2000 hours of the turbine endurance test revealed interesting structures only in the F-48 alloy. As shown in Figures 23 and 24, the contamination of an F-48 specimen at Station One, which operated at a higher temperature, is more extensive after 254 hours than that of an F-48 specimen taken from a lower temperature location downstream of the turbine. After 2000 hours of testing, the surface contamination was much more extensive at the surface of the F-48 specimen located at the turbine inlet, as shown in Figure 25. The contamination has penetrated well over a mil along grain boundaries. The F-48 specimen located aft

of the turbine does not show this same degree of either extensive surface contamination or of intergranular penetration (see Figure 26).

Four finish machined TZC tensile test specimens were installed immediately downstream of the test turbine after 254 hours of the 2000-hour endurance test. At the end of the endurance testing these specimens had been exposed to the second stage turbine exhaust environment (1240°F and 92% potassium vapor quality) for 1746 hours; they were tensile tested at various temperatures and the data was compared with that for TZC specimens aged at 1400°F in vacuum for 1000 hours. At the lower test temperatures, the ductility of the TZC exposed to the turbine atmosphere was decreased, but was still acceptable at 250°F turbine preheat conditions; at 1400°F, the strength and ductility characteristics of the turbine-tested TZC compared very favorably with the vacuum-aged. This provided further evidence of the suitability of this heat of TZC for continued use as turbine blades in the potassium test turbine. These data are presented in Table XII.

VI. CORROSION, EROSION, AND MATERIAL TRANSFER

Various portions of the turbine components experienced metal loss due to the corrosive action of liquid metal. The dissolution and mass transfer of material within the Type 316 stainless steel facility also resulted in the formation of metallic, dust-like deposits, the development of metal coatings on turbine components and the transfer of solid metal foil deposits from their point of disengagement in the 8-inch potassium vapor line to the turbine inlet guide vanes and to turbine blade surfaces.

In general, corrosion and erosion did not present significant operational problems; however, liquid metal corrosion of turbine components of a severe nature was observed after the 35-hour period of operation in October 1964 when freshly condensed potassium was sprayed into the turbine inlet. During the endurance run, the formation of surface films and an apparent surface diffusion effect was noted on the U-700 buckets; the molybdenum alloy buckets exhibited various minor forms of liquid metal surface corrosion, accentuated by aerodynamic effects; and a likely example of impact erosion was observed in a stationary U-700 specimen installed at a point of liquid droplet impingement aft of the 2nd stage turbine.

Materials transfer was noted (1) during the operation of the C.D. nozzle, (2) at various positions within the turbine facility during the boiler modification work and (3) in the 8-inch line and as films less than 0.001-inch thick on turbine components after the turbine performance test. The specific facility operating conditions under which these deposits formed is dealt with more fully in the topical report on turbine test facilities.

The following documents the changing nature of the corrosion, erosion and metal transfer experienced during the program.

A. Corrosion and Erosion

1. Corrosion During Initial Turbine Testing

A substantial amount of corrosion damage was observed in turbine components under undesirable, not to be repeated, operating circumstances

following the completion of the initial 35-hour period of turbine checkout on potassium vapor. During this time, (1) boiler instability was observed with the possibility that considerable amounts of liquid potassium were carried over from the boiler into the turbine, (2) liquid potassium was sprayed into the 8-inch vapor line upstream of the turbine for the purpose of achieving low quality vapor in the turbine and (3) an instrumentation leak at the bottom of the turbine casing resulted in the ingestion of air into the turbine and in an internal fire which burned axially along the second stage nozzle and tip shroud. The second of the above factors, liquid metal spray, was considered to be most significant in its corrosive effects. The damage which resulted from the passage of liquid through the turbine and from the fire are treated separately, but the latter, by locally contaminating the potassium with oxygen, may have accelerated the liquid metal corrosion damage.

Damage by liquid metal occurred in many places and resulted in the removal of metal from the components. A single set of L-605 nozzle partitions, which were used for all turbine tests, were lightly corroded at their leading edges as shown in Figure 27. The trailing edges of the first stage partitions were corroded by liquid droplets rebounding from the first stage blades and the honeycomb turbine tip shroud was corroded where droplets were slung in a radial direction from the turbine blades; see Figure 28. The damage to the first stage wheel assembly can be seen in Figure 29. Rene' 41 turbine blade fasteners were corroded along the upstream sides of the turbine wheels as seen in Figure 30. Some corrosion occurred along the face of the first stage wheel near the bucket dovetails. Severe solution corrosion occurred underneath the bucket platforms of the first stage buckets as shown in Figure 31. Corrosion patterns on the bucket are shown in Figures 32, 33 and 34. Damage to the second stage was significantly less as indicated by the appearance of these turbine buckets, shown in Figure 35.

The fire damage to the second stage stator and turbine shroud is shown in Figures 36, 37 and 38. Air entering through a leak in the instrumentation line aft of the first stage turbine wheel produced an internal fire which melted a portion of the second stage nozzle diaphragm and vanes and destroyed a portion of the honeycomb turbine shroud.

The flow of liquid potassium through the turbine and its responsibility for the above turbine corrosion damage is next described.

Liquid potassium droplets either carried in the vapor from the boiler or injected into the 8-inch diameter vapor line at the spray nozzle were collected on the bullet nose and flowed through the first stage nozzle partition along the inner band. Other liquid potassium droplets, which did not collect on the bullet nose, passed directly through the nozzle diaphragm; some of these larger droplets collected on the nozzle partitions and left the trailing edge of the partitions as slow moving droplets which were subsequently struck by the convex side of the leading edge of the first stage blades. In all cases, the liquid flow into the turbine appeared to have occurred in fairly large quantities over a limited time as would occur during operation of the spray line system. The distribution of this flow, as deduced from later inspection of the hardware, is shown in Figure 39.

When the liquid metal flowed over the inner band of the nozzle diaphragm, a stream of liquid (or drops) struck the face of the wheel at the blade dovetail causing solution corrosion of the wheel face and of the blade locking strips. Liquid impacting against the blade dovetail flowed under the blade platform and resulted in the formation of a severe groove in the blade immediately under the platform at the leading edge of the blade. Liquid under the platform was forced between the edges of the platforms of adjacent blades by centrifugal force. A grooving type of metal removal occurred on the blade platforms at this point. The liquid then flowed radially along the convex surface of the adjacent blade and over the tip of the blade where it was slung against the honeycomb tip shroud.

The forward, convex airfoil portion of the blade surface was subjected to impacting liquid droplets at a rate sufficient to maintain a film of flowing liquid metal on the surface of the blade. The character of this liquid metal flow is deduced from the inspection of the blades, as shown in Figure 40. Had the actual droplet velocity been zero, only the leading edge of the blade airfoil would have been affected and the impacting velocity would have been 710 feet per

second, the blade tip velocity. The actual droplet velocity was appreciable as indicated by the fact that impacting occurred over an area along the convex airfoil surface. Figure 40 also shows the method used to estimate the relative angle of impacting droplets; the velocity of the droplets from the nozzle blade trailing edges had increased to about 310 feet per second at the time of impact and the droplet impacting velocity relative to the blade was approximately 410 feet per second, which was appreciably less than the blade tip velocity of 710 feet per second. Liquid metal in the impact area flowed forward under high contact pressures due to both the blade momentum and the impact of liquid potassium droplets. Here, high velocity solution corrosion appeared a likely explanation for metal removal as evidenced by the rivulations, previously noted in Figure 32, which flow toward the leading edge. A narrow axial area appeared on the convex side of the blade just aft of the aforementioned rivulations where the impacting liquid appeared to flow rearward to a point which was shadowed from the impacting droplets by the preceding blade. A radial line of pits on the convex side of the blade marked the point at which the high liquid contacting forces produced by the impacting droplets no longer existed; from the line of pits aft, evidences of radial liquid flow on the convex surface were noticed. These pits may represent a form of cavitation corrosion in which pulsations in liquid flow might accelerate corrosion. Cavitation corrosion is also suspected along the blade trailing edge where pits were noted as seen in Figure 41. Cavitation corrosion may have occurred also at those places on the blade where, for aerodynamic reasons, alternate vaporization and condensation may have occurred or where eddying accumulations of liquid metal gathered for aerodynamic reasons.

As shown earlier in Figure 34 liquid flowing over the tip of the blade resulted in a rounding and grooving of the convex side of the blade at its tip and the deposit of a thin fin of metal on the concave side of the blade tip. This metal evidently was deposited from the liquid potassium as it left the blade tip. Other metallic deposits occurred as thin films on the concave side of the blade aft of the mid-chord position as seen in Figure 42.

The metal loss from the blades, described in the above discussion of

liquid flow, are believed to have occurred as the result of solution corrosion; however, impact erosion, washing or wire drawing erosion, and cavitation erosion are also considered.

The following types of metal loss which have been observed in the steam turbine operation, and in other applications, merit consideration: (1) Impact erosion has been observed in steam turbines and is believed to be the result of mechanical damage produced by droplet impact and flow. The most significant erosion of this type occurs on the convex side of blade leading edges. In hard erosion shields, the metal loss occurs as needle-like pits and is accompanied by microcracks at the base of the pits. An example of this type of mechanical erosion, entirely unlike that observed on these potassium turbine blades, is shown in Figure 43. (2) Washing erosion is another type of metal removal caused by the continuous flow of liquid over a surface; the mechanism of this form of erosion is not known but may involve wear or solution corrosion. (3) Wire drawing is a similar form of smooth erosion which occurs when a fluid flows through a small constriction under a high pressure differential; again the mechanism is not known but may involve wear or solution corrosion. (4) Direct solution corrosion in liquid metals is always a likely possibility; it involves the chemical dissolution of the metal component part in the alkali metal in an attempt to satisfy the solubility of the liquid for the solute elements comprising the part. At high droplet impacting pressures or under the influence of cavitation, liquid boundary layer films can be very thin and have very high velocities in the vicinity of droplet impact; the solution corrosion mechanism of metal removal may be more severe under such conditions than under the nominal solution corrosion experienced in pumped liquid metal loops where the liquid velocity is relatively low.

A first stage turbine blade was sectioned in several places and metallographically examined to determine, if possible, the nature of the metal removal process and the nature and extent of any sub-surface metallographic changes in the U-700 microstructure produced by exposure to potassium vapor. Several photomicrographs were made of the blade edges; these are shown in relation to their location on the blade in Figure 44. While local attack was not

preferential with respect to the U-700 microstructure; that is evidenced by the absence of preferential attack of either grains or grain boundaries. No sub-surface microstructural changes or diffusion zones were evident; microhardness traverses from the blade edge inward showed no variation in hardness. Extensive additional metallographic observations were made of the surfaces of turbine blades in the area of liquid droplet impact and flow in an attempt to determine evidence of mechanical damage by impacting droplets. Turbine blade airfoil surfaces were electroplated with nickel to preserve edge effects and were then mounted and polished for optical examination at magnifications to 2000X and/or evaluation by electron microscope. Although a thin film of uncertain origin was found on the convex surface of the blade in the pitted region, it was not evident, even in electron micrographs, whether the debris was a deposited film or mechanically damaged surface material. However, an electron microprobe trace of this area for iron, nickel, and chromium indicated the presence of iron in substantial quantity and clearly revealed the debris to be a deposited film of metal taken from the boiler, carried over as solute in the liquid metal droplets and deposited on the blade. Figure 45 shows the optical nature of this area, Figure 46 shows its electron microprobe oscilloscope plot and Figure 47 shows the distribution of iron, nickel, and chromium from the U-700 matrix to the surface debris and the electrodeposited nickel plate.

It was concluded that, (1) no evidence of liquid droplet mechanical impact damage could be found, (2) the removal of metal from the blades was caused by solution corrosion by fresh potassium condensate supplied through the liquid metal spray line system and (3) surface debris on the blade was actually deposited metal carried over in liquid droplets from the boiler. The fact that more metal deposits were not found on the blades was undoubtedly due to their being cleaned and corroded by liquid metal from the spray line. Further examples of metal transfer to the blade airfoils in additional performance testing are described below.

2. Lack of Corrosion During Performance Testing

During the brief 12-hour and 56-hour periods of performance testing,

no evidence of metal loss of the solution corrosion type was noted from the turbine blades; on the contrary, mass transfer of material carried over from the boiler (as solute dissolved in liquid metal droplets) was believed responsible for an accumulated metal film on both the first and second stage blades. In addition, metal foil deposits were found impacted upon the convex leading edges of the turbine blades. These metal transfer effects are discussed in a subsequent section. Photomicrographs of the blades did not reveal any unusual sub-surface effects, such as alloy depletion or cracks, which might indicate corrosion or erosion.

3. Corrosion/Erosion During Endurance Testing

General Corrosion Stains - Following the 2,000-hour endurance test, the turbine and the 8-inch vapor line were maintained at an elevated temperature and under vacuum for a long time after the remaining portions of the loop had cooled. The purpose was to prevent condensation of potassium within the turbine. Examination of the turbine after its removal from the facility did not disclose evidence of condensed potassium on turbine components. A comparison of the appearance of the second stage turbine wheel assembly before and after test is shown in Figure 48. The turbine was thoroughly steam cleaned and disassembled. Figure 49 shows a portion of the second stage turbine wheel assembly after the test. Two types of deposits were observed on these blades and similar deposits were noted on the first stage blades and on the first and second stage nozzle diaphragms. One deposit was very nearly white; the other was dark brown in color.

The two deposits were carefully collected, separately, by scrapping in order to obtain as pure a sample as possible; however, some mixing of the two did occur. Non-destructive x-ray diffraction analysis was performed on the samples prior to spectrographic analysis because of the small quantity of the brown deposit available for analysis. Patterns were obtained, but compounds could not be satisfactorily identified for either of these deposits because of the great number of lines produced in the patterns.

The remainder of the white sample, which was available in sufficient

quantity, was then spectrographically analyzed. The qualitative analysis, which follows, gives only the metallic elements; since the deposits were not metallic in nature, they may have contained significant quantities of gaseous elements. However, there was an insufficient amount of material available on which to perform analysis of oxygen, nitrogen and hydrogen.

Spectrographic analysis indicated the white deposit from the first stage blades contained chromium in major amounts (over 10%), cobalt, nickel and titanium in minor amounts (less than 10%), and aluminum, iron, manganese and silicon, in trace amounts (less than 1%). The white deposit from the second stage blades contained minor amounts of manganese, molybdenum and silicon and strong trace elements of cobalt, chromium, iron, nickel and titanium. Larger foil-like particles scrapped from the blades gave spectrograph evidence of minor amounts of cobalt, chromium, nickel, titanium, manganese and silicon and strong traces of aluminum, iron and molybdenum.

A very light vapor blast, of the type used to maintain tolerances within 0.0002-inch, was used to clean these deposits from the turbine blades and from other turbine components without damaging the underlying metal configuration; i.e., surface irregularities of a very minute nature were still apparent and unaffected after removal of these very thin oxide-like deposits. The nature of the turbine blade surfaces after this vapor blasting operation is shown in Figure 50. These deposits were undoubtedly a light form of corrosion product which was distributed through the turbine flow passages. Blade weight changes of only 0.038% and 0.147% in the first and second stages, respectively, indicated that the extent of this general corrosion was insignificant. The strong possibility existed that these deposits may have formed during the cleaning operations as the result of minute amounts of potassium retained in crevices and porous materials on the surfaces of the flow passages. Similar types of deposits have been noted in the past when valves and other potassium containing components have been steam cleaned. In any event, they represent no serious impairment to further operation of the turbine.

Turbine Blade Corrosion - The post-test appearance of the first stage U-700 turbine blades is shown in Figures 51 through 54 and that of the second

stage U-700 blades are shown in Figures 55 through 58. The principal areas of leading and trailing edge corrosion in second stage TZM blades are shown in Figures 59 and 60. The first stage U-700 blades appeared to have a very slightly more severe surface corrosion reaction than occurred on the second stage U-700 blades and also exhibited significant metal film deposits in the dovetail area which were not observed in the second stage blades. The appearance and the severity of surface corrosion were similar for both TZC and TZM blades in the second stage; only one TZM blade was available for destructive evaluation. These refractory alloy blades were more severely corroded than were the U-700 blades

Corrosion patterns were very similar in all cases. Very minor corrosion occurred in the U-700 blades along the full length of the airfoil surfaces behind the leading edge of the concave side and forward of the trailing edge of the convex side. Corrosion in these same positions was more severe in TZM blades. These localized areas of limited corrosion were believed to have occurred when liquid metal accumulated in these locations as the result of fluid dynamic influences. The relative depth of these corrosion areas is shown in a macrophoto of a TZM turbine blade airfoil cross section and in related micrographs shown in Figure 61.

The extent of corrosion experienced in the two-stage potassium turbine endurance test is by no means excessive in terms of the types and severity of metal loss experienced in other turbine applications. For example, the 2.8 mils of localized leading and trailing edge corrosion which occurred during 2000 hours on the TZM alloy potassium vapor turbine blades compares, in a favorable way, with the 62-190 mils maximum depth of erosion noted on some blades in the last stage of the low pressure end of the Yankee turbine after 18 months of operation⁷.

Assuming a linear rate of water droplet erosion, for the sake of simplicity, steam turbine experience would indicate 9.3 to 29 mils depth of impact erosion and metal loss as compared to 2.8 mils localized leading and trailing edge metal loss in the potassium turbine blades for an equivalent time of 2000 hours. This

comparison is not intended to be precise, but merely to illustrate the relative minor nature of metal loss experienced in potassium vapor turbine testing to date.

The vapor velocity vector diagrams are of some importance in assessing the evidence of localized corrosion obtained during the endurance test. The pitch-line velocity vector diagrams, determined by off-design analysis, are shown in Figure 62. Shown also are the blade inlet angles. The indications are that the first- and second-stage blades were operating with negative angles of attack amounting to 18 and 11 degrees, respectively. Negative angles of attack on the rotating blades cause a steep negative velocity gradient on the pressure (concave) surface near the leading edge. The result was undoubtedly a stagnant vapor region caused by flow separation where liquid would not be swept off the blade; instead it would be centrifuged radially to the tip. A similar phenomenon apparently occurred on the suction surface near the trailing edge. As the flow was turned through about 125 degrees in passing through the rotating blades, the flow tended to separate from the convex side of the blade near the trailing edge. When separation occurred, the boundary layer tended to stagnate because the gas stream did not supply enough energy to keep it moving. Under these conditions, condensed liquid could accumulate in these places of local separation with resultant corrosion.

TZM Blade Micrographs - The photomicrographs of leading and trailing edge corrosion were shown in Figure 61. The re-entrant nature of the concave leading edge corrosion cavity is indicated; its depth was approximately 2.8 mils. A corrosion groove on the convex side of the airfoil just forward of, and parallel to, the trailing edge also had a depth of 2.8 mils; the corrosion product tended to adhere on the upstream side of this corrosion groove.

Figure 63 shows the location of typical corrosion areas on the convex surface and tip surfaces of a second stage TZM blade. Figure 64 illustrates the corrosion groove on the convex side of the airfoil which runs parallel to the tip surface just below the tip. This groove is 4 mils deep, three mils wide and has additional cavities running toward both the blade tip and the dovetail which are each 1/2-mil deep, in themselves. The accumulated corrosion product can be

seen in this cavity, which was apparently produced by active eddies of liquid metal which collected ahead of the advancing convex surface of the blade.

The location of a corrosion groove, located along the length of the convex airfoil surface, appears to be controlled by aerodynamic forces and is thought to represent a channel in which local liquid metal accumulations migrate toward the tip of the blade. The characteristics of this groove are shown in Figure 65; it is about 1-mil deep and 2 1/2 mils wide with corrosion product accumulations along its edges. Figure 66 illustrates a deposit which was localized just aft of this groove.

At the tip of the blade, re-entrant grooves have been cut into the surface along the major corrosion trace; these are shown in Figures 67 and 68. At the blade tip and away from the principal corrosion trace, corrosion crevices were noted as shown in Figure 69; it is possible that these represent a form of cavitation corrosion activated perhaps by pressure pulsations as the blade tips pass the pockets in the honeycomb turbine tip shroud.

In the previously discussed photomicrographs no fine cracks were found at the base of the corrosion grooves or crevices; corrosion attack showed neither preference for grain boundaries nor preferred grain orientation effects.

The above observations are the first conducted on these blades; further detailed studies are planned for blades subjected to an additional 3000 hours of testing and for new blades tested in the 3000-hour endurance test.

U-700 Blade Micrographs - Figure 70 (sketch) illustrates the locations of typical corrosion areas of a first stage U-700 alloy turbine blade which were examined metallographically for comparison with similar areas of the TZM turbine blade previously discussed. Photomicrographs of these and other areas of interest are shown in Figures 71 through 82.

Figure 71 shows the re-entrant nature of the concave leading edge corrosion cavity which is approximately 2 mils deep. Figure 72 shows a surface reaction product 0.7-mil deep which formed immediately aft of the leading edge corrosion

cavity. This formation was observed in several areas of the blade, through the depths measured generally less than 0.2 mil. Figure 73 shows a high magnification of the surface deposit on the concave surface at the leading edge. Figure 73 shows the light surface corrosion and metallic deposit at the concave tip.

Figure 75 shows the light surface corrosion and metallic deposit at the tip on the convex side of the airfoil. Notice the absence of a corrosion groove in this alloy compared with that previously noted at this location on the TZM blade.

Figure 76 indicates very little localized corrosion but a large amount of metallic deposit on the convex side of the airfoil just forward and parallel to the trailing edge.

Figure 77 illustrates a corrosion groove located along the length of the convex airfoil surface which appears to be controlled by aerodynamic forces. It is thought to represent a channel in which local liquid metal accumulations migrate toward the tip of the blade. The groove at this location is about 2 mils deep and 5 mils wide.

A very general type of alloy depletion was present on all surfaces of the U-700 blades from the endurance test which was not observed after any of the previous tests. The metallic film deposits, when apparent, were observed to overlay this layer. Figure 78 shows this condition on the area of the concave surface airfoil. Observe that on etching (see Figure 79), the depth of alloy depletion appears deeper than in the unetched condition. Furthermore, the alloy depletion appears to be preferential at the grain boundaries.

Figures 80 and 81 illustrate the extent of alloy depletion observed on the dovetail surfaces. The dovetail stresses, being considerably higher than the airfoil stresses, could have influenced the coalescence of the particles, probably $M_{23}C_6$ carbides, in the alloy depleted layer visible in dovetail photomicrographs. Figure 82 illustrates an area of the dovetail which had constant contact with the wheel; in this area, which had restricted contact with liquid potassium, no alloy depleted layer is present.

Electron Microprobe Evaluation - Electron microprobe traces were made across the cross section of a first stage U-700 turbine blade from the 2000-hour endurance test hardware. Nickel, iron, chromium, cobalt, molybdenum, titanium, and aluminum content were determined in the nickel electroplate, across the surface of the blade and to a depth of approximately 150 microns (.006 inches) below the surface of the blade. From the traces presented in Figure 83 it is evident that the elements molybdenum, chromium, and cobalt were gradually depleted in the base alloy to a depth of about 4 mils. The iron content was increased to a similar depth from an original value of 5 percent to an average of 15 percent, and the nickel in this same region was reduced from an original value of 50 percent to 20-30 percent. It is also evident that the titanium and aluminum content were altered near the surface. The surface debris was enriched in nickel and iron; it contained approximately 60-80 percent nickel and approximately 10 percent iron. That the surface debris was a deposit was confirmed by (1) its appearance in the photomicrographs, (2) the high iron content diffused into the U-700, and (3) the presence of a high nickel content layer over an area of U-700 which was depleted in nickel.

In addition to the above microprobe trace of a surface debris area, a microprobe trace was made of a surface reaction product observed at the convex airfoil surface immediately aft of the leading edge corrosion groove of a 2000-hour, first stage U-700 blade. This phase, which appeared pink when viewed with the optical microscope was found to contain the surprising amount of 40-50 percent copper to a depth of about 2 mils; an increase of 8-9 percent iron over the nominal base metal composition was also observed. The nickel content was found to have dropped to approximately 25 percent from the normal 50 percent alloy content. The electron microprobe traces of this pink phase are presented in Figure 84; in general, study of the other traces indicate that no change occurred in the molybdenum, aluminum, titanium, chromium and cobalt within this phase as compared to the base metal; however, the characteristic compositions of the surface debris were similar in both the above microprobe traces with respect to the base composition.

Erosion Inserts - Erosion inserts of the type shown in Figure 85 were installed behind the second stage of the turbine during the endurance test. The purpose of these inserts was to evaluate various materials under the influence of impacting potassium droplets coming from the second stage blade tips at turbine tip speeds of 770 ft/sec and at temperatures of about 1260°F. Three specimens each of aged U-700, stress relieved TZM, recrystallized TZM and as-received TZC were installed on the aft side of the second stage turbine shroud as shown in Figure 86 (the relative strengths of these materials are shown in Table XIII as an indication of their expected resistance of impact erosion). Impacting liquid droplets from the blade trailing edge tips struck the specimens along the narrow face of the projecting tab of the insert near the 90° milled recess. The vapor quality entering the second stage turbine blades was 96.7%; it was the liquid condensate in this vapor which collected on the second stage blades and which produced erosion effects on the inserts as the droplets were slung from the second stage blade tips.

Binocular examination of the inserts after 2000 hours of testing disclosed minor, non-uniform surface deposits and discoloration. These deposits are found to consist of corrosion products and mass transported material similar to that observed on the endurance test blades. Figure 87 shows a typical example of the light surface corrosion and discoloration found on the erosion inserts.

The weight change data for these specimens are shown in Table XIV to an accuracy of 0.0002 grams. The increase in weight of these specimens in spite of some metal loss, particularly in the case of U-700 which experienced a deep needle-hole form of impact erosion, can be explained by the corrosion products accumulated on their surfaces. After a light vapor blast, which cleaned the specimens to their metal surfaces, the relative weight losses become more significant. The larger losses in U-700 are indicative of the needle-hole type of impact erosion in which the largest amount of metal removal was noted.

All of the erosion inserts were examined macroscopically before and after surface vapor blasting at magnifications as high as 60X for evidence of erosion. Macrophotos of these are shown in Figures 88 and 91.

The U-700 inserts were clearly the most affected; a cluster of deep holes was readily apparent at a location adjacent to the passing trailing edge tips

of the second stage blades as seen in Figure 88. These holes in the U-700 erosion inserts were examined metallographically at several planes through the impact erosion area. The holes were found to have a depth-to-diameter ratio of approximately 3 to 5 for the deeper holes. The interior surfaces of the holes were crazed with very small cracks penetrating inward approximately 0.0005-inch in some areas. Photomicrographs of the impact erosion area of U-700 erosion insert number A-3 are presented in Figures 92 through 96. Alloy depletion similar to that observed on the U-700 blades was observed on the U-700 erosion insert as seen in Figures 96 and 97; this surface effect was apparently unrelated to liquid impact as it was present on all exposed surfaces of the insert; this implied that a thin corrosive liquid potassium film was present over the entire insert surface.

These erosion inserts gave the first evidence of what could be classical liquid droplet impact erosion in the U-700 specimens and similar in nature to steam turbine erosion as seen earlier in macro form in Figure 43, and at larger magnification in Figure 98. The deep holes formed in the exact area where droplets would have been released from the second stage trailing edge blade tips and would have impacted on the erosion insert. The micro-cracks at the base of the holes are indicative of the impact erosion or cavitation erosion methods or mechanical damage. The surface areas between adjacent holes deteriorated either by an apparent randomness in the location of impacting droplets or by disruption of the surface between adjacent holes. At the periphery of the cluster of holes there existed occasional deep holes, with depths 4 to 5 times that of their diameters; these holes had formed in the original surface of the U-700 insert without doing damage to the adjacent surface. This type of erosion was similar to that reported by Hays⁸ for ductile materials in steam turbine erosion. In other examples of erosion, pits in otherwise unaffected surfaces have been noted in multiple droplet impact specimens and in cavitation damaged specimens. In water droplet impact in Stellite 6B erosion shields in steam turbines, deep pits or irregular cross section have been observed with depths of one to two diameters in areas where no adjacent surface damage was noted.

Kulp and Altieri⁹ have observed, to a very limited extent, the formation of well rounded cavitation pits in Type 316 stainless steel pump impellers operating

in potassium at 1400°F; these pits, which they believed were caused by the implosion of a single bubble, were of approximately equal diameter and depth. They occurred to depths of five and nine mils in areas in which no immediately adjacent surface damage was noted. The circular surface rim of the pit was forced upward as if by some internal force. While they assume that the metal removal occurred as a single event, the microstructure does not appear to show sufficient evidences of deformation to account for all the metal loss within the pore. The flow of liquid into, and out of, the pore in repeated events could have resulted in removal of the metal by solution corrosion; no microcracks, which would have indicated mechanical removal of the metal were apparent.

Cavitation damage of a more general nature, noted in Kulp's and Altieri's liquid potassium pump tests, penetrated to a maximum to 50 mils; this damage was apparently caused by severe working of the surface in which relatively large amounts of the surface were removed. Other examples of cavitation damage, as experienced by Robinson and Hammitt¹⁰, have given the appearance of low order changes in surface profile, as contrasted to the above samples of deeper pitting. The pits formed in various materials under the influence of cavitation in mercury venturi flow passages and had diameter-to-depth ratios of 20 to 1, entirely unlike that observed in the U-700 erosion inserts. On the other hand, Hammitt¹¹ has also pointed out that a deep type of cavitation pitting has been observed in water pump impellers and is referred to as "worm holing."

Kovacevitch¹² has conducted multiple impact erosion tests in water and potassium on various turbine materials. His test involved whirling round bar specimens which cut through a stream of water or potassium at right angles to the plane of specimen rotation. In tests at 1400°F, molybdenum base alloys were as resistant to potassium as were Stellite 6B specimens in water droplet impact at room temperature under comparable conditions of impact velocity, stream diameter and nozzle-to-specimen distance. Columbium and tantalum alloys lost from 20 to 200 times the weight lost in the molybdenum alloys. The mechanism of material loss was not reported, but it was concluded that the testing method

was inadequate in comparison to actual turbine tests. Low impacting velocities of only 212 feet per second and the possibility of contamination of the potassium (the oxygen content was not reported) tend to make the results difficult to interpret.

It is apparent, then, that impacting erosion has resulted in the mechanical removal of metal from the U-700 potassium turbine erosion inserts.

Refractory alloy erosion inserts (stress relieved TZM and as-received TZC) were examined metallographically in an attempt to define more clearly possible indications of corrosion and erosion observed on those specimens. A photomicrograph showing the corroded area on the tip of insert C-3 is presented in Figure 99; it can clearly be seen, by the absence of microcracks and the presence of corrosion products, that corrosion was the cause of metal loss in this particular area.

A close binocular scrutiny of a TZC refractory alloy erosion insert, specimen D-3, revealed, in addition to machining marks which were on the surface prior to test, very small indications of what appeared to be localized solution corrosion under the influence of impacting liquid potassium droplets.

Corrosion cavities were seen metallographically in the area corresponding to the cratered area of the U-700 erosion insert. The interior of the cavities gave the appearance of a porous or leached structure, and the bottom of the leached area could not be clearly defined. No cracks indicative of mechanical damage could be distinguished in the material surrounding the craters which tended to support solution corrosion as the failure solution. Photomicrographs of this cratered area of the TZC specimens are presented in Figures 100 and 101.

Corrosion and Erosion Summary - While gross evidences of corrosion were experienced during an early period of turbine operation, in which quantities of freshly condensed potassium in large droplet sizes were introduced into the turbine, the corrosion experienced in 2000-hour endurance testing has been relatively minor. The worst corrosion was only 2-3 mils deep in TZM after 2000 hours. Very subtle indications of alloy depletion and the formation of very thin

metal deposits at the surface of blade airfoil and dovetail sections were noted in metallographic and electron microprobe examination. Limited evidences were indicated of depletion of nickel (and to a lesser extent, of cobalt, chromium and molybdenum) to a depth of 4 mils and of the formation of nickel and iron rich deposits or debris to a thickness of approximately 0.1-mil. In one instance a high copper concentration was diffused into the surface of a U-700 airfoil to a depth less than 2 mils; in some cases metal deposits resulted in an apparent diffusion of iron into the U-700 airfoil surface. Where visible corrosion occurred, its depth in aerodynamically preferred areas was almost as severe in the first stage U-700 blades as in the second stage TZM blades. The second stage U-700 blade corrosion was less severe than either of the above.

No evidences were noted of direct liquid droplet impingement damage on turbine blades during the well-controlled, long-duration endurance test. Instead, the liquid responsible for corrosion is believed to have accumulated on the blades in minor amounts, as the result of aerodynamic forces, and in a highly active state, as the result of high frequency aerodynamic effects generated as the blades passed partitions and shroud components. Mechanical impact erosion was confirmed in only one location and in one material; i.e., in the stationary U-700 erosion inserts located aft of the second stage blade tips. The mechanical nature of the damage was attested by the formation of microcracks at the forefront of the impact erosion area.

In none of the corrosion evaluation were any effects noted of a nature which could be considered detrimental to continued turbine operation.

B. Material Transfer

Thin porous metal film deposits were observed in the turbine and turbine facility on various occasions since the facility began operation in October, 1963. These deposits were found, first, downstream of the convergent-divergent nozzle during the first test of the turbine facility; second, as a powdery deposit in the vapor drum of the boiler during the boiler repair; third, as a foil deposit (a) on the refractory metal probe which had been inserted in the 8-inch vapor line, (b) on the inlet guide vanes, and

(c) on turbine rotating parts during turbine performance testing; and fourth, (a) on the face of the first stage wheel, (b) on turbine bucket dovetails and airfoils and (c) on the erosion insert surfaces during the endurance test. For instances preceding the endurance test, the deposits were believed to have originated as metal taken into solution in the boiler, then precipitated either in the vapor drum, in the heated 8-inch vapor line, or on other surfaces as the droplets of potassium were evaporated. The high cobalt content of deposits on the first stage wheel during the endurance test indicates that metal may have been transported from the L-605 partitions or H-33 braze.

1. C. D. Nozzle Testing

When the convergent-divergent nozzle test section was removed for flange modifications in November 1963, a thick metallic deposit occurred on the far side of the inside surface of the elbow leading into the condenser. The deposit was thickest directly opposite the nozzle, and from that location thinned-out in all directions. The deposit, at its thickest, measured approximately 0.030-inch, and appeared to consist of large laminated particles sintered together. Photomicrographs showing the structure of this deposit are presented in Figure 102. Qualitative spectrographic analysis of the deposit indicated a major concentration of nickel (greater than 10%), a minor concentration of iron (less than 10%) and trace concentrations of chromium, aluminum and cobalt (less than 1%).

2. Performance Testing

The metallic, mass-transfer deposits which occurred during performance testing were observed in several places. A foil deposit on the 8-inch turbine inlet vapor line immediately downstream of the throttling valve resulted when liquid droplets containing metallic elements in solution were dried-out as they passed through the partially closed valve. This foil deposit was porous and appeared to have grown from the evaporation of liquid droplets and not as impacted, or sintered solid particles of the type previously observed in the convergent-divergent nozzle test. The foil thickness ranged between 0.005-to 0.010-inch thick. The texture of the foil deposit from the 8-inch line is shown in Figure 103.

During performance testing, after the facility had been modified to supply drier vapor, a portion of foil deposit, of the above origin, became detached from the inner surface of the 8-inch line and was carried downstream by the high velocity potassium vapor to be re-deposited upon surfaces such as the refractory alloy specimen probe and the inlet guide vanes. Figure 104 shows the nature of foil deposits on the first stage nozzle diaphragm. Figure 105 shows some of these foil particles on the convex side of the first stage turbine blades and to a very minor extent on the second stage blades. Apparently, the foil was ground into very small particles within the first stage, allowing most of these fine particles to pass through the second stage without becoming attached to the airfoil surfaces. The microstructure of impacted foil deposits on the convex airfoil surface of a first stage blade is shown, at two magnifications, in Figures 106 and 107. These foil deposits on the blades were identical in texture to the foil pieces taken from the wall of the 8-inch vapor line downstream of the throttling valve.

In addition to the presence of impacted metallic foil on the turbine blades, which was noted after performance testing, thin metallic films formed directly on the blades from the evaporation or cooling of liquid droplets in two separate instances. First, very minor traces of such deposits were found on the grossly corroded turbine blades after the first period of turbine checkout, in which the film was detected by electron microprobe analysis. Second, during the 12- and 56-hour periods of performance testing, in which corrosive liquid potassium was not sprayed into the vapor line, a uniform, but thin film of deposited metal accumulated on the airfoil sections of blades from both stages in the turbine. The uniform film thickness on the first stage blades was 0.5-mil as seen in Figure 108 and only 0.2-mil on the second stage blades as seen in Figure 109. As the result of pickup of metallic elements, the first stage blades experienced an average weight gain of 1.13% per blade and the second stage blades gained an average of only 0.023% per blade.

During boiler modification, a fine metallic powdery deposit was removed from the upper header of the boiler. The analyses of a sample of the powdery deposit removed from the boiler header and of a sample of the foil removed from the 8-inch line are presented in Table XV, along with analyses of other deposits.

The metallic deposits in the upper drum of the boiler and those found in both the CD nozzle tests and in the 8-inch vapor line during performance testing, all gave compositional evidence of having originated from the Type 316 stainless steel loop material as a source.

Considering the relatively large area in the boiler and the relatively small area in which droplet evaporation occurred, the formation of the amount of deposits noted during turbine testing was not considered to be indicative of significant corrosion in the boiler. X-ray measurements were made of the wall thickness of the boiler tubes in various locations prior to endurance testing and no reduction in the tube wall thickness was noted. Most of the metal deposits observed in the 8-inch line may have formed during the earlier periods of turbine performance operation when the throttle valve was partially closed to control turbine inlet temperature. After liquid droplet carry-over had been materially reduced by boiler modifications and the throttling valve was operated in the full open position, this condition became less serious. A more significant effect than deterioration of the facility by this degree of metal transport was the possibility that these metal deposits could become disengaged from the wall and pass into the turbine where blockage of vapor flow or mechanical erosion could result.

Prior to the endurance run, the 8-inch vapor line was mechanically cleaned to remove any foil deposits and the endurance test was run without throttling and with the boiler liquid level at a position to minimize liquid droplet carry-over. This proved successful inasmuch as this type of foil deposition and detachment was not observed during the endurance test.

3. Endurance Testing

Minor deposits of metal accumulated on the first stage wheel surface and on turbine blade airfoil sections as shown in Figures 110 and 111. It was expected that the metallic deposits which formed on the first stage wheel and blade surfaces during endurance testing were produced by evaporation or cooling of liquid droplets carried over from the boiler. However, the chemical analysis, also presented in Table XV, shows a significant amount of

cobalt, which indicates that the majority of the metal could have been picked up by liquid potassium from either the L-605, cobalt base inlet duct guide vanes and nozzle partitions or the cobalt-base braze alloy (H-33) used to assemble these components.

The thin metallic film is visible on U-700 blades in the photomicrographs in Figures 112 and 113 and appears overlaying the corroded airfoil surface; the thickness of the foil was found to be between 0.1- and 0.5-mil on an airfoil which had not been vapor blasted.

Weight change data presented in Table XVI are insufficiently conclusive to confirm the presence of metal film buildup or to indicate relative metal loss through corrosion. It is apparent that the previously presented metallographic evaluation alone must be relied upon for such deductions.

VII. PROCUREMENT, HANDLING AND ANALYSIS OF POTASSIUM

A. General Considerations

The two stage potassium turbine requires about 3,500 pounds of potassium. Roughly 2,400 pounds are used in the loop during actual operation (the remainder stays in the dump tank), and of this about 120 pounds are used in the hydrodynamic seal loop. During turbine operation, the potassium in the main loop is recycled through the loop about twice an hour. Due to this high flow rate, small quantities of impurities in the potassium could have deleterious effects on the various parts of the loop and the turbine itself.

It is not possible to set meaningful limitations on the maximum quantity of each possible impurity which the potassium may contain, since the specific effects have not been established in most cases. It is, of course, known that oxygen may cause corrosion of the loop and turbine components and that it may be removed from the potassium by refractory metal parts leading to undesirable changes such as embrittlement.^{13,14,15} There is some evidence also that oxygen content correlates with carbon transfer¹⁶. Carburization can lead to decreases in ductility of various components¹⁷.

Since so little, of a specific nature, is known about the effects of impurities, it has been the policy to maintain the impurity concentrations at the lowest possible levels. This is accomplished in the loop by means of zirconium getters - one in the condenser and one in a by-pass hot trap around the boiler. A titanium getter is also provided in the dump tank to provide purification capabilities between operational periods. Furthermore, the vaporization of the potassium in the boiler is in itself a very effective purification process; consequently, the potassium vapor which reaches the turbine should be of extremely high purity.

Under the conditions of turbine testing, the concentrations of most impurities in the potassium should remain at or below the detection limits of the applicable analytical techniques. Exceptions to this rule are volatile impurities such as sodium. An increase in the concentration of any particular

impurity indicates contamination of the potassium in the loop or contamination during sampling or analysis. The chemical analysis of the potassium, is, thus, more important in understanding or eliminating malfunctions or undesirable operating procedures than it is in maintaining the potassium purity at some specified level.

Oxygen concentrations in potassium have been determined at the SPPS Laboratories using the mercury amalgamation method under inert helium or argon gas. This method is described in detail in SPPS Specification No. 03-0055-00-A, "The Amalgamation Method for Oxygen in Sodium, Potassium and NaK" which is a modification of the method of Pepkowitz and Judd¹⁸.

The emission spectrographic technique which has been applied to the determination of metallic impurities is described in SPPS Specification No. 03-0058-00-A, "Spectrographic Methods for Metallic Impurities in Alkali Metals."

Three methods have been applied to the determination of carbon in potassium, the first used being that developed by S. Kallman of Ledoux and Company, Teaneck, New Jersey. This method consists of the dry combustion of the potassium using an oxygen-inert gas mixture, followed by the release of carbon dioxide by the addition of sulfuric acid. The amount of carbon dioxide is measured conductimetrically. The method is described by S. Kallman and R. Liu¹⁹.

The second method is that in use by Mine Safety Appliance Research Corporation, Callery, Pennsylvania. The method consists of first reacting the potassium with water which converts the potassium to the hydroxide and any carbides present to acetylene. The quantity of acetylene is determined mass spectrometrically. The potassium hydroxide solution obtained in the first step is acidified with sulfuric acid, releasing carbon dioxide from any carbonate present initially. The carbon dioxide is measured mass spectrometrically. Finally, the potassium sulfate resulting from the second step is dried and then oxidized at high temperature with oxygen, converting any elemental carbon present to carbon dioxide which is then determined with the mass spectrometer.

The third technique which has been used was recently developed for potassium at SPPS. It consists of the dry combustion of the potassium in an oxygen-inert

gas atmosphere in the presence of silica. The potassium oxide and potassium carbonate react with the silicon dioxide forming potassium silicate, and carbon dioxide is released in the case of the carbonate. The carbon dioxide is measured with a gas chromatograph.

Prior to the turbine endurance run, the potassium samples which were analyzed were removed from the dump tank, since no provision had yet been made to sample the loop itself; i.e., referring to Figure 114 the tee and connection through valve 6 to valve VML-2 had not yet been made, although the lines between valves 5, 7 and 8 were in. Referring to Figure 114 the procedure for sampling the dump tank was as follows:

1. The sample tube and overflow reservoir system (sampling system) was cleaned, assembled, helium leak checked, baked out at 200°-300°F for 15 minutes at 5×10^{-3} torr and backfilled with Matheson ultra high purity argon.
2. The sampling system was attached to the argon supply between valves 2 and 3. Then with argon flowing from the bottom of the sample tube, the sample tube was connected to valve 7.
3. The sampling system, the overflow tank and the dump tank dip line were heated to 200°-500°F.
4. With valve 7 closed, valves 5 and 8 were opened and about 25 pounds of potassium were flushed from the dump tank into the overflow tank while venting pressure off the overflow tank through valve 10.
5. The overflow tank was then pressurized and emptied back into the dump tank.
6. Step No. 4 above was repeated, thus flushing the dump tank line with about 10 times its volume of potassium.
7. The sample was then taken by closing valve 8, opening valves 1, 2 and 3 and flowing argon through the sampler reservoir, then opening valve 7 and flushing potassium through the sample tube until the reservoir was filled to within 1/2 inch of the top of the overflow line (the dotted line shown in Figure 114).

8. Valves 7 and 1 were closed, the reservoir was pressurized to 5-10 psig, valves 3 and 4 were closed and the sampler was cooled to room temperature.
9. During sample cooling, the overflow tank was pressurized and emptied through valve 8 back into the dump tank.
10. The cool sample was then disconnected and capped off and valve 7 was cleaned in preparation for the next sampling operation.

The procedure used to sample the loop will be described later in this report.

B. Procurement and Initial Purification of Potassium

The potassium in use in the Two Stage Turbine was purchased in March 1963 from Mine Safety Appliance Research Corporation; Callery, Pennsylvania. Two 2000-pound capacity, stainless steel, shipping containers were fabricated by MSAR and filled with their slagged and filtered grade of potassium.

The potassium (3570 lbs.) was transferred to the loop dump tank on September 26, 1963. A sample of potassium was obtained from the fill line during the transfer from Container No. 1. This was subsequently analyzed for oxygen and 154 ppm (Specimen 35, Table XVII) were found.

All analyses for oxygen and carbon in potassium are shown in Table XVII. The values given in the text of this report are weighted averages obtained by dividing the total micrograms of oxygen found by the total of the sample weights for multiplicate analyses.

After transfer of all the potassium to the dump tank, another sample was obtained from the dump tank and analyzed. The oxygen concentration was found to be 775 ppm (Specimen 36). This high value probably indicates contamination by material in the dump tank. The metallic impurities in this sample were also determined. These results are shown in Table XVIII. All elements determined were found to be at acceptably low values.

Subsequent hot trapping with the titanium getter (~ 200 lbs. Ti; ~ 1 g K/in² Ti) in the dump tank for 108 hours at 1100° to 1200°F reduced the oxygen content to 48 ppm (Specimen 42). The potassium was then forced from the dump tank into the condenser, boiler and associated piping where it was circulated for three days at 300° to 500°F by means of the EM pump and controlled argon pressure. It was not possible to circulate the potassium through the 8-inch diameter vapor line or the converging-diverging (C-D) nozzle.

The potassium was returned to the dump tank, resampled and reanalyzed. The increase of oxygen concentration to 87 ppm (Specimen 46) indicated pickup from the loop during flushing. Subsequent hot trapping at 1200°F decreased the oxygen concentration to 44 ppm (Specimen 47).

C. Initial Boiling and Facility Testing

The potassium was returned to the loop and boiling was initiated and sustained for a few hours. Operational difficulties involving a potassium leak and fire at the flange between the C-D nozzle and the condenser required that the potassium be returned to the dump tank. It was again sampled and analyzed with a value of 10 ppm (Specimen 48) being found for the oxygen concentration. This reduction in oxygen content reflects the purification which took place in the loop due to hot trapping and distillation and is also evidence that the leak did not result in significant contamination of the potassium.

The potassium was returned to the loop for the purpose of testing the spray nozzle in the 8-inch vapor line upstream from the C-D nozzle. This system did not operate correctly due to plugging in the in-line, spray line, hot trap. After removal of the hot trap, the potassium was used to flush the loop for 7 hours at 300° to 400°F and again returned to the dump tank. Analysis for oxygen produced a value of 140 ppm (Specimen 57), indicating contamination of the loop during the removal of the hot trap. The potassium was hot trapped in the dump tank at 1150°F and subsequent analysis indicated an oxygen content of 33 ppm (Specimen 58). Testing in the C-D nozzle was completed on December 29, 1963.

D. Initial Turbine Testing

By April 2, 1964 the installation of the two stage turbine was nearing completion, so the dump tank was sampled and the potassium was analyzed prior to flushing the loop. The oxygen content was 67 ppm (Specimen 73). The loop was flushed and the potassium returned to the dump tank and sampled at 950°F. Analysis indicated 30 ppm oxygen (Specimen 74). This reduction in oxygen content is probably indicative of the high flush temperature, since it is known that stainless steel will start to remove oxygen from potassium between 700° and 900°F. It is also probable that zirconium and titanium become effective as getters at about 1000°F. Subsequent hot trapping in the dump tank at 1200°F for 100 hours reduced the oxygen content to 24 ppm (Specimen 75).

The potassium was transferred to the loop and turbine testing was initiated on April 13, 1964; i.e., potassium was placed in the hydrodynamic seal for the first time. This test was aborted when it was found that oil was leaking into the hydrodynamic seal potassium system and into the condenser, and the potassium was returned to the dump tank and sampled. The carbon content was found to be 88 ppm (Specimen 89), indicating contamination of the potassium by oil. The potassium was hot trapped at 1150°F for 100 hours and reanalyzed. The carbon concentration had dropped to 59 ppm and the oxygen content was 17 ppm (Specimen 93). The results of analysis for metallic impurities are shown in Table XVIII and indicate that the material was of superior quality in this respect. Additional hot trapping at 1175°F for 150 hours reduced the carbon content to 43 ppm while the oxygen content did not change appreciably - 18 ppm (Specimen 97). The metallic impurity concentration remained essentially unchanged except for Al, Ca, Fe, Mg and Si. The increases noted for these elements were probably indicative of contamination by dust during conversion to KCl.

By July 15, 1964 the turbine had been operated on potassium vapor for a total of about six hours. Operational difficulties required that the potassium be dumped, so the dump tank and the potassium hydrodynamic seal head tank were both sampled. The head tank sample was analyzed for carbon to determine whether or not oil was getting into this system. A value of 11 ppm carbon (Specimen 101) was found, indicating that no such contamination had occurred. The dump tank

sample (Specimen 102) produced values of 40 ppm oxygen, 42 ppm carbon, and values for metallic impurities (See Table XVIII) which were not significantly different from those obtained for the hydrodynamic seal head tank sample.

The increase in oxygen content may have reflected contamination of the potassium during an efflux line fire, which was one of the difficulties encountered. Another sample was taken (Specimen 110) and 65 ppm oxygen was found, but precision was poor. The carbon content was 32 ppm, which was not significantly different from the previous sample. It was decided to hot trap the potassium. This was done and the material was resampled. Analysis (Specimen 112) indicated that the oxygen content had been reduced to the low value of 6 ppm whereas the carbon content had apparently increased to 200 ppm. The fact that the next specimen (Specimen 115) produced values of 36 ppm carbon and 8 ppm oxygen lead to the conclusion that the value of 200 ppm for carbon was erroneous, but no good reason for this was apparent, especially since the precision was so good on duplicate analyses.

E. Turbine Performance Testing

Specimen 115, mentioned above, was removed from the dump tank prior to flushing the loop in preparation for performance testing. After flushing the loop and returning the potassium to the dump tank, values of 7 ppm oxygen and 52 ppm carbon (Specimen 116) were found. Hot trapping was not considered necessary, so the potassium was returned to the loop for performance testing.

During the course of performance testing a number of malfunctions occurred. One was a potassium leak and fire in the condensate extraction tube on the bottom of the turbine casing. In this case only the condenser was dumped. Analysis (Specimen 117) showed 13 ppm oxygen and 199 ppm carbon. Again there is no reasonable explanation for the high value obtained for carbon.

The most serious occurrence which took place was the leak and fire in the vapor drum of the boiler which occurred on October 13, 1964. The boiler pressure was below atmospheric pressure at the time the leak first started, and the contamination by in-leakage of air is reflected in the high value of 45 ppm

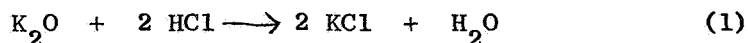
oxygen obtained for Specimen 127. Subsequent hot trapping reduced the oxygen content to 7 ppm (Specimen 158). The carbon content was not reduced substantially (98 ppm).

At this point it was decided to have Mine Safety Appliance Research Corporation, Callery, Pennsylvania perform future analyses for carbon, since their method distinguished between elemental, carbide and carbonate carbon. The dump tank was resampled (Specimen 179) and a specimen was submitted to MSAR. This sample should have been comparable with No. 158. The precision of the analytical results for carbon was not particularly good; however, the average value of 35 ppm for total carbon was considerably less than the value of 98 ppm found by Ledoux. This lower value for total carbon may have been due to the fact that the potassium remained in the dump tank at about 500°F from December 12, 1964 until February 8, 1965; however, the mechanism for its disappearance is not apparent.

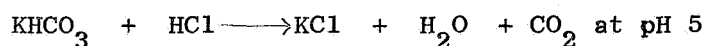
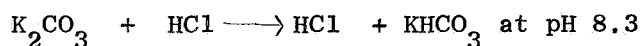
After extensive repair and modification of the boiler, it was flushed with potassium. The analytical results obtained for Specimen 185, obtained after flushing, show the contamination (68 ppm oxygen and 460 ppm carbon) expected from the long period during which the loop was open to the atmosphere and probably also from residual contamination due to the fire. Hot trapping for 100 hours at 1350°F substantially reduced both the carbon (196 ppm) and the oxygen (15 ppm) concentrations (Specimen 187). Subsequent operation of the turbine further reduced the carbon (70 ppm) and oxygen (10 ppm) contents (Specimen 188). Specimen 198 was taken from the dump tank after completion of performance testing and analysis indicated still further reduction in both carbon (45 ppm) and oxygen (6 ppm). Analytical data for metallic impurities for Samples 185, 187, 188, and 198 are shown in Table XVIII and indicate that the concentrations of these impurities remained quite low.

Specimen 206 was removed from the dump tank between performance and endurance testing at the request of the NASA Program Monitor for the purpose of obtaining comparison analyses. The large increase in carbonate carbon is not understood.

An unusual and, as yet, unresolved discrepancy appears in the data presented. This is the lack of correlation between the carbonate carbon and the oxygen concentrations. Since the amalgamation residue is analyzed by titration with HCl, assuming that the only titratable species is K_2O , whereas K_2CO_3 is also titratable, there should be a definite proportionality between carbonate and oxygen. That there should be a correlation between carbonate and what is calculated and reported as oxygen is arrived at as follows. Two chemical equations apply:



It is clear that in the titration with HCl, one gram-atom of oxygen in equation (1) is equivalent to one gram-atom of carbonate carbon in equation (2). Therefore, 16 micrograms of oxygen are equivalent to 12 micrograms of carbonate carbon. It follows that 1 ppm of carbon as carbonate is equivalent to 1.33 ppm of oxygen and would be reported as such, using the amalgamation method. Consequently, the oxygen and carbonate carbon data for specimens 185 and 187 are not in agreement. For example, if the carbonate carbon concentration were actually 350 ppm in specimen 185, the amalgamation method should have detected it as about 465 ppm oxygen. Furthermore, the presence of this much carbonate should have been obvious from the titration curve since the neutralization takes place in two steps:



resulting in two inflections in the titration curve. No such behavior was observed.

It is similarly difficult to invalidate the carbonate determination because when such high levels were found, MSAR checked their technique using some sodium of known carbonate content and found the correct amount. Segregation in the long sampling tube during cooling is a possible explanation for the non-correlation; however, the good agreement between duplicate analyses for both

carbon and oxygen indicates that this was not the cause. Contamination of the MSAR specimens during handling by SPPS or during transit is also highly unlikely.

F. Turbine Endurance Testing

During the period between the completion of performance testing and the initiation of endurance testing, the potassium sampling system was modified to allow sampling from the loop during operation as well as from the dump tank during shutdown. This arrangement permitted the removal of potassium samples which were more representative of the potassium to which the turbine was exposed.

The modified apparatus is shown schematically in Figure 114, and the sampling procedure was as follows:

1. Connect a clean, argon filled overflow reservoir (with new sample tube attached) to the sampling system, making use of the Swagelok fitting between valves 2 and 3.
2. Purge the overflow reservoir and the sample tube through valves 2 and 3 while removing the swagelok cap from the bottom of the sample tube and making the connection at valve 7.
3. Open valve 1 and continue the argon purge while wrapping heating tapes on the sample tube and overflow reservoir and during heat-up of the entire sampling system.
4. Heat all lines and valves, the overflow tank and the overflow reservoir to about 400°F.
5. Adjust the pressure in the overflow tank to about 15 psia.
6. Reduce the heat rejection in the heat exchanger to give a potassium temperature of about 400°F.
7. Open valve VML-2 to fill the line to valve 6.
8. Open valve 6 to fill lines between valves 5, 7 and 8.
9. Open valve 8 and flow a quantity of potassium into the overflow tank which is equal to one to two times the volume of the lines between valve VML-2 and valve 8. Close valve 8.

10. Open valve 7 and flow a quantity of potassium through the sample tube into the overflow reservoir which is equal to one to two times the volume between valve 7 and the top of the overflow tube in the overflow reservoir.
11. Close valves 1 and 7 and pressurize the overflow reservoir to about 10 psig.
12. Close valve VML-2 and open valve 8 to drain the potassium out of the lines between valves 5, 7 and VML-2.
13. Close valves 2, 3 6 and 8 and turn off all heat to the sampling system.
14. When the potassium has reached room temperature, disconnect the sample tube at valve 7 and cap the sample tube.
15. Disconnect the overflow reservoir at valve 2.
16. Clean valve 7 back to the valve seat.

The sample tube and attached overflow reservoir were submitted for analysis for oxygen, carbon and metallic impurities in the potassium. The analytical data obtained are shown in Tables XVII and XVIII.

The valve, VML-2, is just downstream of the 450 Btu heat exchanger which supplied potassium to the argon reclamation system and to the fill line for the hydrodynamic seal loop. Normally, the potassium supplied by this heat exchanger is at a temperature near 250°F. This was considered to be too low a temperature for obtaining representative specimens, so, during sampling, the heat rejection of the exchanger was reduced so that the potassium temperature was above 300°F and was generally between 350° and 400°F. Although an even higher sampling temperature was preferred, this was not possible because the argon reclamation system should be supplied with liquid potassium at as low a temperature as possible, since it is a counterflow device intended to remove potassium vapor and droplets from the argon.

The source of the potassium which is supplied to the 450 Btu heat exchanger is the line (containing valve VPL-8) which is attached to the main loop just downstream from the EM pump. The potassium sampled is representative of that

which has passed through the turbine to the condenser; and should, therefore, be extremely pure after an initial period during which contaminants are being cleaned out of the 8-inch turbine feed line, the turbine and the condenser.

During the first 250-hour period of endurance testing, Specimens 225 through 235 were removed from the main loop and analyzed. Specimen 225 was taken from the loop after filling the dump tank, but before starting potassium vapor flow through the turbine. The relatively high oxygen value of 27 ppm obtained is indicative of some contamination during the long shutdown just prior to test. The values obtained for the carbon content and the metallic impurity concentrations will be discussed later.

Specimen 226 was removed from the loop two hours after the initiation of vapor flow through the turbine. The high concentration of oxygen (69 ppm) was probably due to some oxygen pickup along the 8-inch turbine feed line and the condenser during the shutdown. The following low value (14 ppm) for oxygen for Specimen 227 indicated that the combination of distillation and hot trapping which takes place during loop operation had quickly and effectively removed the oxide, washed down from the 8-inch line and condenser, from the potassium passing through the turbine.

The high value for oxygen (17 ppm) found for Specimen 231 was due to contamination during analysis. The air leak found in the analytical apparatus was repaired before the remainder of the analyses were performed. The reason that the precision was good on duplicate samples was because both samples were run simultaneously in the same apparatus and so were exposed to the same atmosphere.

Specimen 236 was removed from the dump tank subsequent to the shutdown after returning the loop potassium to the dump tank.

A similar sampling and analyzing schedule was maintained during startup and operation for the final 1750-hour period of endurance testing. The results indicate that little, if any, contamination occurred during the shutdown period. The high value for oxygen concentration found for Specimen 240 may be due to such



Figure 6. First Stage U-700 Blade Dovetail After 2000-Hour Endurance Test Showing Concentration of Accicular Structure Presumed to be Sigma Phase. (B322411)

Etchant: 3% H_2O_2

Mag: 500X



Figure 7. First Stage U-700 Blade Dovetail After 2000-Hour Endurance Test Showing Concentration of Accicular Structure Presumed to be Sigma Phase. (B322311)

Etchant: 3% H_2O_2

Mag: 2000X

All results for the determination of metallic impurities in the potassium during endurance testing are shown in Table XVIII and involve specimens 225 through 290. The data are reported as ppm in potassium chloride. The high values found for calcium concentration are fallacious. By a long process of elimination it was finally discovered that the source of the calcium was a red rubber bulb on a hydrochloric acid dispenser which was used in the preparation of potassium chloride from the potassium specimens. The potassium chloride prepared as Specimens 225A, 289A, and 290A was prepared without using the dispenser, whereas in the preparation of Specimens 225, 289B and 290B the dispenser was used. These data indicate that the concentrations of all impurity elements considered probably remained at very low levels through the endurance test. The reduction in the concentrations of aluminum and silicon noted for Specimens 225A, 289A, 289B, 290A and 290B is evidently not associated with the high calcium. This has not been explained.

The analytical data presented indicate that the potassium passed through the turbine was of extremely high purity except during startup. This is confirmed by the fact that only relatively small quantities of impurities were picked up by the refractory alloy metal specimens during the testing. This is especially evident when it is realized that during the 2000-hour endurance run about ten million pounds of potassium were passed through the turbine.

VIIIL CONCLUSIONS AND RECOMMENDATIONS

The experiences and information gained during the construction, assembly, operation and evaluation of the turbine led to the following principal conclusions and recommendations:

1. The non-refractory alloys and materials used in the two stage turbine have demonstrated their adequacy for this application. No significant changes in materials or processes are required for further turbine testing.

2. While gross turbine blade solution corrosion was produced by a deliberately introduced coarse spray of liquid potassium into the turbine and possible liquid droplet carry-over from the boiler, these effects were readily eliminated in subsequent testing by eliminating the spray, more effectively filtering the potassium vapor from the boiler, and by modifying the boiler operating procedure.

3. Probably limited amounts of metal were transferred from the boiler to the turbine when metal solute within liquid metal droplets was carried from the boiler. This situation has been greatly improved by operating the boiler liquid level at a lower position within the upper header and by the use of an additional separator at the boiler outlet. While some minor mass transfer may still be expected in future testing, it should not represent a hazard to the safety of the turbine.

4. Impact erosion, which produced loss of metal by mechanical damage, was positively identified in only one instance: Stationary U-700 erosion test inserts located behind the trailing edge tips of the second stage blades developed significant impact erosion pits during the 2000-hour endurance test.

5. The "gettering" types of refractory alloys, such as the columbium base alloys, are readily contaminated with carbon, oxygen and nitrogen in the Type 316 stainless steel turbine facility; however, molybdenum alloys are much more resistant to such contamination.

6. The chemical analytical data obtained for the oxygen and metallic impurity concentrations in the potassium used in the turbine loop indicate that the analytical techniques applied are adequate for monitoring the potassium

for these impurity elements. In order to quickly determine whether or not there is an air leak in those portions of the system which operate below atmospheric pressure, it is recommended that the oxygen concentration be determined continuously using an indicating galvanic cell type oxygen meter or other device in the loop system.

7. The data obtained for carbon concentrations in potassium are confusing due to the lack of reproducibility and to the discrepancy noted between the carbonate carbon values and the oxide values. However, those data for carbon obtained most recently, using techniques developed in General Electric Company, Space Power and Propulsion Section Laboratories, are in much better agreement with the oxygen data and indicate that the carbon content of the potassium was quite low, about 20 ppm.

8. It is clear, from the carbon and oxygen analyses, that the potassium can become contaminated by turbine malfunctions, by in-leakage of air, or by opening the loop for repair or replacement of parts. However, the data also show that the gettering and distillation processes, which take place during operation of the loop act as a "self-cleaning" process to quickly reduce the impurity levels to very low values.

9. The testing program has demonstrated that a stainless steel test facility can successfully be used to evaluate molybdenum alloy turbine components for Rankine Cycle power generating systems at inlet temperatures near 1500°F and rotor blade tip velocities to 765 ft/sec.

REFERENCES

1. Semmel, Jr., J. W., Nichols, H. E., Yount, R. E., and Frank, R. G., "Two Stage Potassium Test Turbine-Volume I, Materials Support," GE63FPD238, Contract NAS 5-1143, May 8, 1963.
2. Chang, W. H., "A Study of the Influence of Heat Treatment on the Micro-structure and Properties of Refractory Alloys," ASD TDR-62-211, April 1962, p. 86.
3. Prater, T. A., "Recrystallization Behavior of a Dispersion Hardened Molybdenum Base Alloy," Reactive Metals, Interscience Publishers, (AIME), New York, 1958, p. 207.
4. Chang and Perlmutter, I., "Solution and Aging Reactions in Molybdenum Base Alloys," Proc. High Temp. Metals Conference, Detroit, Michigan, April 1961.
5. Harrison, R. W., and Delgrosso, E. J., "Low Pressure Oxidation of Columbium-1 Zirconium," CNIM-5351, United Aircraft Corporation, April 20, 1964.
6. Frank, R. G., "Materials for Potassium Lubricated Journal Bearings," Qtrly. Progress Report #3, NASA Contract NAS 3-2534, NASA-CR-64073, January 22, 1964.
7. "Basic Investigation of Turbine Erosion Phenomena," Anon., WANL-PR(DD)-009, Contract NAS 7-390, February, 1966, p. 9.
8. Hays, L. G., "Turbine Erosion Research in Great Britain," Tech. Memo. No. 33-271, Jet Propulsion Laboratory, Pasadena, California, March 1966.
9. Kulp, R. S., and Altieri, J. W., "Cavitation Damage of Mechanical Pump Impellers Operation in Liquid Metal Space Power Loops," NASA-CR-165, July 1965.
10. Robinson, M. J., and Hammitt, F. G., "Technical Report No. 16 on the Detailed Flow Structure and the Corresponding Damage to Test Specimens in a Cavitating Venturi," 03424-16-T, NS G-3960, University of Michigan, August 1965.
11. Hammitt, F. G., University of Michigan, Personal Communication, 3/10/66.
12. Kovacevitch, E. A., "Erosion Properties of Selected Turbine Materials in Water and Potassium," AFAPL-TR-65-130, January 1966.
13. DeStefano, J. R., and Hoffman, E. E., "Corrosion Mechanisms in Refractory Metal - Alkali Metal Systems," Section IV of the Science and Technology of Tungsten, Tantalum, Molybdenum, Niobium and Their Alloys, Edited by N. E. Promisel, Pergamon Press, New York, 1964.
14. DeVan, J. H., and Hoffman, E. E., Work Done at Saclay Reported in Foreign Trip Report, June 4-28, 1962, ORNL Central Files, Number 63-12-66.

15. DeVan, J. H., Hoffman, E. E., Scott, J. L. and Manly, W. D., "Mass Transfer Studies in High Temperature Sodium and NaK Systems," presented at the Sixth Annual Corrosion Symposium, Battelle Memorial Institute, June 18-20, 1957.
16. Lyashenko, V. S. and Nezorov, B. A., "The Mechanism of Carbon Transfer in Liquid Sodium," Conference on the Corrosion of Reactor Materials, International Atomic Energy Agency, Vienna, CN-13/41, (1962).
17. Andrews, W. J., "Carburization of Austenitic Stainless Steel in Liquid Sodium, NAA-SR-5282, September 1, 1960.
18. Pepkowitz, L. P., and Judd, W. C., "The Determination of Sodium Monoxide in Sodium," Anal. Chem. 22, 1283 (1950).
19. Kallman, S., and Liu, R., "The Determination of Total Carbon and Sodium Carbonate in Sodium Metal," Analytical Chemistry 36 590 (1964).

TABLE I

ROOM TEMPERATURE

TENSILE PROPERTIES OF U-700 TURBINE BLADE MATERIALS

BEFORE AND AFTER 2000-HOUR ENDURANCE TEST

<u>First Stage Blade No.</u>	<u>Turbine Test Temperature °F</u>	<u>UTS (ksi)</u>	<u>.2%YS (ksi)</u>	<u>%E</u>	<u>%RA</u>
45	1360	175	121	12	13
56	1360	175	125	12	10
58	1360	178	125	10	9
<u>Second Stage Blade No.</u>					
1	1260	191	131	10	17
20	1260	198	130	12	19
58	1260	199	141	15	15
<u>Heat Treated Blade Blank</u>					
A	Untested	185	124	19	18
B	Untested	190	129	17	18
C	Untested	188	125	20	18

TABLE II
COMPARATIVE PROPERTIES OF TZM, F-48, AS-30, TZC, AND Cb-132M

ALLOY	Test Temp.-°F	0.2% Yield Strength - psi	Ultimate Strength - psi	Elong. in 1" - %	Reduction in Area - %
<u>TZM</u>					
Stress Relieved 1 Hr./2300°F	RT	104,000	110,000	24	58
Stress Relieved 1 Hr./2300°F	1400	81,000	88,000	14	83
<u>F-48</u>					
Stress Relieved 1 Hr./2500°F	RT	101,000	116,000	21.2	31.9
Stress Relieved 1 Hr./2500°F	1400	59,000	87,000	22	50
<u>AS-30</u>					
Stress Relieved 1 Hr./1900°F	RT	100,000	127,000	13	30
Stress Relieved 1 Hr./1900°F	1400	75,000	90,000	8	55
<u>TZC</u>					
As Rolled at 2912°F	RT	97,800	103,100	1	1
As Rolled at 2912°F	1400	58,700	66,400	14	74
<u>Cb-132M</u>					
Stress Relieved 1 Hr./2200°F	RT	-	121,500	0.3	0.5

Note: See Tables VI and VII for further TZC data. The poor ductility of Cb-132M and its sensitivity to cracking was the reason for its limited evaluation.

Tests were performed on an Instron tensile test machine at a crosshead speed of 0.005 in/in/min up to the yield point, then at 0.05 in/in/min to failure.

TABLE III

Cb-132M RAW MATERIAL DATA AND
PROCESSING HISTORY

PIECES RECEIVED:

Piece #1: 0.6" x 3" x 5 1/4"

Piece #2: 0.6" x 3 3/8" x 3 7/16"

SOURCE:

Universal Cyclops Steel Corporation

HEAT NO:

KCl416

COMPOSITION:

Cb, 19.77 Ta, 14.93W, 5.07 Mo, 2.18 Zr, 0.10 C, 120 ppm Si, 100 ppm Fe, 50 ppm Cu, 20 ppm Pb, 2 ppm Mn, 32 ppm O₂, 49 ppm N₂, 19 H₂.

REPUTED PROCESSING HISTORY:

- EB Melted
- Vacuum Arc Remelted
- Extruded Above 3100°F at 2.8 to 1 Reduction (64%)
- Heat Treated 4 Hours at 2800°F.
- Cross Rolled at 2400°F to about 50% Reduction in Area.
- As Received Condition:

Structure - Equiaxed.

Grain Size - ASTM 0 to 00.

Hardness - R_A 65.5 after 2200°F S.R. (305 DPH)

TABLE IV
TZC RAW MATERIAL DATA AND
PROCESSING HISTORY

PIECES RECEIVED:

Piece #1 1 1/2" x 3/4" x 4"

Piece #2-8; 1 1/2" x 1 1/4" x 3/4" (on order, June 22 delivery)

SOURCE:

General Electric Company, Lamp Metals and Components Department

HEAT NO:

RMP No. 89

COMPOSITION:

Mo, 1.1 Ti, 0.13 Zr, 0.13 C, 100 ppm Cb, 18 ppm Si, 10 ppm each Pb, V, Sn, 8 ppm Al, 13 ppm Fe, 5 ppm Co, 2 ppm each Cu and Mg, 1 ppm each Mn, Ni and Cr, 4 ppm O₂, 1 ppm N, 1 ppm H₂.

PROCESSING HISTORY:

- Vacuum arc melted to 5" diameter finish machined ingot.
- Extruded at 1700°C (3092°F) at 2.3 to 1 reduction to 4 1/8" x 2.22" sheet bar
- Cross Rolled at 1600°C (2912°F) to 0.740" thick plate
- As received condition:

Structure - fibrous in both extruded and
rolled directions.

Hardness - R_A 61.0 (245 DPH)

TABLE V

Cb-132M AND TZC ROOM TEMPERATURE AND ELEVATED TEMPERATURE TENSILE TEST RESULTS

Material	Specimen	Condition**	Test Temp. - °F	0.2% Load- Time Dev. - ksi	Ult. Str. - ksi	Elong. - %	Reduct. in Area - %
Cb-132M	6	A; S.R.2200°F	RT	----	79.7	0	0
Cb-132M	12	A; S.R.2200°F	RT	----	121.5	0.3	0.5
Cb-132M*	9	C; S.R.2600°F, Pickled	RT	----	96.4	0	0
TZC	1	B; As Rolled	RT	97.8	103.1	1.0	1.0
TZC	2	B; As Rolled	RT	----	103.0	0.2	0.5
TZC	25	B; As Rolled	RT	81.2	97.4	1.0	1.0
TZC	26	B; As Rolled	RT	84.5	88.0	1.0	0
TZC	20	B; As Rolled	150	83.7	107.0	6.0	9.0***
TZC	22	B; As Rolled	150	72.5	104.0	10.0	17.0
TZC	23	B; As Rolled	150	73.3	97.4	13.0	38.0
TZC	21	B; As Rolled	1400	58.7	66.4	14.0	74.0
TZC	24	B; As Rolled	1400	61.8	69.0	11.0	53.0
TZC	17	E; As Rolled & Pickled	RT	89.0	108.0	6.0	7.0***
TZC	18	E; As Rolled & Pickled	150	71.0	103.0	18.0	41.0
TZC	16	E; As Rolled & Pickled	250	61.2	91.6	16.0	38.0
TZC	19	E; As Rolled & Pickled	1400	60.0	68.0	8.0	53.5
TZC	4	D; Aged 2750°F & Pickled	RT	67.8	99.5**	7.0	10.0****
TZC	15	D; Aged 2750°F & Pickled	RT	74.0	99.0	7.0	10.0
TZC	14	D; Aged 2750°F & Pickled	250	53.3	86.5	18.0	40.0
TZC	13	D; Aged 2750°F & Pickled	1400	47.6	58.5	13.0	54.0
TZC	3	D; Aged 2750°F & Pickled	1400	51.1	60.3	14.2	58.5
TZC(Prater)	--	F Annealed 2400°F	RT	111.5	135.5	22.0	--

*/Condition

- A. Hot rolled at 2400°F, ultrasonically inspected, machined by stress-free grinding, stress relieved 1 hour at 2200°F, Zyglo inspected.
- B. Hot rolled 2912°F, ultrasonically inspected, machined by stress-free grinding, Zyglo inspected.
- C. "A", above, plus 1 hour at 2600°F at 10^{-5} torr, pickle in 20 HF - 20 HNO₃ - 60 H₂O to remove 0.001 inch of surface.
- D. "B", above, plus 25 hours at 2750°F at 10^{-5} torr, pickle in 85 HNO₃ - 15 H₂SO₄ - 5 H₃PO₄ - 2 HF to remove 0.0005 inch of surface.
- E. "B", above, plus pickle in 85 HNO₃ - 15 H₂SO₄ - 5 H₃PO₄ - 2 HF to remove 0.0005 inch of surface.
- F. Worked at 2462°F (1350°C), annealed at 2400°F.

*Specimens 1, 2, 6, and 12 were tested at 0.05 inch/inch/minute, crosshead speed to 0.6% elongation; all others were tested at 0.005 inch/inch/minute.

**Fracture did not occur at minimum area.

***0 at break.

****3.5 at break.

TABLE VI

TRANSVERSE AND AGED TENSILE PROPERTIES OF TZC ALLOY*

<u>Condition</u>	<u>Temp. °F</u>	<u>0.2% Yld. Str.</u> <u>- psi</u>	<u>Ultimate</u> <u>Str. - psi</u>	<u>Elong.</u> <u>- %</u>	<u>R. A.</u> <u>- %</u>
Transverse to	150	76,000	89,300	1.8	4.9
Rolling	150	55,500	68,700	15.1	68.7
Direction	1400	66,300	70,600	9.3	50.7
Aged 1,000	150	71,300	96,400	5	6
Hours At	250	67,500	92,000	19	33.5
1400°F	1400	54,300	66,900	14	58.5
	1400	56,500	68,200	17	71.0

*G.E. Heat RMP-89, As-Received

TABLE VII
WEIGHT CHANGE AND CHEMICAL ANALYSIS EVALUATION OF REFRACTORY ALLOY
PROBE SPECIMENS AFTER TURBINE PERFORMANCE TESTING

Specimen No.	Material	Original	Final	Wt. Change	Location*	Chemical Analyses -ppm			
		Wt.-gr.	Wt.-gr.	- gr.		C	O	N	H
Run #1 - 12 Hours Above 1400°F (March, 1965):									
1	F-48	9.2162	9.1885	-0.0277	Surface	340	309	155	6
					Core	240	55	22	4
					As-Rec'd	270	34	70	1
2	F-48	9.1781	9.1704	-0.0077	Reinstalled in Run #2				
3	TZM	10.0498	10.0467	-0.0031	Surface	210	35	13	2
					Core	180	37	6	1
					As-Rec'd	200	12	4	1
4	TZM	10.0259	10.0227	-0.0032	Reinstalled in Run #2				
5	AS-30	9.2701	9.2521	-0.0180	Reinstalled in Run #2				
6	AS-30	9.2513	9.2125	-0.0388	As-Rec'd	710/1040	79/50	180/210	7/10
					Contaminated in Welding; Reinstalled in Run #2				
Run #1 and #2 - 68 Hours Above 1400°F (March to May - 1965):									
1-5	AS-30	9.2491	9.2371	-0.0120	Surface	1180/1210	557	379	16
					Core	1170/1100	95	183	13
2-2	F-38	9.2491	9.2371	-0.0256	Surface	580	257	183	14
					Core	270	38	28	9
3-4	TZM	10.0224	10.0229	+0.0005	Surface	210	49	15	2
					Core	160	25	6	1
Run #2 only - 56 Hours Above 1400°F (May - 1965):									
4	F-48	8.8727	8.8554	-0.0173	Surface	410	397	169	16
					Core	290	115	54	10
5	TZM	9.5042	9.5045	+0.0003	Surface	980	31	9	1
					Core	170	20	2	1
6-6	AS-30	9.2091	9.1375	-0.0716	Surface	1160/1100	562	305	14
					Core	1120/1120	120	186	13

* Surface analyses were performed on specimens machined from the test rings to leave the original surface to a depth of 0.030-inch. Core analyses were made on specimens machined to remove surface material to a depth of 0.030-inch.

NOTE: The protective sleeve over the first 3 specimens was coated with a metallic deposit during Run #2. This may have influenced the pickup of contaminating gases and resulted in generally lower contamination of F-48 Specimen 2-2 as compared to Specimen 4.

See also Tables IX and X for additional data on other tests.

TABLE VIII

TENSILE PROPERTIES OF TZC SPECIMENS AFTER
EXPOSURE IN A LIQUID POTASSIUM-CARBON MIXTURE
FOR 100 HOURS AT 1400°F

<u>Test Temp.</u> <u>- °F</u>	<u>Ultimate Strength</u> <u>- psi</u>	<u>0.2% Yld. Strength</u> <u>- psi</u>	<u>Elong.</u> <u>- %</u>	<u>R. A.</u> <u>- %</u>
150	72,600	72,600	0	0
500	62,200	62,200	0	1
650	70,900	63,400	0	1
1200	69,200	65,500	13	52

Note: Tensile tests were performed in a vacuum of 1×10^{-6} torr at a crosshead rate of 0.005-inch per minute to 0.6% load-time deviation and then at a rate of 0.05-inch per minute to failure.

TABLE IX
WEIGHT CHANGE AND CHEMICAL ANALYSIS EVALUATION OF REFRACTORY
METAL PROBE SPECIMENS AFTER 254 HOURS OF TURBINE ENDURANCE RUN

Specimen No.	Material	Original Wt.-gr.	Final Wt.-gr.	Wt. Change - gr.	Location*	Chemical Analyses -ppm			
						C	O	N	H
Probe I Located at Station 1 (1520°F):									
I-1	TZC	9.7607	9.7611	+0.0004	Continued on Test				
I-2	TZM	9.6369	9.6371	+0.0002	" " "				
I-3	F-48	9.1933	9.1550	-0.0383	" " "				
I-4	TZC	9.6353	9.6355	+0.0002	Surface	980			
						1060			
					Core	1460			
						1800			
						1400			
I-5	TZM	9.9288	9.9290	+0.0002	Surface	150/70	30	5	3
					Core	340/230	46	5	2
I-6	F-48	9.2441	9.170	-0.0741	Surface	550/470	172	278	7
					Core	240/350	28	21	6
Probe II Located in the Condenser (1260°F):									
II-1	TZC	9.7246	9.7234	-0.0012	Surface	1280			
						1300			
					Core	1460			
						1480			
II-2	TZM	9.8626	9.8621	-0.0005	Surface	220/210	31	12	3
					Core	270/170	39	5	2
II-3	F-48	9.3720	9.2860	-0.0860	Surface	440/260	77	95	6
					Core	230/170	30	5	5
II-4	TZC	9.6495	9.6490	-0.0005	Surface	1170/1260			
						2850/1180			
						4730**			
II-5	TZM	9.7889	9.7884	-0.0005	Core	1450/1400			
II-5	TZM	9.7889	9.7884	-0.0005	Surface	320/280	31	37	2
					Core	250/250	42	4	2
II-6	F-48	9.1358	9.0275	-0.1083	Surface	490/530	65	111	5
					Core	270/370	42	24	4
As-Received Specimens:									
	TZC					1470			
						1760			
	TZM					1490	5	1	1
	F-48					200	12	4	1
						270	34	70	1

* Surface analyses were performed on specimens machined from the test rings to leave the original surface to a depth of 0.030-inch. Core analyses were made on specimens machined to remove surface material to a depth of 0.030-inch.

**High carbon analyses for the surface of specimen II-4 may have resulted from the retention of zygl inspection fluid in cracks which formed during deformation tests.

See also Tables VII and X for additional data on other tests.

TABLE X

WEIGHT CHANGE AND CHEMICAL ANALYSIS EVALUATION OF REFRACTORY ALLOY
PROBE SPECIMENS AFTER 2000 HOURS OF TURBINE ENDURANCE TESTING

Specimen No.	Material	Original	Final	Wt. Change	Location*	Chemical Analyses - ppm			
		Wt.-gr.	Wt.-gr.	- gr.		C	O	N	H
<u>Probe I Located at Station 1 (1520°F):</u>									
I-1	TZC	9.7607	9.7603	-0.0004	Surface	1100	34	21	8
					Core	1100	58	8	6
					As-Received	1490	5	1	1
I-2	TZM	9.6369	9.6369	0.0000	Surface	250/190	83	7	1
					Core	300/280	61	13	1
					As-Received	200	12	4	1
I-3	F-48	9.1933	9.1457	-0.0476	Surface	500/460	241	337	1
					Core	350/280	75	42	6
					As-Received	270	34	70	1
I-4**	TZC	9.5018	9.5019	+0.0001	Surface	1400/1600	51	5	3
					Core	1500/1800	46	6	2
I-5**	TZM	9.5885	9.5880	+0.0005	Surface	210/230	119	8	5
					Core	240/290	81	9	5
I-6**	F-48	9.3358	9.3256	-0.0102	Surface	300/500	97	156	5
					Core	210/240	22	21	4
<u>Probe III Located in the Condenser (1260°F):</u>									
III-1	TZC	9.7825	9.7821	-0.0004	Surface	1000/1100	38	6	2
					Core	1200/1100	38	6	3
III-2	TZM	9.7981	9.7980	-0.0001	Surface	160/220	66	8	2
					Core	250/270	50	7	1
III-3	F-48	9.4324	9.3687	-0.0637	Surface	580/470	116	172	4
					Core	210/190	25	13	2
III-4	TZC	9.6130	9.6133	+0.0003	Surface	1000/1100	34	4	1
					Core	1200/1200	26	2	1
III-5	TZM	9.8445	9.8442	-0.0003	Surface	170/240	18	2	3
					Core	230/190	33	5	2
III-6	F-48	9.2600	9.1905	-0.0695	Surface	320/320	131	175	6
					Core	290/280	46	20	6

* Surface analyses were performed on specimens machined to leave the original surface to a depth of 0.030-inch. Core analyses were made on specimens machined to remove surface material to a depth of 0.030-inch.

** These specimens were installed after 254 hours of the 2000-hour endurance test.

See also Tables VII and IX for additional data on other tests.

TABLE XI

COMPRESSION LOADED "C" RING TESTS FOR EVALUATION OF TZC DUCTILITY
AFTER 254 HOURS OF THE TURBINE ENDURANCE RUN

Specimen No.	Ring Thickness - Inch	Ring Length - Inch	Test Temperature - °F	Maximum Load -lbs.	Deflection - Inch	Bend Ductility
Turbine Specimens:						
I-4 (Station 1, 1520°F)	0.044	0.374	650	91	0.154	1T, 120°
II-1 (Condenser, 1260°F)	0.047	0.347	650	89	0.183	1T, 120°
II-4 (Condenser, 1260°F)	0.044	0.349	500	103	0.164	1T, 120°

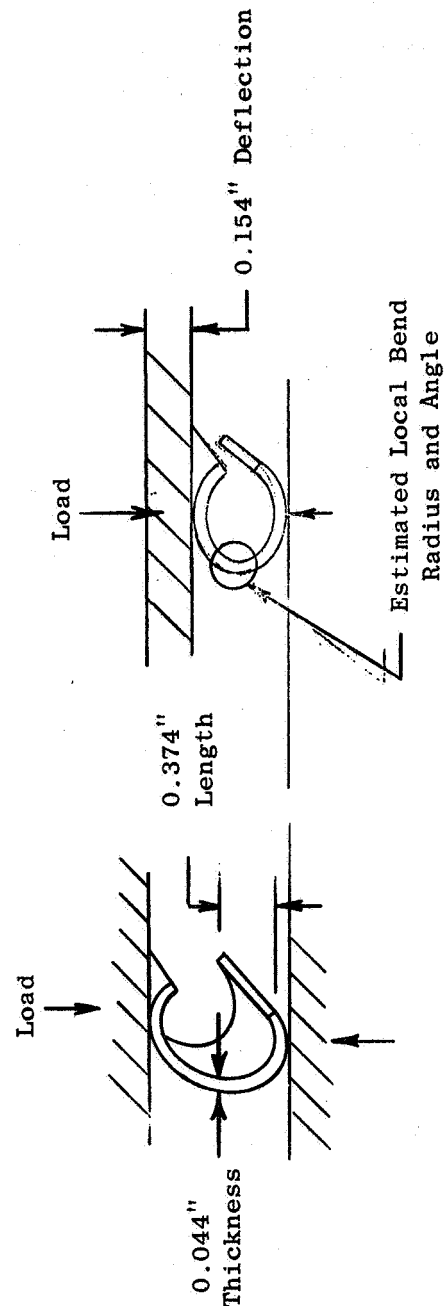


TABLE XII

TENSILE PROPERTIES OF TZC TEST BARS AGED IN VACUUM FOR 1000 HOURS AT 1400°F AND
EXPOSED TO 1260°F POTASSIUM TURBINE EXHAUST FOR 1746 HOURS OF ENDURANCE TESTING

<u>Test Temp.</u> <u>°F</u>	<u>Condition</u>	<u>Ultimate Tensile Strength - ksi</u>	<u>0.2% Yield Strength - ksi</u>	<u>Elong.</u> <u>- %</u>	<u>R. A.</u> <u>- %</u>
150	Vacuum Aged	103/107	71/83	18/6	41/9
	Turbine Tested	109	89.4	5.5	6
250	Vacuum Aged	91.6	61.2	16	38
	Turbine Tested	100/91.5	81.1/73.6	9.8/5.0	22.4/7.0
1400	Vacuum Aged	66.9	54.3	14	58.5
	Turbine Tested	64.7	58.2	15.7	70.6

TABLE XIII
RELATIVE STRENGTHS OF
U-700, TZM, and TZC ALLOYS*

<u>Alloy</u>	<u>Test Temp.</u> <u>°F</u>	<u>Condition</u>	<u>Ultimate</u> <u>Tensile</u> <u>Strength - ksi</u>	<u>0.2%</u> <u>Yield</u> <u>Strength - ksi</u>	<u>Elong.</u> <u>- %</u>	<u>R. A.</u> <u>- %</u>
U-700	RT	2125°F-2Hrs.A.C.	170	140	5	7
	1500°F	1975°F-2Hrs.A.C.	105	88	15	32
		1550°F-24Hrs.A.C.				
		1400°F-16Hrs.A.C.				
TZM	RT	Stress Relieved	108	102	24	60
	1400°F	2200°F/1 Hr.	88	80	13	83
TZM	RT	Recrystallized	81	52	22	43
	1400°F	2850°F/1 Hr.	43	27	25	92
TZC	RT	As Rolled at 1700°C	109	89	10	22
	1400°F	(3092°F)	65	58	16	70

* Data obtained from tests performed on material received for component fabrication.

TABLE XIV

EROSION INSERT WEIGHT CHANGES AFTER 2000

HOURS ENDURANCE TESTING

<u>U-700 Alloy</u>	<u>Condition</u>	<u>Wt. Before Test - gms</u>	<u>Wt. Change After Test - gms</u>	<u>Wt. Change After Vapor Blast - gms</u>
A-1	2125°F-2Hrs.A.C.	22.3236	+0.0169	-0.0241
A-2	1975°F-2Hrs.A.C.	22.6031	+0.0216	-0.0242
A-3	1550°F-2Hrs.A.C.	22.4609	+0.0124	-0.0195
	1400°F-2Hrs.A.C.			Average -0.0226
<u>TZM Alloy</u>				
B-1	Recrystallized	28.5138	+0.0096	-0.0105
B-2	2850°F/1 Hr.	28.4526	-0.0017	-0.0109
B-3*				Average -0.0107
<u>TZM Alloy</u>				
C-1	Stress Relieved	28.6116	+0.0020	-0.0087
C-2	2200°F/1 Hr.	28.5160	+0.0011	-0.0070
C-3		28.5479	+0.0024	-0.0078
				Average -0.0078
<u>TZC Alloy</u>				
D-1	As Rolled at 1700°F	28.2277	-0.0138	-0.0258
D-2	(3092°F)	28.1585	-0.0119	-0.0144
D-3		27.9436	+0.0016	-0.0063
				Average -0.0155

* This specimen was machined during final turbine assembly to fit properly; no original weight available.

TABLE XV

CHEMICAL COMPOSITION OF METAL DEPOSITS AND

COMPONENT MATERIALS IN THE

TWO STAGE TURBINE FACILITY WEIGHT PERCENT

	C. D. Nozzle Deposits *	Upper Drum Boiler Deposits	8-Inch Vapor Line Deposits- Performance Test	First Stage Wheel Deposits Endurance Test	L-605	H - 33 Braze	Type
Iron	Mi	70.4	49.5	2.8	3 Max.	---	66.5
Chromium	T	12.2	5.2	10.4	20	21	17
Nickel	Ma	8.2	38.4	58.1	10	21	12.5
Cobalt	T	8.8	----	27.4	52	46.5	----
Aluminum	T	----	----	----	--	----	----
Titanium	T	----	----	----	--	----	----
Tungsten	-	----	----	----	15	3.5	----
Others	T	----	----	----	--	Si 8.0	Si 1.0 Mo 3.0
Carbon	-	----	0.52	0.14	0.5	----	0.08

* Spectrographic Analysis

Ma - Major element, greater than 10%

Mi - Minor element, less than 10%

T - Trace element, less than 1%

TABLE XVI

WEIGHT CHANGES OF FIRST AND SECOND STAGE TURBINE
BLADES AFTER 2000 HOUR ENDURANCE TEST

<u>Turbine Blade</u>	<u>Weight Change - %</u>	
	<u>As Cleaned</u>	<u>After Vapor Blasting</u>
U-700 First Stage	+0.038	-0.304
U-700 Second Stage	+0.147	-0.019
TZM Second Stage	-0.044	-0.105

NOTE: U-700 First Stage Nominal Bucket Weight - 16.1 gr.

U-700 Second Stage Nominal Bucket Weight - 22.1 gr.

TZM Second Stage Nominal Bucket Weight - 27.8 gr.

TABLE XVII
ANALYTICAL DATA FOR OXYGEN AND CARBON IN POTASSIUM

Service No.	Sampling Date	Oxygen Analysis Date	Oxygen Data				Carbon Data				Specimen Identity and Remarks
			Sample Weight, Grams	PPM O	Weighted Average PPM O	Analytical Lab.	Sample Weight, Grams	PPM Elem. C	PPM Carbide C	PPM Total C	
35	8-26-63	8-27-63	1.607	176	154						Sample taken from fill line during transfer from shipping container #1 to dump tank
* 36	9-2-63	9-2-63	1.085	116	775						Taken from dump tank at ~500°F after initial fill
			1.621	774							
			1.380	636							
			1.086	960							
42	9-11-63	9-14-63	1.623	48							From dump tank at 500°F after hot trapping at 1100-1200°F for 110 hours
46	9-26-63	9-26-63	1.853	72	87						From dump tank after flushing loop at 500°F
			1.185	107							
			1.317	101							
47	10-1-63	10-2-63	1.915	51	44						From dump tank at 600°F after hot trapping at 1200°F 13 μ gm analytical blank subtracted
			0.242	92							From Dump tank after boiling and condensing (C-D Nozzle) in loop for a few hours after fire at flange. 11.5 μ gm analytical blank subtracted
48	10-6-63	10-7-63	1.920	16	10						From dump tank at 500°F after trying spray nozzle. Spray line hot trap plugged. It was removed. Potassium returned to loop for flush of boiler and condenser for 7 hours at 300 to 400°F.
			0.272	54							From dump tank after hot trapping at 1150°F
			1.920	105	140						From dump tank before hot flushing.
			1.048	205							
57	11-18-63	11-19-63									From dump tank at 950°F after hot flushing.
58	11-21-63	11-22-63	1.888	32.6	33						From dump tank at 580°F after hot trapping ~100 hours at 1100°F
73	4-2-64	4-2-64	1.623	68	67						From dump tank after oil contamination during hydrodynamic seal leak.
			0.641	71							
74	4-4-64	4-6-64	1.638	34	30						
			0.547	43							
75	4-9-64	4-11-64	1.105	24	24						
89	5-6-64	5-6-64				Ledoux	6.27			106	
							6.14			65	
							4.80			96	
* 93	5-15-64	5-27-64	1.646	10	17						From dump tank after 100 hours hot trapping at 1100°F
			1.157	24		Ledoux				60	
			0.540	23						58	
* 97	6-8-64	6-24-64	2.702	22	18						From dump tank after 150 hours hot trapping at 1100°F
			1.646	10		Ledoux				43	
101	7-15-64	7-16-64				Ledoux	4.2			24	From slinger seal head tank
							7.5			7	
							4.4			5	

TABLE XVII (Continued)

Service No.	Sampling Date	Oxygen Analysis Date	Oxygen Data			Carbon Data							Specimen Identity and Remarks
			Sample Weight, Grams	PPM O	Weighted Average PPM, O	Analytical Lab.	Sample Weight, Grams	PPM Elem. C	PPM Carbide C	PPM Carb. C	Total PPM C	Weighted Average PPM C	
* 102	7-15-64	7-23-64	2.194 1.079	39 43	40	Ledoux	10.8 10.7 11.2				36 53 37	42	After 6 hours of operation of turbine on vapor.
110	7-23-64	9-24-64	3.887 3.922	32 98	65	Ledoux					32 32	32	From dump tank
112	~ 9-23-64	9-26-64	3.879	4	6	Ledoux					197	200	From dump tank after hot trapping at 1000°F. Re-sampled because of high value found for #110.
115	~ 9-27-64	10-1-64	3.949	7		Ledoux					204		
116	~ 9-27-64	10-1-64	3.969 3.918	8 6	8 7	Ledoux					36 52	36 52	From dump tank before flushing loop. From dump tank after flushing loop.
117	10-5-64	10-5-64	2.021 3.920 2.010	10 14 12	13	Ledoux					199	199	From dump tank after leak.
127	10-13-64	10-13-64	1.236 3.910 2.002	26 52 43	45	Ledoux					114 119	117	From dump tank after boiler fire.
158	12-22-64	12-22-64	4.039 1.900	6 8	7	Ledoux					102 94	98	From dump tank.
179	2-8-65	2-9-65				MSAR		27 18	<5 <5	19 6	46 24	35	
* 185	3-3-65	3-3-65	3.898 1.650	74 54	68	MSAR		124 86	<5 <5	356 355	480 441	460	From dump tank after flush of boiler and condenser.
187	3-10-65	3-10-65	3.929 1.693	15 14	15	MSAR		58 61	<5 <5	132 142	190 203	196	From dump tank after 100 hours hot trapping at 1350°F.
188	4-2-65	4-2-65	3.828 2.014	10 9	10	MSAR		81 41	<5 <5	10 8	91 49	70	From dump tank at 620°F.
198	5-27-65	5-27-65	3.711 1.838	5 9	6	MSAR		33 48	<5 <5	5 5	38 53	45	From dump tank after turbine test run.
206	7-9-65	7-12-65	3.949 4.559 1.904	13 9 14	11	MSAR		55 72	<5 <5	80 76	135 158	146	From dump tank (for NASA).
* 225	9-13-65	9-13-65	1.62 2.76	26 27	27	MSAR		25 41	<0.5 <0.5	112 59	138 100	119	Zero hours on vapor. Sampled at 350°F.
						SFPS	0.32 0.51 0.30 0.43				30 13 9 19	17	
* 236	9-13-65	9-13-65	3.847 1.916 4.137 1.885	74 61 69 64	69	MSAR		17 19	<0.5 <0.5	172 189	189 208	198	Two hours on vapor. Sampled at 350°F.

TABLE XVII (Continued)

Service No.	Sampling Date	Oxygen Analysis Date	Oxygen Data				Analytical Lab.	Sample Weight, Grams	Carbon Data				Total PPM C	Weighted Average PPM C		Specimen Identity and Remarks
			Sample Weight, Grams	PPM O	Weighted Average PPM, O	PPM Carbide C			PPM Carb. C	PPM Elem. C	PPM Carbide C	PPM Carb. C				
* 227	9-13-65	9-14-65	3.871	12	14	MSAR		102	<0.5	240	342	207	Five hours on vapor. Sampled at 350°F.			
								28	<0.5	112	140					
			1.873	18				67	<0.5	166	233					
								13	<0.5	100	73	76				
						SPPS					79					
228	9-14-65	9-14-65	3.754	10	12								Ten hours on vapor. Sampled at 310°F.			
			1.713	16												
229	9-14-65	9-14-65	4.375	7	9								25 hours on vapor. Sampled at 365°F.			
			2.197	12												
230	9-15-65	9-28-65	3.883	7	8								42 hours on vapor. Sampled at 400°F.			
			1.912	8												
231	9-15-65	9-15-65	2.198	15	17								50 hours on vapor. Sampled at 350°F. High oxygen values due to leak in analytical apparatus.			
			4.04	19												
* 232	9-17-65	9-17-65	2.002	11	11	MSAR		20	<0.5	12	32	35	100 hours on vapor. Sampled at 370°F.			
								25	<0.5	14	39					
233	9-20-65	9-20-65	2.463	8	9								150 hours on vapor. Sampled at 275°F.			
			1.392	12												
234	9-22-65	9-22-65	1.58	10	11								200 hours on vapor. Sampled at 335°F.			
			2.68	12												
* 235	9-24-65	9-24-65	3.844	11	11	MSAR		21	<0.5	6	27	27	250 hours on vapor. Sampled at 320°F.			
			1.904	11				19	<0.5	7	26					
236	9-28-65	9-28-65	3.941	12	13								Sample from dump tank after shutdown - 400°F.			
			1.994	14												
* 238	10-8-65	10-8-65	4.055	7	9	MSAR		112	<0.5	154	266	132	Zero hours on vapor. Sampled at 300°F.			
								50	<0.5	87	137					
			1.697	13				11	<0.5	33	44					
								15	<0.5	68	83					
* 239	10-8-65	10-8-65	3.722	6	6								Two hours on vapor. Sampled at 360°F.			
240	10-8-65	10-8-65	2.067	13	19								Five hours on vapor. Sampled at 350°F.			
			3.941	22												
241	10-8-65	10-9-65	3.883	3	4								Ten hours on vapor. Sampled at 335°F.			
			1.822	5												
242	10-9-65	10-10-65	3.840	5	7								25 hours on vapor. Sampled at 355°F.			
			1.920	11												
243	10-10-65	10-10-65	1.932	7	5								50 hours on vapor. Sampled at 250°F.			
			3.879	4												
* 244	10-12-65	10-12-65	4.231	3	4	MSAR		50	<0.5	87	137	128	100 hours on vapor. Sampled at 250°F.			
			1.916	5				37	<0.5	82	119					

TABLE XVII (Continued)

Service No.	Sampling Date	Oxygen Analysis Date	Oxygen Data				Carbon Data										Specimen Identity and Remarks
			Sample Weight, Grams	PPM O	Weighted Average PPM, O	Analytical Lab.	Sample Weight, Grams	PPM Elem.	PPM Carbide		Total PPM C	Weighted Average PPM C					
									C	C							
246	10-14-65	10-14-65	4.317	3	4										150 hours on vapor. Sampled at 350°F.		
			2.162	4											200 hours on vapor. Sampled at 350°F.		
247	10-16-65	10-17-65	4.116	5	7												
			2.119	10													
* 248	10-18-65	10-19-65	4.051	9	9	MSAR								166	250 hours on vapor. Sampled at 250°F.		
			1.963	10										149	300 hours on vapor. Sampled at 300°F.		
249	10-21-65	10-21-65	3.847	5	5									150	350 hours on vapor. Sampled at 350°F.		
			2.123	5										182	400 hours on vapor.		
250	10-23-65	10-23-65	3.761	6	6										450 hours on vapor. Sampled at 380°F.		
			1.920	7											500 hours on vapor. Sampled at 400°F.		
251	10-25-65	10-25-65	3.908	4	5										550 hours on vapor. Sampled at 400°F.		
			1.916	6											600 hours on vapor. Sampled at 380°F.		
252	10-27-65	10-27-65	2.194	6	8										650 hours on vapor. Sampled at 350°F.		
			3.664	10											700 hours on vapor. Sampled at 400°F. High oxygen values due to contamination during sampling.		
253	10-29-65	10-29-65	2.205	7	8										747 hours on vapor. Sampled at 400°F.		
			4.407	8											800 hours on vapor. Sampled at 400°F.		
254	10-31-65	10-31-65	1.908	9	9										850 hours on vapor. Sampled at 350°F.		
			3.875	9											900 hours on vapor. Sampled at 400°F.		
256	11-2-65	11-2-65	4.109	5	5										950 hours on vapor. Sampled at 350°F.		
			2.178	7											1000 hours on vapor. Sampled at 350°F.		
259	11-4-65	11-5-65	2.209	6	6										1050 hours on vapor. Sampled at 400°F.		
			4.457	6													
260	11-6-65	11-8-65	2.272	41	43												
			4.442	44													
261	11-8-65	11-8-65	1.928	9	11												
			3.844	11													
263	11-10-65	11-10-65	3.562	8	9												
			1.760	10													
264	11-12-65	11-13-65	2.162	11	18												
			4.461	19													
265	11-15-65	11-15-65	3.765	6	7												
			1.935	8													
266	11-17-65	11-17-65	3.930	5	5												
			1.939	6													
* 267	11-19-65	11-19-65	2.229	6	7												
			4.301	7													
268	11-21-65	11-21-65	3.265	6	6												
			1.654	7													

TABLE XVII (Continued)

Oxygen Data										Carbon Data									
Service No.	Sampling Date	Oxygen Analysis Date	Sample Weight, Grams	PPM O	PPM C	Weighted Average PPM, O	Sample Weight, Grams	Analytical Lab.	Elem. C	PPM Carbide	Total PPM C	Weighted Average PPM C	Specimen Identity and Remarks						
270	11-23-65	11-23-65	4.383 2.244	5 8	6								1100 hours on vapor. Sampled at 400°F.						
271	11-25-65	11-25-65	2.276 4.426	6 7	7								1150 hours on vapor. Sampled at 390°F.						
272	11-27-65	11-29-65	3.300 1.989	10 16	12								1200 hours on vapor. Sampled at 375°F.						
273	11-29-65	11-30-65	3.394 2.200	8 15	11								1250 hours on vapor. Sampled at 400°F.						
* 274	12-2-65	12-2-65	3.140 2.033	8 10	9								1315 hours on vapor. Sampled at 400°F.						
276	12-3-65	12-6-65	3.206 1.689	6 8	7								1350 hours on vapor. Sampled at 400°F.						
277	12-5-65	12-6-65	1.697 3.292	10 13	12								1400 hours on vapor. Sampled at 400°F.						
278	12-7-65	12-8-65	2.295 1.079	11 13	12								1450 hours on vapor. Sampled at 400°F.						
279	12-10-65	12-10-65	1.060 4.367	62 67	66								1500 hours on vapor. Sampled at 415°F. High oxygen values due to contamination during sampling.						
280	12-10-65	12-10-65	1.960 1.323	17 16	17								1514 hours on vapor. Sampled at 400°F.						
* 282	12-12-65	12-13-65	2.229 1.132	9 13	10								1550 hours on vapor. Sampled at 400°F.						
* 283	12-14-65	12-14-65	2.240 1.466	11 11	11								1600 hours on vapor. Sampled at 400°F.						
286	12-16-65	12-16-65	1.361 2.405	10 16	14								1650 hours on vapor. Sampled at 410°F.						
287	12-18-65	12-20-65	2.440	7	6		SPPS					<20	1700 hours on vapor. Sampled at 405°F.						
288	12-18-65	12-23-65	1.623 3.175 0.547 2.823 1.591 2.252 1.144	6 8 19 7 9 8 12	9							<20 <20 <20	1700 hours on vapor. Sampled at 405°F. A root mean square analysis was performed on these results. The regression line for $\mu\text{gms oxygen versus grams sample}$ was, $y = 4.82x + 7.3$; i.e., $\mu\text{gms oxygen} = 4.82 \mu\text{gms/gm}$ (Sample weight in grams) $+ 7.3 \mu\text{gms}$. Therefore, the oxygen content was 4.82 ppm and the analytical blank was 7.3 $\mu\text{gms oxygen}$. The standard deviation, σ , was 1.52 μgms and the correlation coefficient, r was 0.9462.						

TABLE XVII (Continued)

Service No.	Oxygen Data			Carbon Data							Specimen Identity and Remarks	
	Sampling Date	Oxygen Analysis Date	Sample Weight, Grams	PPM O	Weighted Average PPM, O	Analytical Lab.	Sample Weight, Grams	PPM Elem. C	PPM Carbide C	PPM Total C		Weighted Average PPM C
* 289	12-20-65	12-20-65	2.229	6	5							1750 hours on vapor. Sampled at 405°F. Last sample removed from loop prior to shutdown.
			2.100	5								
* 290	12-22-65	12-22-65	2.976	6	8	SPPS	0.35			21	20	Sampled at 600°F. Sample taken from dump tank after endurance test.
			1.074	12			0.40			<20		

* Sample prepared for spectrographic analysis.

TABLE XVIII
METALLIC IMPURITIES IN POTASSIUM

Service No.	Sampling Date	Analytical Lab	Impurity Concentrations Reported as PPM in Potassium Chloride																		
			Ag	Al	B	Ba	Be	Ca	Cb	Co	Cr	Cu	Fe	Mg	Mn	Mo	Na	Ni	Pb	Si	Sn
36	9-2-63	NUMEC	<1	<2	<10	<3	<1	75	<1	<5	<5	3	75	10	5	3	<3	90	<5	<5	<25
93	5-15-64	AEFD	1	<1				<1	<1	1	<1	1	<1	1	<1	<1	15	<1	<1	1	<1
97	6-8-64	AEFD	1	10				>25	<5	<1	<1	<1	10	10	<1	<1	25	1	<5	10	<1
102	7-15-64	AEFD	5	5				>25	<1	<1	<1	<1	5	1	<1	<1	>25	<1		5	<1
185	3-3-65	AEFD	5	1				25	<5	<1	<1	<1	1	1	<1	<1	>25	<1	<1	1	<5
187	3-10-65	AEFD	1	5				>25	<1	<1	<1	<1	1	<1	<1	<1	>25	1	<1	1	<1
188	4-2-65	AEFD	5	1				1	<1	<1	<1	<1	<1	<1	<1	<1	25	<1	1	1	<1
198	5-27-65	NUMEC	3	2	<10	<3	<1	4	<5	<5	<1	<1	<5	<2	<1	<3	35	<5	<5	<25	<5
225	9-13-65	AEFD	5	>25	<25			1	<5	<5	1	1	<1	25	<1	<1	>25	<1	<5	<15	<5
225A		AEFD	5	1	<25			<1	5	<5	1	1	<1	1	<1	<1	25	<1	<5	1	<5
226	9-13-65	NUMEC	15	3	<10	<3	<1	>400	<25	<5	<5	2	<5	5	<1	<3	<50	<5	<5	<25	<5
227	9-13-65	AEFD	1	15	<25			>250	<5	<1	<1	<1	<1	5	<1	<1	>25	<1	<5	15	<5
232	9-17-65	NUMEC	<1	3	<10	<3	<1	>900	<25	<5	<5	<1	<5	7	<1	<3	<50	<5	<5	<25	<5
235	9-24-65	NUMEC	<1	<2	<10	<3	<1	>300	<25	<5	<5	<1	<5	5	<1	<3	<50	<5	<5	<25	<5
238	10-8-65	AEFD	1	15	<25			>250	<5	<1	<1	<1	<1	25	<1	<1	>25	<1	<5	>15	<5
239	10-8-65	AEFD	1	10	<25			>250	<5	<1	<1	<1	<1	10	<1	<1	>25	<1	<5	15	<5
244	10-12-65	AEFD	<1	10	<25			>250	<5	<1	<1	<1	<1	10	<1	<1	>25	<1	<5	15	<5
248	10-18-65	AEFD	<1	10	<25			>250	<5	<1	<1	<1	<1	10	<1	<1	>25	<1	<5	15	<5
267	11-19-65	AEFD	<1	10				>100	<1	<1	<1	<1	1	10	<1	<1	>100	<1	<10	10	<5
274A	12-2-65	AEFD	<1					>250	<5	<1	<1	<1	1	10	<1	<1	>25	<1	<5	5	<5
274B		AEFD	<1					250	<5	<1	<1	<1	<1	5	<1	<1	>25	<1	<5	5	<5
282	12-12-65	AEFD	<1	5	<25			>250	<1	<1	<1	<1	<1	10	<1	<1	25	<1	<5	15	<5
283	12-14-65	AEFD	<1	5	<25			>250	<1	<1	<1	<1	<1	10	<1	<1	25	<1	<5	1	<5
289A	12-20-65	AEFD	<1	1	<25			>250	<5	<1	<1	<1	<1	1	<1	<1	25	<1	<5	1	<5
289B		AEFD	<1	1	<25			250	<5	<5	1	<1	1	5	<1	<1	25	<1	<5	1	<5
290A	12-22-65	AEFD	5	1	<25			>250	<5	<5	<1	1	<1	1	<1	<1	>25	<1	<5	1	<5
290B		AEFD	5	1	<25			250	<5	<5	<1	<1	<1	5	<1	<1	>25	<1	<5	1	<5

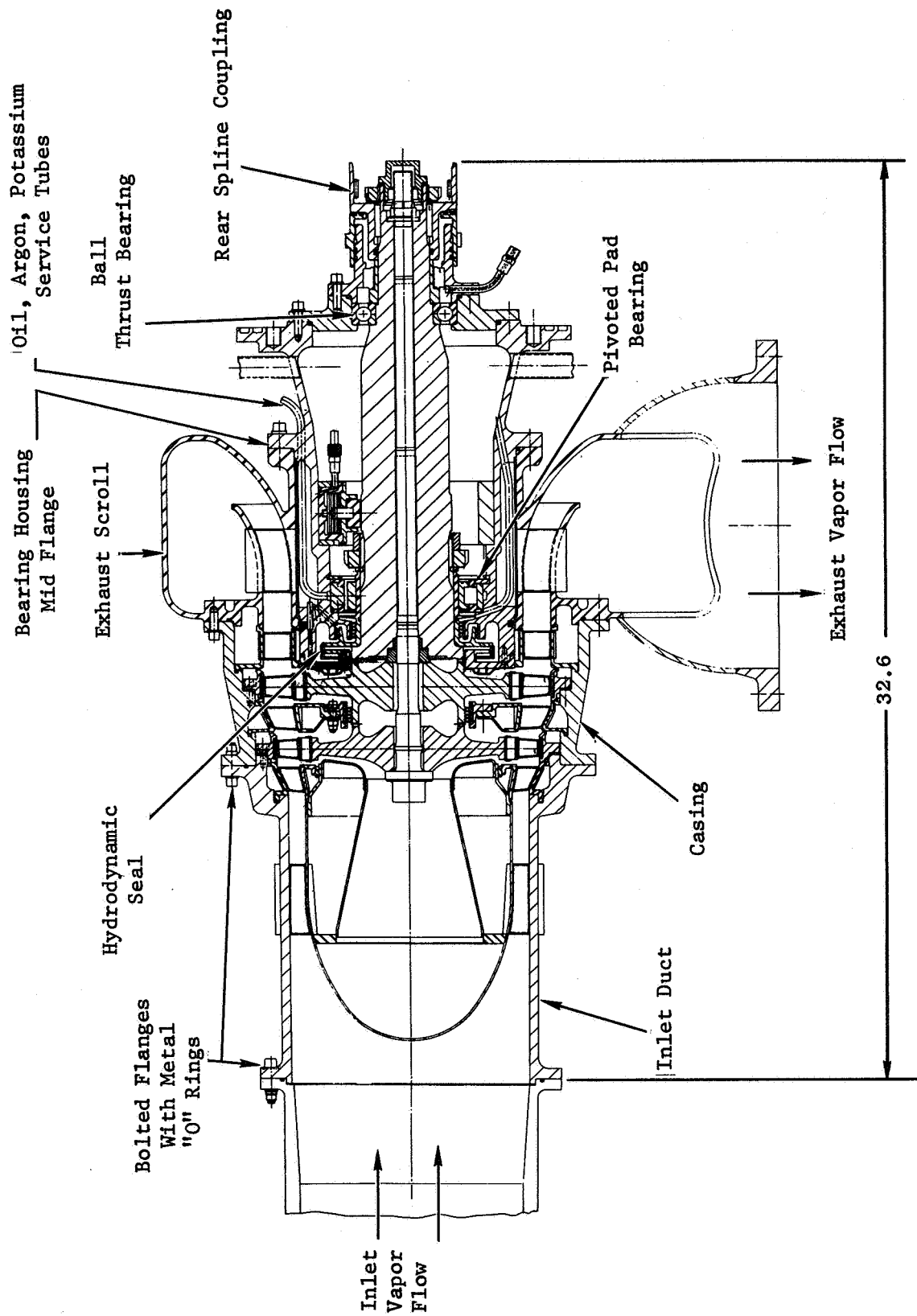


Figure 1. Cross Sectional View of Potassium Test Turbine Showing the Original Design.

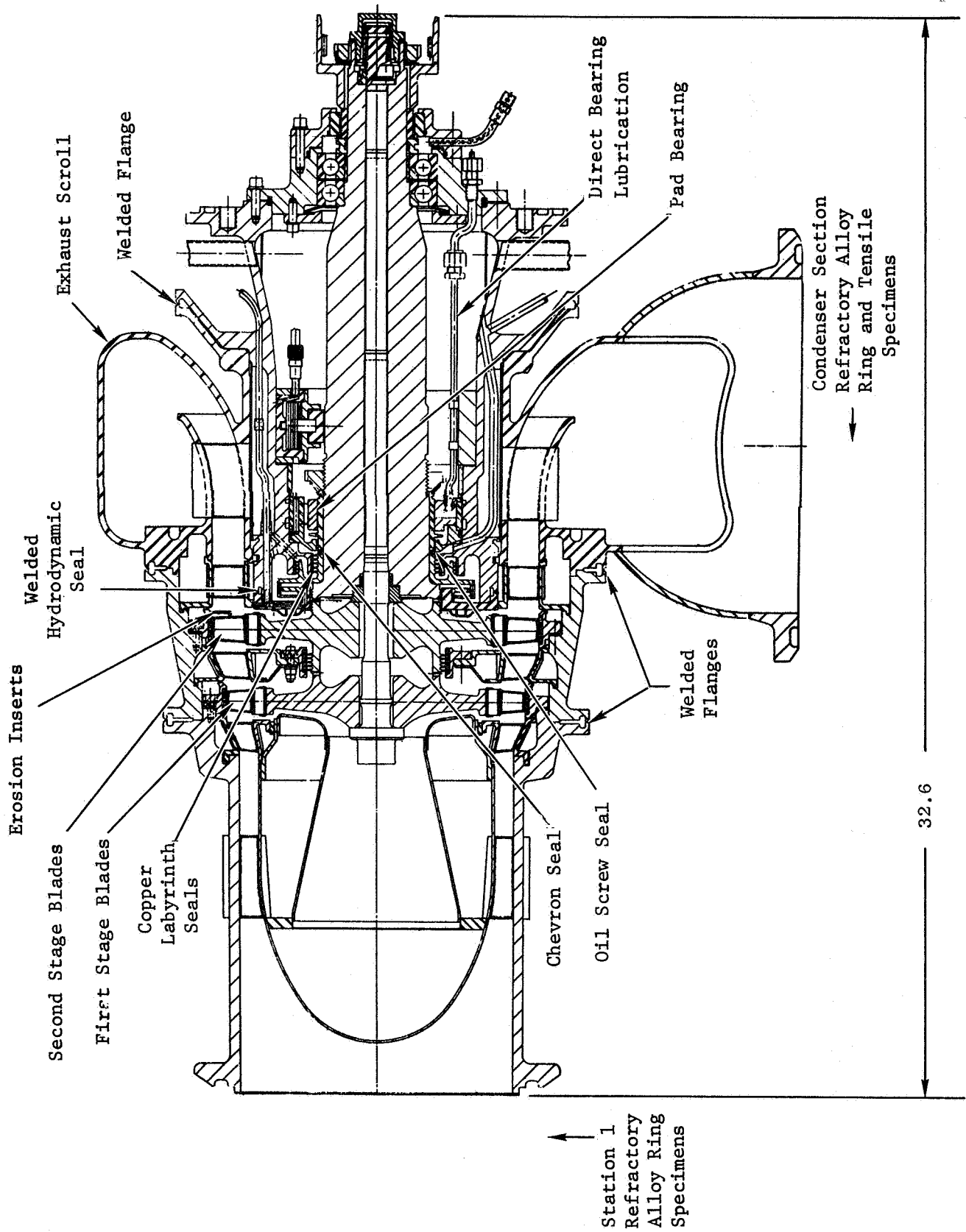


Figure 2. Cross Sectional View of Potassium Test Turbine Showing Final Design.

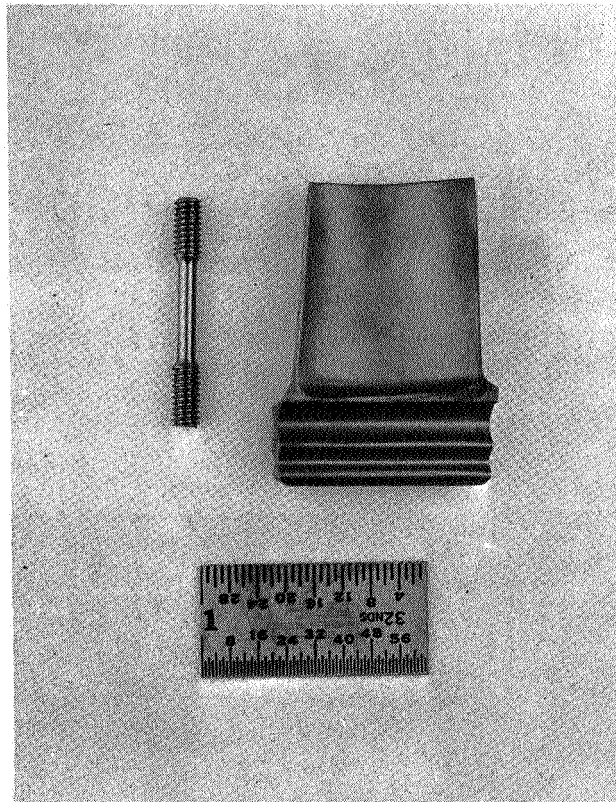


Figure 3. Miniature Tensile Bar Taken From a Second Stage U-700 Blade After 2000 Hours Test at 1260°F. A Second Stage U-700 Blade is Shown for Comparison. (MCRA 3043)

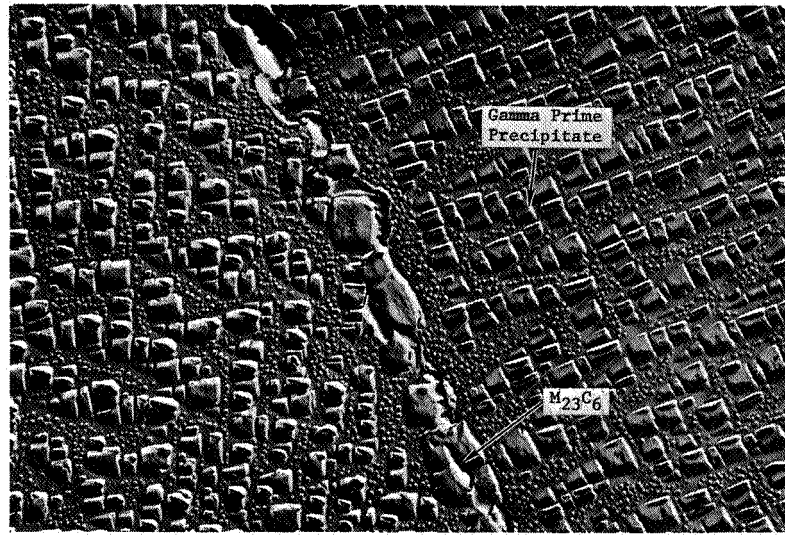


Figure 4. Electron Micrograph of a U-700 First Stage Blade Before Testing and in the Fully Heat Treated Condition. (A7501)

Carbon Replica

Mag: 10,000X

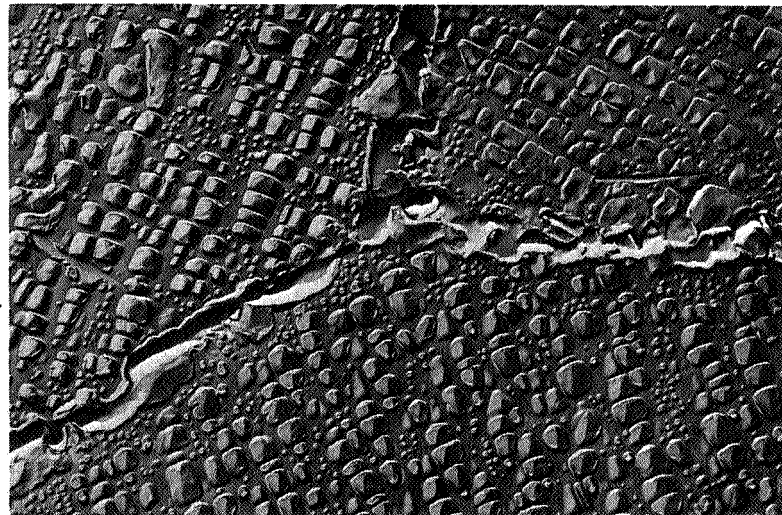


Figure 5. Electron Micrograph of a U-700 First Stage Blade After 2000-Hour Endurance Test at Approximately 1450°F. Note Coalescence of Gamma Prime Precipitate Within Grains and Growth of Intergranular M₂₃C₆ Carbides. (B3215)

Carbon Replica

Mag: 10,000X

contamination, but it is more probable that it was due to contamination during sampling or analysis. The high values found for Specimens 260 and 279 were definitely due to contamination during sampling. It should be pointed out that whenever a high oxygen value was found, the loop was resampled as soon as possible.

Specimen 288 was intentionally larger so that a statistical analysis of multiplicate analytical results could be made. This statistical investigation of the relationship between the oxygen found and the sample weights produced the regression line:

$$\mu \text{ gms } O = 4.82 \mu \text{ gms/gm (Sample Wt. in gms)} + 7.3 \mu \text{ gms}$$

That is, the oxygen concentration was 4.82 ppm and the analytical blank was 7.3 micrograms. The standard deviation, σ , was 1.52 micrograms. The correlation coefficient, r , indicating a linear relationship between the weight of oxygen found and the sample weight, was 0.946.

If the analytical blank determined for Specimen 288 is generally applicable to all analyses, then all values reported for oxygen concentration are somewhat high, and it may be concluded that the oxygen content of the potassium passing through the turbine was exceptionally low, on the order of 5 ppm or less.

The generally high values found for the carbon content of the potassium, particularly carbonate carbon, are virtually impossible to explain. Recently, during the development of the analytical method for total carbon, Specimens 225 and 227 were reanalyzed by SPPS personnel (See Table XVII). In neither case were the high values reported by MSAR confirmed.

More recently, eight additional samples of potassium from Specimen 225 were analyzed. The average value for total carbon was 28 ppm. The standard deviation, σ , was 5 ppm. The percent recovery of carbon added as potassium carbonate was 94% for four samples.

This carbon analysis problem is still under investigation.

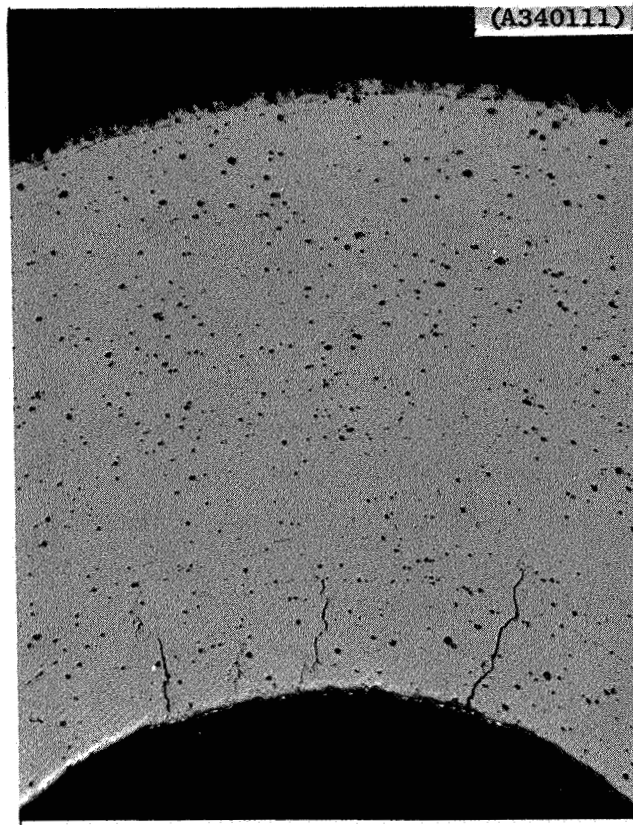


Figure 8. Forward Radius of Rene' 41 Turbine Blade Locking Strip Showing Strain Age Cracking. (A340111)

Etchant: None

Mag: 100X

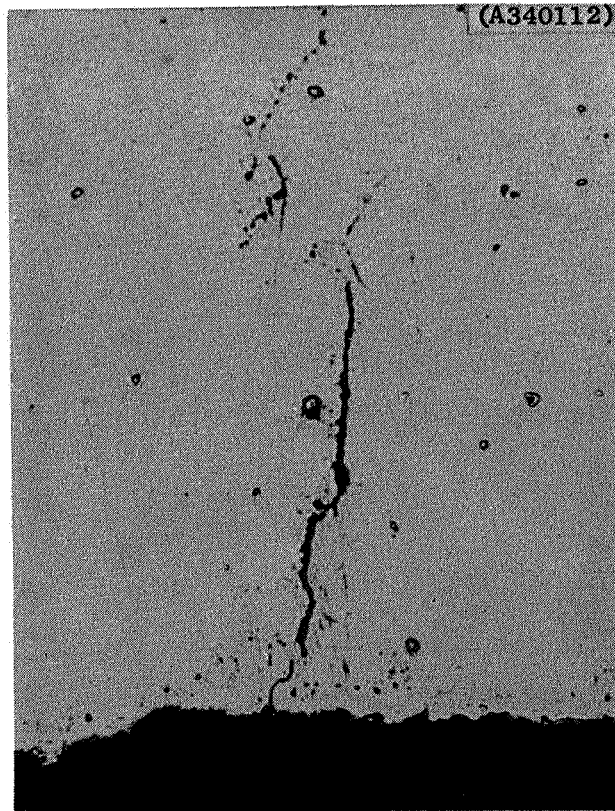


Figure 9. Forward Radius of Rene' 41 Turbine Blade Locking Strip Showing Strain Age Cracking. (A340112)

Etchant: None

Mag: 500X

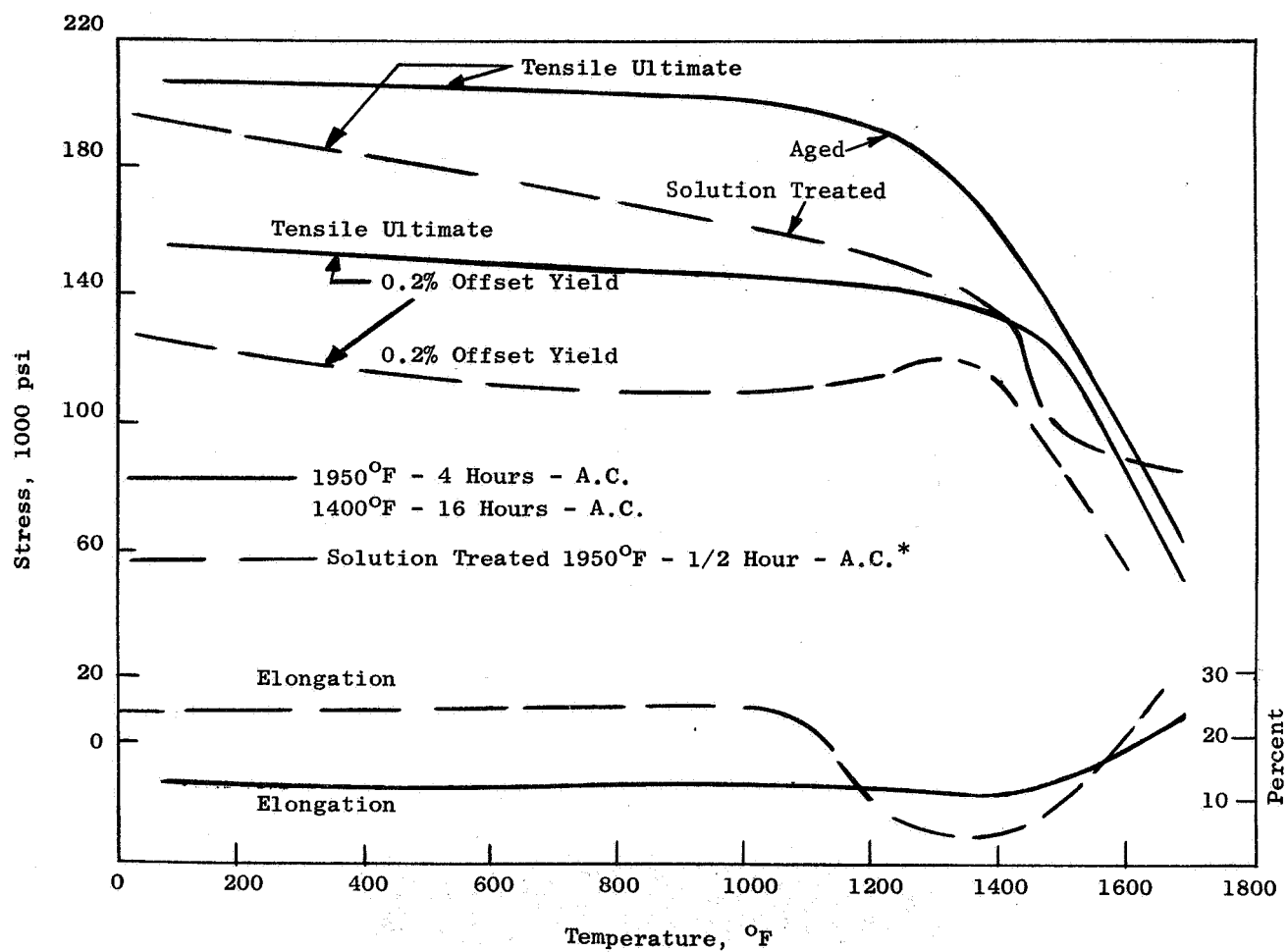
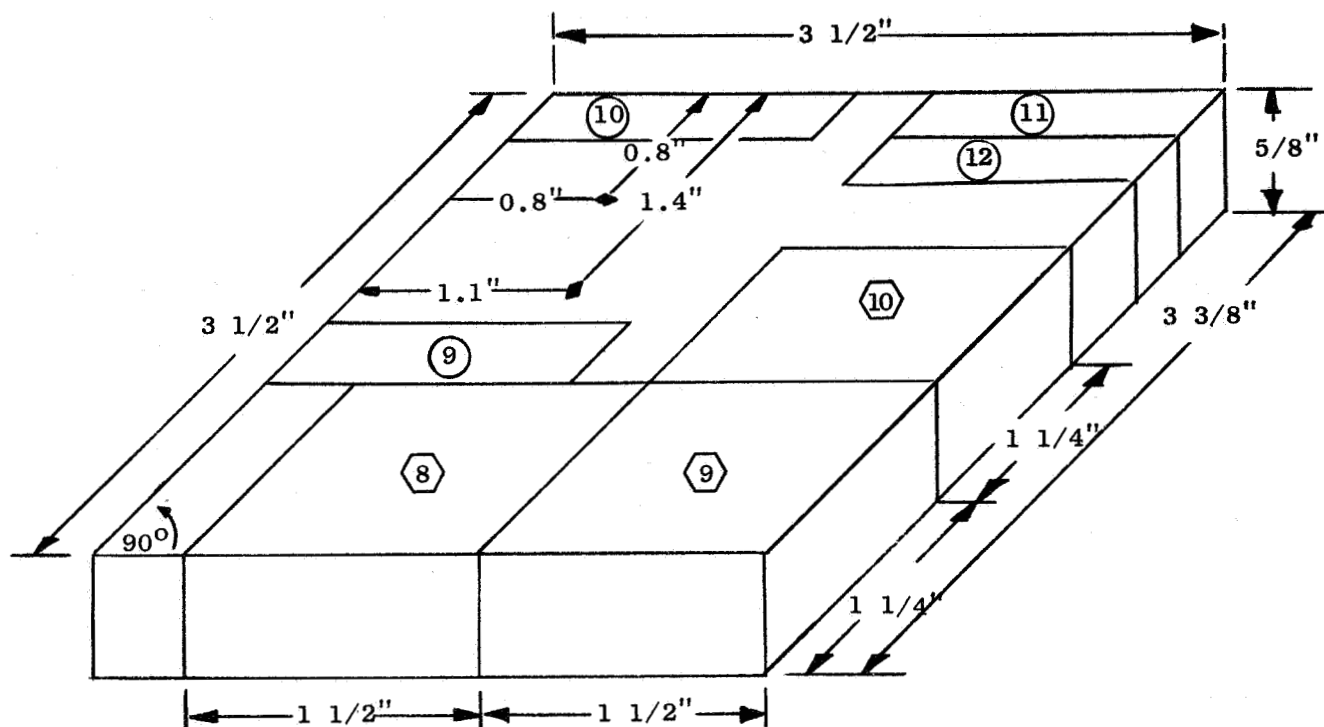


Figure 10. Rene' 41 Tensile Properties

*Barker, J.F., "Solution Treated Properties of R-41 Alloy," General Electric Company, Report DM57-187, dated 12-6-57.






-  Blade Blank
-  Test Specimen
-  Location of Internal Defect

Figure 12. Cb-132M Refractory Alloy Blade and Test Specimen Layout - Second Piece.

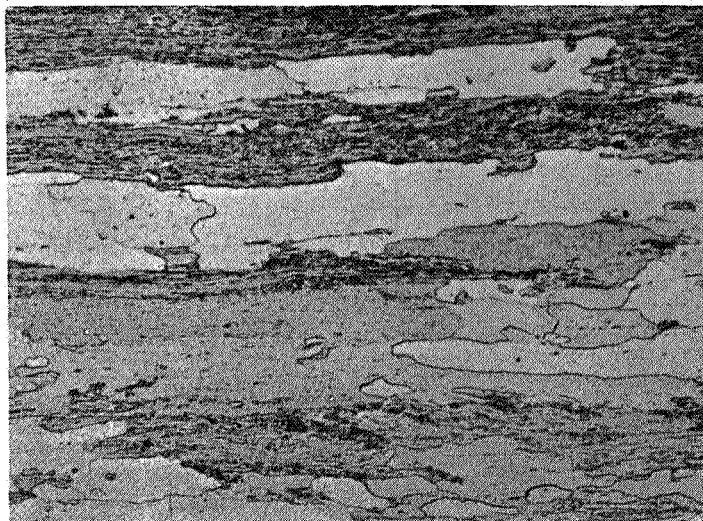


Figure 13. Longitudinal Photomicrograph of TZC Alloy, As Received.
(A290111)

Etchant: As Polished (H_2O_2)

Mag: 100X

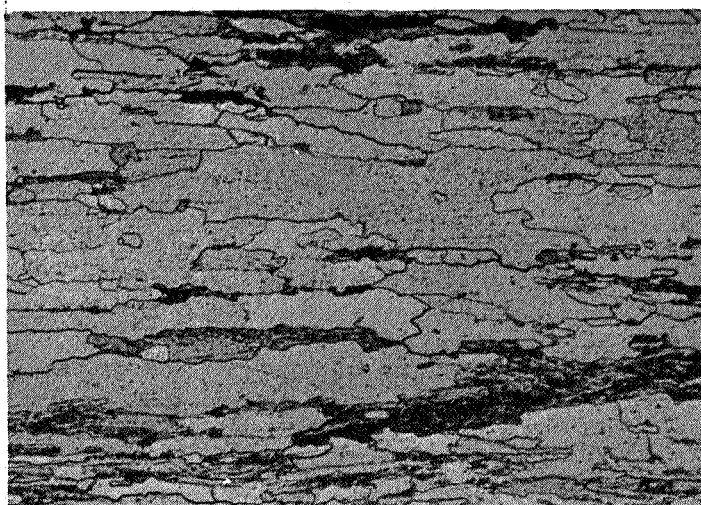


Figure 14. Transverse Photomicrograph of TZC Alloy, As Received.
(A290212)

Etchant: As Polished (H_2O_2)

Mag: 100X

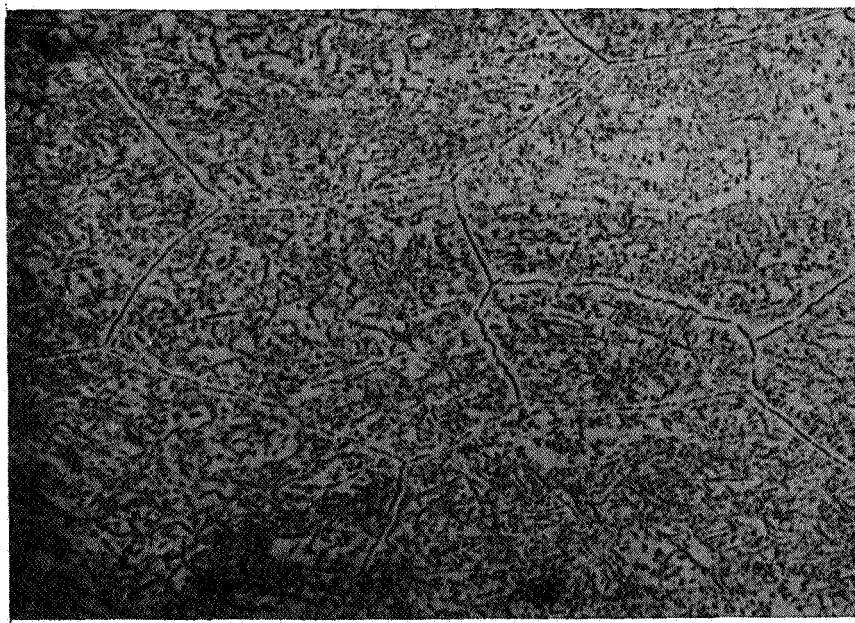


Figure 15. Photomicrograph of Cb-132M as Received and Stress Relieved One Hour at 2200°F. (A260311)

Etchant: 60 H₂O-20 HF - 20 HNO₃

Mag: 100X

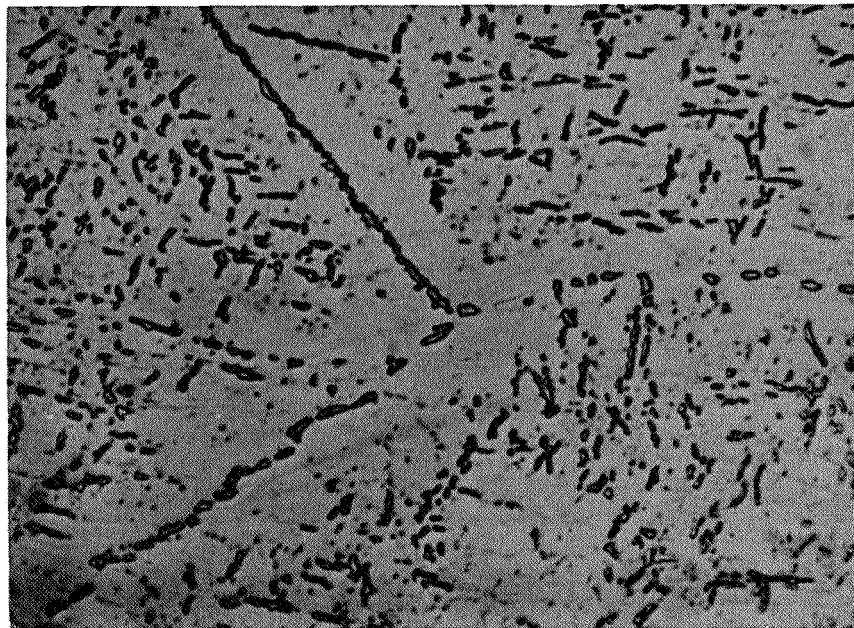


Figure 16. Photomicrograph of Cb-132M as Received and Stress Relieved One Hour at 2200°F. (A260312)

Etchant: 60 H₂O-20-HF - 20 HNO₃

Mag: 500X

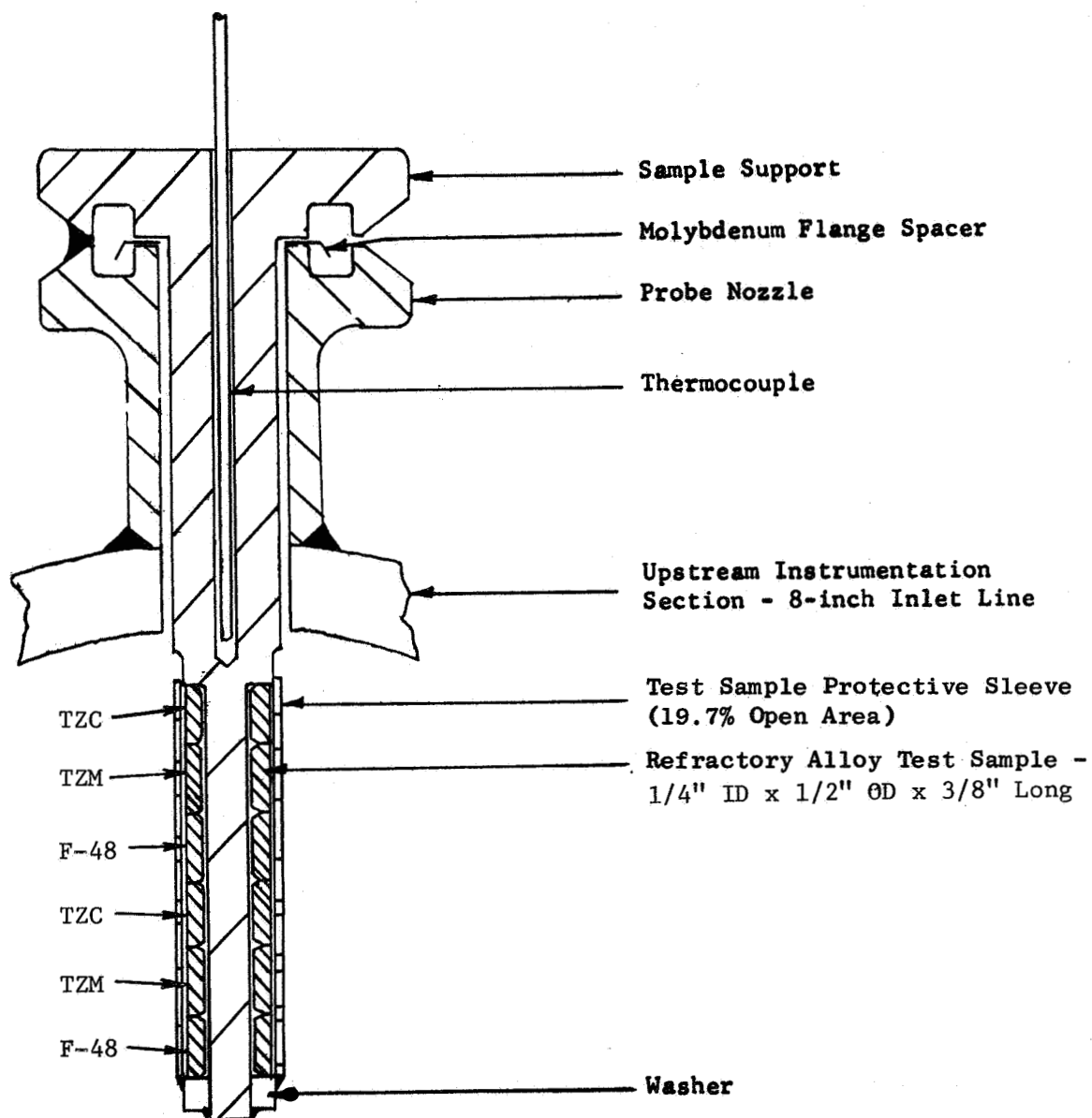


Figure 17. Refractory Alloy Immersion Probe
(Scale 1/1)

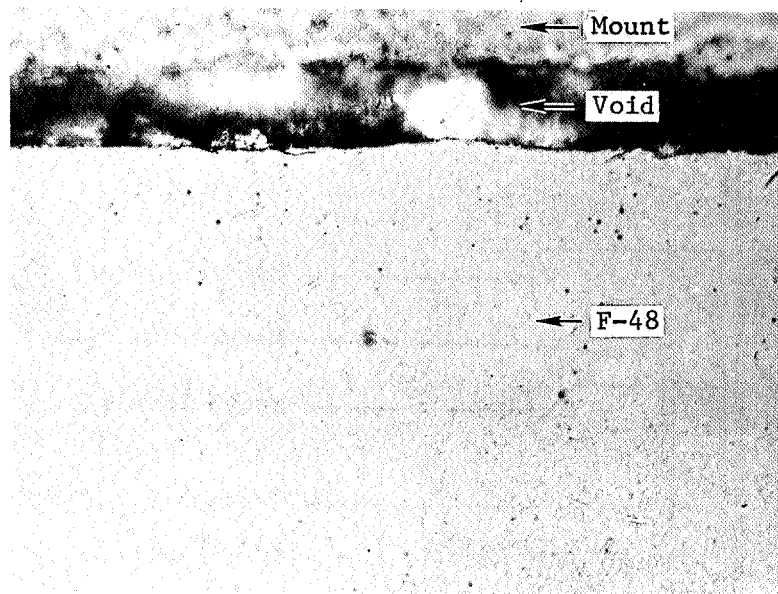


Figure 18. Contaminated Surface of F-48 Probe Specimen from Station One After 12 Hour Exposure to Inlet Potassium Vapor During Turbine Performance Test. (A320113)

Etchant: Electrolytic Anodize*

Mag: 1000X

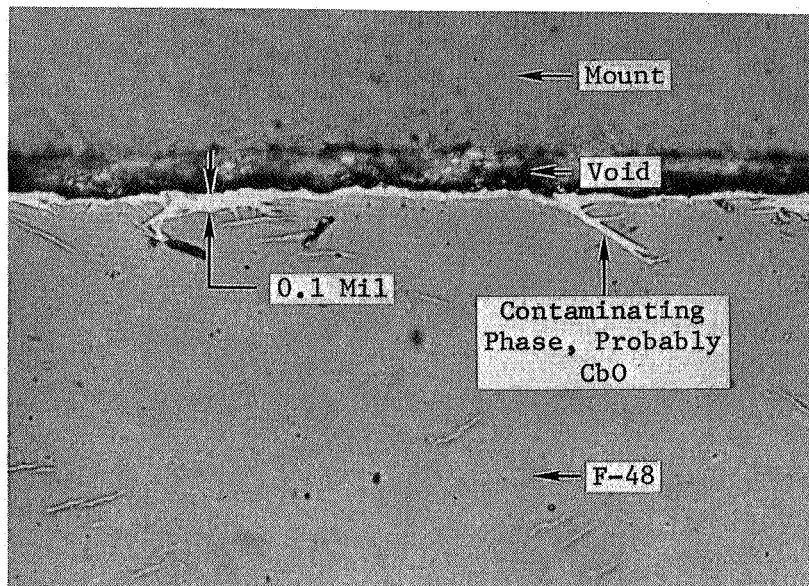


Figure 19. Contaminated Surface of F-48 Probe Specimen from Station One After 56 Hour Exposure to Inlet Potassium Vapor During Turbine Performance Test. (A320614)

Etchant: Electrolytic Anodize*

Mag: 1000X

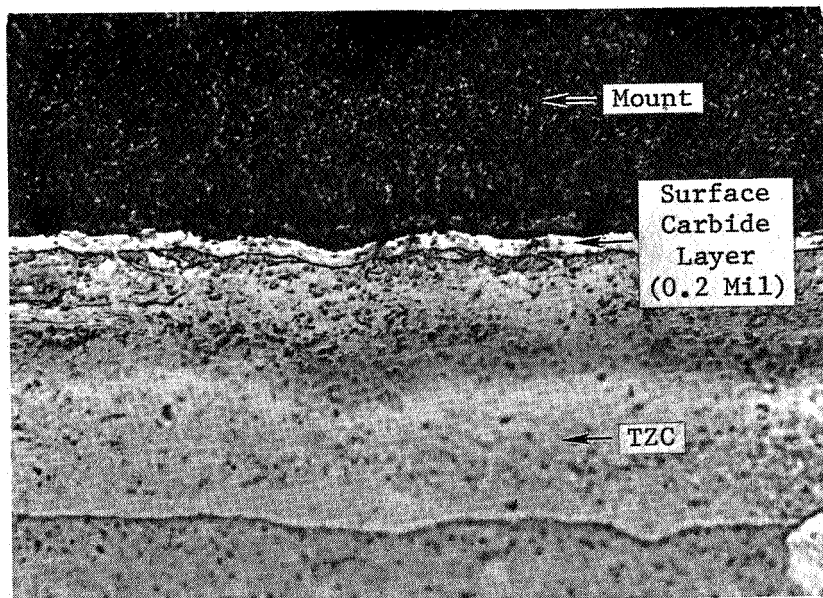


Figure 20. Carbide Formed at the Surface of TZC Exposed for 100 Hours at 1400°F in Liquid Potassium Containing Carbon. (A890111)

Etchant: Murakami's

Mag: 500X

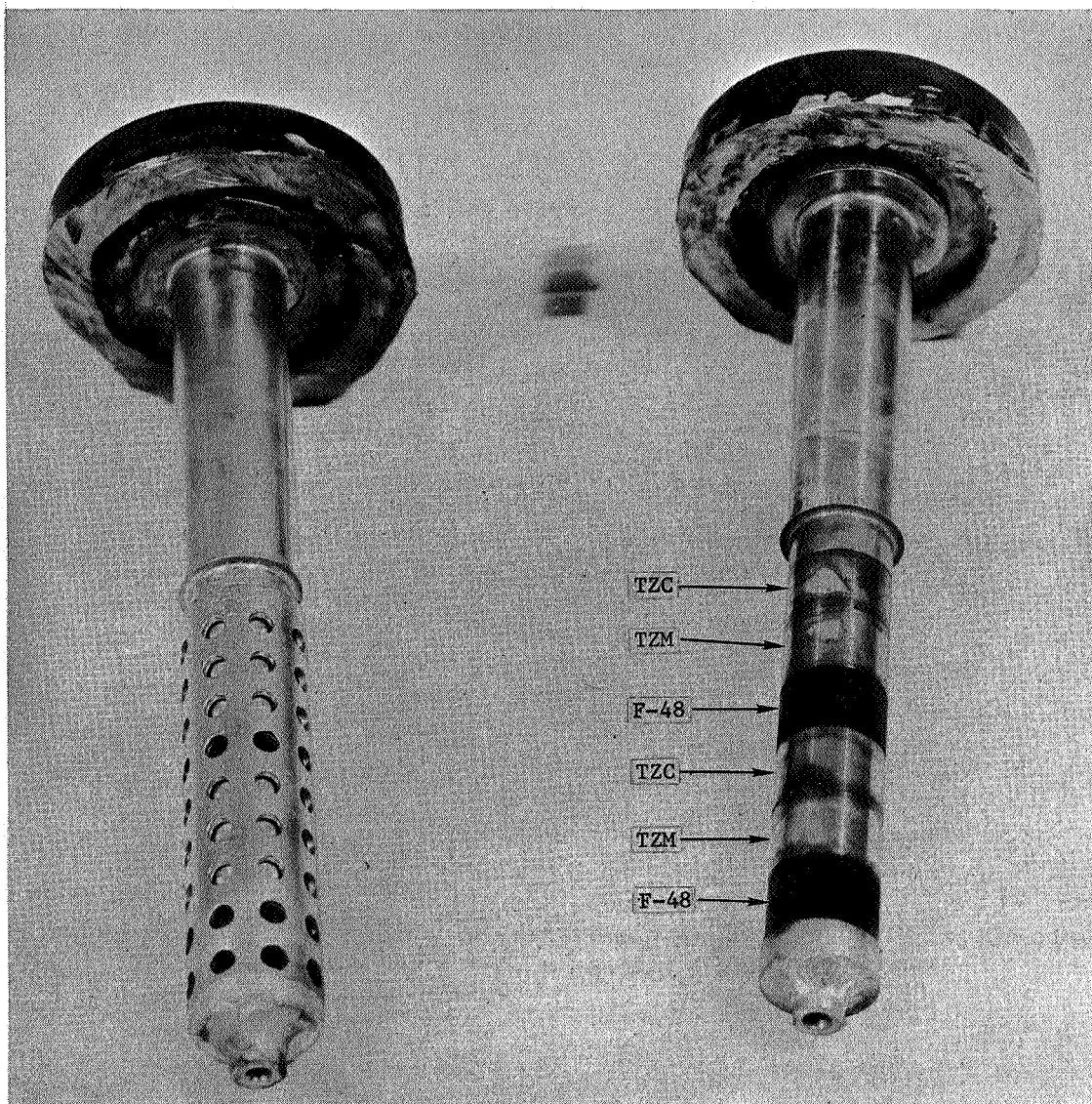


Figure 21. Refractory Alloy Specimen Probes from Station One, Left, and Condenser, Right. (Note Darkening of F-48 Specimens)
(C65032822)

Mag: 1X

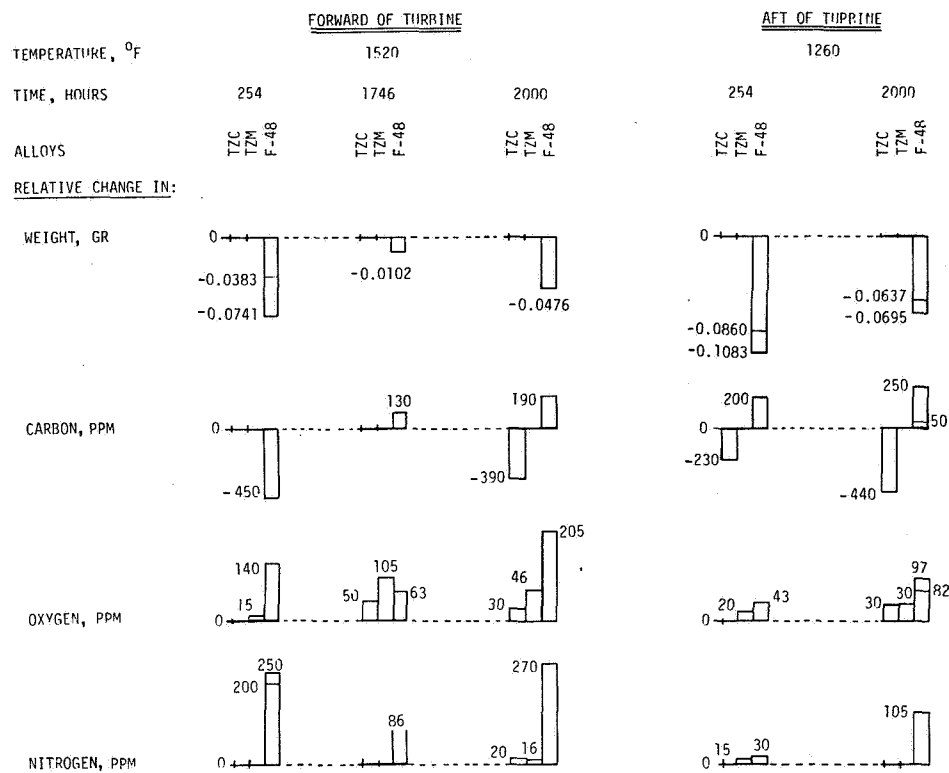


Figure 22. Summary of Changes in Weight and in Carbon Oxygen and Nitrogen Content of TZC, TZM and F-48 Alloy Ring Specimens During Turbine Endurance Testing.

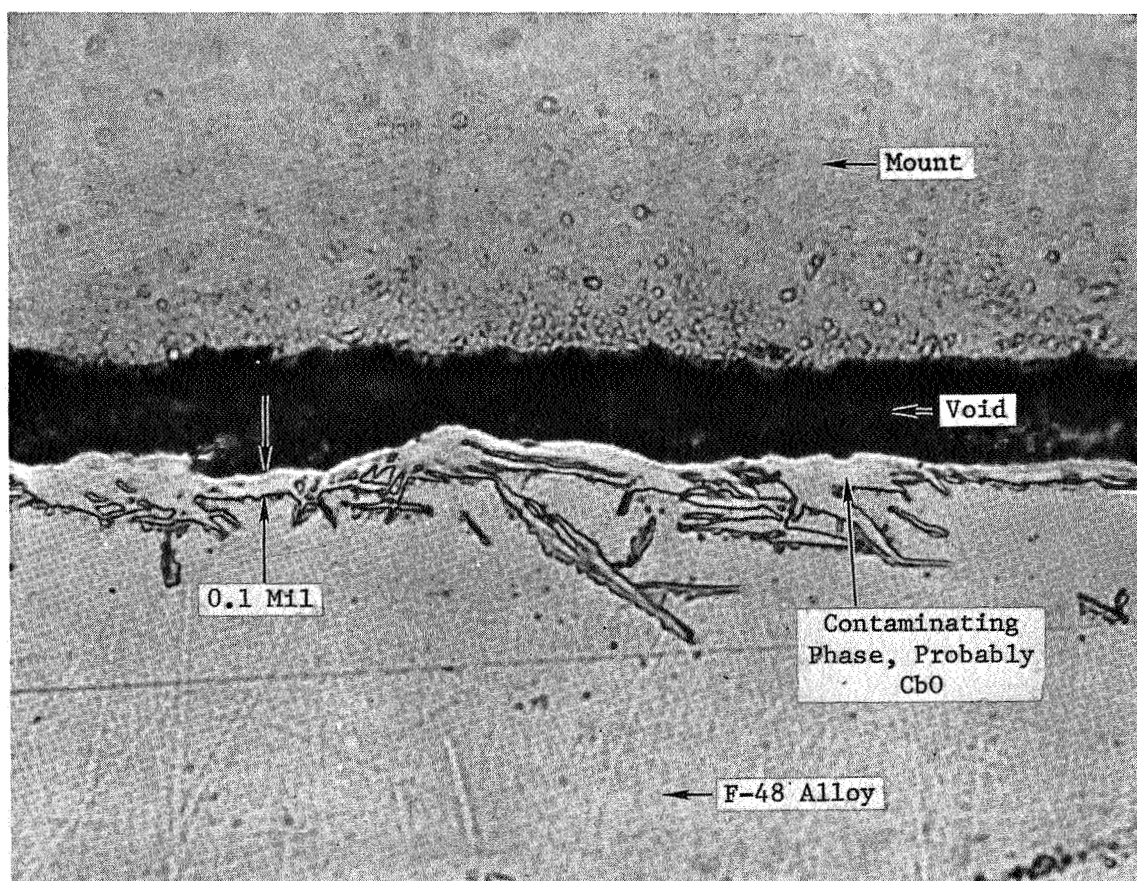


Figure 23. Contaminated Surface of F-48 Specimen from Station One After 254-Hour Exposure to Inlet Potassium Vapor During Turbine Endurance Test. (A930114)

Etchant: 60% Glycerine - 20% HF - 20% HNO₃

Mag: 1000X

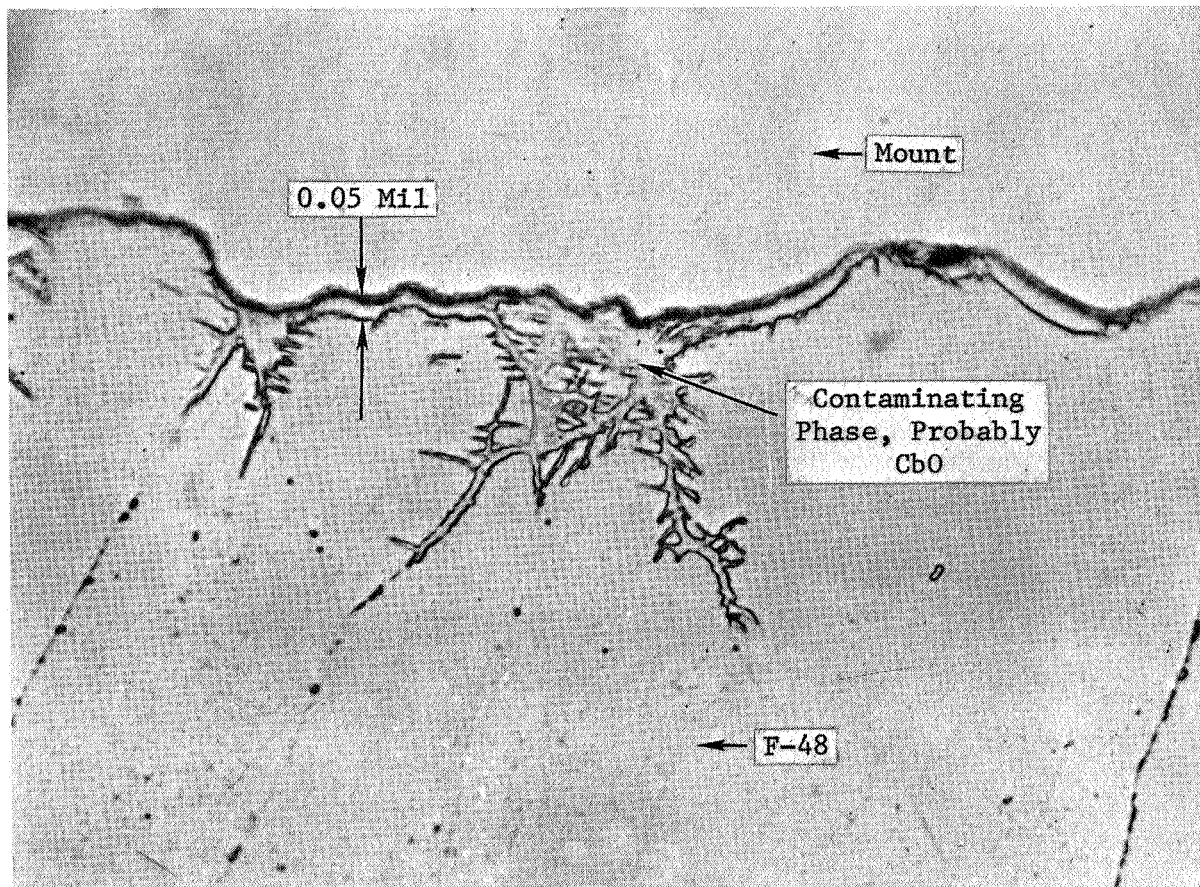


Figure 24. Contaminated Surface of F-48 Specimen from Condenser After 254-Hour Exposure to Exit Potassium Vapor During Turbine Endurance Test. (A930312)

Etchant: 60% Glycerine - 20% HF - 20% HNO₃

Mag: 1000X

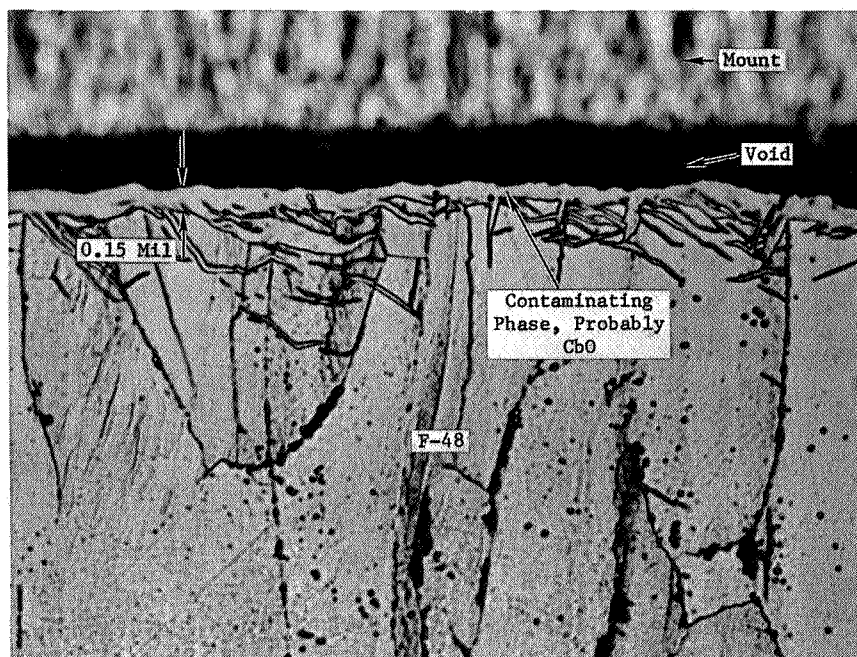


Figure 25. Contaminated Surface of F-48 Specimen from Station One After 2000 Hour Exposure to Inlet Potassium Vapor During Turbine Endurance Test. (B280911)

Etchant: 60% Glycerine - 20% HF - 20% HNO₃ Mag: 1000X

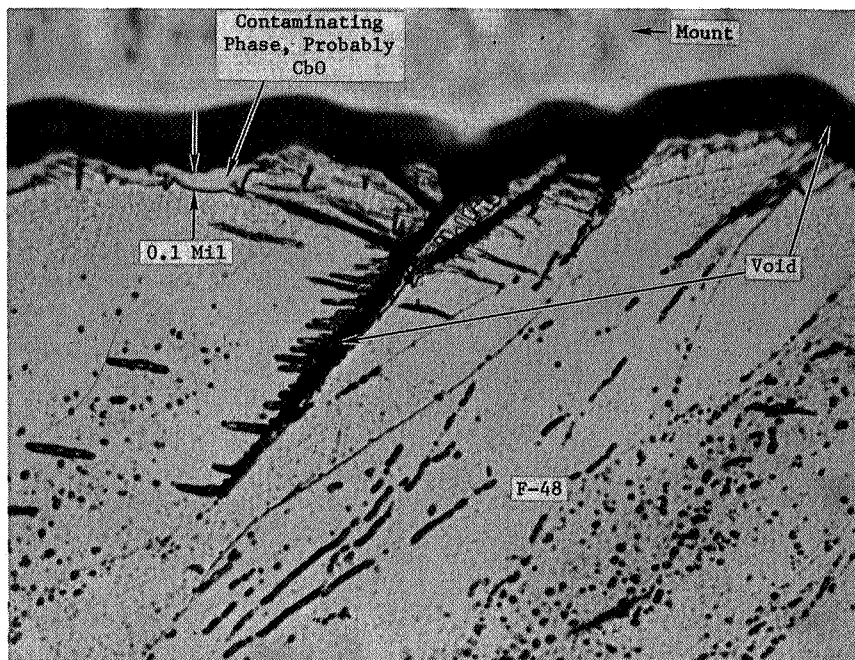


Figure 26. Contaminated Surface of F-48 Specimen from Condenser After 2000 Hour Exposure to Exit Potassium Vapor During Turbine Endurance Test. (B281212)

Etchant: 60% Glycerine - 20% HF - 20% HNO₃ Mag: 1000X

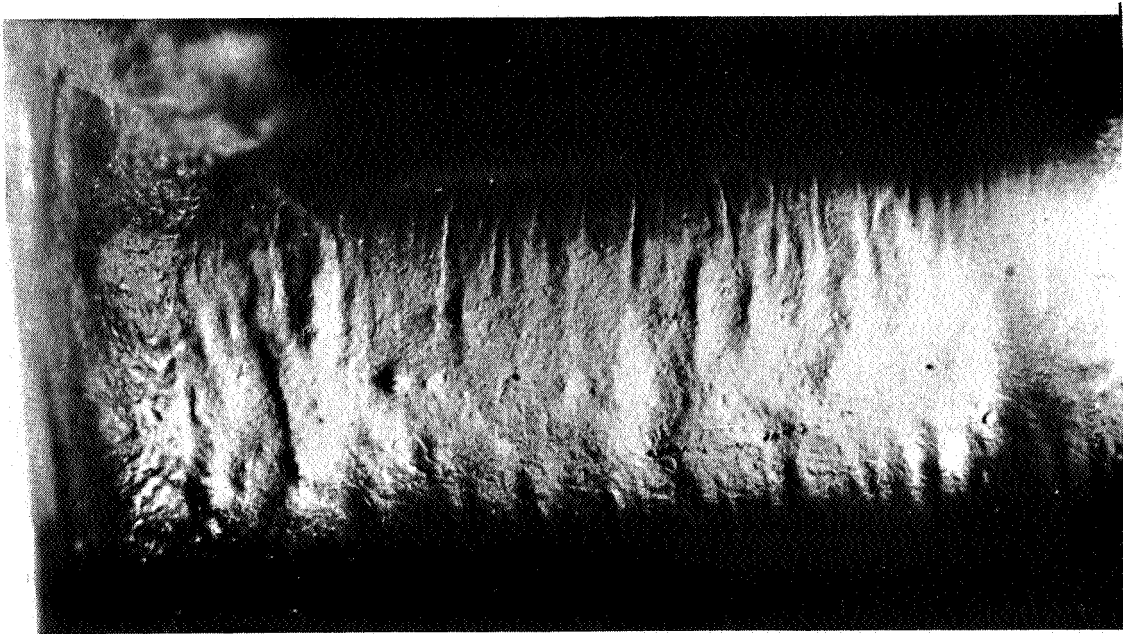
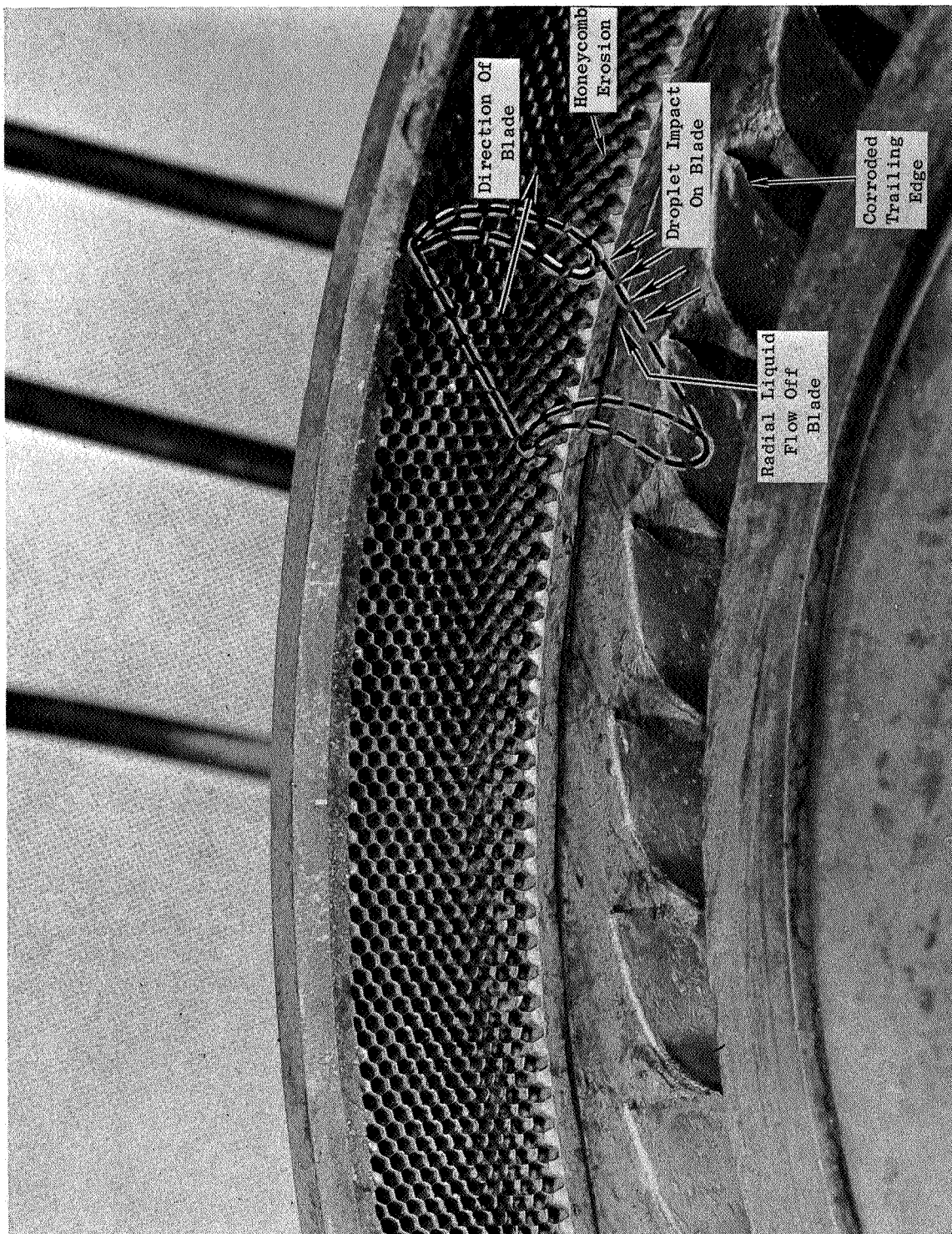


Figure 27. Enlarged View of Leading Edge of the First Stage L-605 Nozzle Vane. (C64122369) Mag: 9X



Mag: 1.4X

Figure 28. First Stage Honeycomb Tip Seal. (C64120409)

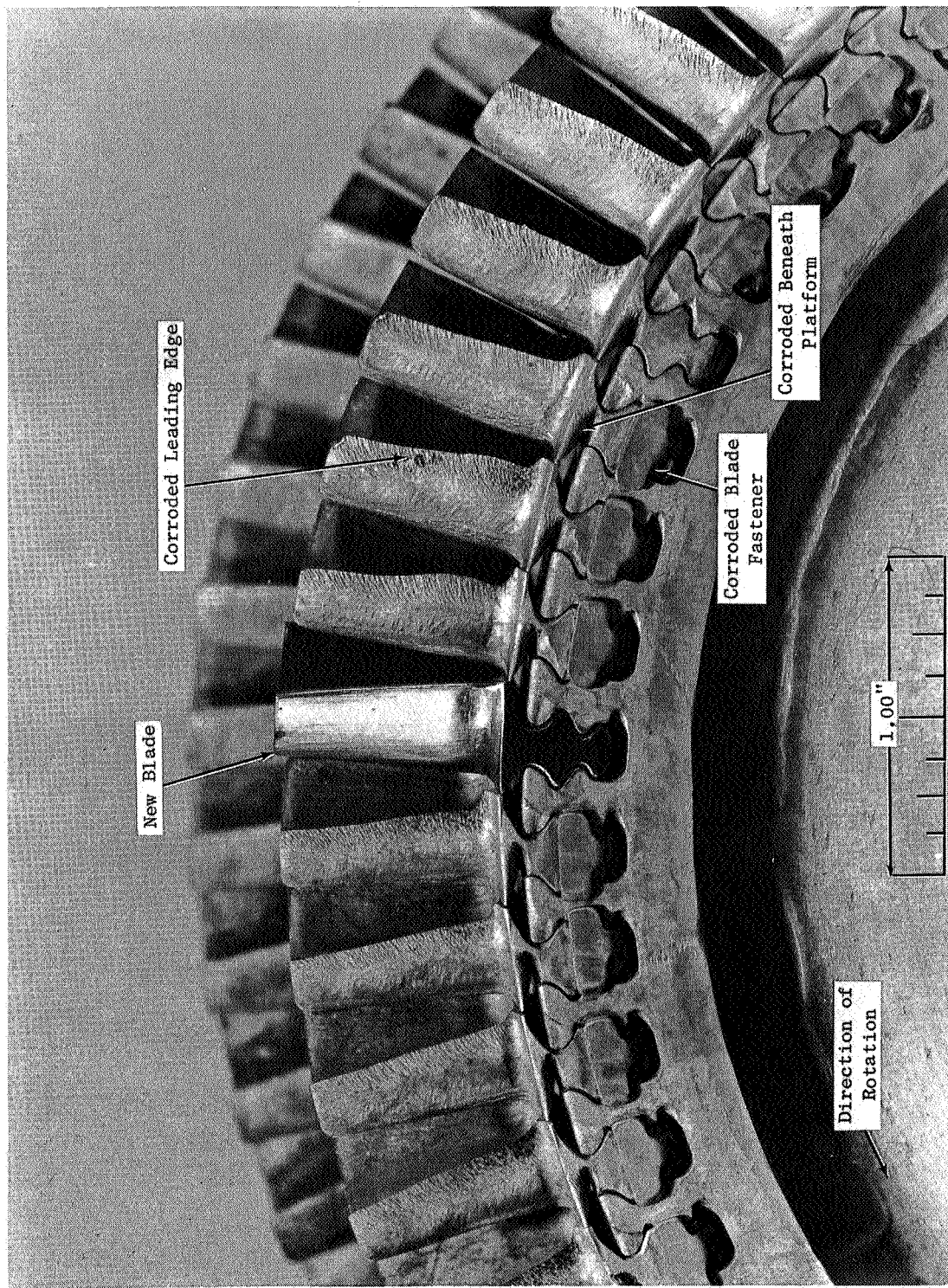
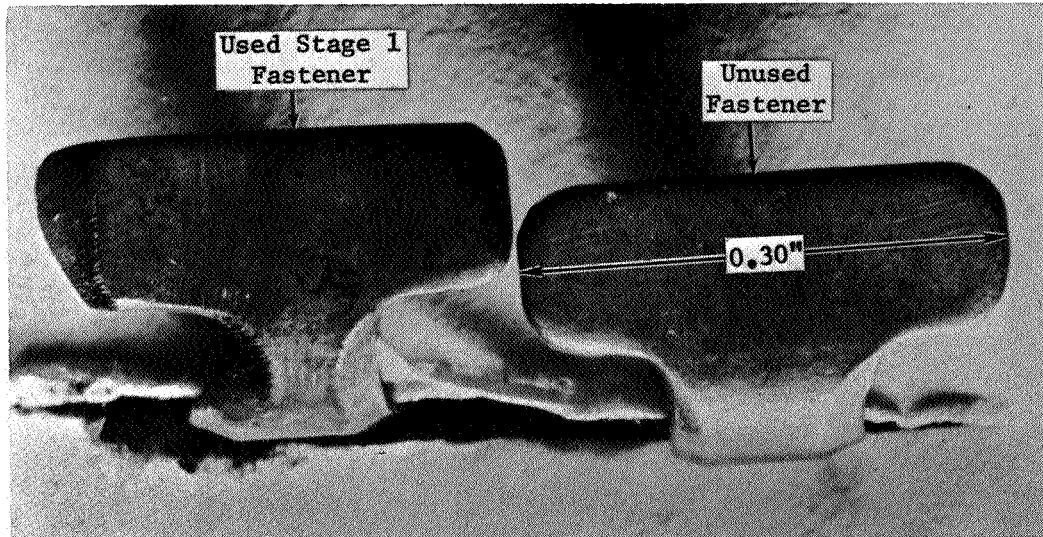
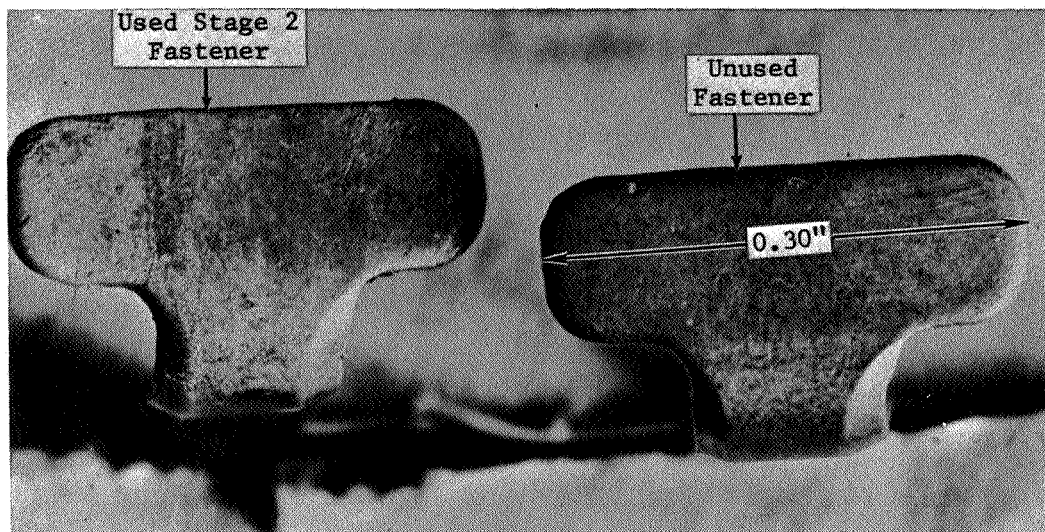


Figure 29. First Stage Turbine Rotor Blades. (C64120410)



(C64122208)



(C64122207)

Figure 30. Comparison of Blade Locking Strips Before and After 35-Hour Turbine Checkout.

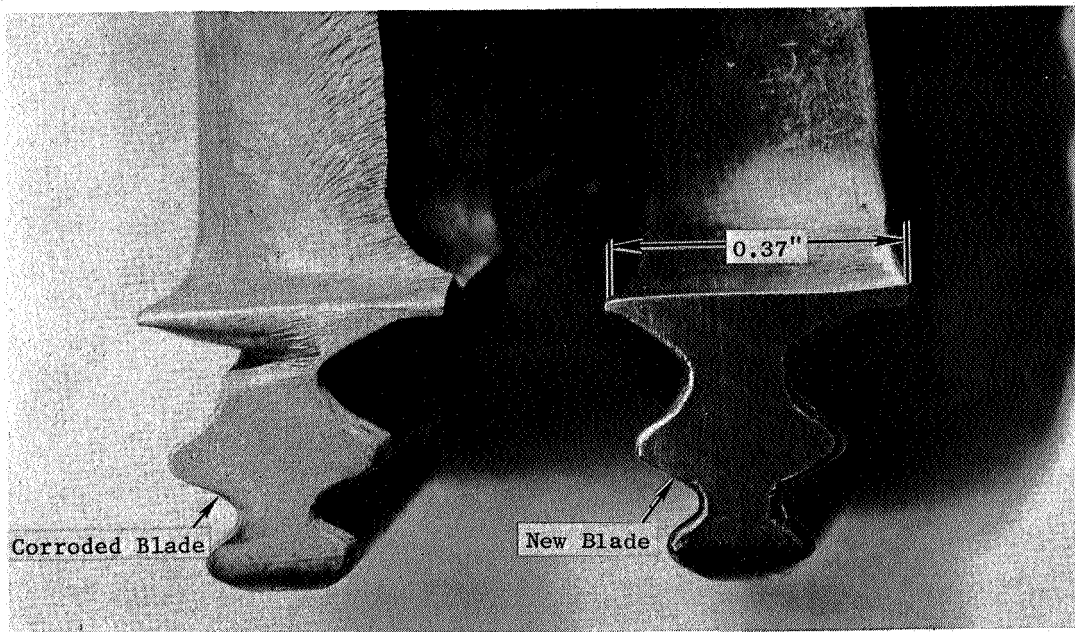
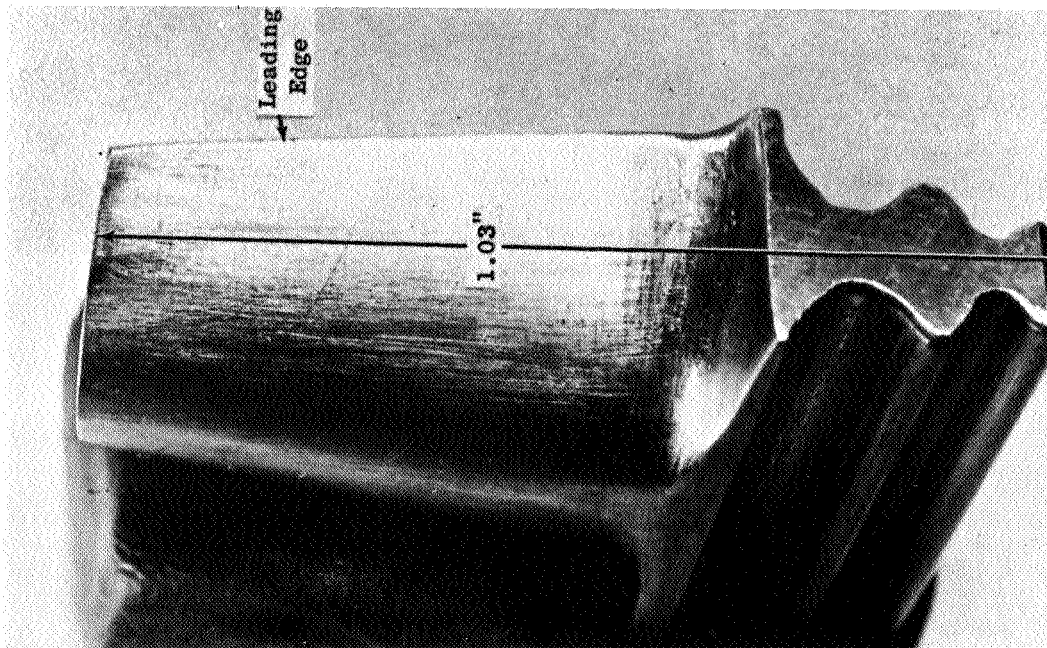
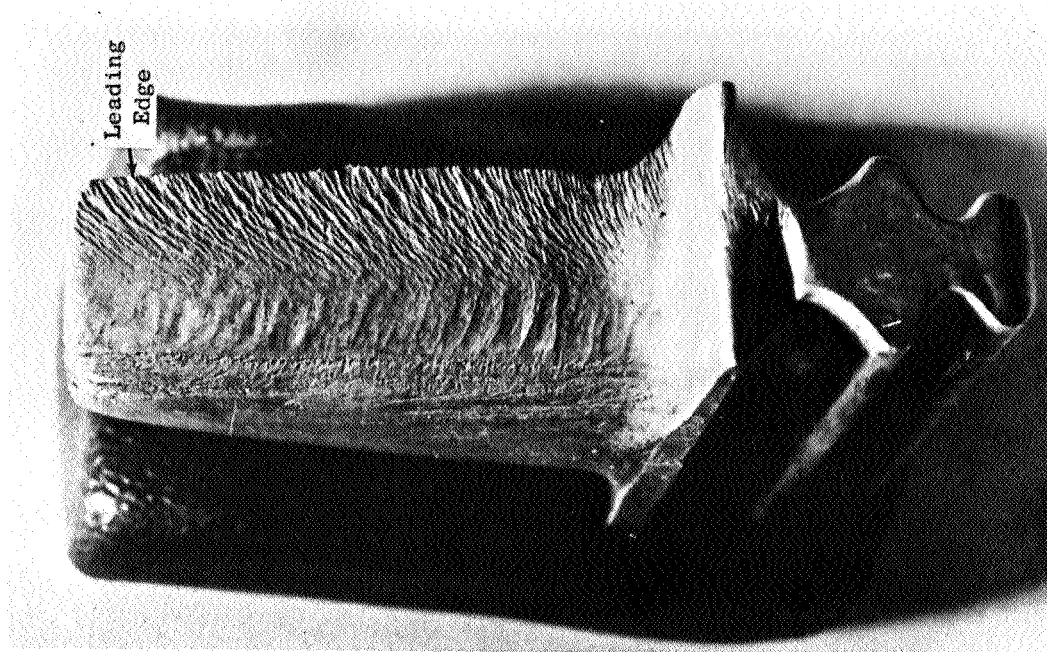


Figure 31. Comparison of Root-Region of First Stage Blade Before and After 35 Hour Turbine Checkout. (C64120910)

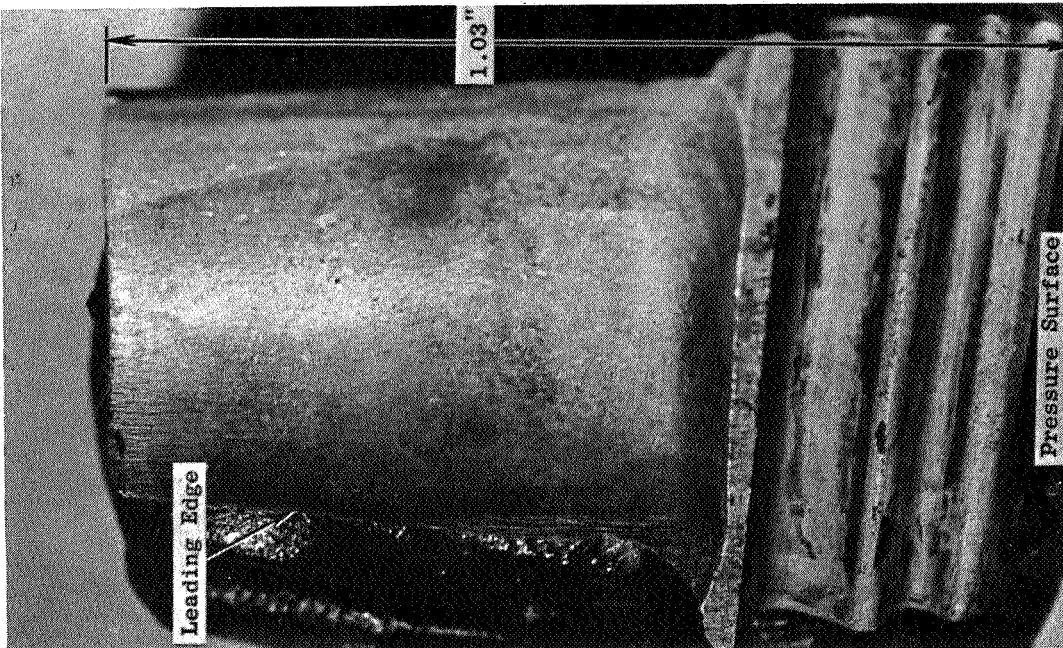
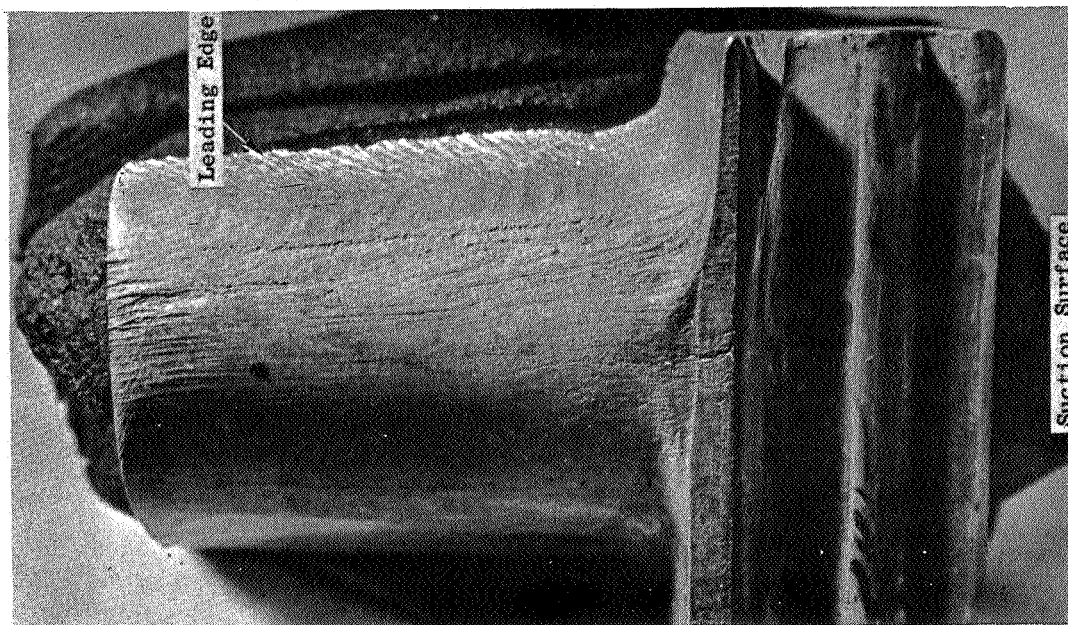


(C64I20912)



(C64I20913)

Figure 32. Comparison of a First Stage Blade Before and After 35-Hour Turbine Checkout.



4120915)

(C64120914)

Figure 33. Suction and Pressure Surfaces of a First Stage Blade After 35-Hour Turbine Checkout.

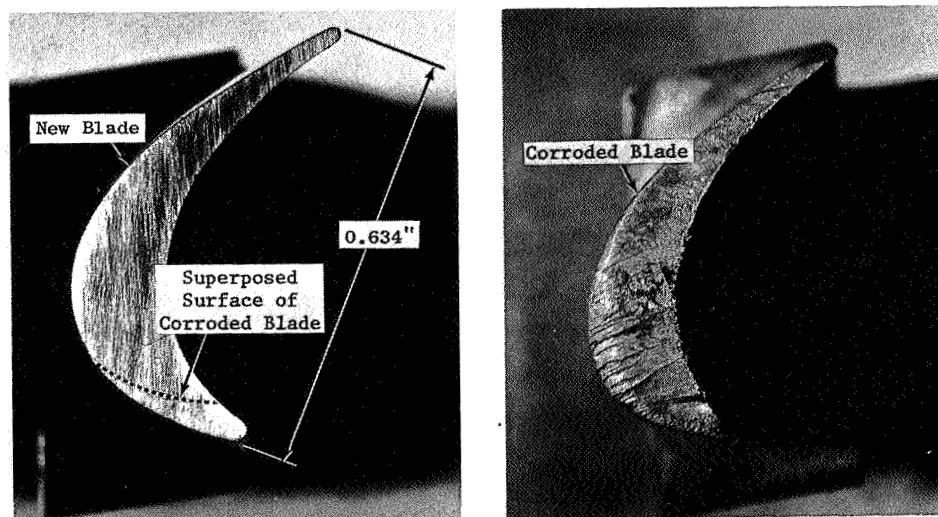
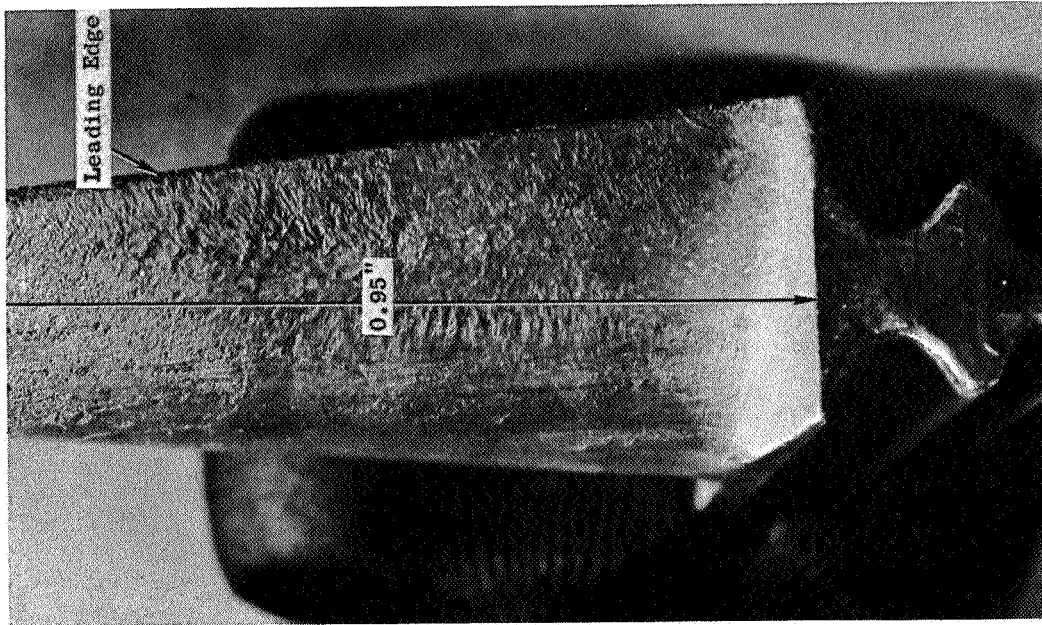


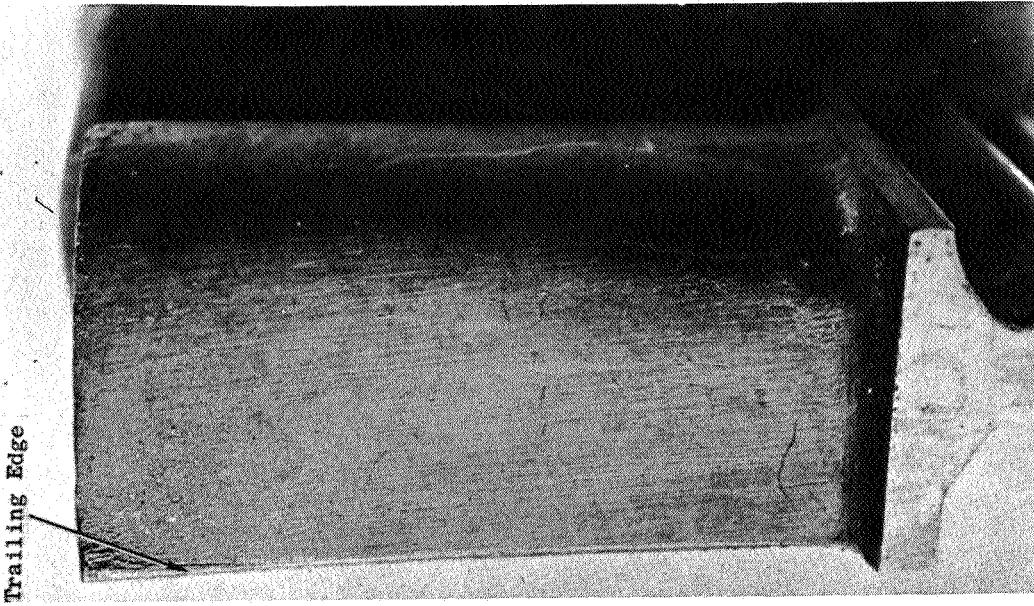
Figure 34. Comparison of Tip Section of First Stage Blade Before and After 35 Hour Turbine Checkout. (C64120911)



(C64121502)

(C64121505)

Figure 35. Leading and Trailing Edge of a Second Stage Blade After 35-Hour Turbine Checkout.



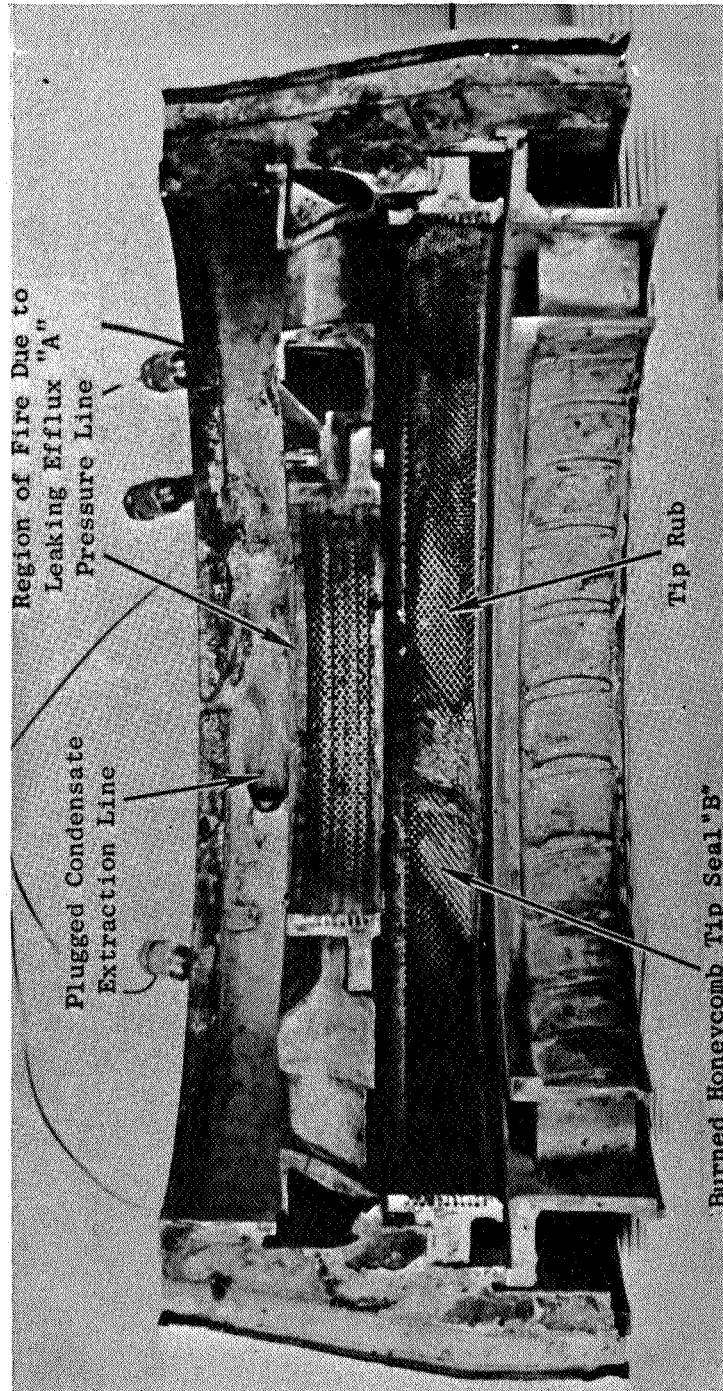


Figure 36. Fire Damage in Second Stage Tip Seal During 35-Hour Turbine
Checkout. (C64120413) Mag: 1/2X

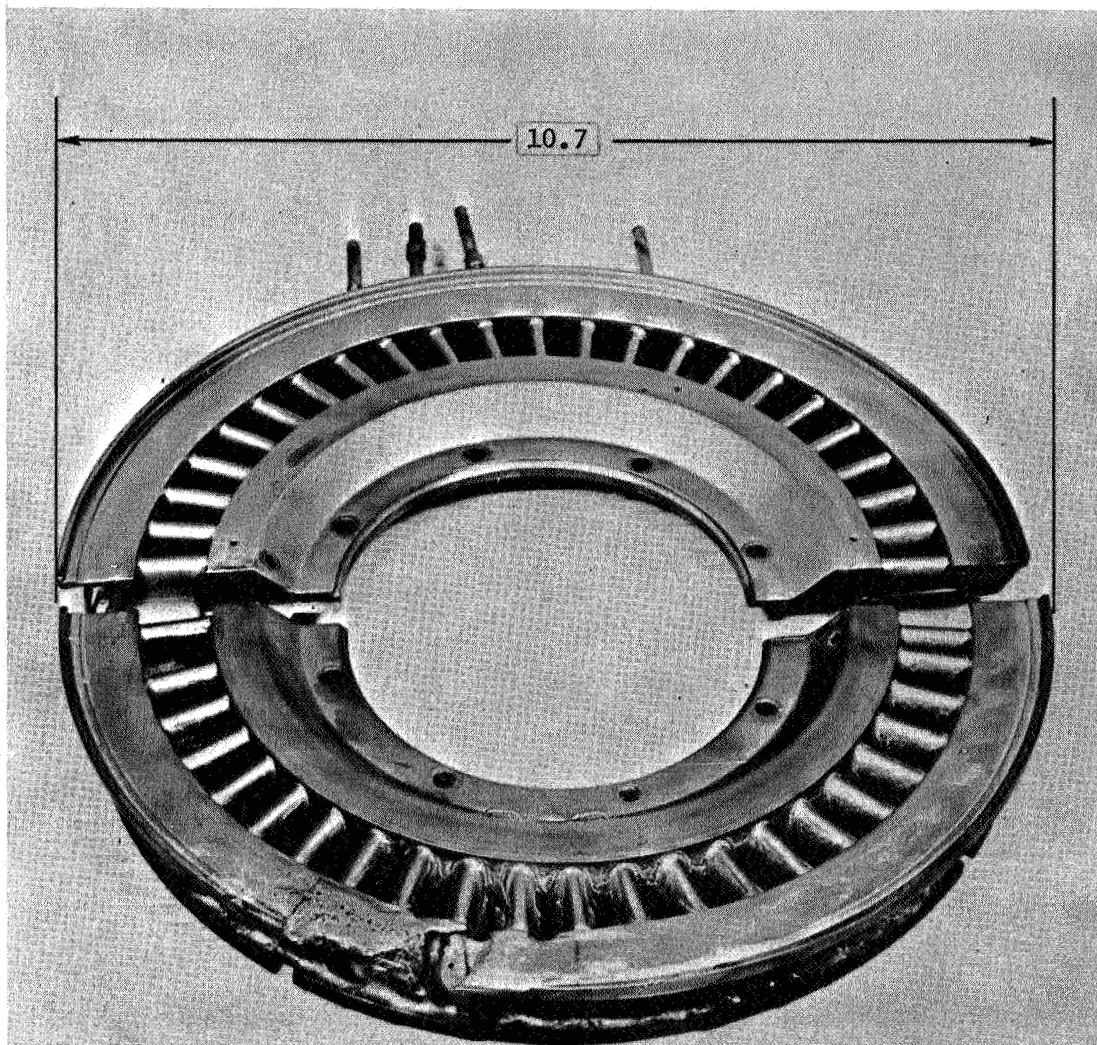


Figure 37. Second Stage Nozzle Diaphragm After Removal from Casing Following 35-Hour Turbine Checkout. (C64121805)

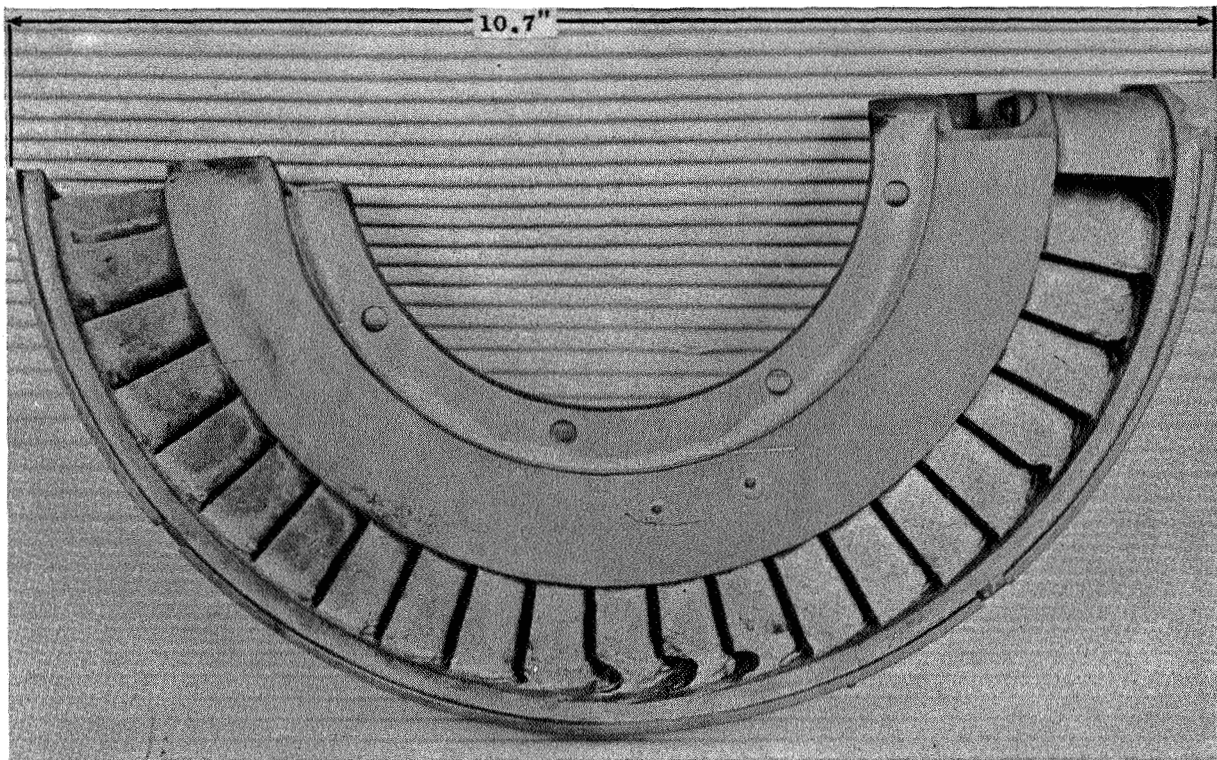


Figure 38. Fire Damage to Second Stage Nozzle Diaphragm Vanes During 35-Hour Turbine Checkout. (C64121803)

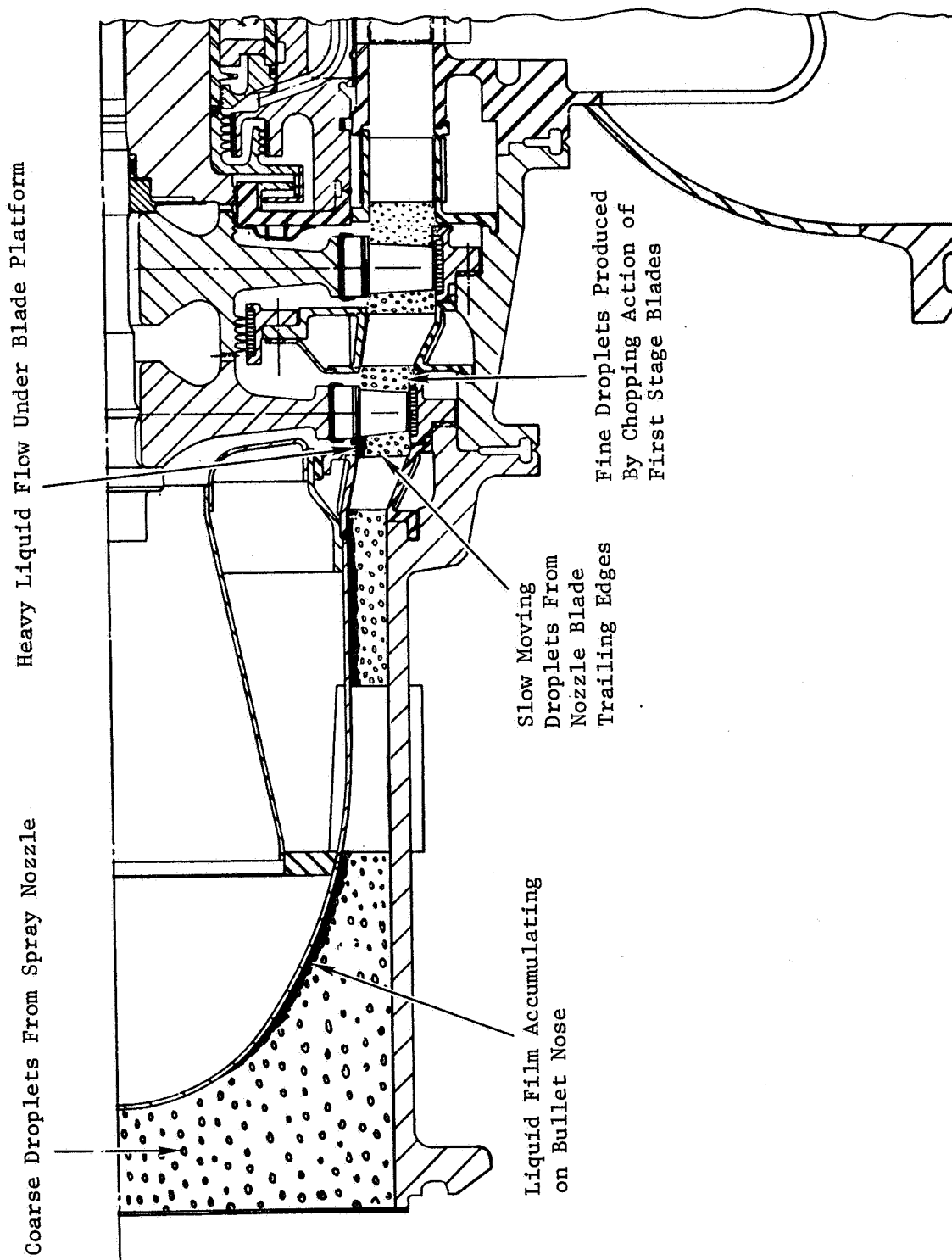


Figure 39. Schematic Diagram of Suspected Flow of Liquid Potassium in the Turbine During Operation of the Spray Line.

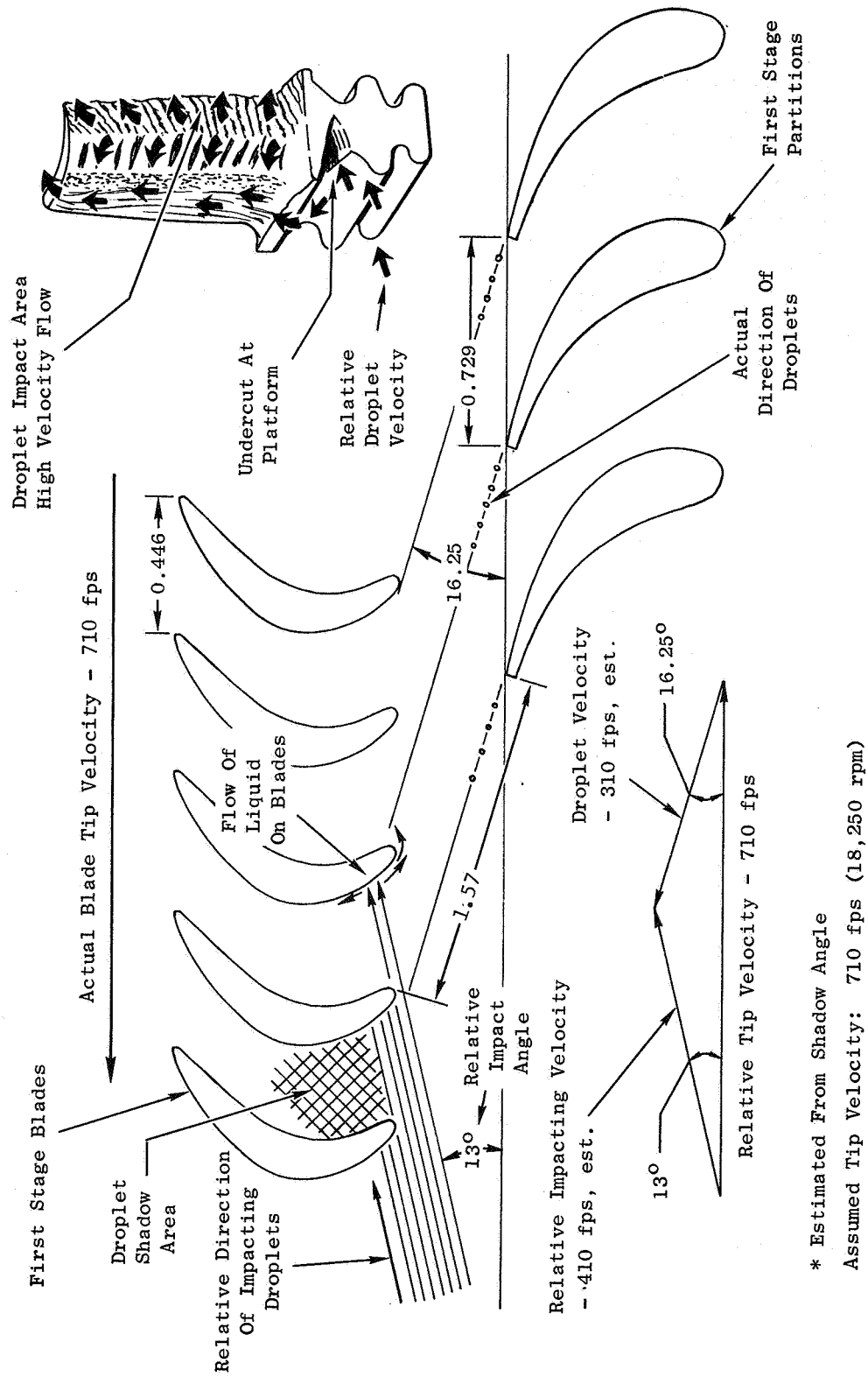


Figure 40. Estimated Droplet Velocity Vector Diagrams and Impacting Droplet Flow Conditions During Liquid Potassium Spray Injection Into the Turbine.

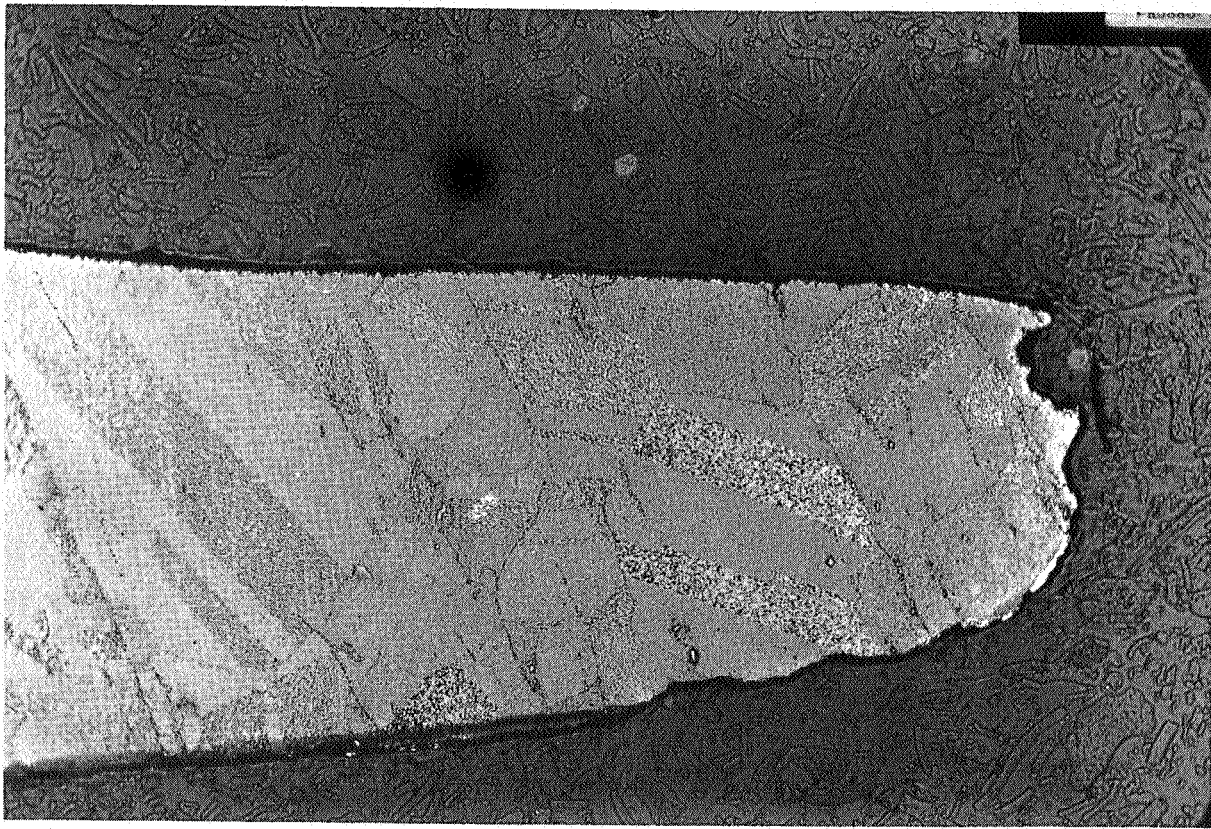


Figure 41. Suspected Cavitation Corrosion in First Stage Blade Trailing Edge After 35-Hour Turbine Checkout. (K5880)

Etchant: 100 EtOH - 100 HCl - 30 3% H₂O₂, Electrolytic

Mag: 250X

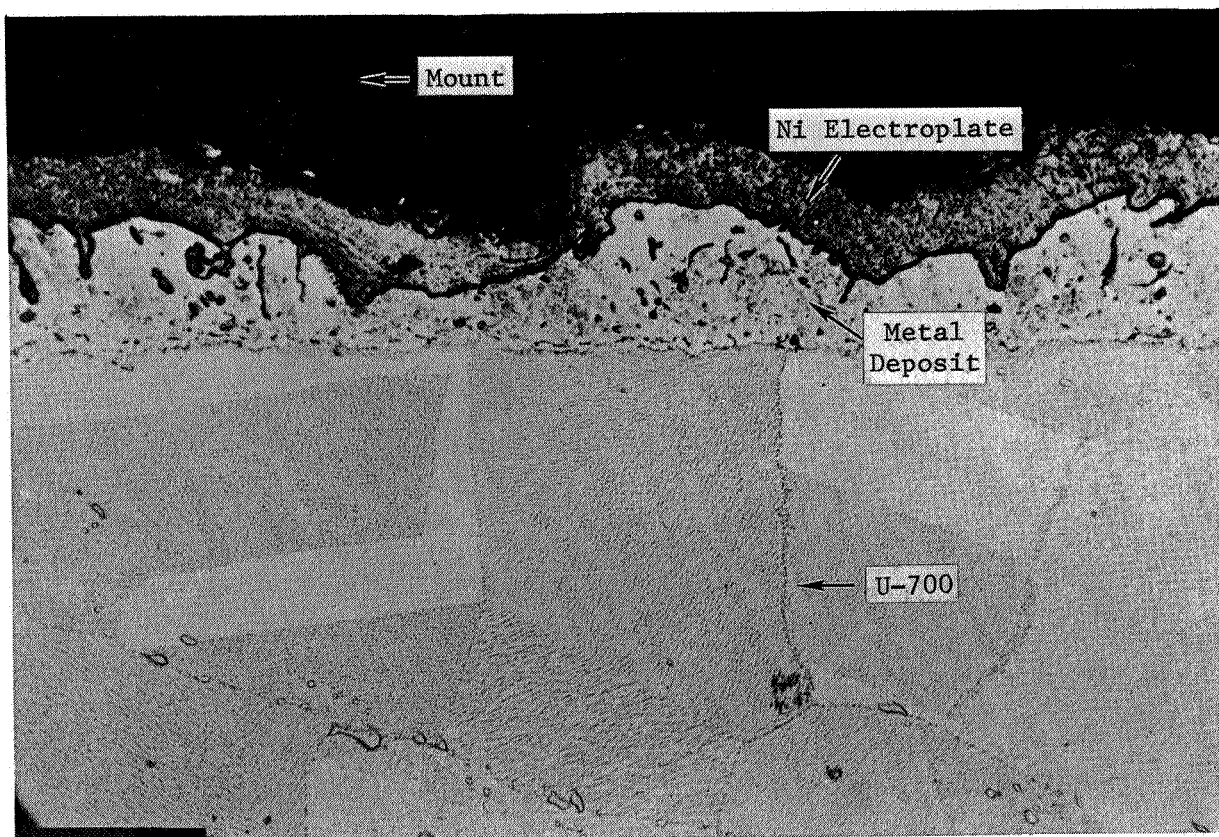


Figure 42. Metal Deposit on First Stage Blade Concave Surface After 35 Hour Turbine Checkout. (L171)

Etchant: 100 Et OH-100 HCl-30 3% H_2O_2 , Electrolytic Mag: 500X

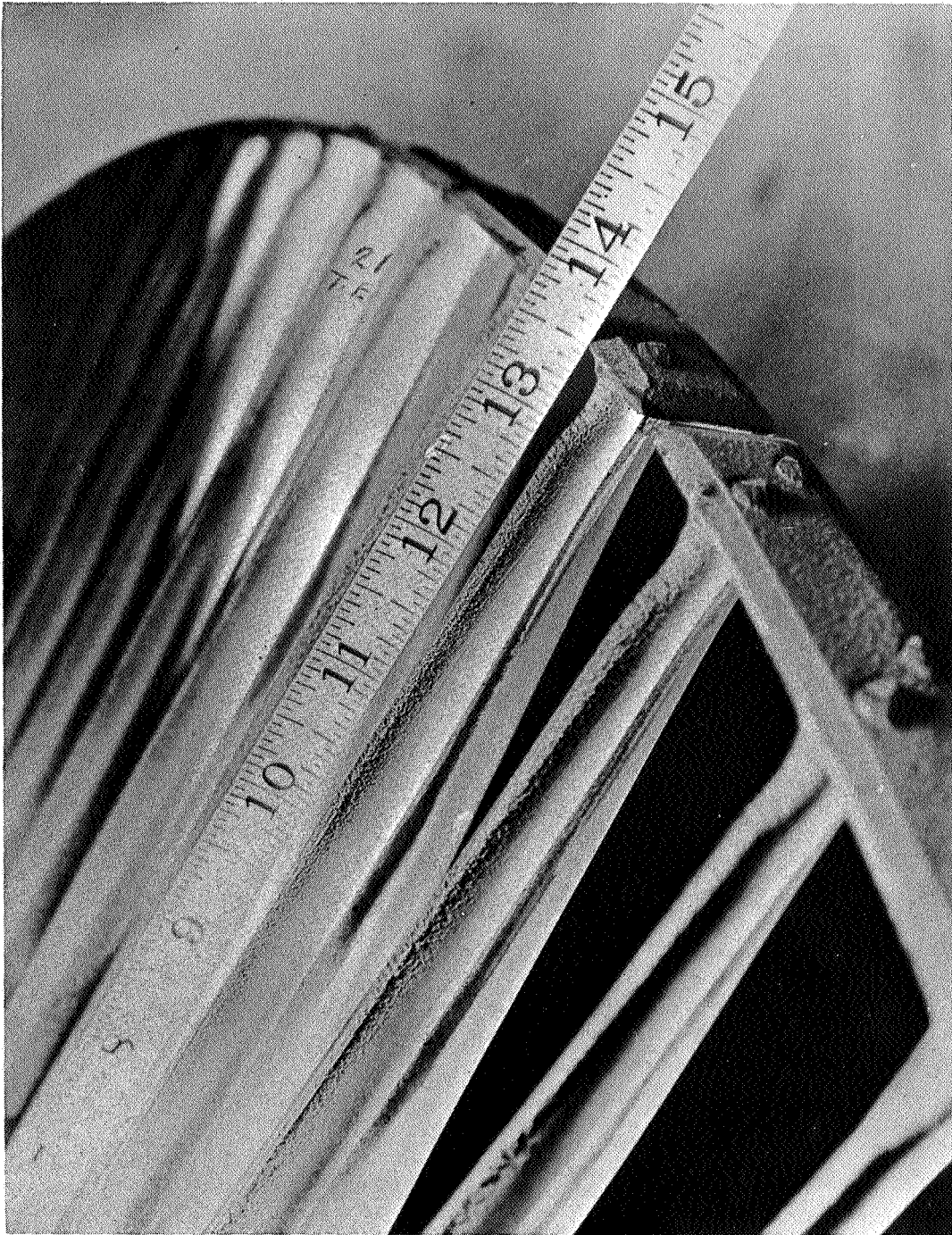


Figure 43. Impact Erosion in the Last Stage of a Central Station Steam Turbine.

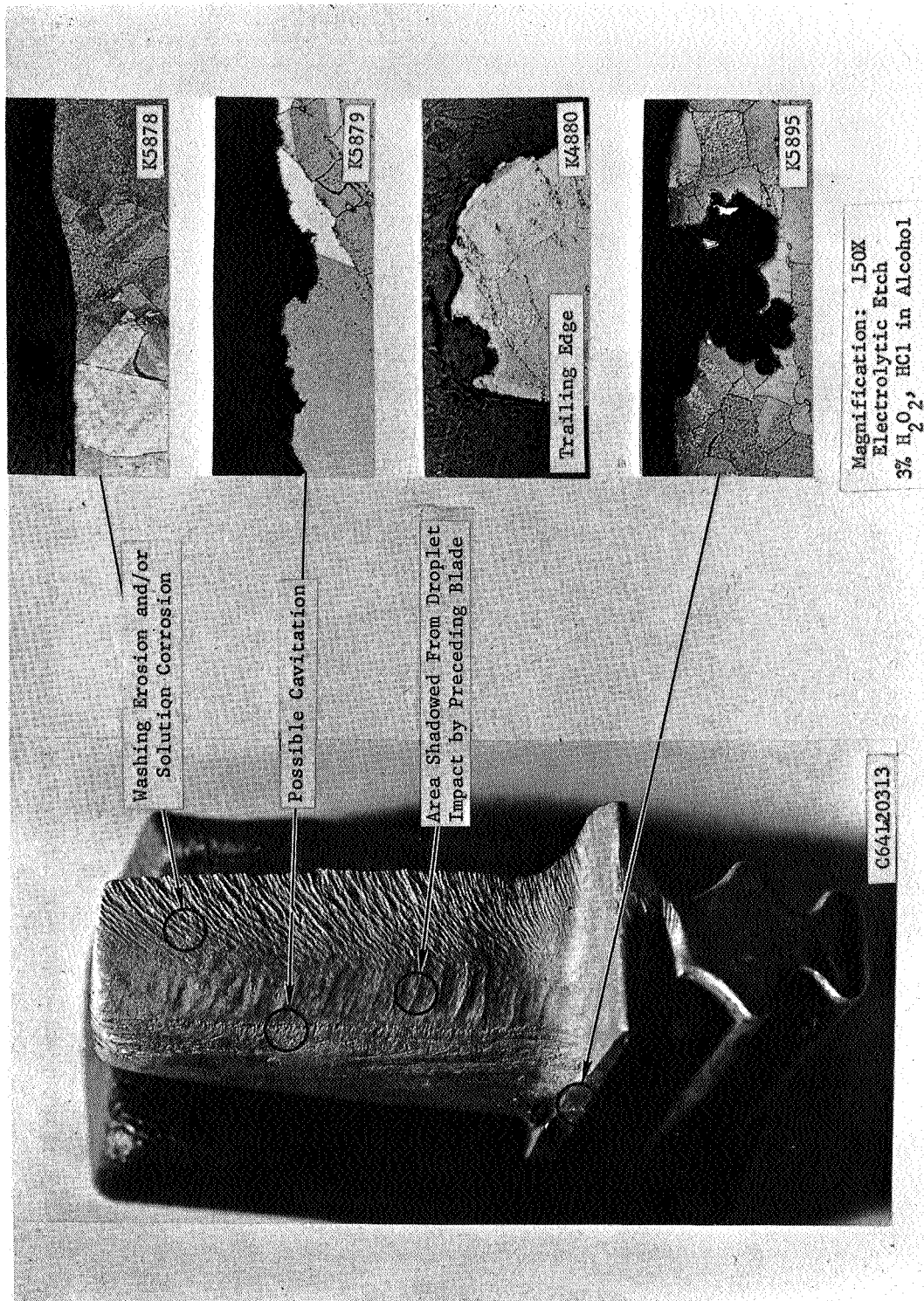


Figure 44. Photomicrographs Showing Nature of Metal Removal from Surface of First Stage Turbine Blade After 35-Hour Turbine Checkout.

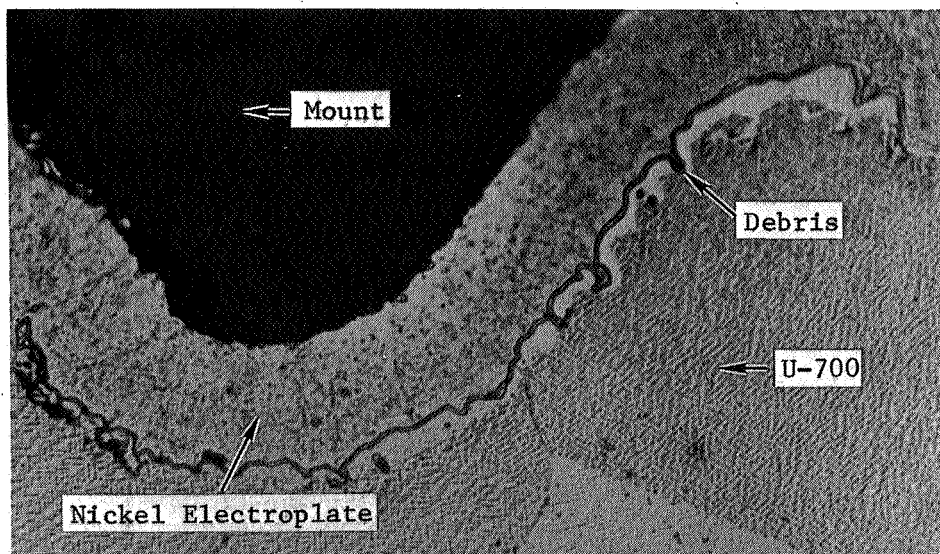


Figure 45. Optical Photomicrograph of Area of Electron Microprobe Analysis, Convex Surface of Stage One Blade.

Mag: 1000X

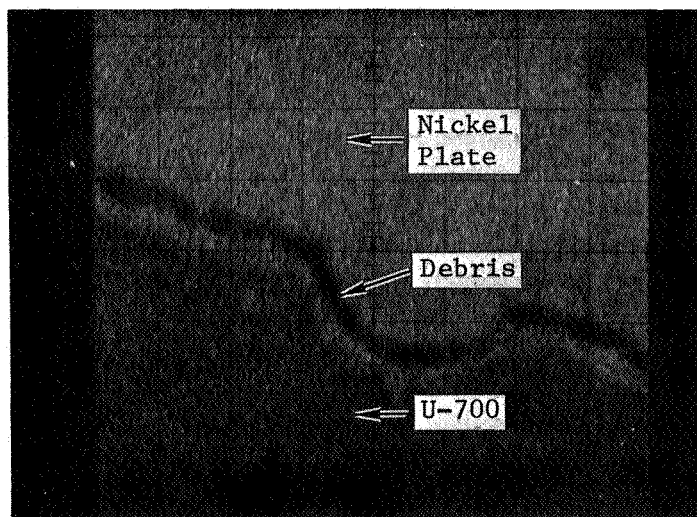


Figure 46. Electron Microprobe Oscilloscope Plot of Nickel Trace at the Convex Surface of a First Stage Blade.

Mag: 890X

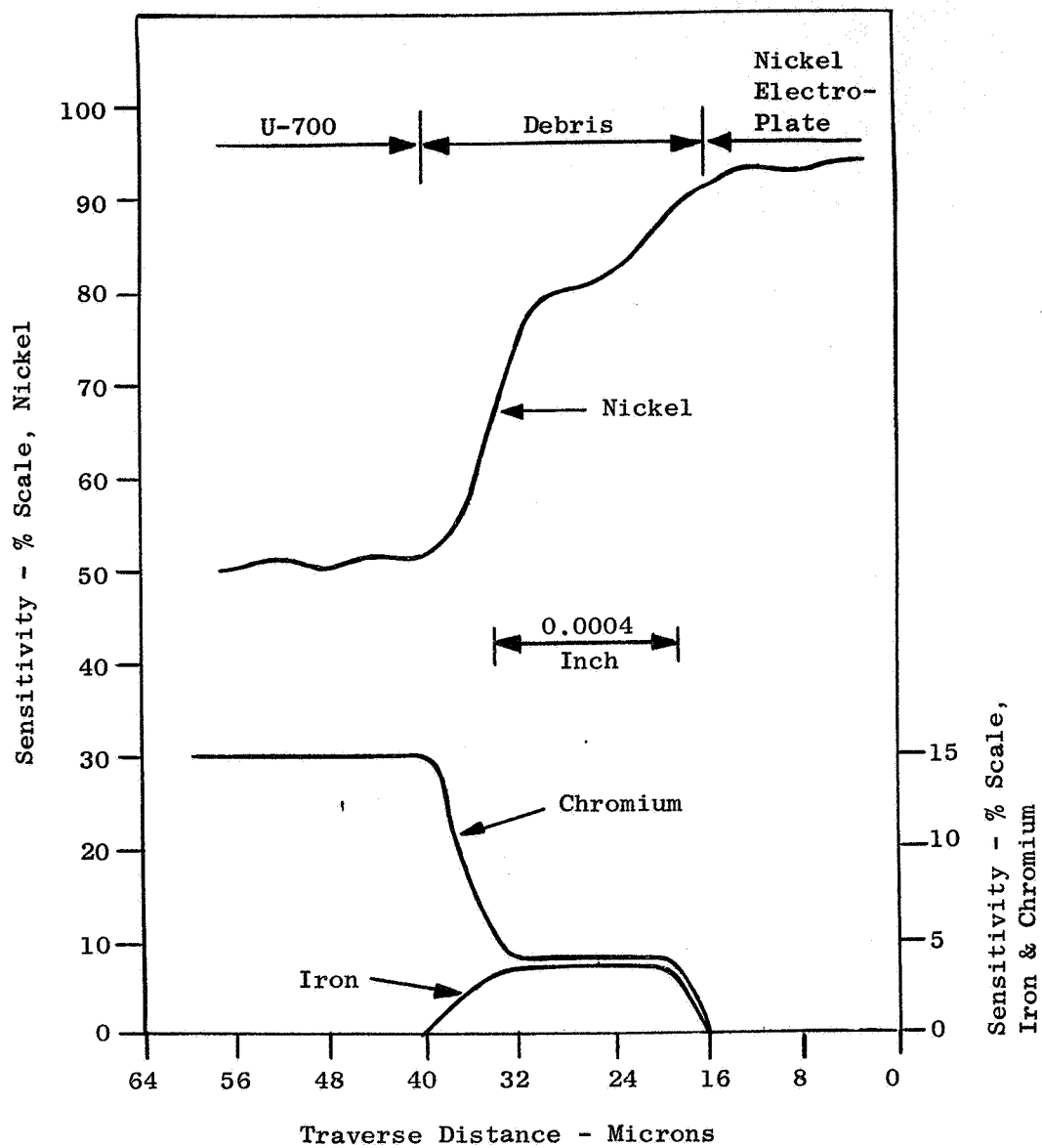


Figure 47. Electron Microprobe Beam Traverse of U-700 Blade.

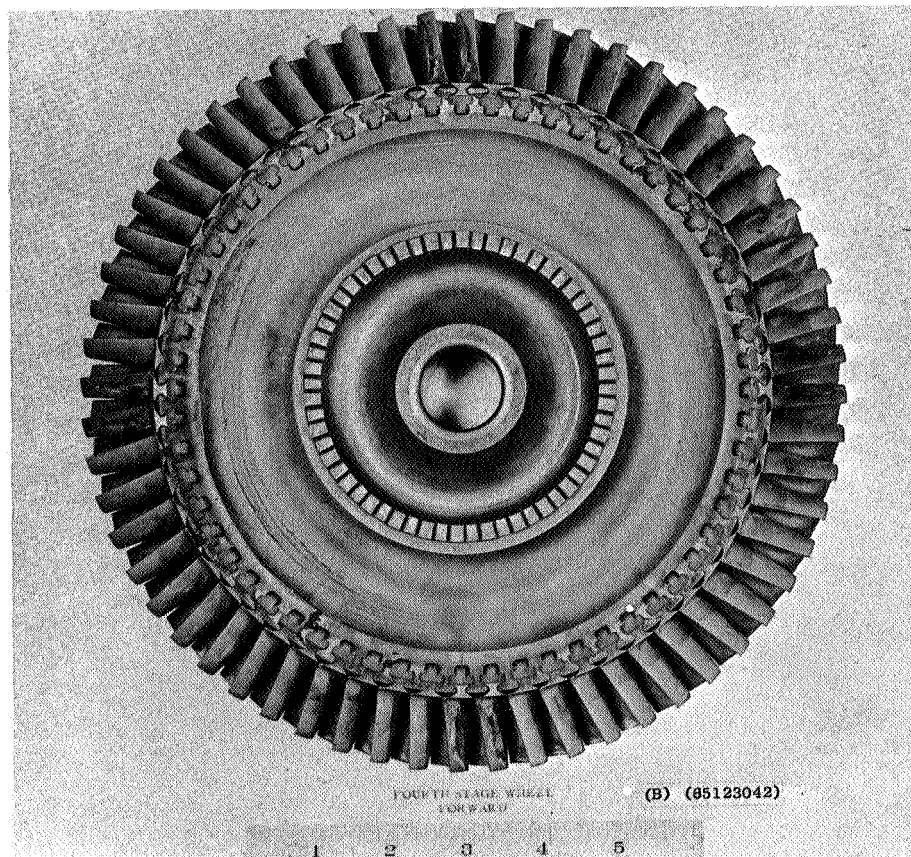
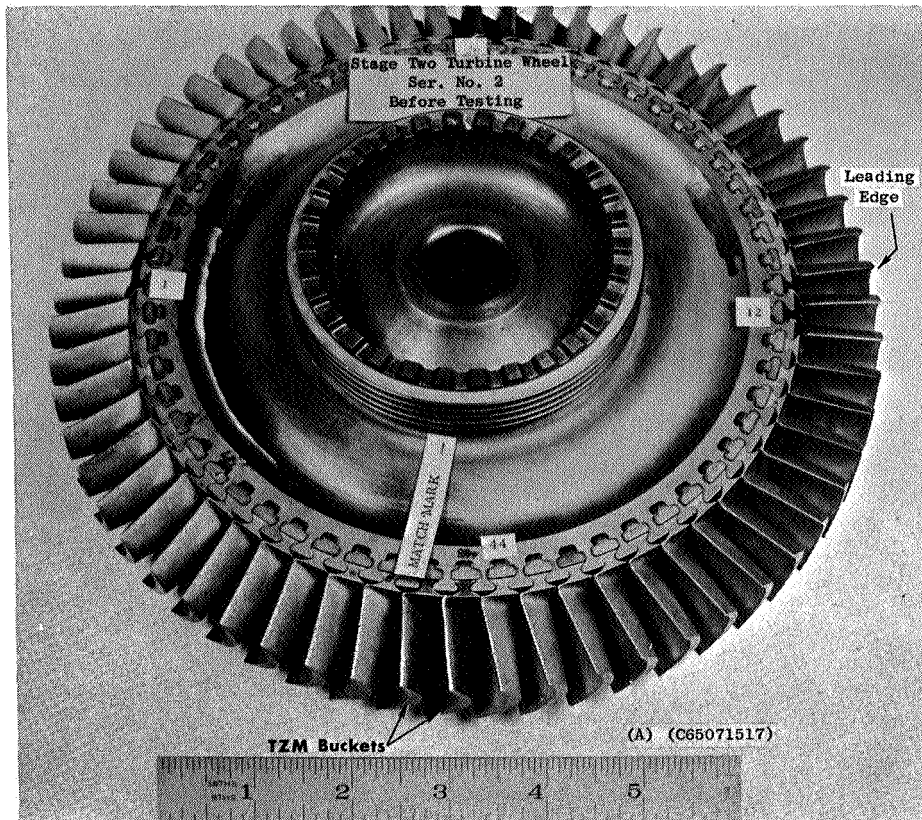


Figure 48. Second Stage Turbine Wheel Assembly Before, (A) and After, (B), 2000 Hour Endurance Test.

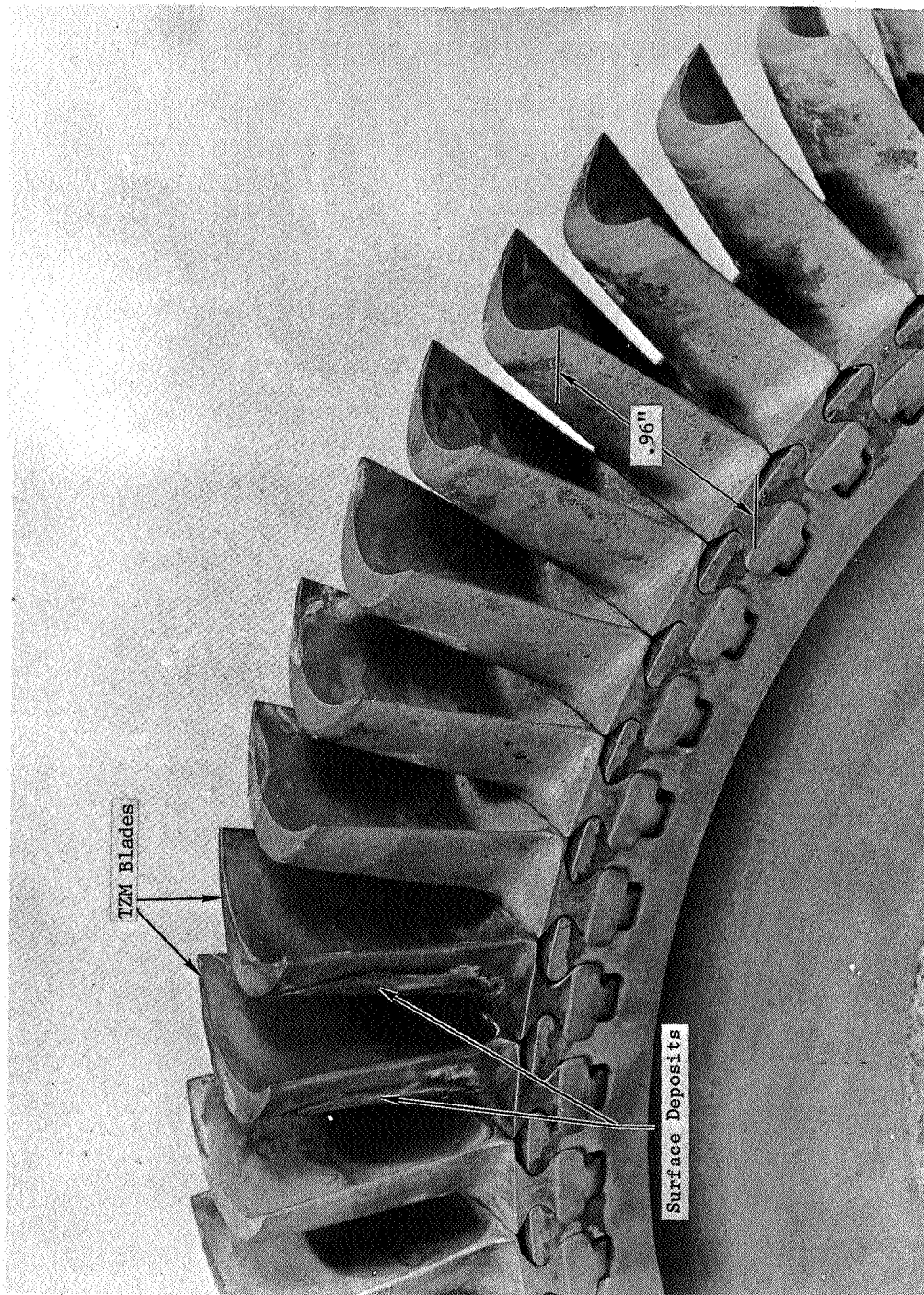


Figure 49. Second Stage Turbine Wheel Assembly After 2000 Hour Endurance Test. (C65123016)

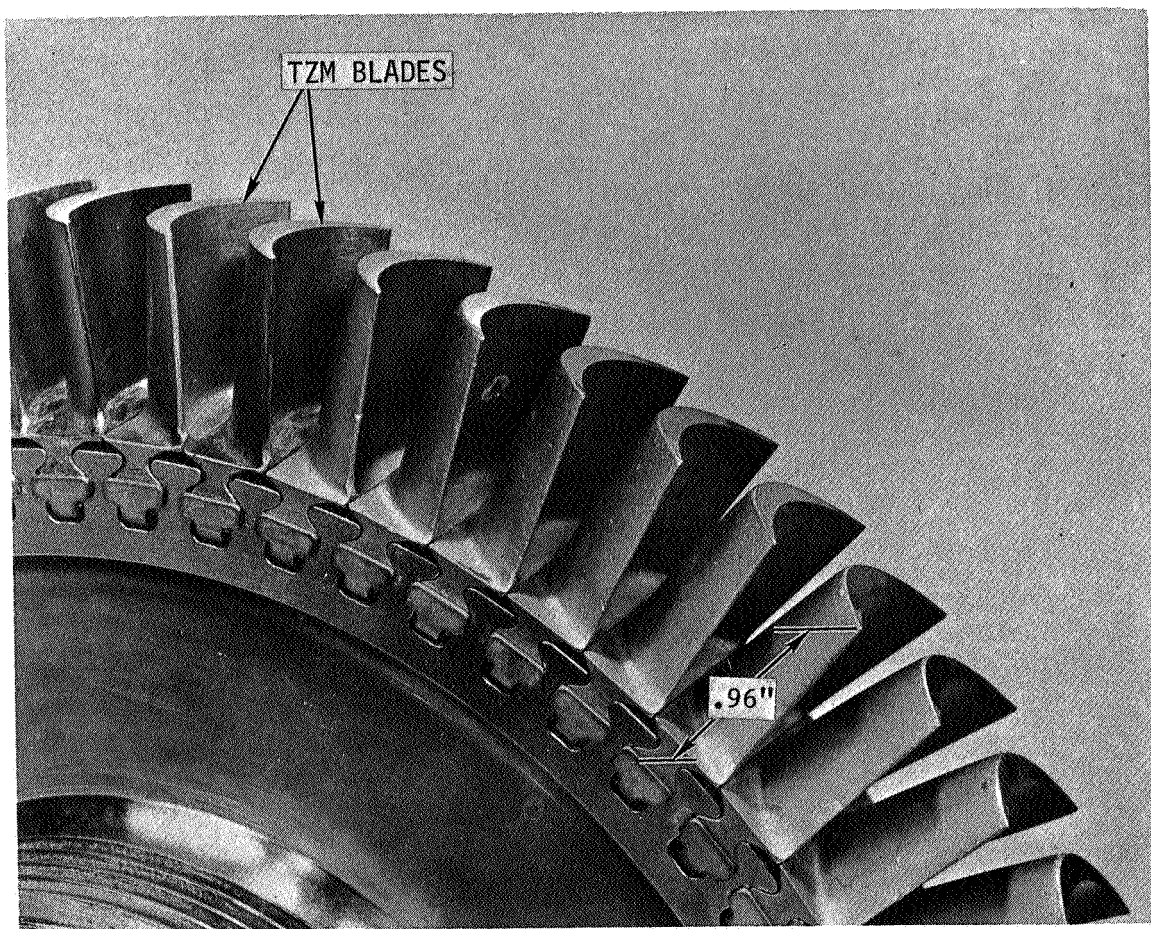


Figure 50. Second Stage Turbine Wheel Assembly After 2000 Hour Endurance Test, Vapor Blast Cleaning and Reassembly. (C6602215)

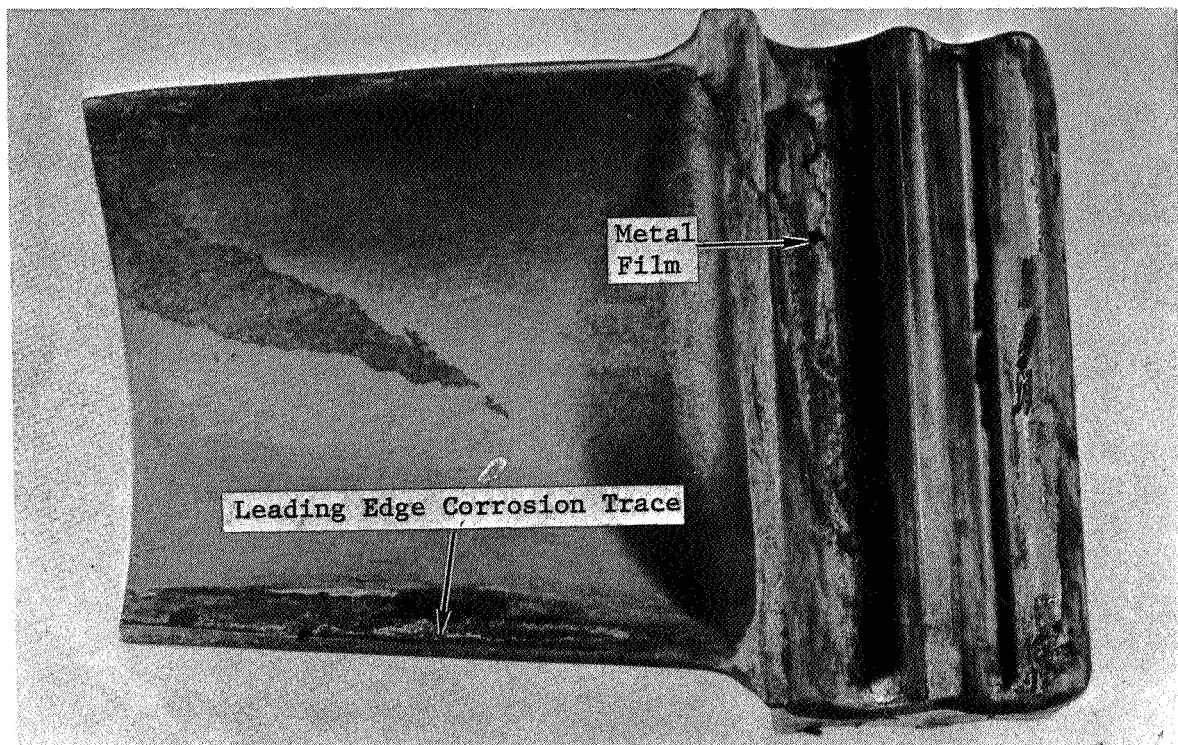


Figure 51. Concave Side of U-700 First Stage Turbine Blade After 2000 Hour Endurance Test. (C66011343)

Mag: 5X

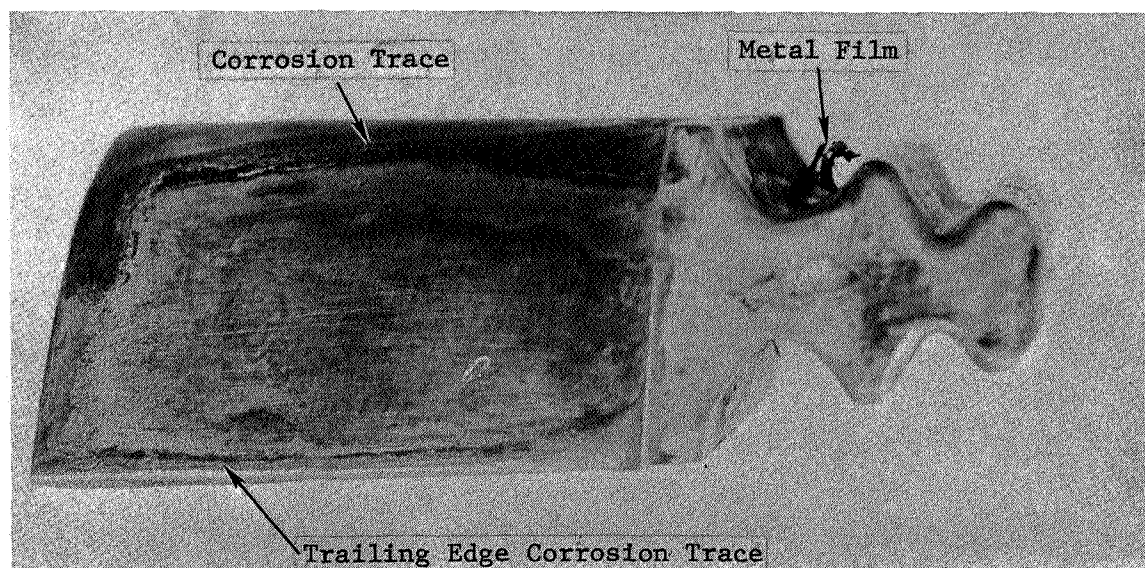


Figure 52. Trailing Edge of U-700 First Stage Turbine Blade After 2000 Hour Endurance Test. Note Metal Foil on Dovetail. (C66011340)

Mag: 5X

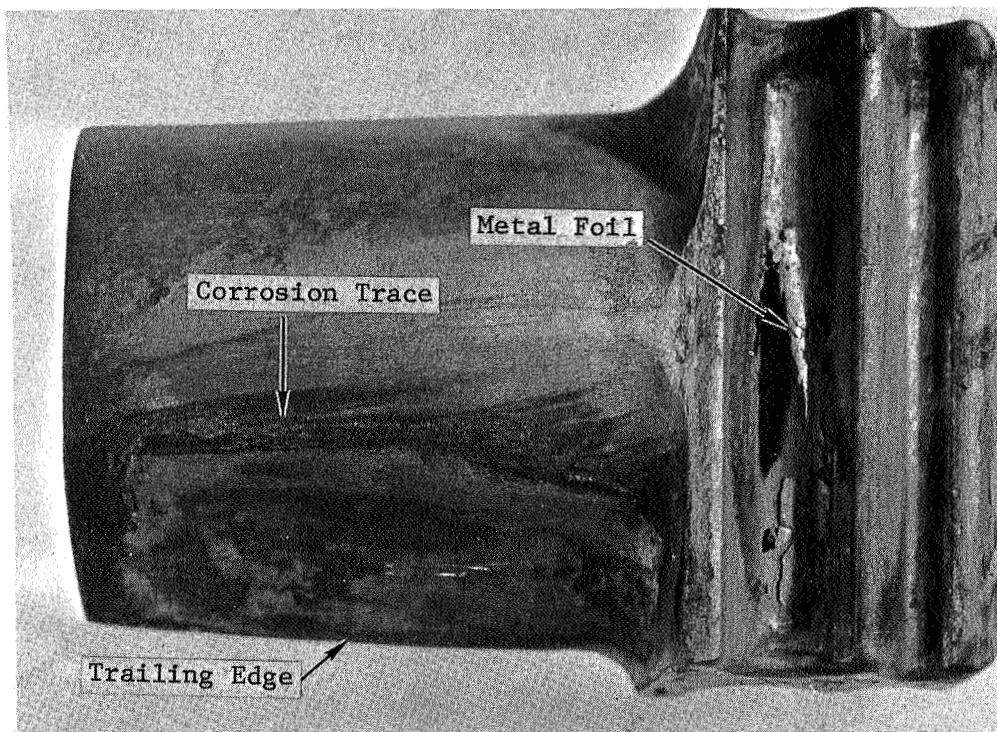


Figure 53. Convex Side of U-700 First Stage Turbine Blade After 2000-Hour Endurance Test. (C66011346) Mag: 5X

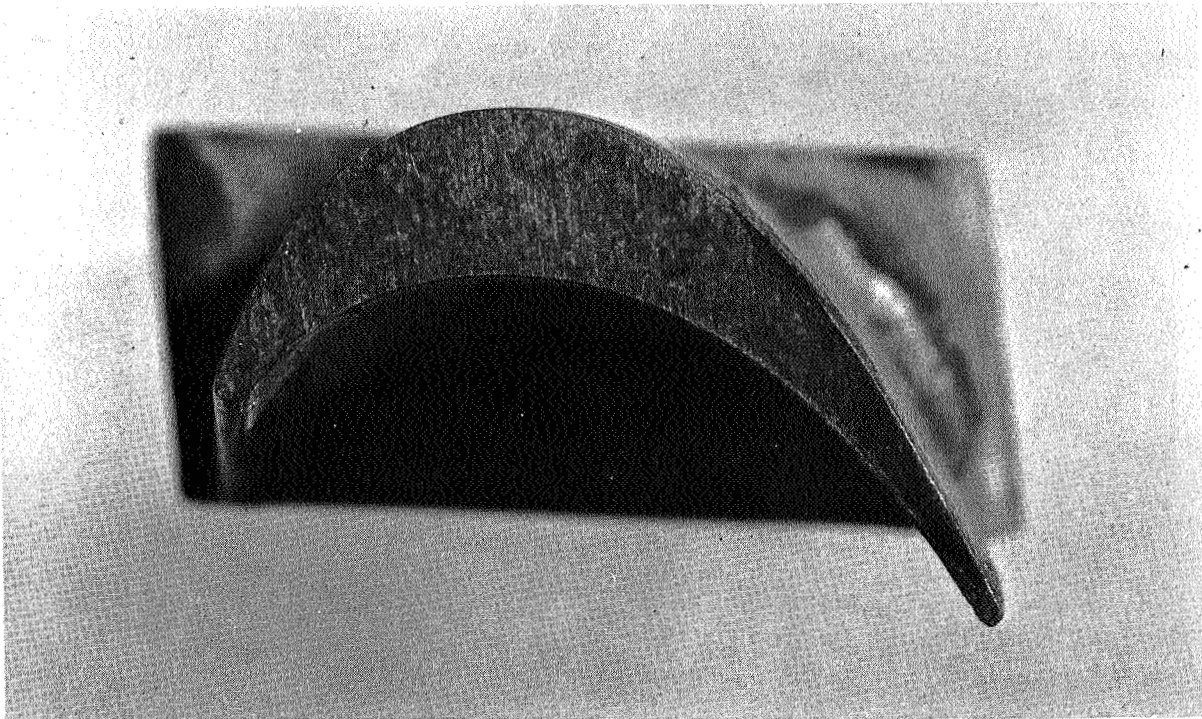


Figure 54. Tip of U-700 First Stage Turbine Blade After 2000 Hour
Endurance Test. (C66011338)

Mag: 5X

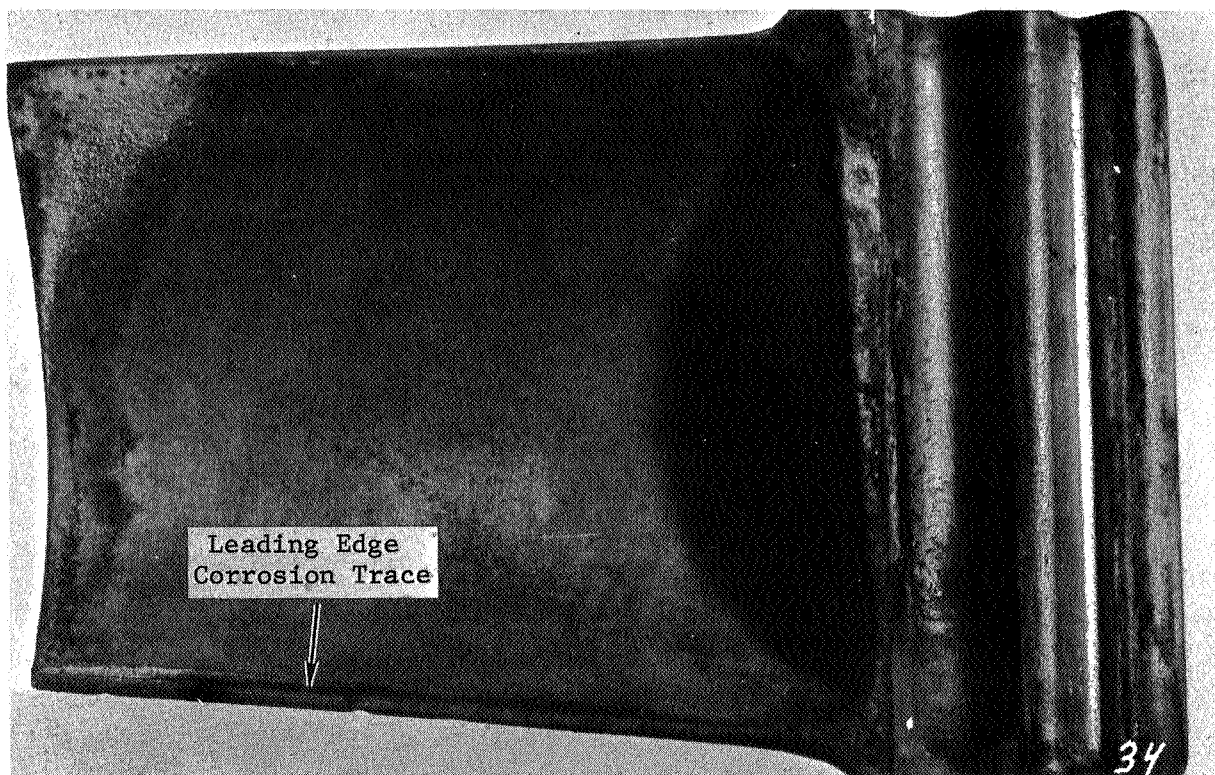


Figure 55. Concave Side of U-700 Second Stage Turbine Blade After
2000-Hour Endurance Test. (C66011345) Mag: 5X

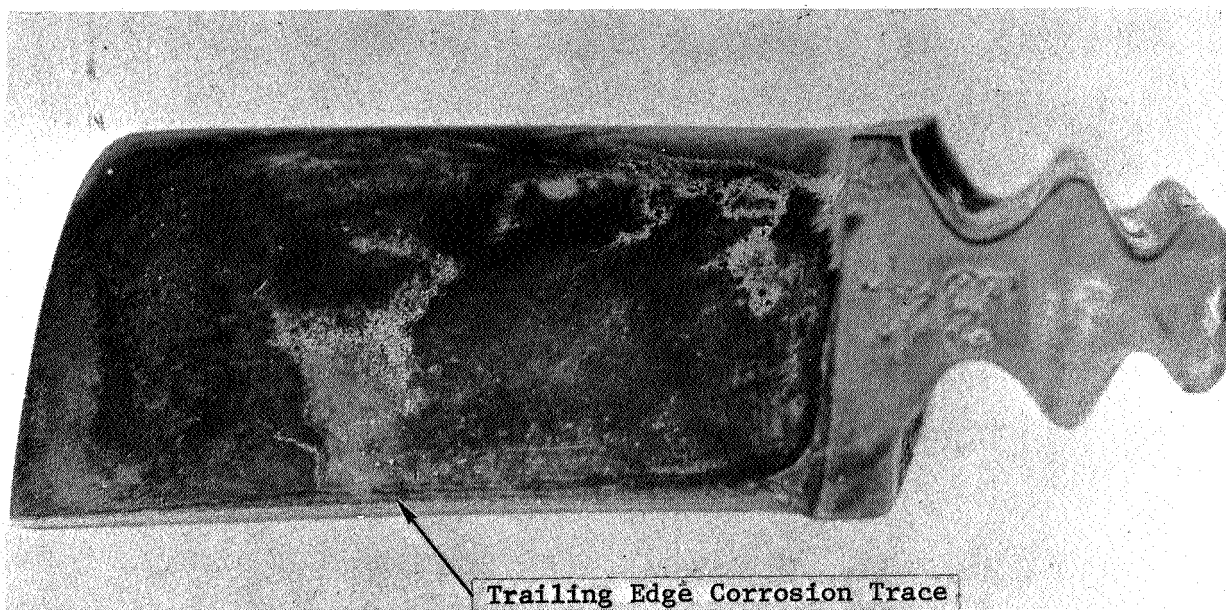


Figure 56. Trailing Edge of U-700 Second Stage Turbine Blade After
2000-Hour Endurance Test. (C66011341) Mag: 5X

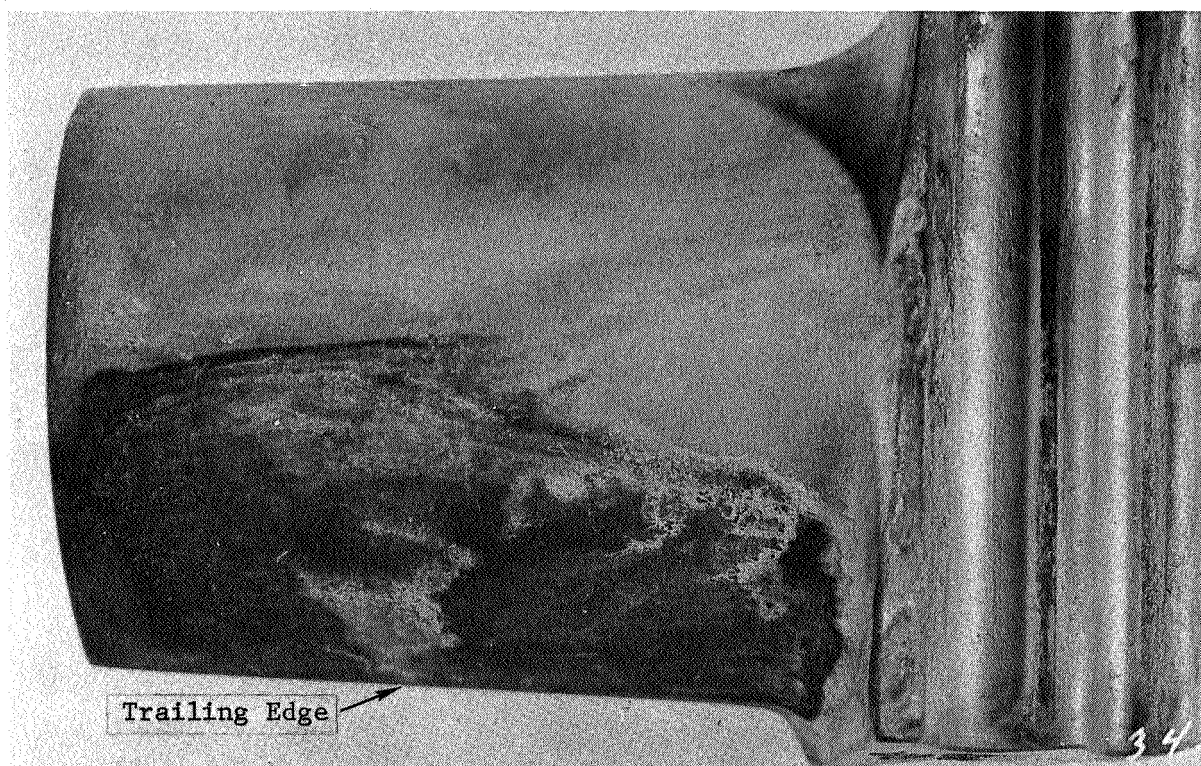


Figure 57. Convex Surface of U-700 Second Stage Turbine Blade After
2000-Hour Endurance Test. (C66011344) Mag: 5X

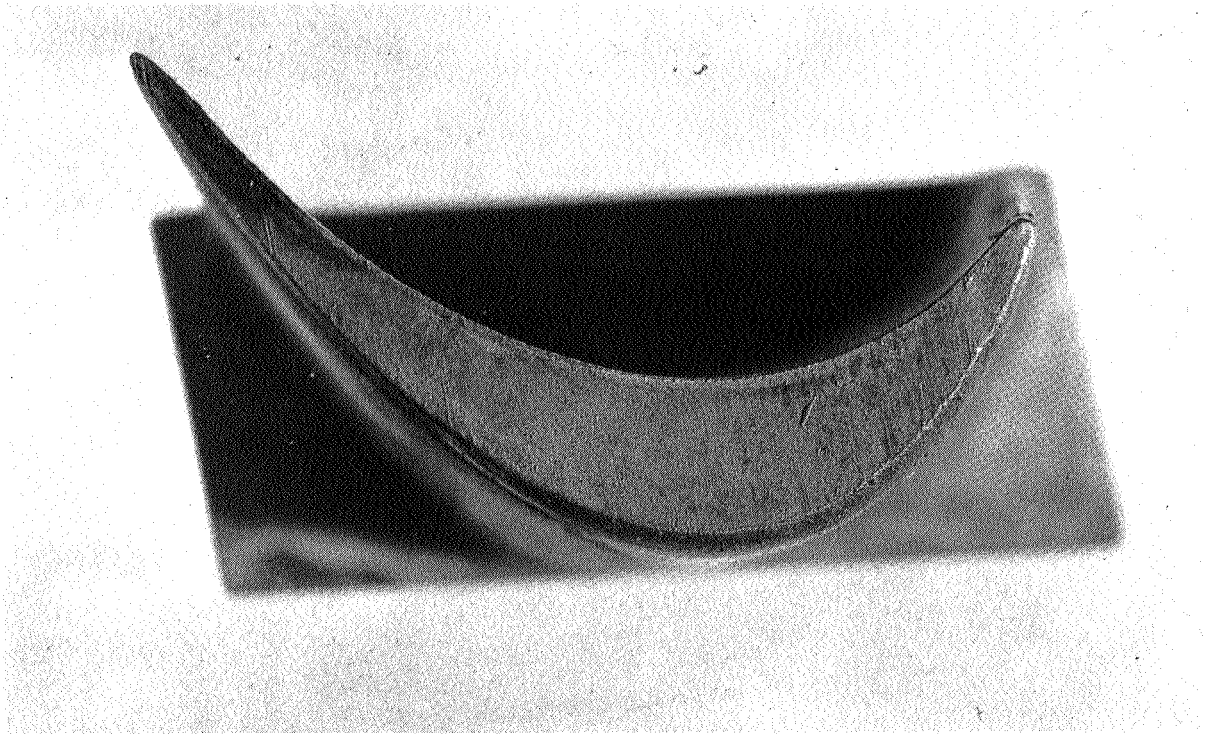


Figure 58. Tip of U-700 Second Stage Turbine Blade After 2000 Hour
Endurance Test. (C66011337)

Mag: 5X

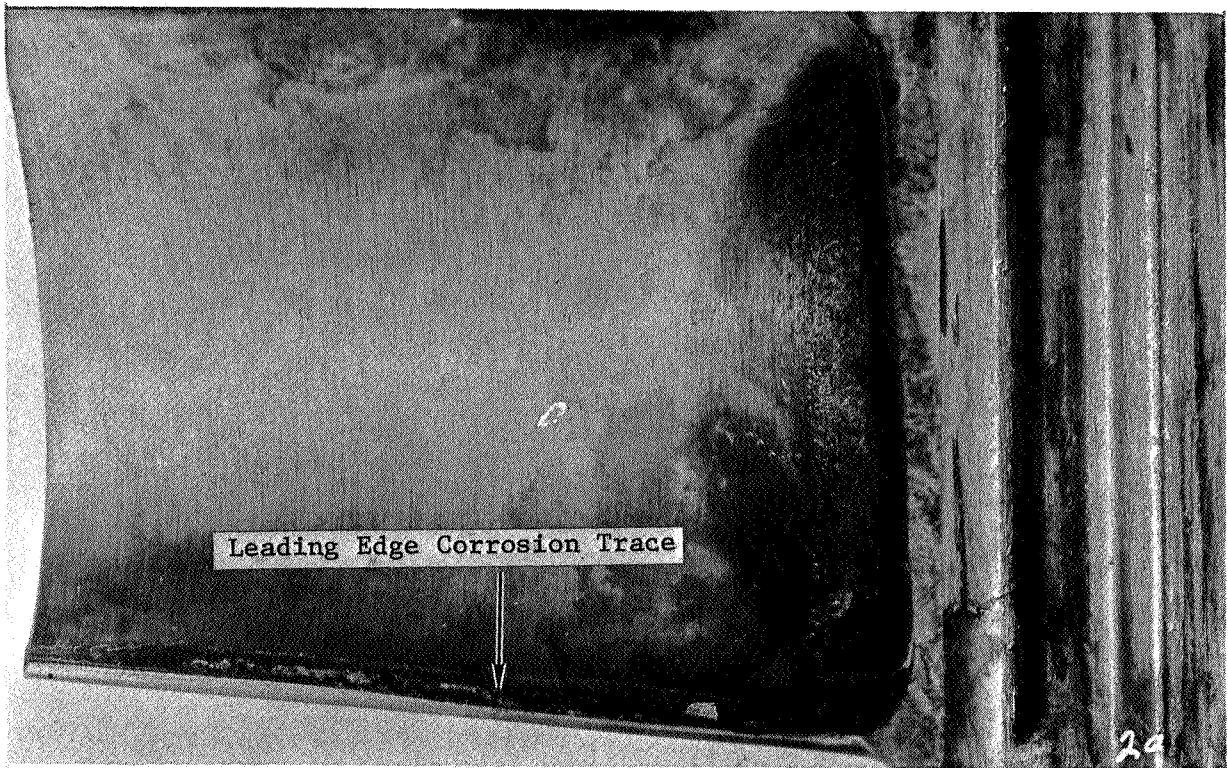


Figure 59. Concave Side of TZM Second Stage Turbine Blade After 2000-Hour Endurance Test. Note Leading Edge Corrosion. (C66011348)

Mag: 5X

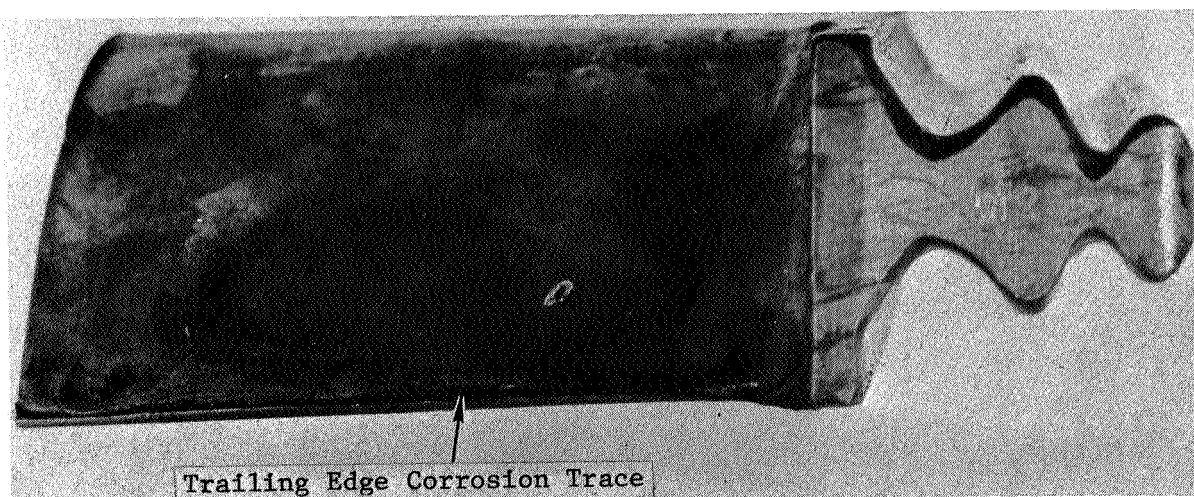
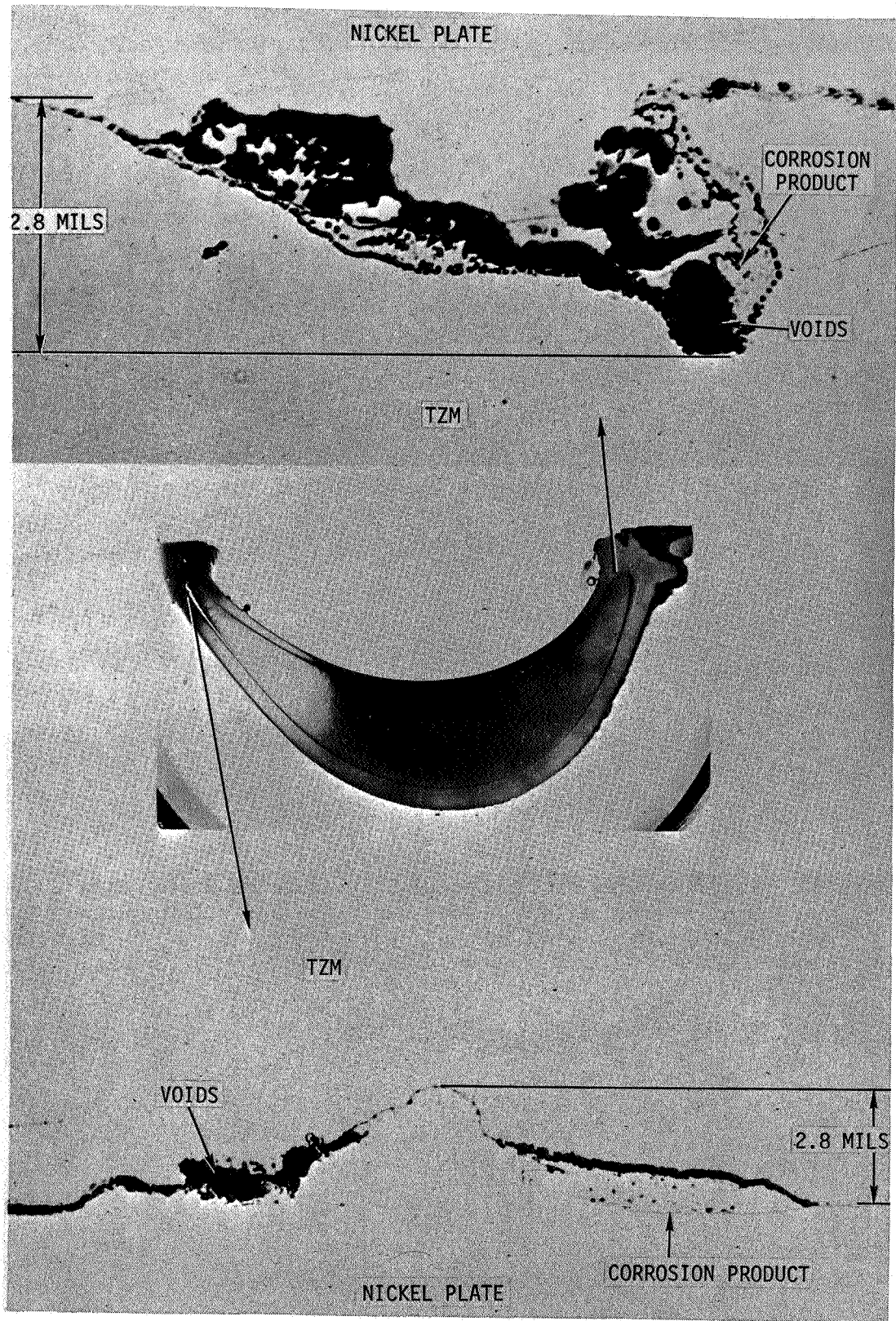


Figure 60. Trailing Edge of TZM Second Stage Turbine Blade After 2000-Hour Endurance Test. Note Corrosion at Trailing Edge.
(C66011328) Mag: 5X

CONCAVE LEADING EDGE

UNETCHED

MAG: 350X



UNETCHED

CONVEX TRAILING EDGE

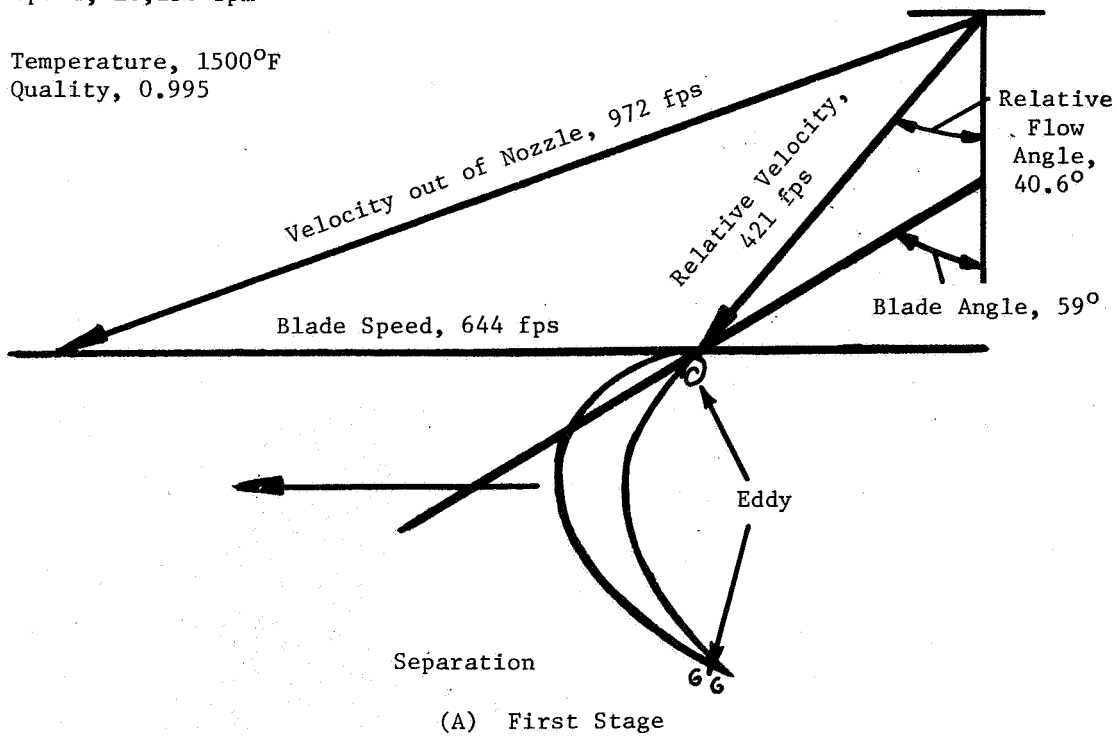
MAG: 175X

Figure 61. Leading and Trailing Edge Corrosion Traces and Micrographs of a Second Stage TZM Blade After 2000 Hour Endurance Test.

Speed, 18,250 rpm

Temperature, 1500°F

Quality, 0.995



Temperature, 1390°F

Quality, 0.967

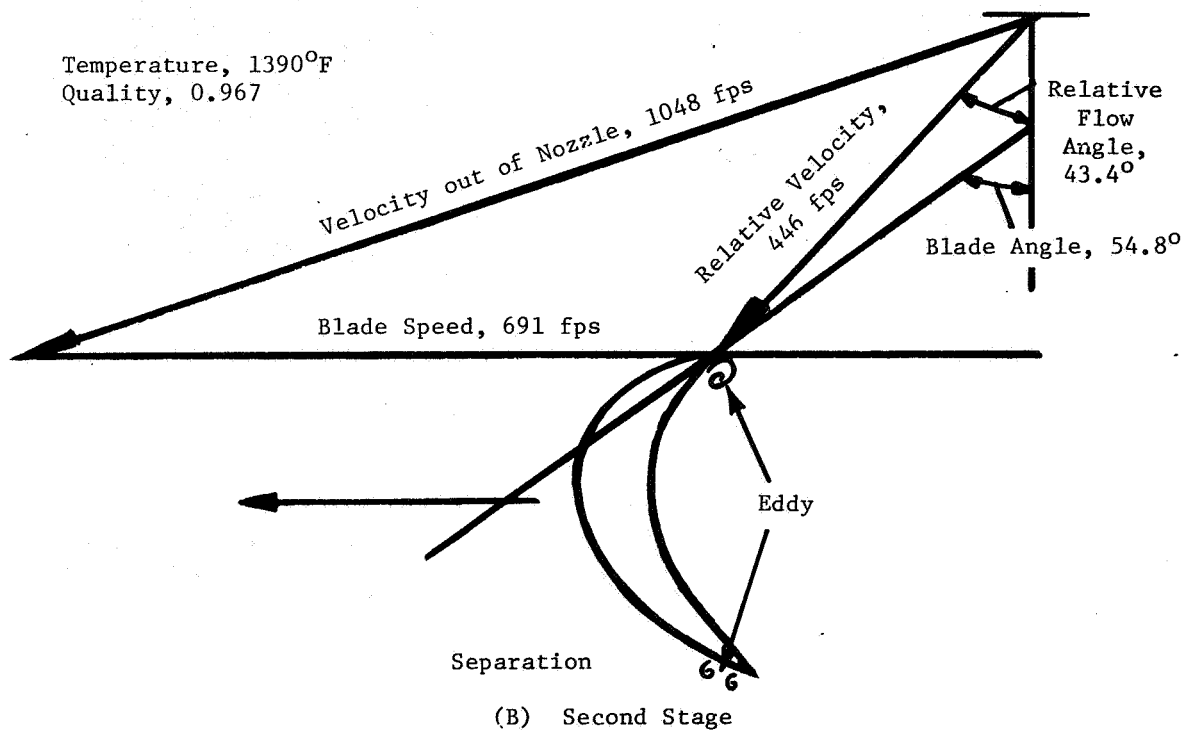
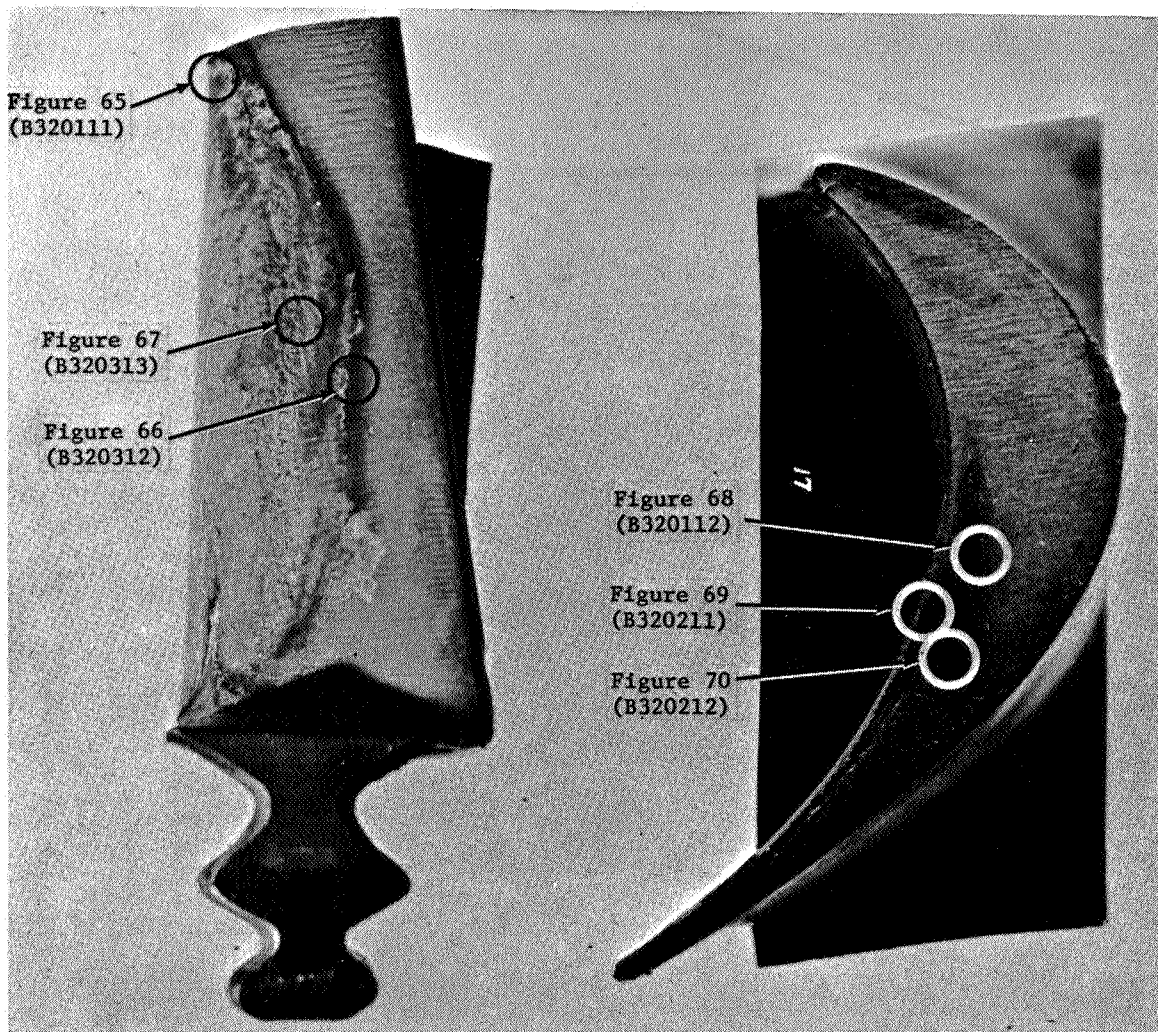


Figure 62. Flow Vector Diagrams for First and Second Stage Turbine Inlet Conditions.



(C66012445)

(C66012451)

Figure 63. Location of Selected Micrographs Taken from the Convex Airfoil Surface and Tip of a TZM Second Stage Blade After 2000-Hour Test.

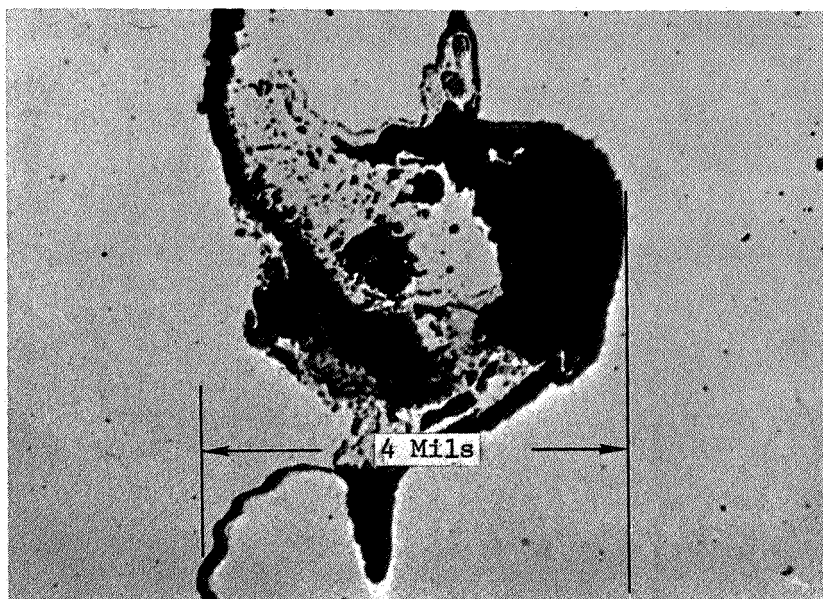


Figure 64. Convex Surface Near Tip of TZM Second Stage Blade After 2000 Hour Test. (B320111)

Etchant: Unetched

Mag: 500X

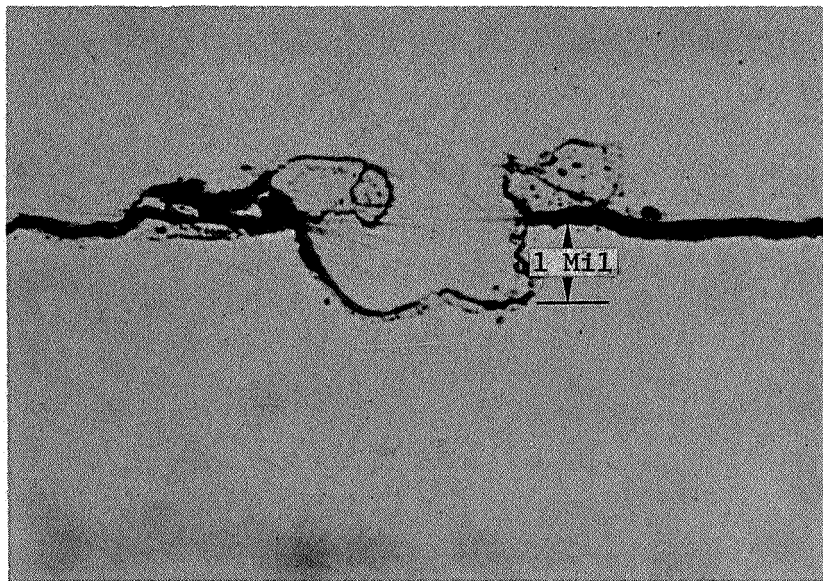


Figure 65. Convex Surface of TZM Second Stage Blade at Major Corrosion Area After 2000 Hour Test. (B320312)

Etchant: Unetched

Mag: 500X

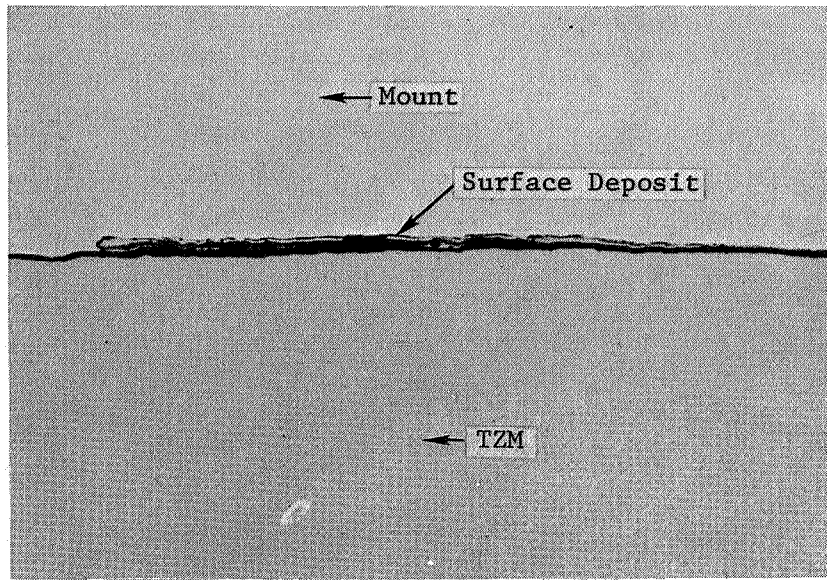


Figure 66. Convex Surface of TZM Second Stage Blade After 2000 Hour Test. (B320313)

Etchant: Unetched

Mag: 100X

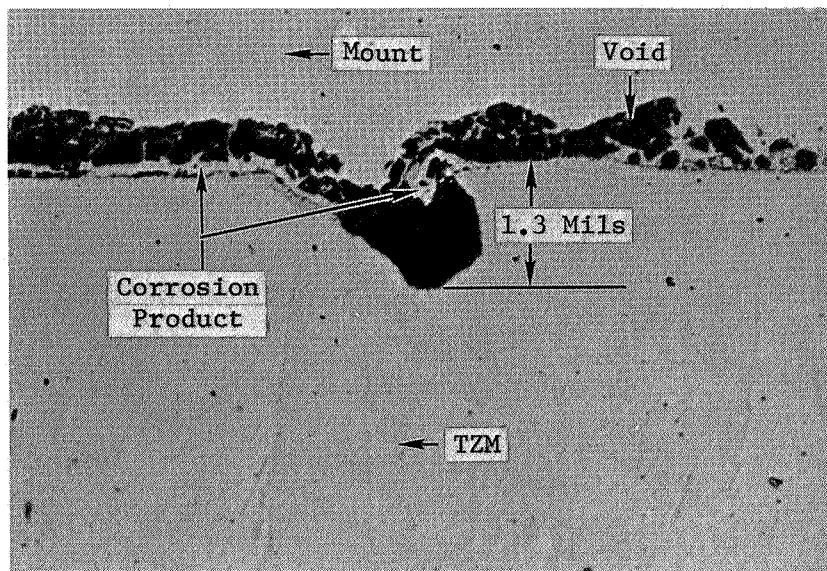


Figure 67. Tip of TZM Second Stage Turbine Blade at Major Corrosion Trace After 2000 Hour Test. (B320112)

Etchant: Unetched

Mag: 500X

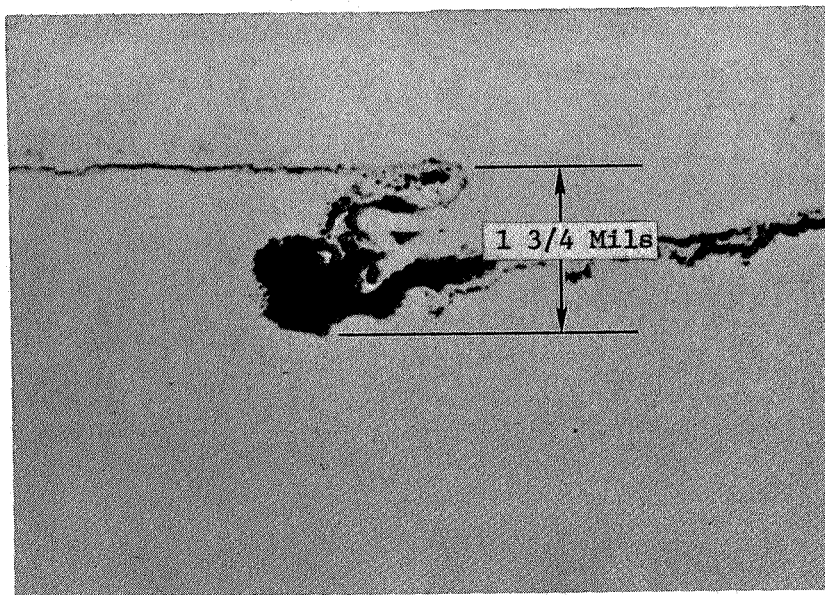


Figure 68. Tip of TZM Second Stage Turbine Blade at Major Corrosion Trace After 2000 Hour Test. (B320211)

Etchant: Unetched

Mag: 500X

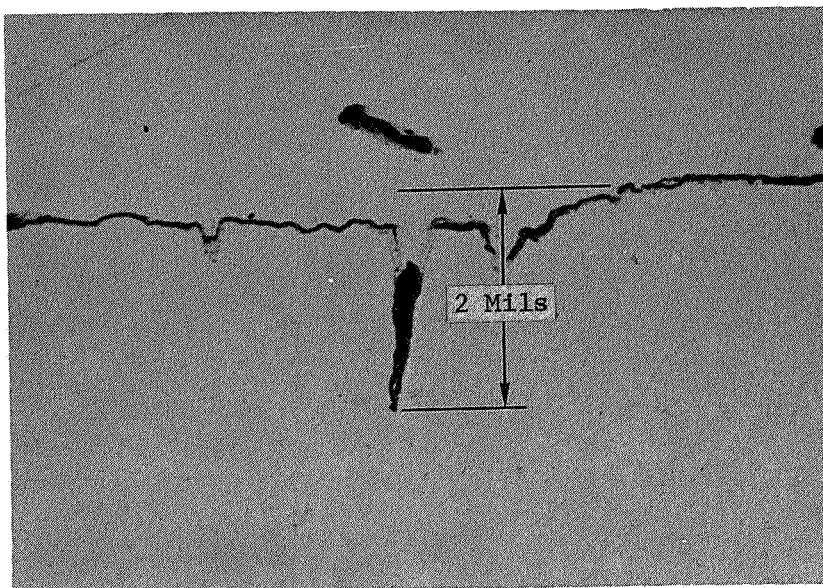


Figure 69. Tip of TZM Second Stage Turbine Blade Away from Major Corrosion Trace After 2000 Hour Test. (B320212)

Etchant: Unetched

Mag: 500X

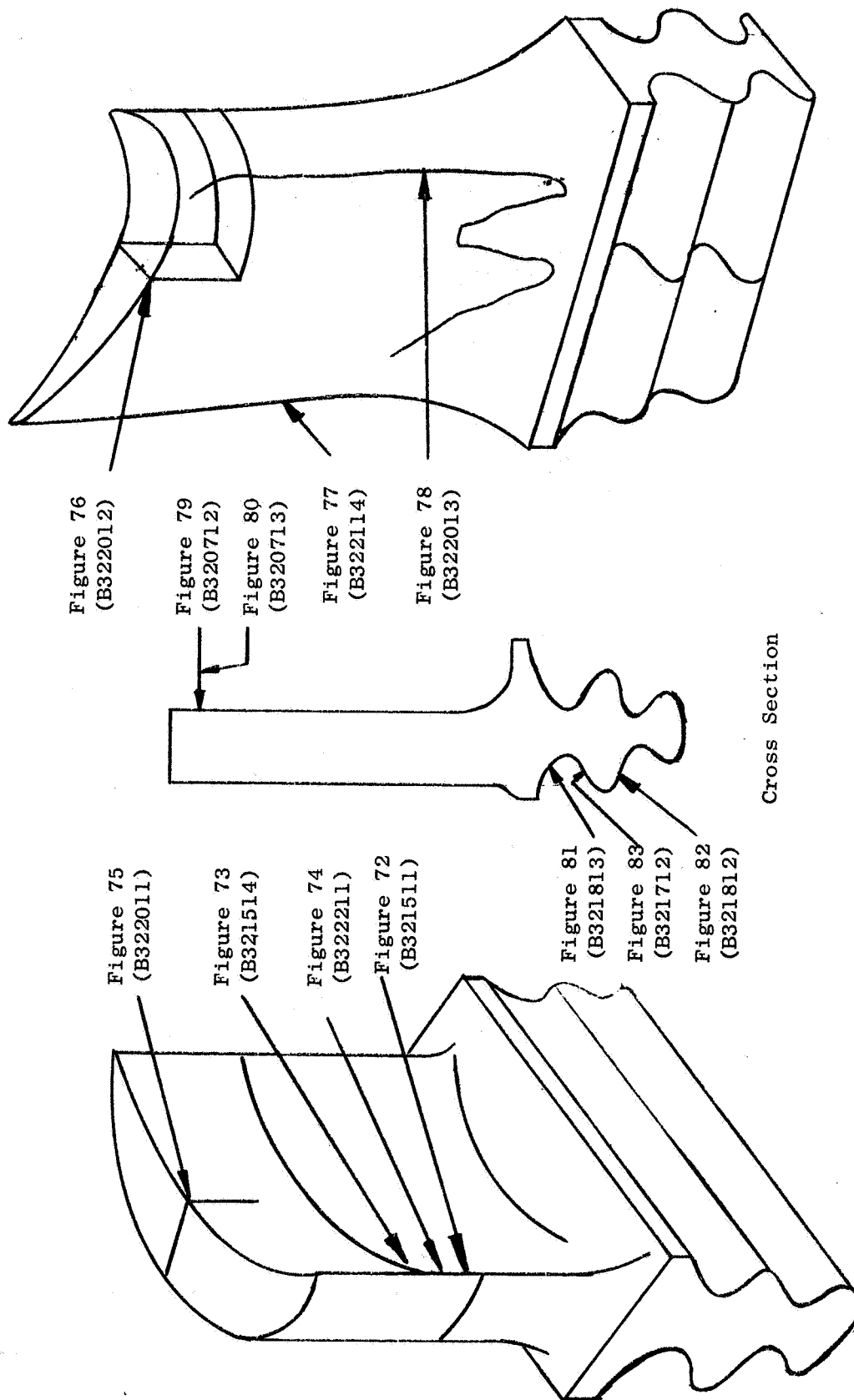


Figure 70. Location of Selected Micrographs of a U-700 First Stage Blade after 2000-Hour Endurance Test at Approximately 1450°F.

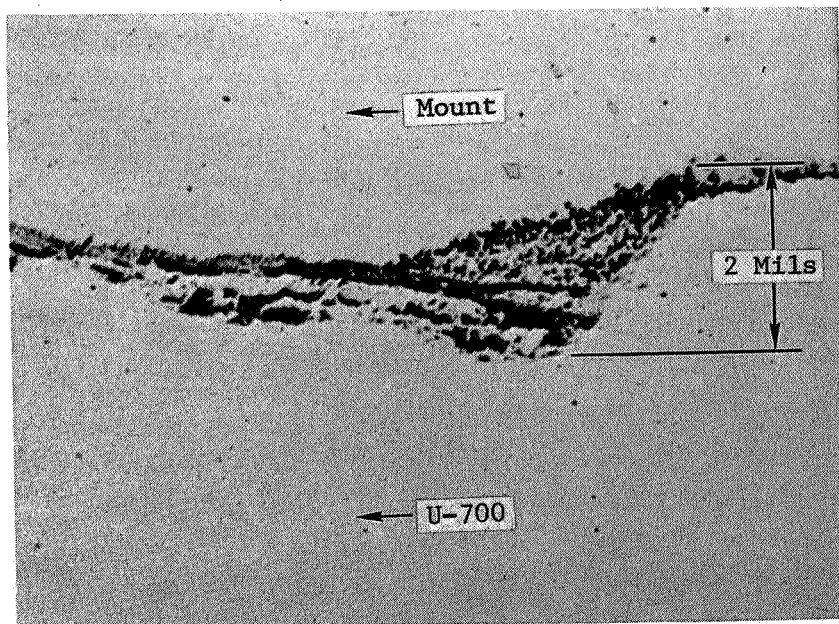


Figure 71. Corrosion Cavity at Concave Leading Edge of a First Stage U-700 Blade After 2000 Hour Endurance Test. (B321511)

Etchant: Unetched

Mag: 500X

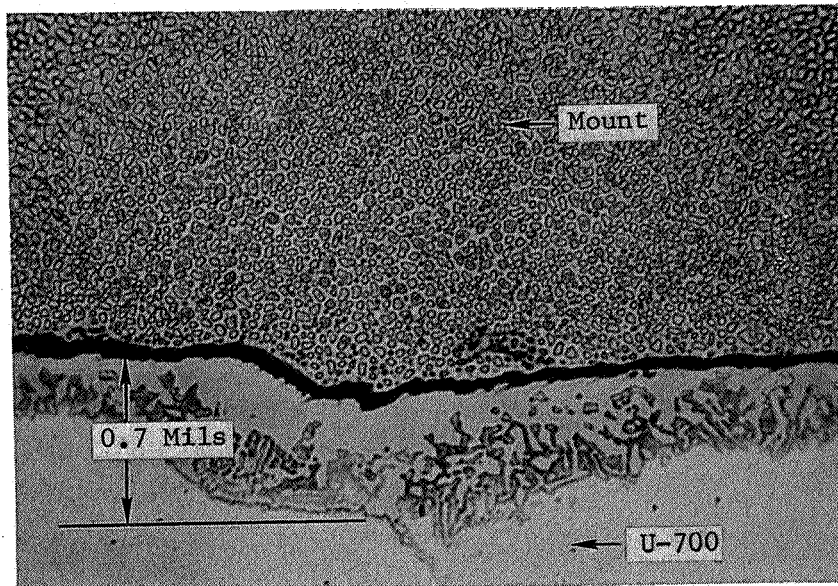


Figure 72. Surface Reaction Product at Concave Leading Edge of a First Stage U-700 Blade After 2000 Hour Endurance Test. (B321514)

Etchant: 3% H_2O_2 , Electrolytic

Mag: 1000X

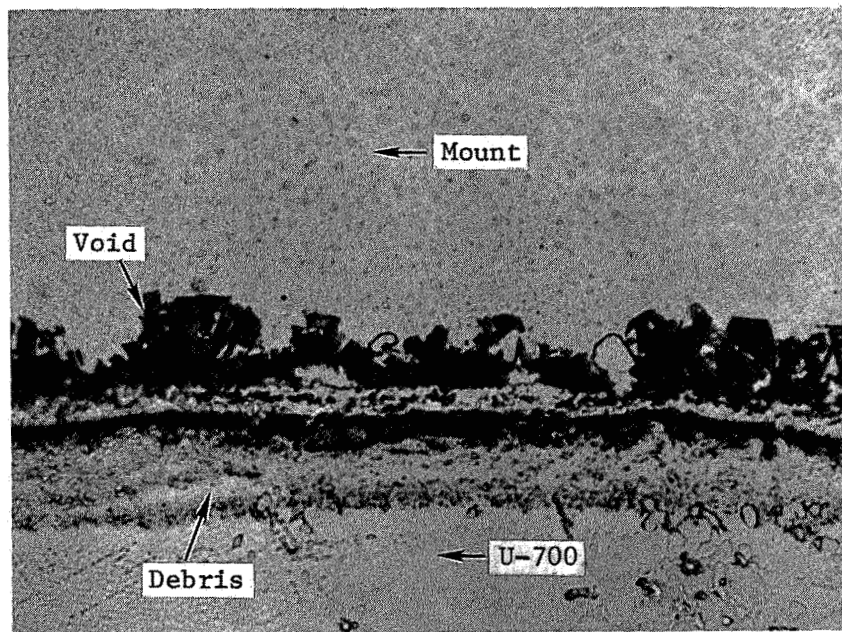


Figure 73. Surface Deposit on the Concave Leading Edge of a First Stage Turbine Blade After 2000 Hour Endurance Test. (B322211)

Etchant: Unetched

Mag: 1000X

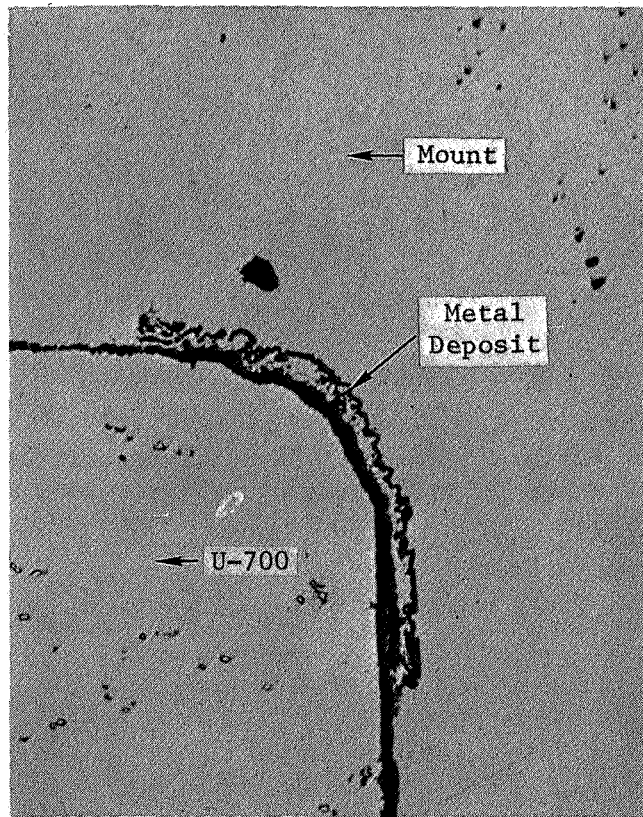


Figure 74. Surface Corrosion and Metal Deposit at Concave Tip of a U-700 First Stage Turbine Blade After 2000 Hour Endurance Test. (B322011)

Etchant: Unetched

Mag: 100X

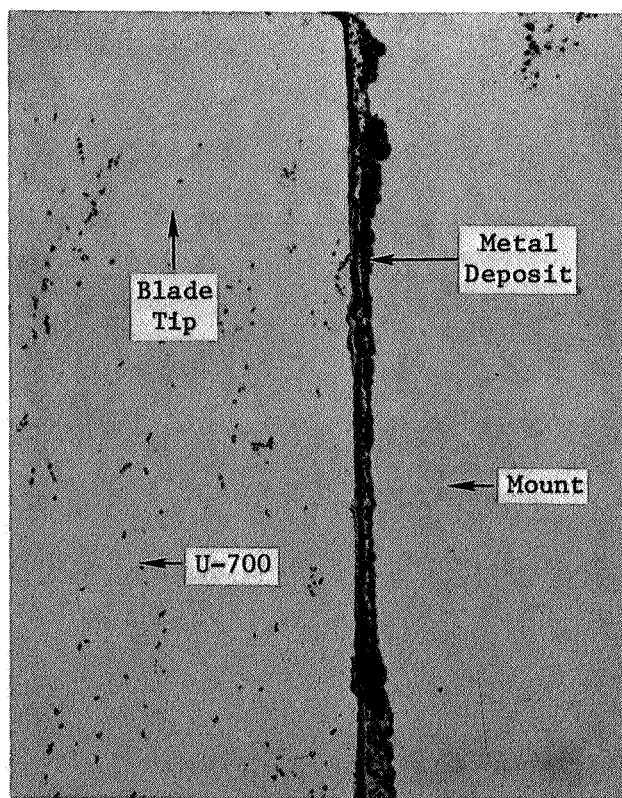


Figure 75. Light Surface Corrosion and Metal Deposit on Convex Tip of a First Stage U-700 Turbine Blade After 2000 Hour Test. (B322012)

Etchant: Unetched

Mag: 100X

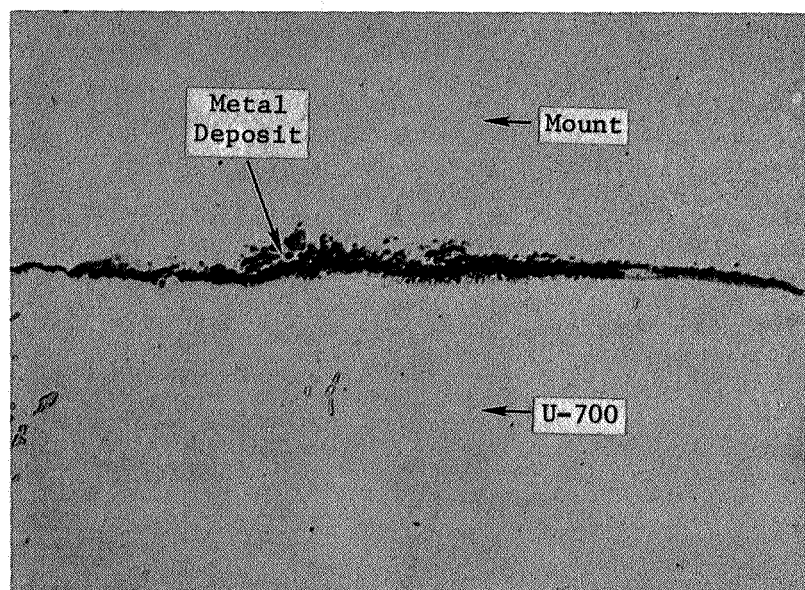


Figure 76. Corrosion and Metal Deposit on Convex Trailing Edge of a First Stage U-700 Turbine Blade After 2000 Hour Test. (B322114)

Etchant: Unetched

Mag: 250X

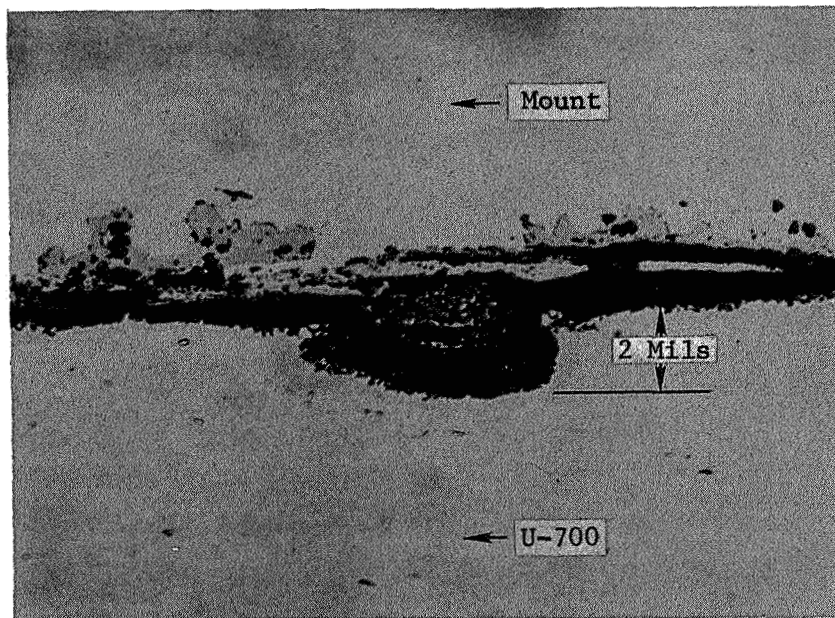


Figure 77. Corrosion Groove on Convex Airfoil Surface of a U-700 First Stage Turbine Blade After 2000 Hour Endurance Test. (B322013)

Etchant: Unetched

Mag: 250X

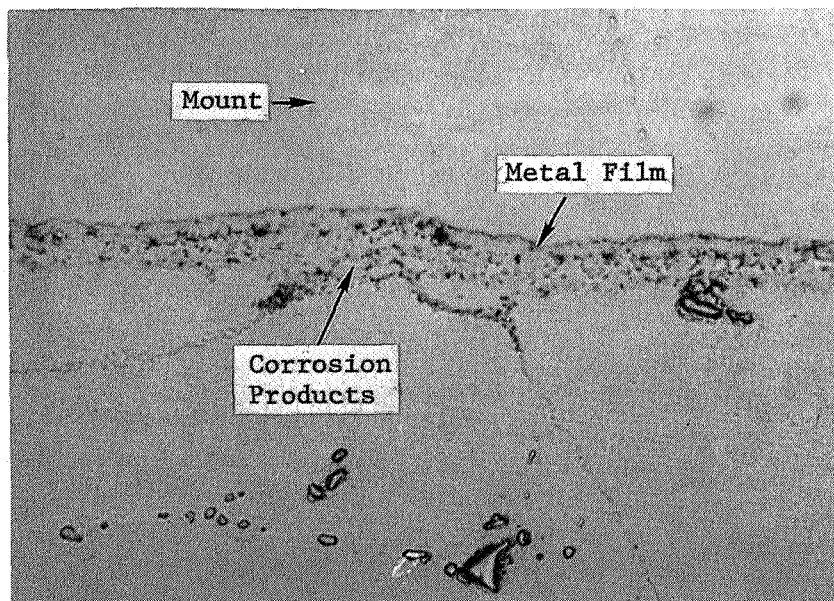


Figure 78. Metal Film Deposit Overlaying Corrosion Products on the Concave Tip Surface of a First Stage U-700 Turbine Blade After 2000 Hour Test (B320712)

Etchant: Unetched

Mag: 1000X

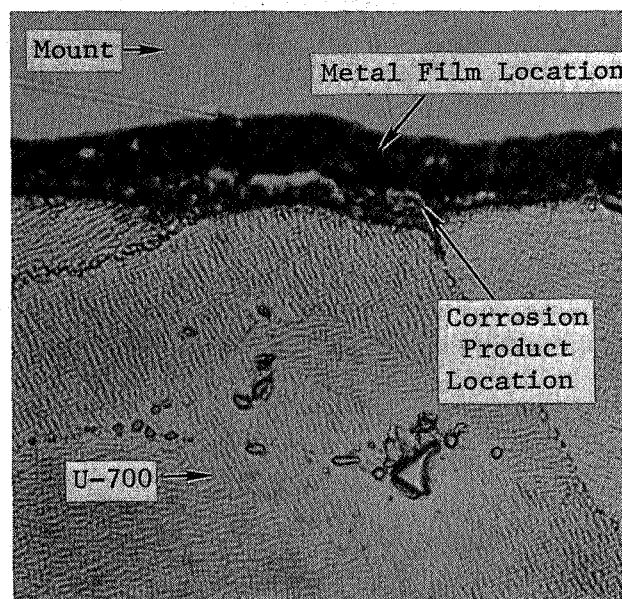


Figure 79. Metal Film Deposit Overlaying Corrosion Products on the Concave Tip Surface of a First Stage U-700 Turbine Blade After 2000 Hour Test. (B320713) Area Shown is that of Figure 78.

Etchant: 3% H_2O_2 , Electrolytic

Mag: 1000X

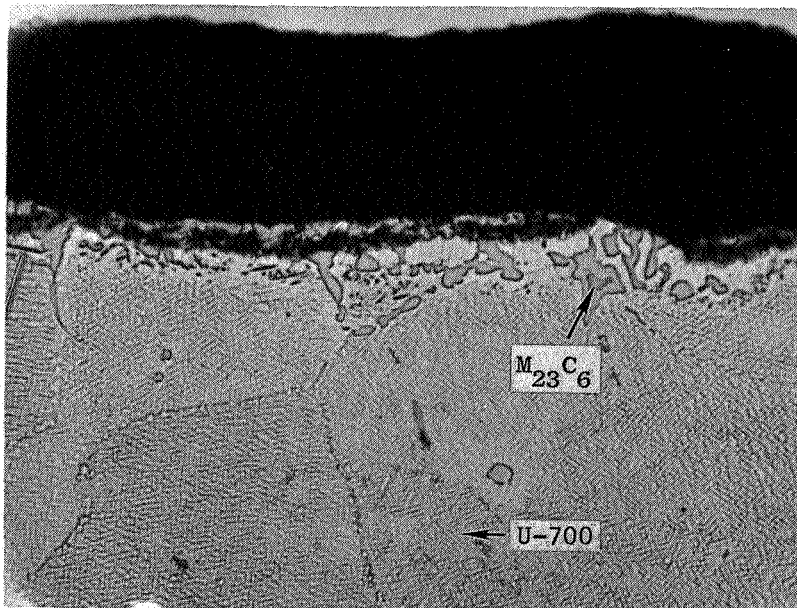


Figure 80. Alloy Depletion at Dovetail Surface of a First Stage U-700 Turbine Blade After 2000 Hour Test. (B321813)

Etchant: 3% H_2O_2 , Electrolytic

Mag: 1000X

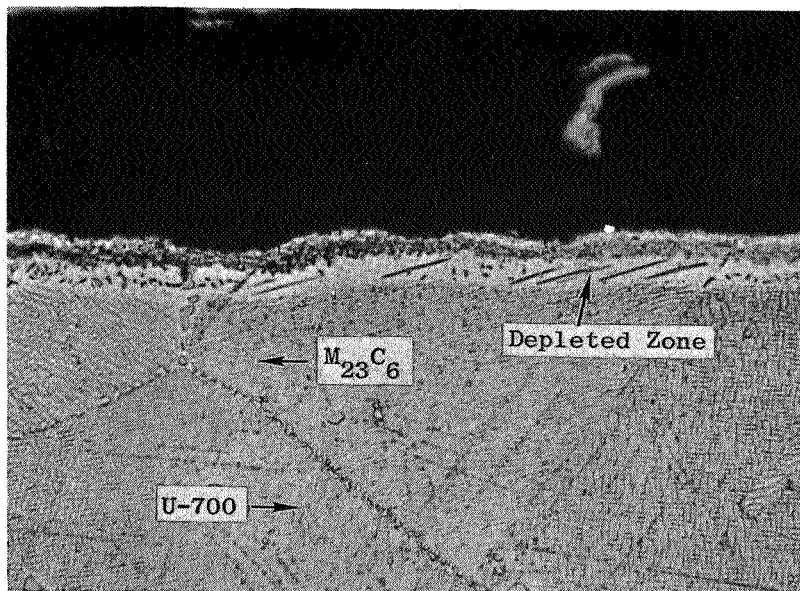


Figure 81. Alloy Depletion at Dovetail Surface of a First Stage U-700 Turbine Blade After 2000 Hour Test. (B321812)

Etchant: 3% H_2O_2 , Electrolytic

Mag: 1000X

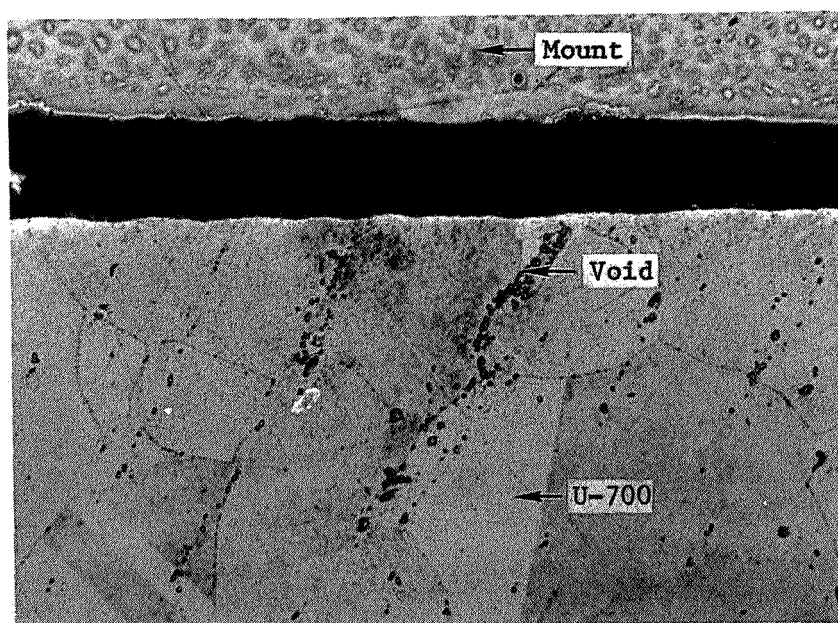


Figure 82. Dovetail Contact Area of a U-700 First Stage Turbine Blade After 2000 Hour Test. Note Lack of Depletion or Corrosion in Area Protected from Potassium. (B321712)

Etchant: 3% H_2O_2 , Electrolytic

Mag: 250X

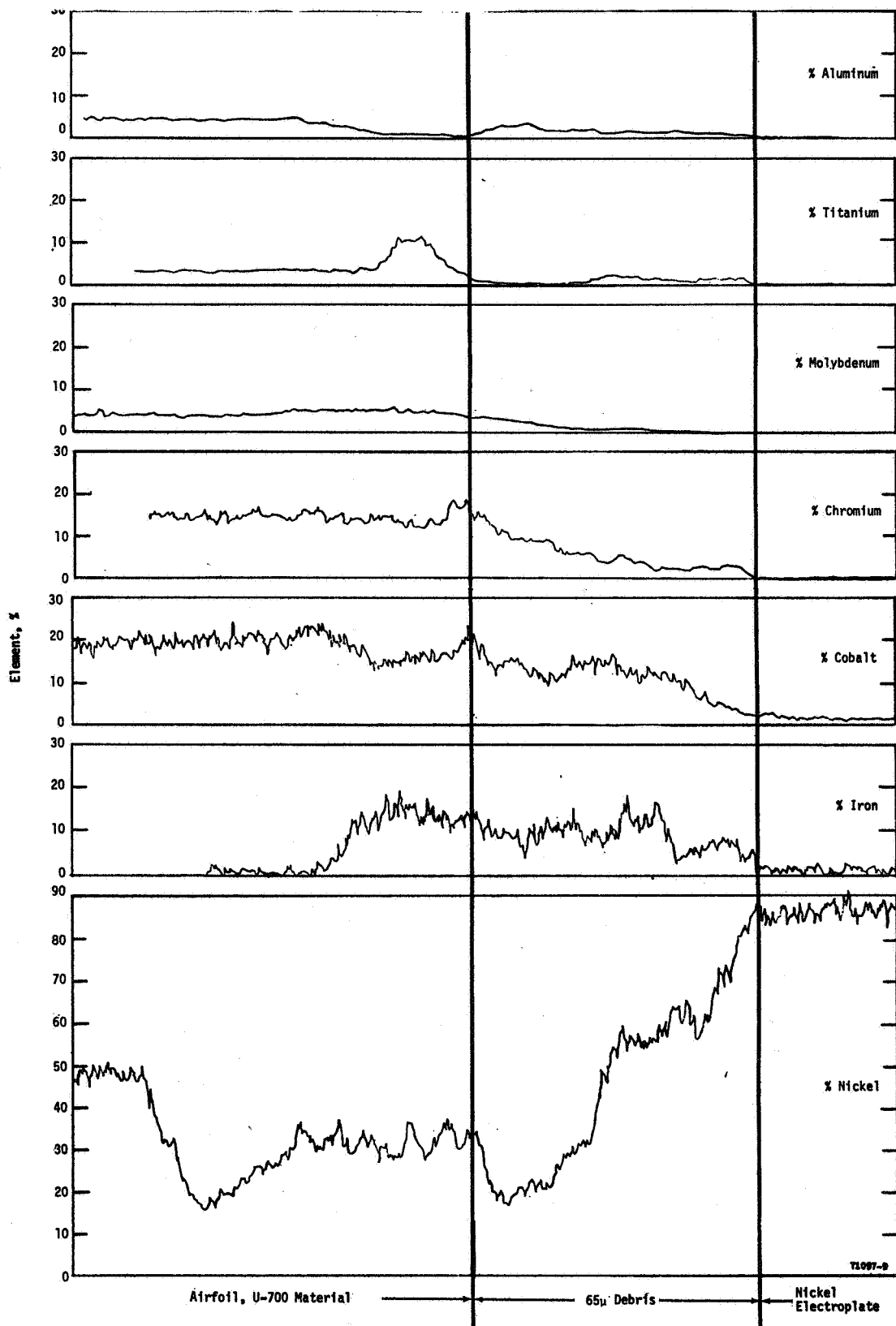


Figure 83. Electron Microprobe Traces of Surface Debris on First Stage U-700 Turbine Blade from the 2000-Hour Endurance Test.

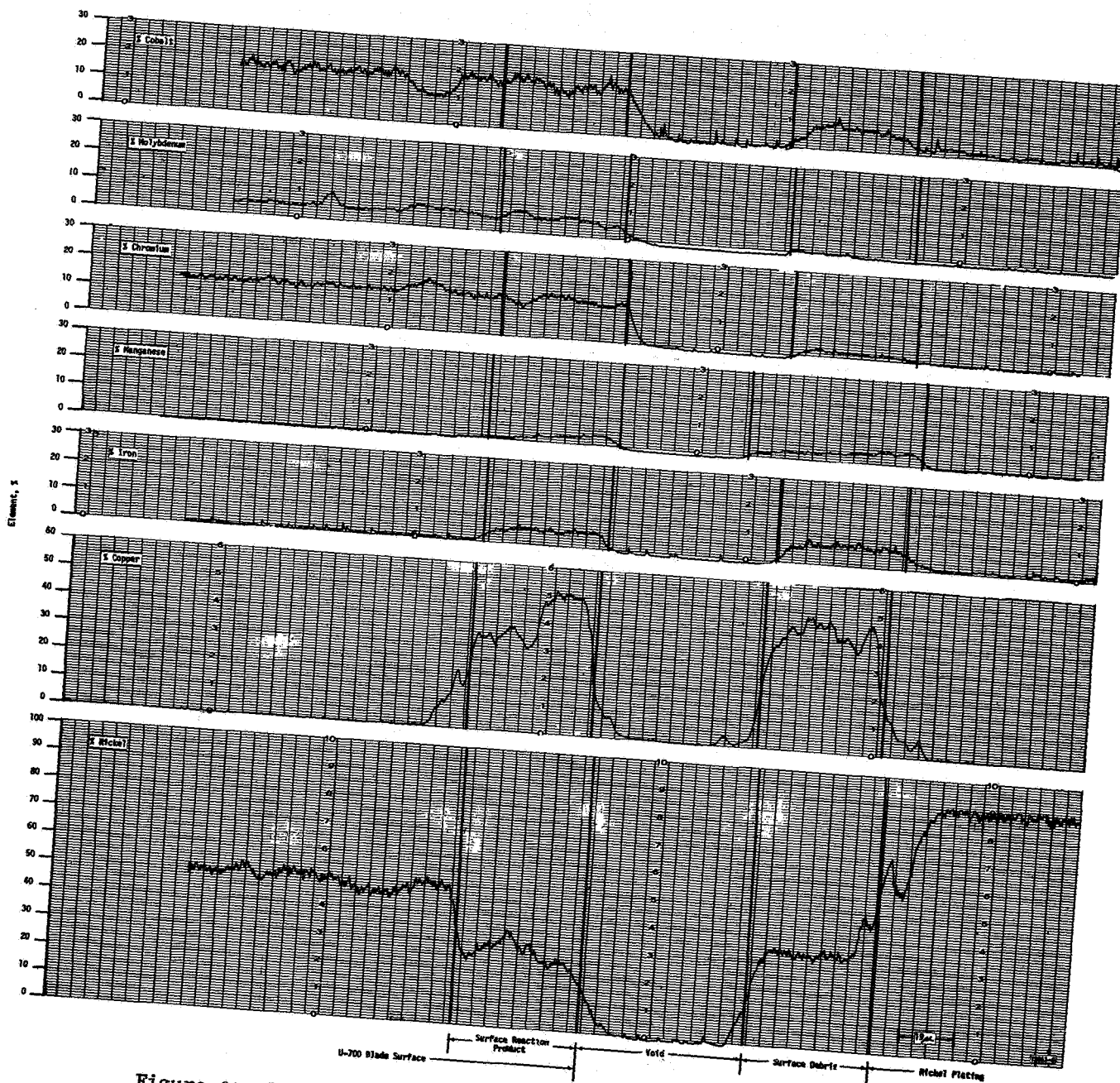


Figure 84. Electron Microprobe Traces of Surface Reaction Product and Overlaying Debris of First Stage Blade from 2000-Hour Test.

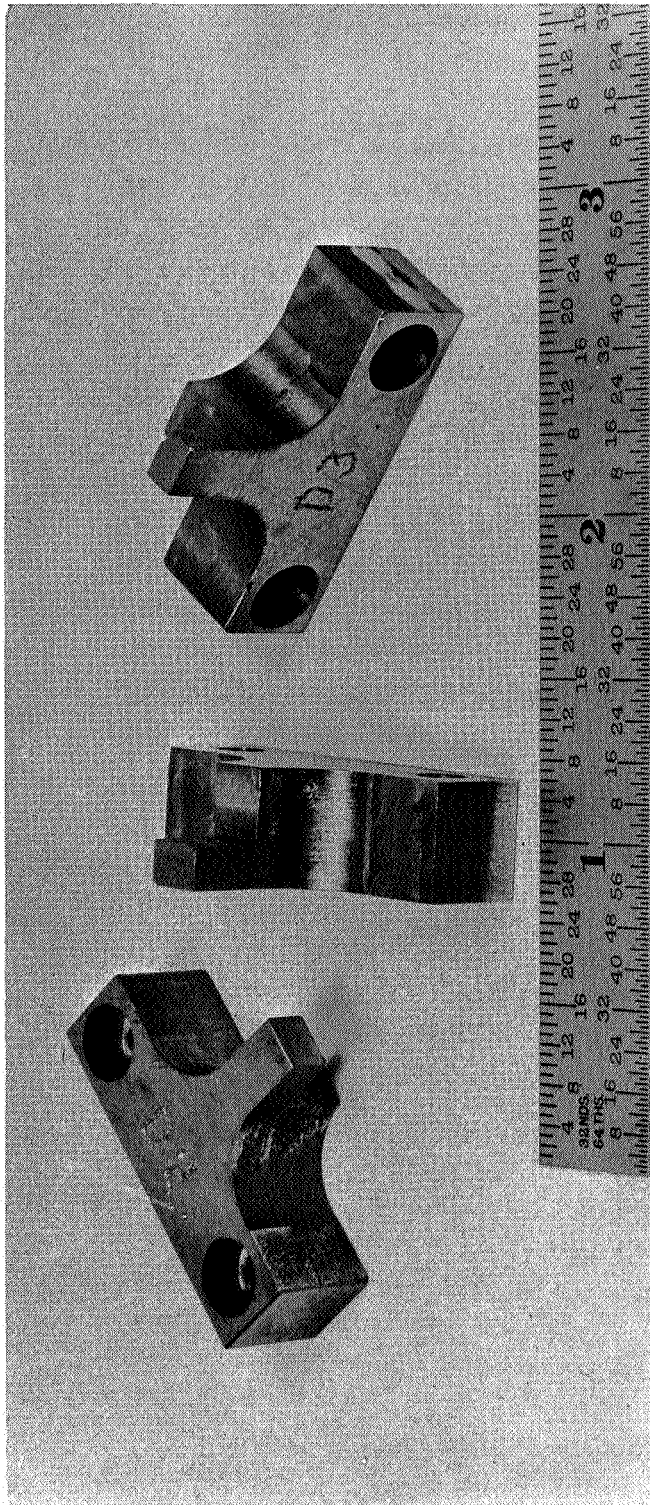


Figure 85. Molybdenum Alloy TZC Erosion Inserts Before Installation for 2000-Hour Endurance Test. (C65082408)

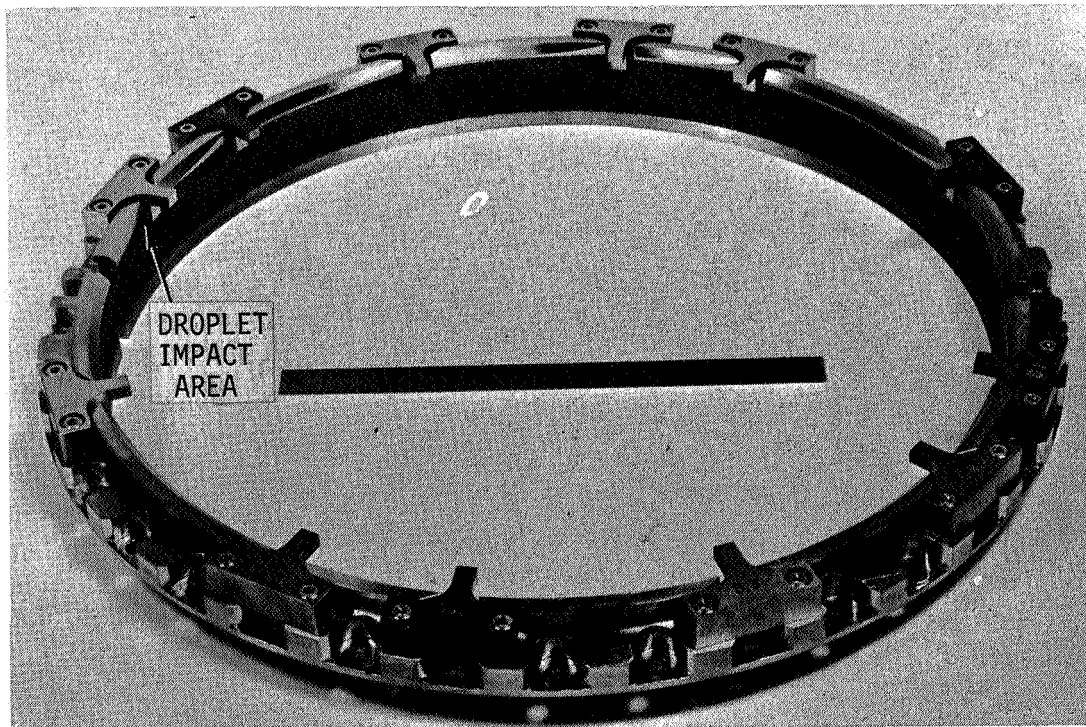


Figure 86. Erosion Inserts Installed in Second Stage Turbine Shroud.
(C65082408)

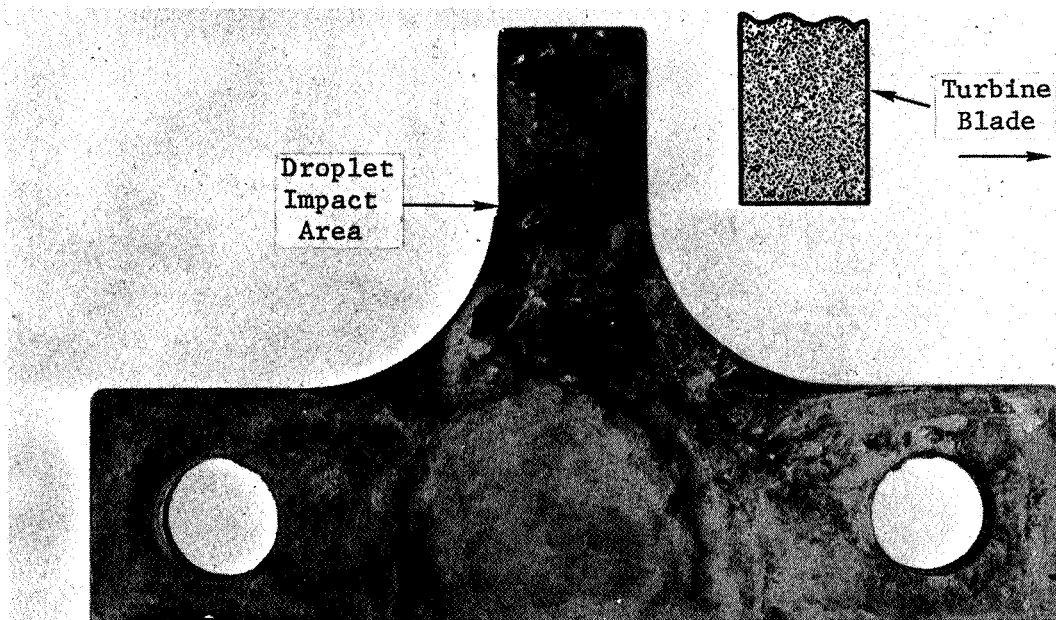


Figure 87. Erosion Insert Showing Typical Discoloration.
(C66012437) Mag: 4X



Figure 89. Liquid Potassium Impact Surface of Recrystallized TZM Erosion Insert Specimen Number B-2. Mag: 9X (C66012761)

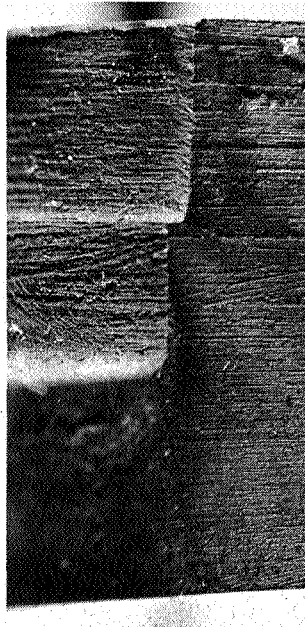


Figure 90. Liquid Potassium Impact Surface of Stress Relieved TZM Erosion Insert Specimen Number C-1. (C66012763) Mag: 9X



Figure 91. Liquid Potassium Impact Surface of As-Received * TZC Erosion Insert Specimen Number D-2. (C66012757) Mag: 9X

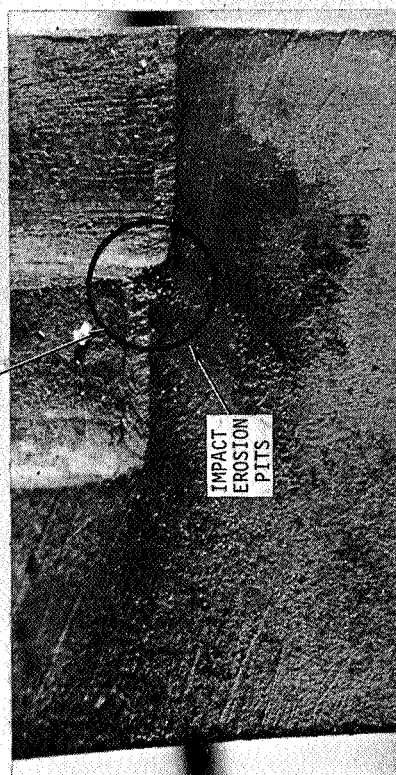
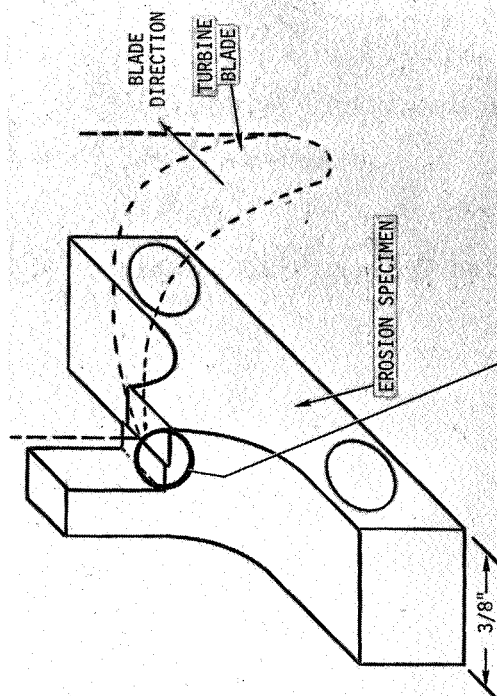


Figure 88. Liquid Potassium Impact Surface of U-700 Erosion Insert Specimen Number A-1. Note Impact Erosion at Upper Center. Mag: 9X

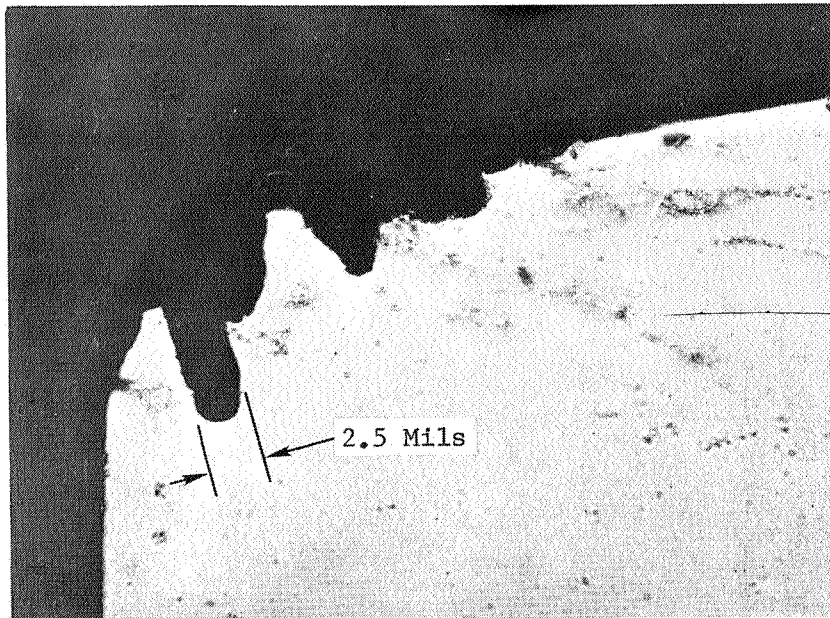


Figure 92. Impact Erosion Pits in U-700 Erosion Insert A-3. (B340111)
Etchant: Unetched Mag: 100X

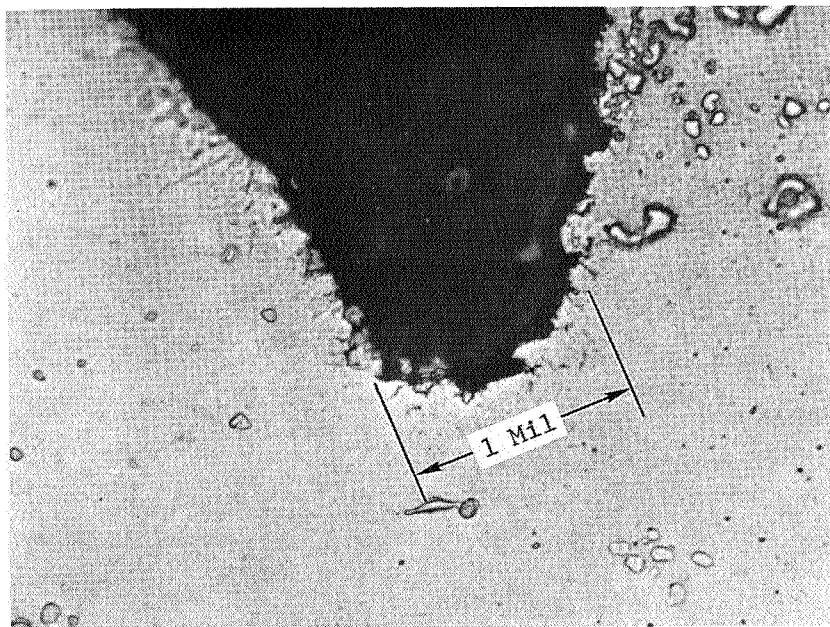


Figure 93. Impact Erosion Pits in U-700 Erosion Insert A-3 (Center Pit
in Above Figure). (B340112)
Etchant: Unetched Mag: 1000X

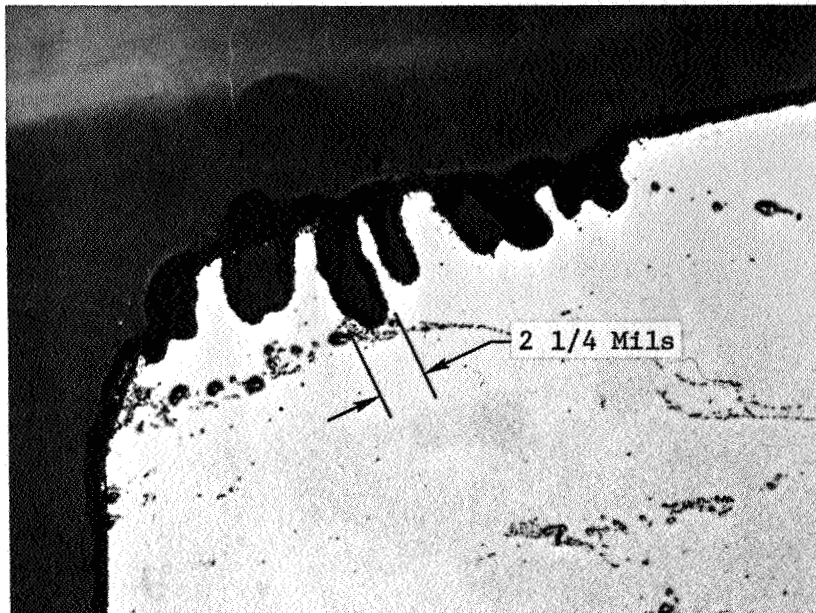


Figure 94. Impact Erosion Pits in U-700 Insert A-3 at a Third Planar Position. (B340117)

Etchant: Unetched

Mag: 100X

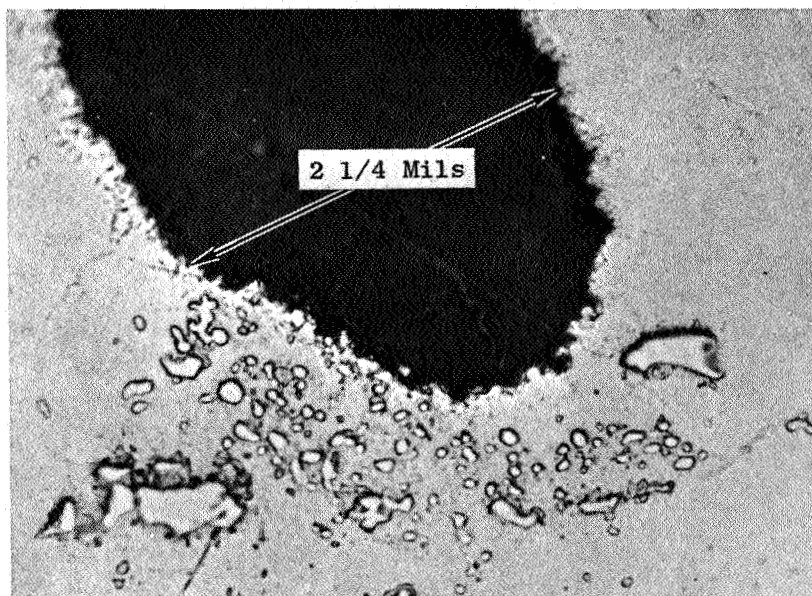


Figure 95. Impact Erosion Pit in U-700 Erosion Insert A-3. (Deepest Pit in Above Figure). (B340116)

Etchant: Unetched

Mag: 1000X

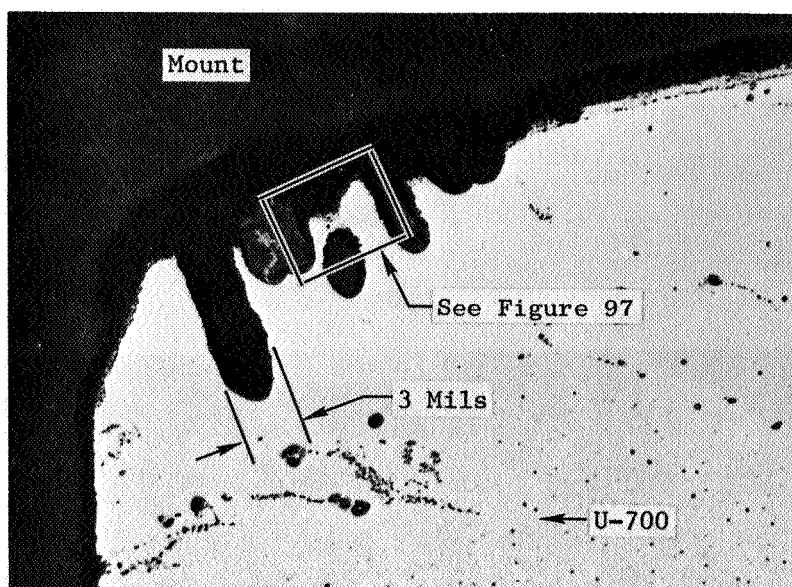


Figure 96. Impact Erosion Pits in U-700 Erosion Insert A-3 at a Second Planar Position. (B340113)

Etchant: Unetched

Mag: 100X

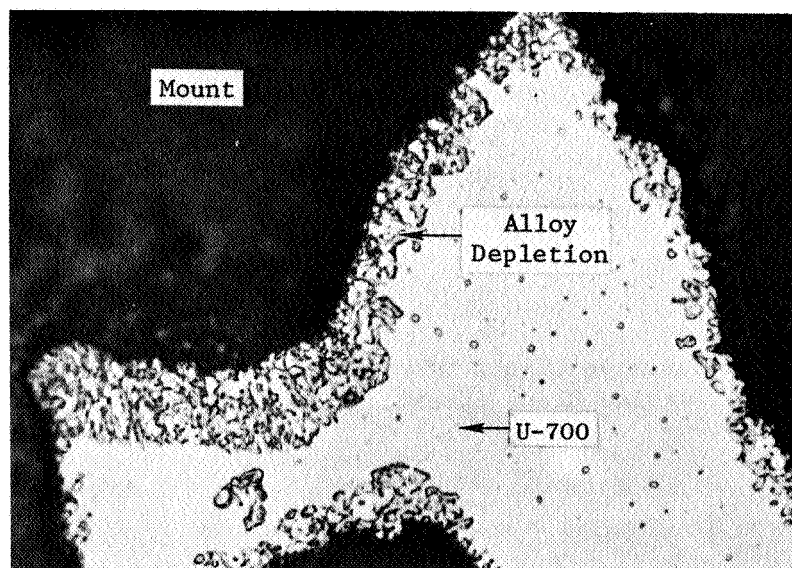


Figure 97. Alloy Depletion in Area of U-700 Impact Erosion Pits (See Above Figure). (B340115)

Etchant: 3% Nitrol

Mag: 1000X

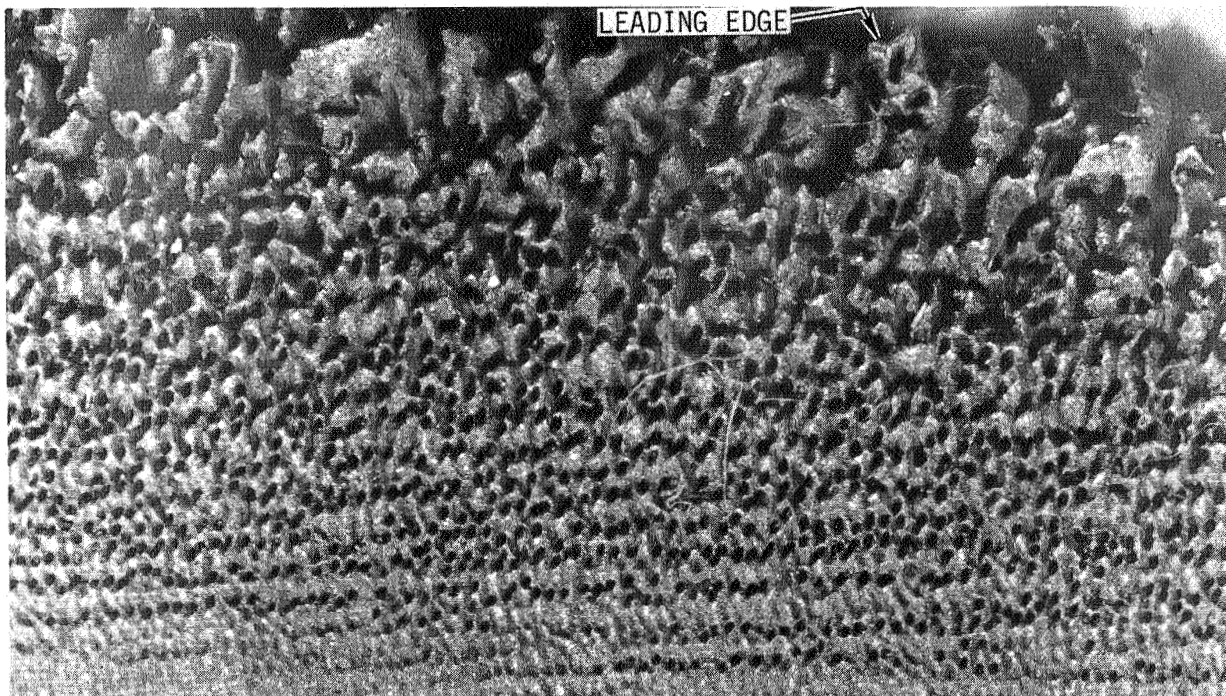


Figure 98. Characteristic Liquid Droplet Impact Erosion on Stellite 6B Steam Turbine Blade Insert. (C65061410)

Mag: 13X

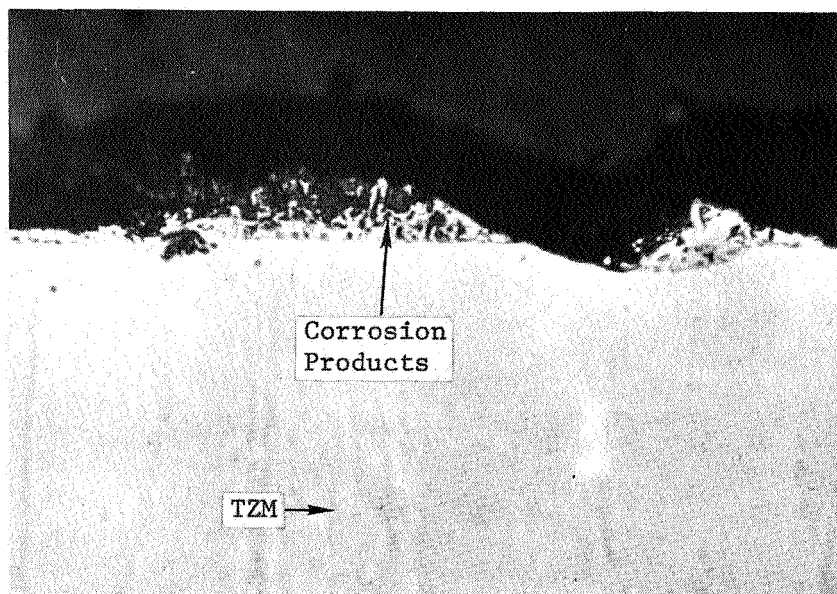


Figure 99. Liquid Potassium Impact Surface of Stress Relieved TZM Erosion Insert. (B370111)

Etchant: Unetched

Mag: 500X

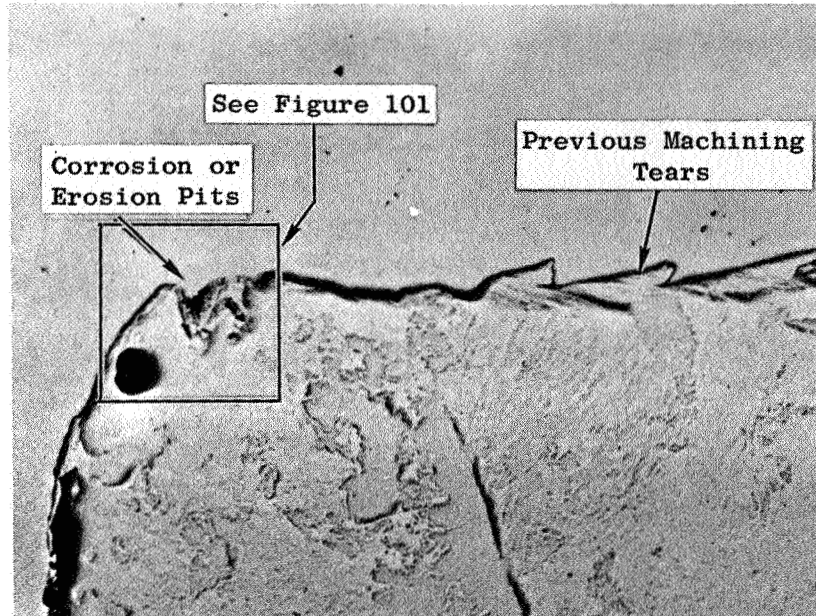


Figure 100. Corrosion Pits in TZC Erosion Insert Specimen D-2.
Etchant: Unetched Mag: 100X

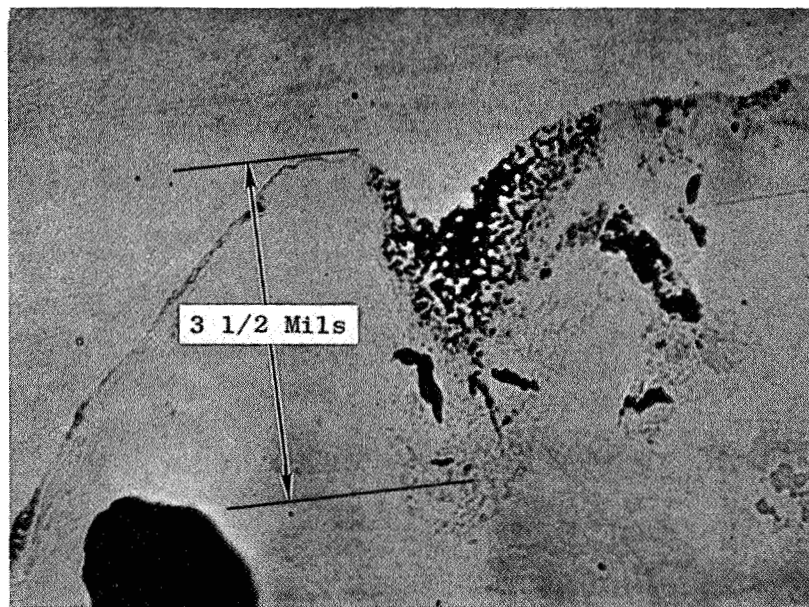


Figure 101. Corrosion Pit in TZC Erosion Insert Specimen
Etchant: Unetched Mag:

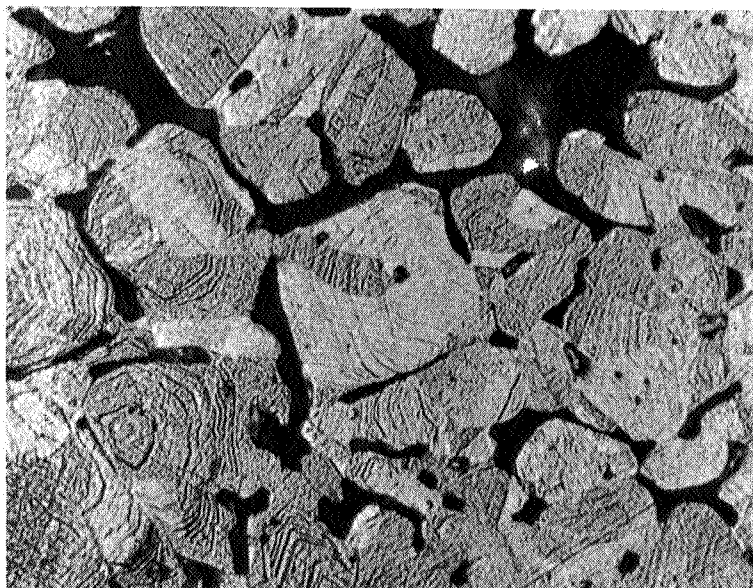
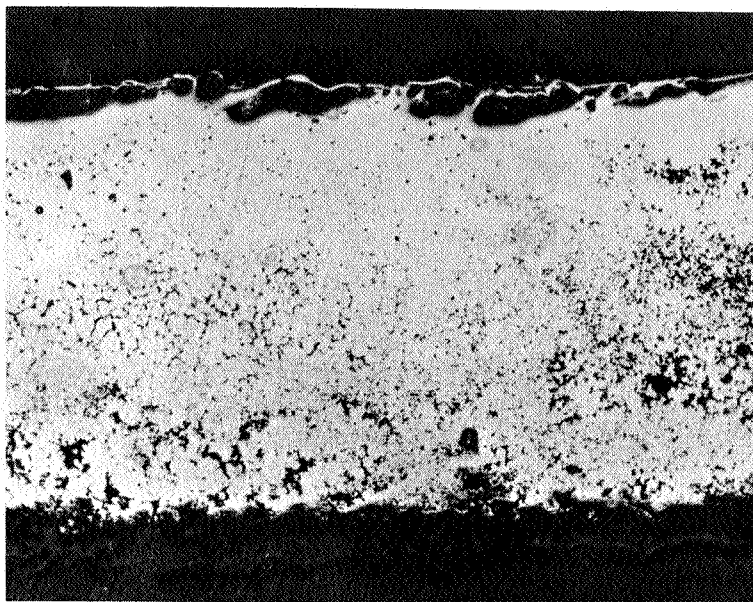


Figure 102. Cross Section of Metallic Deposit from CD Nozzle Test, 100X (Top); Enlarged and Etched Section of Metallic Deposit from CD Nozzle Test Showing Vapor Deposition Characteristics, 1000X (Bottom). (C63121252)

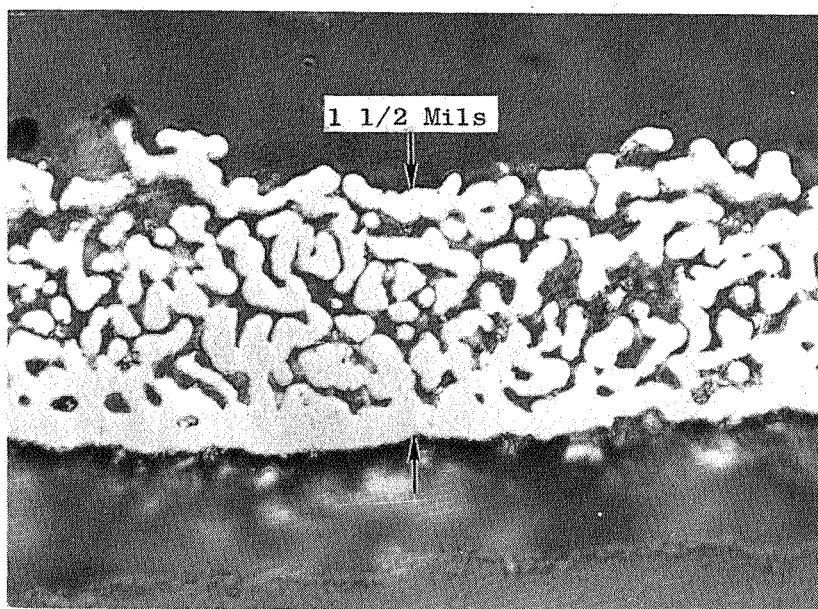


Figure 103. Metal Foil Removed from the 8-Inch Vapor Line of the 3000 KW Turbine Facility After Performance Testing. (A680111)

Etchant: Unetched

Mag: 1000X

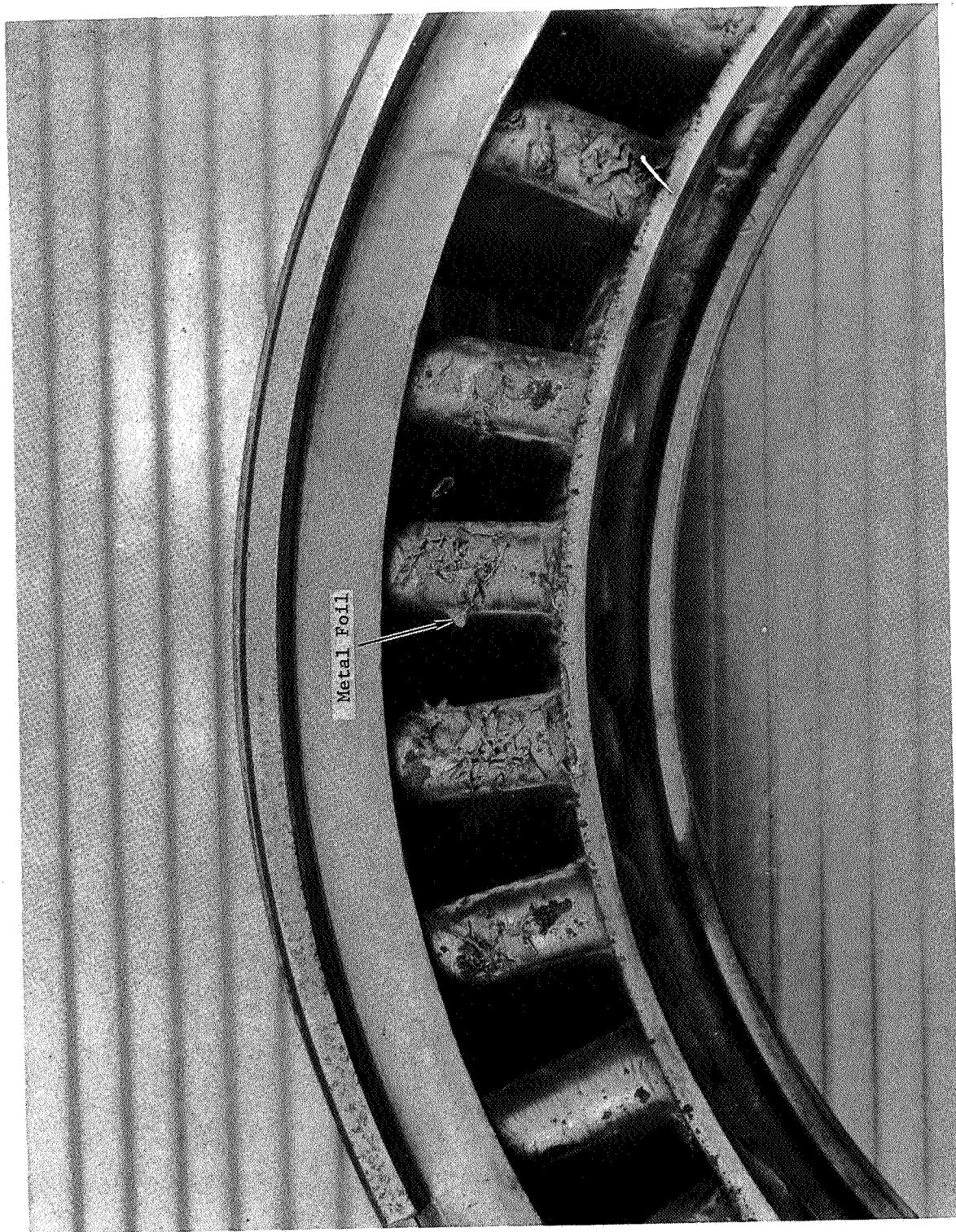


Figure 104. Metal Foil Deposits Impacted on the First Stage Turbine Nozzle
Diaphragm After Performance Testing. (C65061516)

Mag: 1.45X

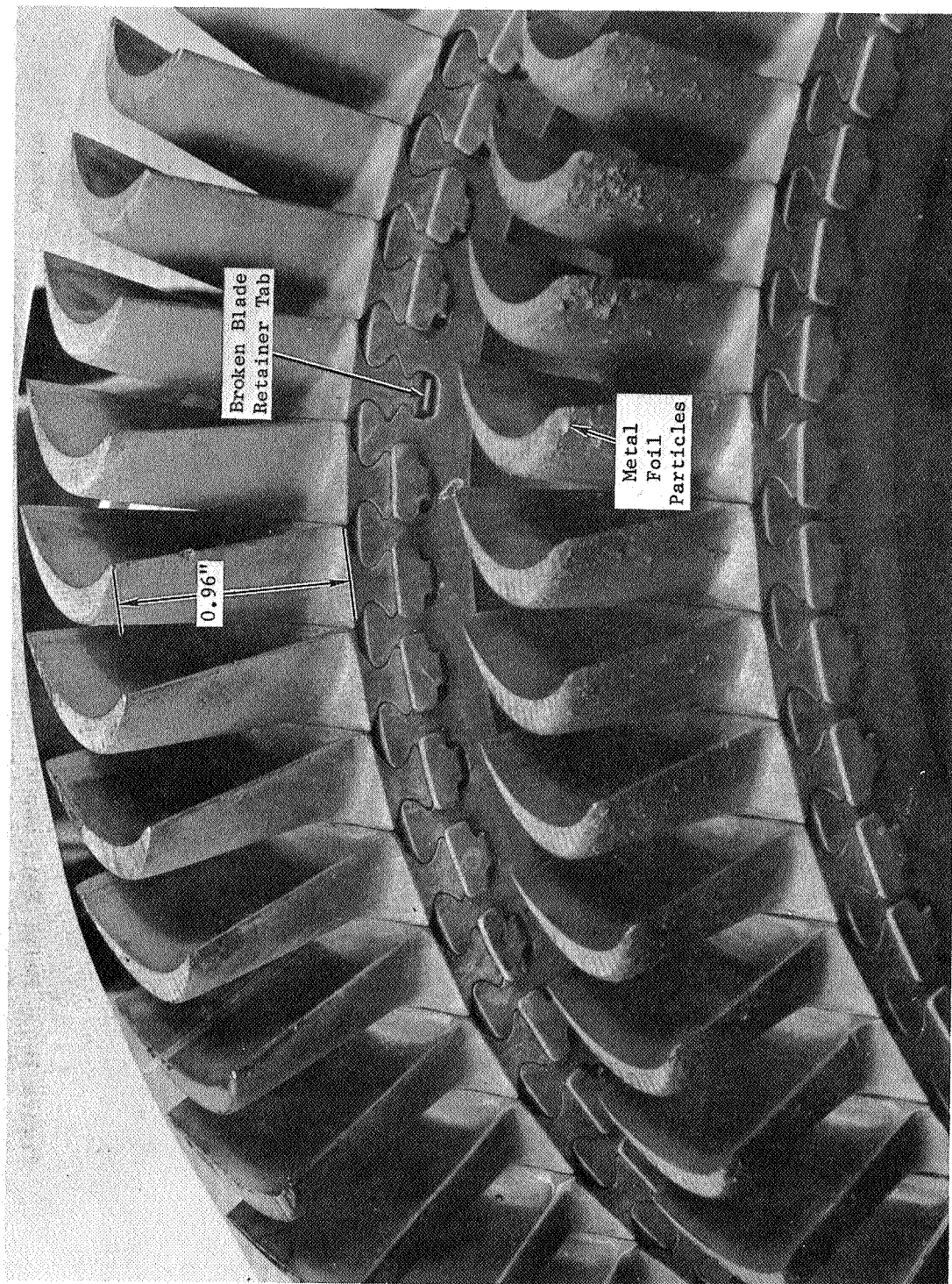


Figure 105. Close-up of Rotor Blades Showing Metal Foil Particles Impacted on First and Second Stage Blades. (C65060726)

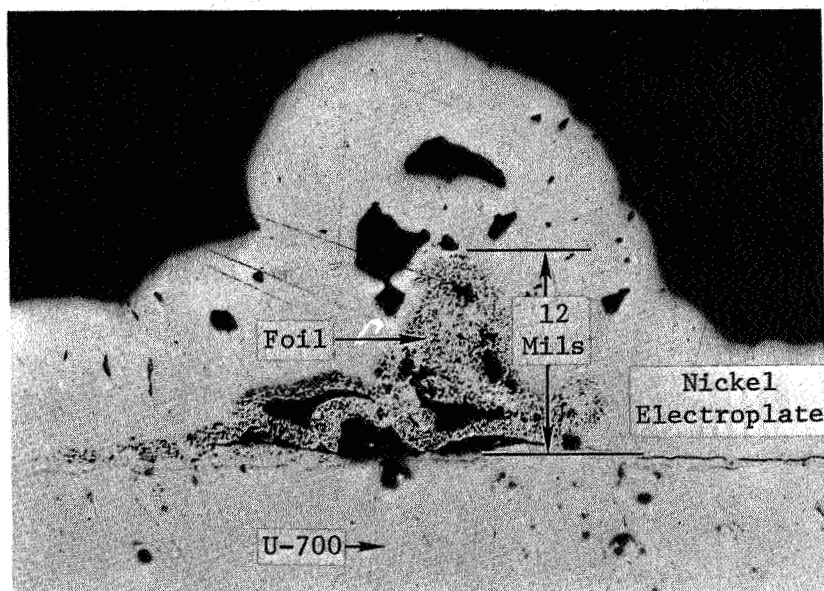


Figure 106. Foil Deposit Impacted on a Stage One Blade During Performance Testing. (A610111)

Etchant: Unetched

Mag: 100X

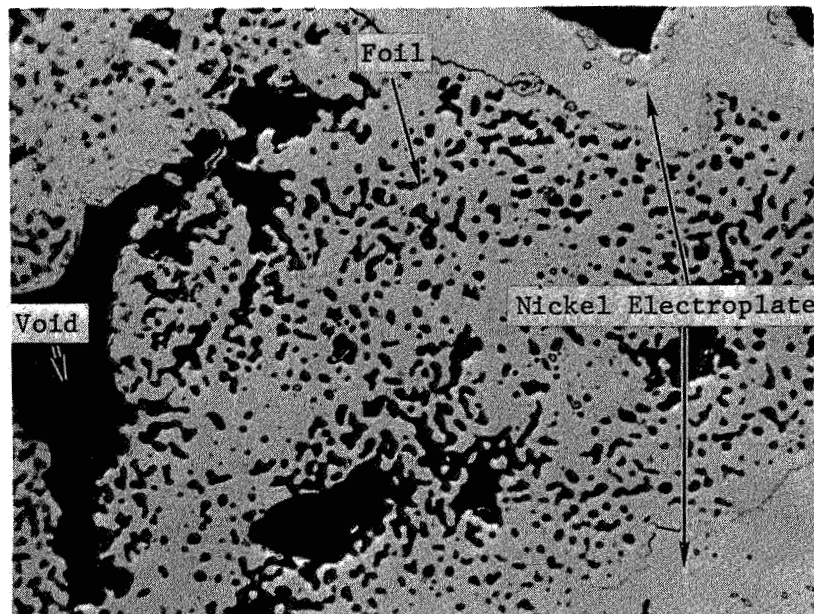


Figure 107. Foil Deposit Impacted on a Stage One Blade During Performance Testing (A610117)

Etchant: Unetched

Mag: 500X

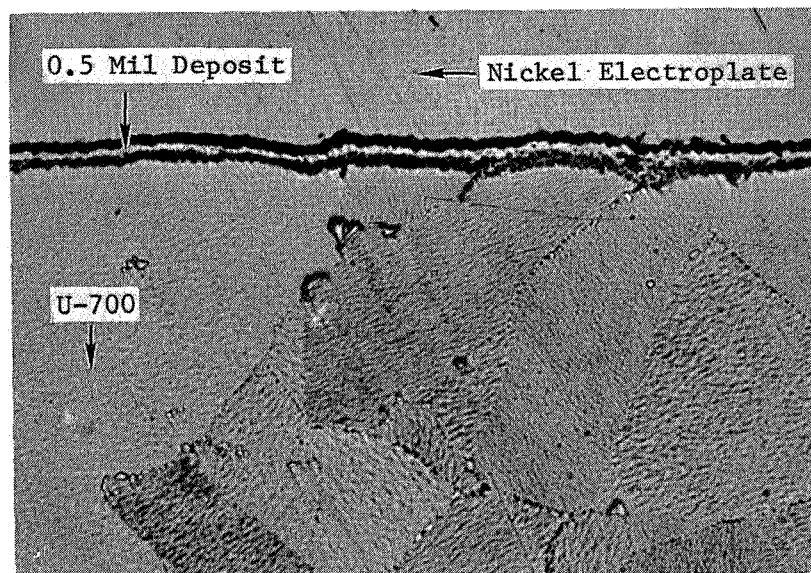


Figure 108. Uniform Metal Film Deposit on a First Stage Blade After 65-Hour Performance Test. (A61011-10)

Etchant: 100 H_2O - 50 HCl - 5 gr Fe Cl_3

Mag: 500X

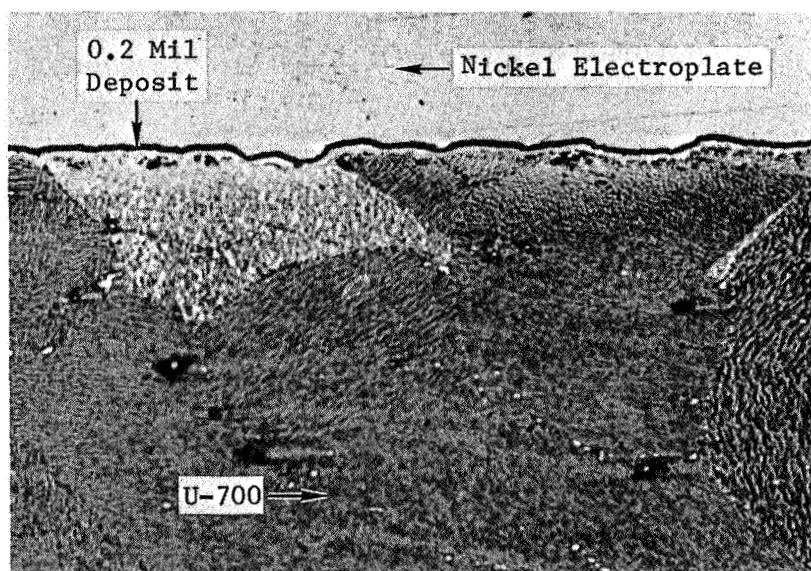


Figure 109. Uniform Metal Film Deposit on a Second Stage Turbine Blade After 65-Hour Performance Test. (A750118)

Etchant: 100 H₂O - 50 HCl - 5 gr FeCl₃ Mag: 500X

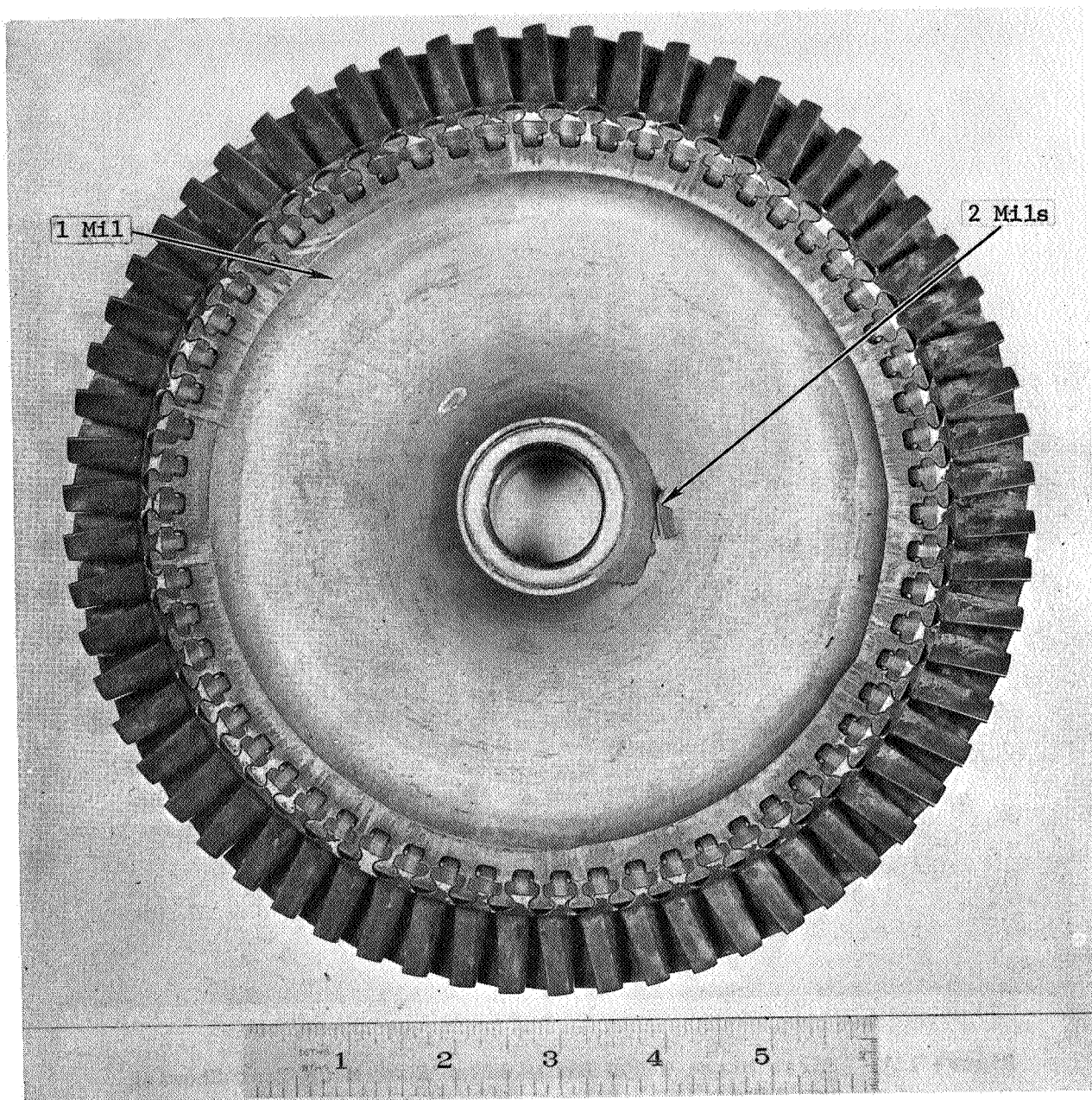


Figure 110. Forward Face of First Stage Turbine Wheel After 2000 Hour Endurance Test Showing Deposited Metal Film. (C65123043)

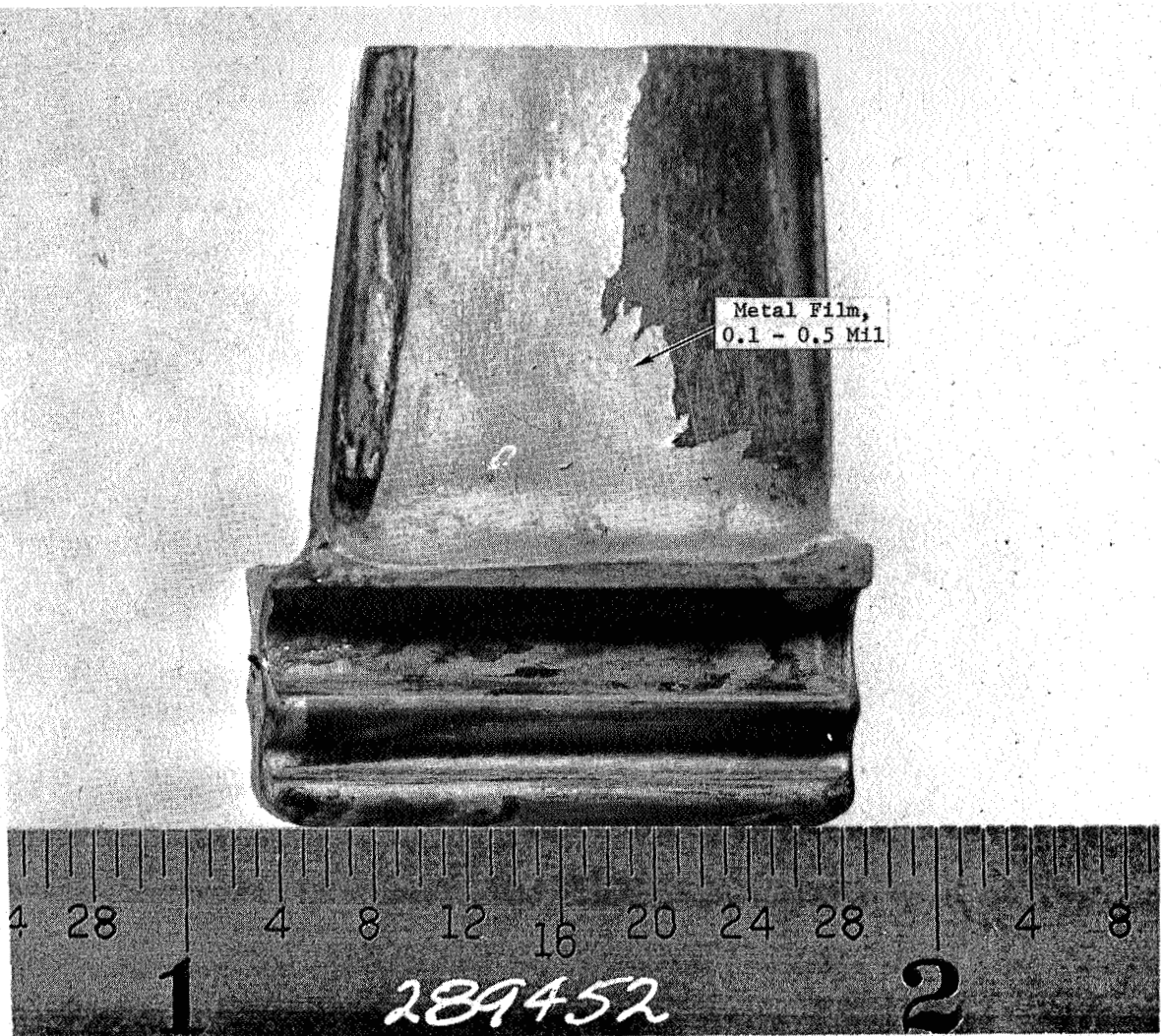


Figure 111. First Stage U-700 Blade After 2000 Hour Test Showing Deposited Metal Film. (289452)

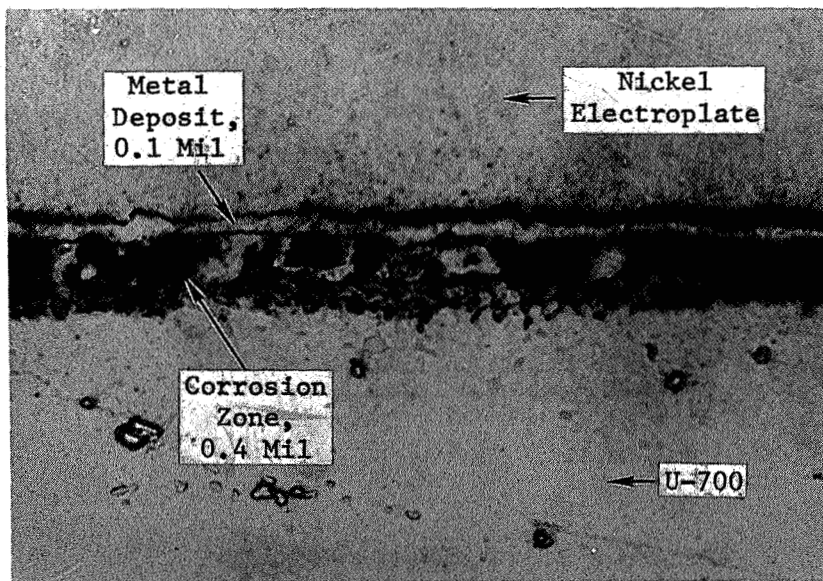


Figure 112. Concave Surface of First Stage U-700 Endurance Test Blade Near Leading Edge Showing Metallic Film Deposit and Underlying Corrosion. (B322112)

Etchant: Unetched

Mag: 1000X

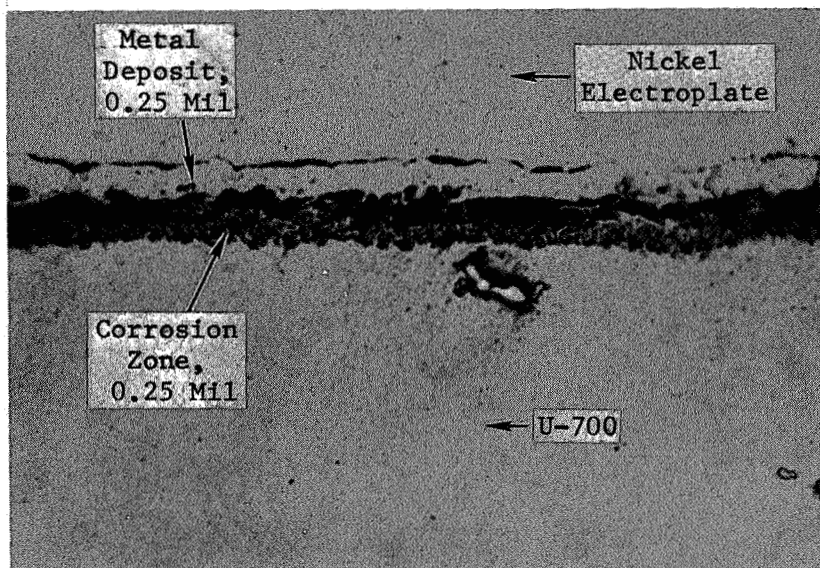


Figure 113. Convex Surface of First Stage U-700 Endurance Test Blade Near Leading Edge Showing Metallic Film Deposit and Underlying Corrosion. (B322113)

Etchant: Unetched

Mag: 1000X

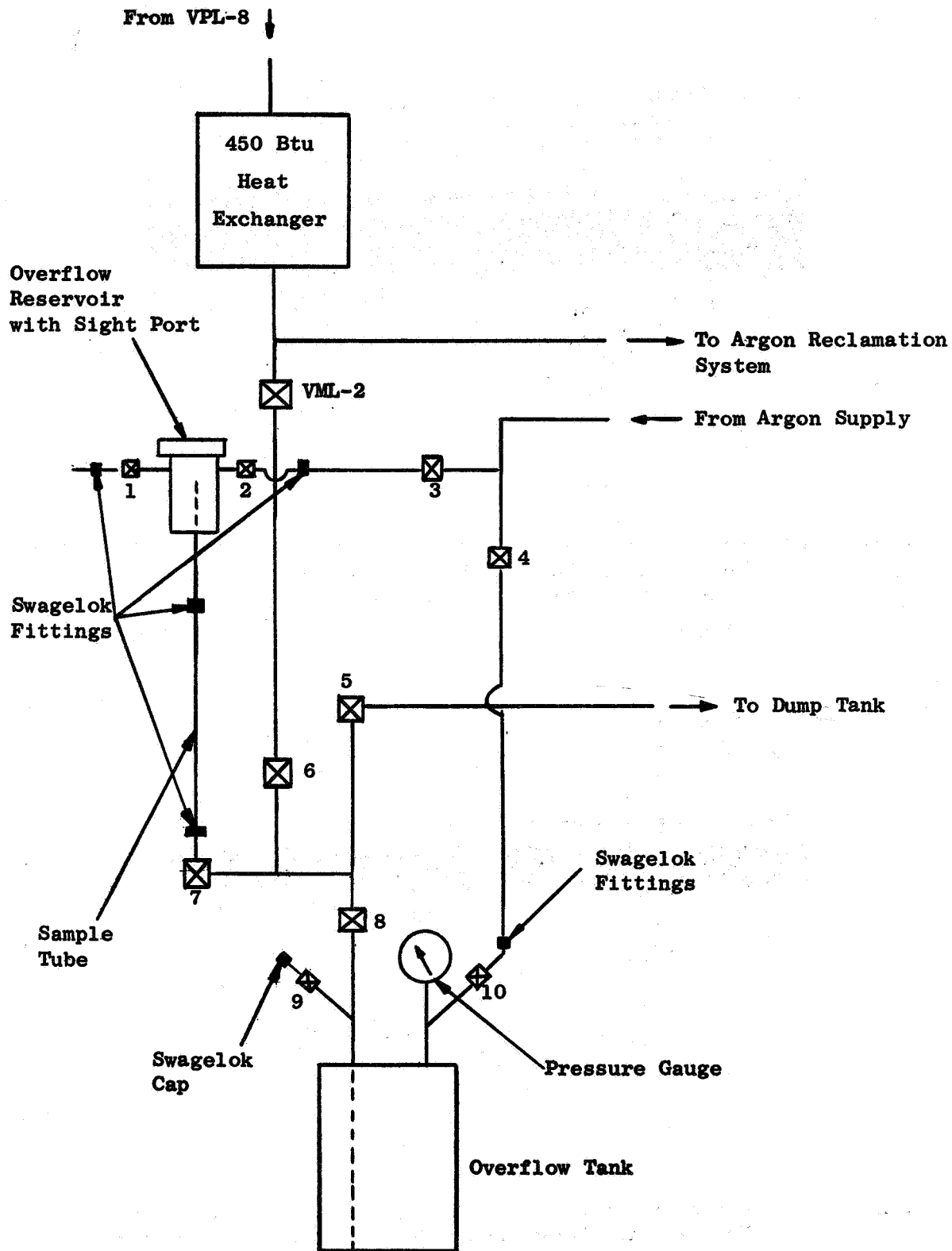


Figure 114. Schematic Diagram of Potassium Sampling Apparatus for the Two Stage Potassium Test Turbine.

"The aeronautical and space activities of the United States shall be conducted so as to contribute . . . to the expansion of human knowledge of phenomena in the atmosphere and space. The Administration shall provide for the widest practicable and appropriate dissemination of information concerning its activities and the results thereof."

—NATIONAL AERONAUTICS AND SPACE ACT OF 1958

NASA SCIENTIFIC AND TECHNICAL PUBLICATIONS

TECHNICAL REPORTS: Scientific and technical information considered important, complete, and a lasting contribution to existing knowledge.

TECHNICAL NOTES: Information less broad in scope but nevertheless of importance as a contribution to existing knowledge.

TECHNICAL MEMORANDUMS: Information receiving limited distribution because of preliminary data, security classification, or other reasons.

CONTRACTOR REPORTS: Scientific and technical information generated under a NASA contract or grant and considered an important contribution to existing knowledge.

TECHNICAL TRANSLATIONS: Information published in a foreign language considered to merit NASA distribution in English.

SPECIAL PUBLICATIONS: Information derived from or of value to NASA activities. Publications include conference proceedings, monographs, data compilations, handbooks, sourcebooks, and special bibliographies.

TECHNOLOGY UTILIZATION PUBLICATIONS: Information on technology used by NASA that may be of particular interest in commercial and other non-aerospace applications. Publications include Tech Briefs, Technology Utilization Reports and Notes, and Technology Surveys.

Details on the availability of these publications may be obtained from:

SCIENTIFIC AND TECHNICAL INFORMATION DIVISION
NATIONAL AERONAUTICS AND SPACE ADMINISTRATION

Washington, D.C. 20546